



Universitat Autònoma de Barcelona

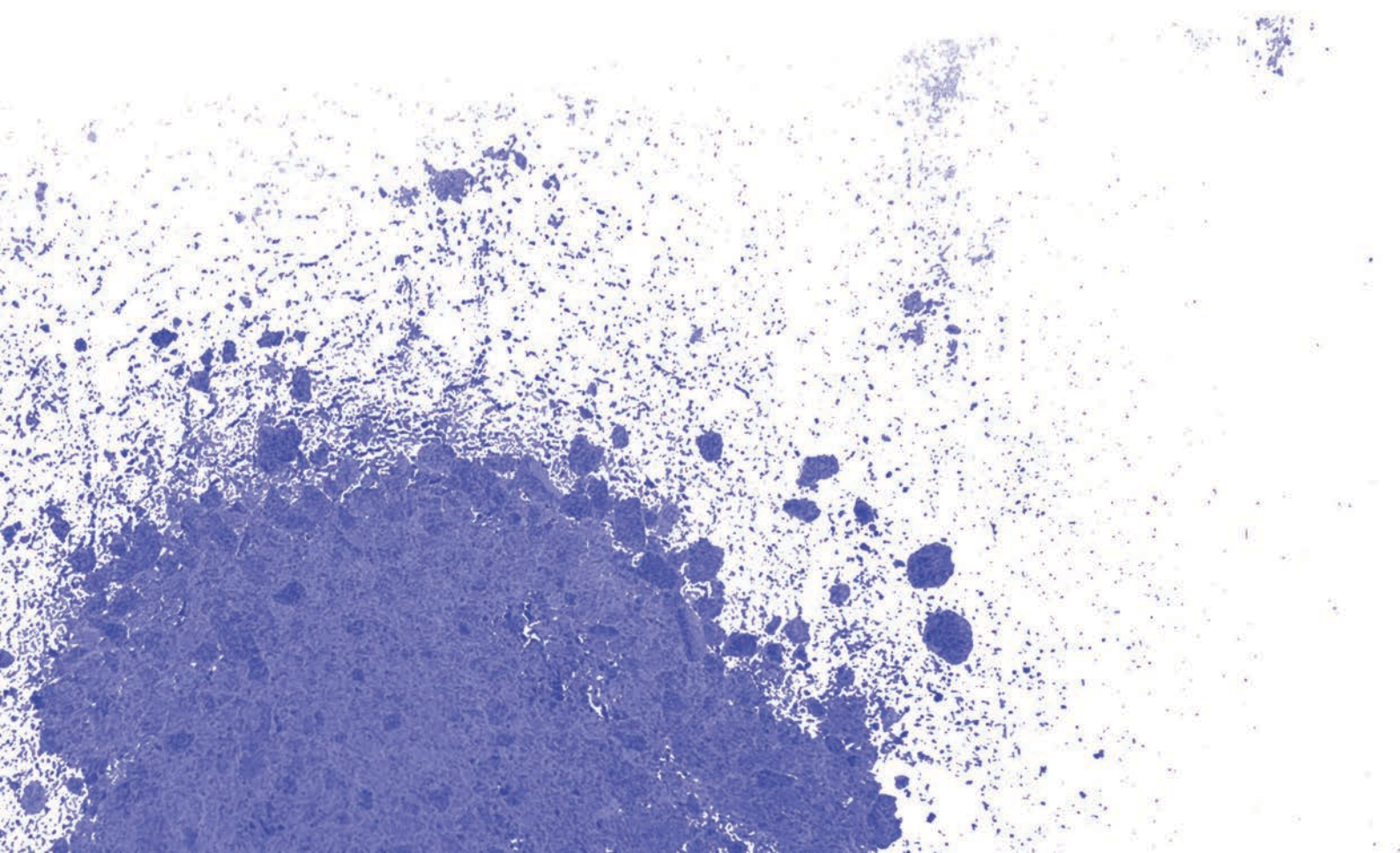
ADVERTIMENT. L'accés als continguts d'aquesta tesi queda condicionat a l'acceptació de les condicions d'ús establertes per la següent llicència Creative Commons:  http://cat.creativecommons.org/?page_id=184

ADVERTENCIA. El acceso a los contenidos de esta tesis queda condicionado a la aceptación de las condiciones de uso establecidas por la siguiente licencia Creative Commons:  <http://es.creativecommons.org/blog/licencias/>

WARNING. The access to the contents of this doctoral thesis it is limited to the acceptance of the use conditions set by the following Creative Commons license:  <https://creativecommons.org/licenses/?lang=en>

**HIGH-RESOLUTION MICRODIALYSIS
APPLIED TO THE STUDY
AND TREATMENT
OF BRAIN METABOLIC DISORDERS**

MARIAN VIDAL JORGE



DOCTORAL THESIS

**High-resolution microdialysis applied to the study and
treatment of brain metabolic disorders**

Report submitted by Marian Vidal Jorge to qualify for Doctorate degree
by the *Universitat Autònoma de Barcelona*.

This thesis has been conducted in the Neurotraumatology and Neurosurgery
Research Unit (UNINN) at Vall d'Hebron Research Institute (VHRI).

PhD directors

PhD student

Juan Sahuquillo Barris

Surgery Department
Faculty of Medicine
Universitat Autònoma de Barcelona

Marian Vidal Jorge

María de las Mercedes Márquez Martínez

Proteomics and Structural Biology Service (SePBioES)
Institute of Biotechnology and Biomedicine (IBB)
Universitat Autònoma de Barcelona

Sara García Gil Perotín

Department of Neurology
Multiple sclerosis and neural regeneration research group
La Fe, University Hospital and Health institute

Barcelona, May 2017

FUNDING AND CONFLICTS OF INTEREST

The present doctoral thesis has been conducted in the Neurotraumatology and Neurosurgery Research Unit (UNINN). The UNINN is supported by a Grant from the Departament d'Universitats, Recerca i Societat de la Informació de la Generalitat de Catalunya (SGR 2014-844). The articles and studies developed in the present thesis has been supported by the Fondo de Investigación Sanitaria (Instituto de Salud Carlos III) with grant FIS PI11/00700, which was co-financed by the European Regional Development Fund (ERDF) and awarded to Dr. J. Sahuquillo.

The authors of the presented studies do not have any conflict of interest in relation to the materials and methods used in these works nor in the results shown. All the articles and the textbooks chapters included in this doctoral thesis have been reproduced with the prior authorization of the copyright holders.

El futur té que començar a algun punt



podria ser aquest

AL MEU PARE

"Parlem de tu, però no pas amb pena.
Senzillament parlem de tu, ..., de les teves
coses, parlem i també dels teus gustos,
del que estimaves i el que no estimaves,
del que feies i deies i senties;
de tu parlem, però no pas amb pena.

I a poc a poc esdevindràs tan nostre
que no caldrà ni que parlem de tu
per recordar-te; a poc a poc seràs
un gest, un mot, un gust, una mirada
que flueix sense dir-lo ni pensar-lo"

Miquel Martí i Pol

INDEX

FUNDINGS AND CONFLICTS OF INTEREST	I
AGRAÏMENTS	II
ABBREVIATIONS AND ACRONYMS	5
INTRODUCTION	14
1. Ischemic Stroke.....	17
2. Traumatic brain injury.....	19
3. Pathophysiology of traumatic brain injury.....	23
3.1. Excitotoxicity and ionic influx	23
3.2. Metabolic changes	25
3.2.1. Brain ischemia Biomarkers: Lactate and the lactate-to-pyruvate ratio.	27
3.2.2. Mitochondrial dysfunction	29
3.3. Phospholipid membrane degradation	31
3.4. Oxidative stress and isoprostanes	32
3.5. Cerebral edema	37
3.5.1. Brain volume regulation.....	37
3.5.2. Types of cerebral edema	39
3.6. Brain tissue hypoxia	43
3.6.1. Classes of tissue hypoxia	44
3.6.2. Molecular adaptation to hypoxia	45
4. Normobaric brain oxygen therapy as a therapeutic maneuver.....	50
5. Multimodal monitoring in TBI patients	54
5.1. Intracranial Pressure	54
5.2. Cerebral microdialysis	55
5.2.1. Methodological considerations	56
5.2.2. Catheter implantation and tissue classification	57
5.2.3. Relative recovery and <i>in vitro</i> calibration.....	59
5.2.4. Metabolic thresholds.....	60
5.2.5. Clinical applications of microdialysis monitoring.....	62
5.3. Brain oxygenation	65
5.3.1. Jugular bulb oxygen saturation	66
5.3.2. Partial brain tissue oxygen tension.....	66

HYPOTHESES AND OBJECTIVES	72
STUDIES CONDUCTED	76
1. <i>Microdiálisis cerebral en el paciente neurocrítico</i>	81
2. Characterization of the Ionic Profile of the Extracellular Space of the Injured and Ischemic Brain: A Microdialysis Study.	91
3. Does normobaric hyperoxia cause oxidative stress in the injured brain? A microdialysis study using 8-iso-PGF ₂ α as a biomarker.....	115
RESULTS AND DISCUSSION	122
1. Characterization of the ionic profile of the extracellular space of the injured and ischemic brain	122
1.1. Ion-selective electrode versus ICP-MS analyzer	123
1.2. Study Group	123
1.3. Control group	124
1.4. Ionic content related to cerebral pathology and microdialysis catheter insertion zone	125
1.5. Glycerol in the normal and injured brain	131
1.6. Discussion	131
1.7. Limitations of the study and future directions	140
2. Normobaric hyperoxia and oxidative stress in the injured brain	141
2.1. Study Group	141
2.2. Normobaric hyperoxia	143
2.3. Systemic and intracranial changes after the hyperoxic challenge	144
2.4. Metabolic response to hyperoxia in the normal and injured brain	145
2.5. Reference range for 8-Iso-Prostaglandin F ₂ α	148
2.6. <i>In vitro</i> relative recovery of 8-iso-PGF ₂ α	149
2.7. Plasma and cerebral 8-iso-PGF ₂ α levels before and after hyperoxia	150
2.8. Discussion	151
2.9. Future directions and study limitations	156
CONCLUSIONS	160
ANNEX	192
1. Human organotypic cultures as an <i>in vitro</i> model.....	192
1.1. Material and methods	192
1.1.1. Cell Culture.....	192
1.1.2. Cell culture characterization.....	193
1.2. Results and discussion	195

2. Human adult neural stem cells as an <i>in vitro</i> model	200
2.1. Material and methods	200
2.1.1. Cell culture	200
2.1.2. Cell culture characterization.....	201
2.2. Results and discussion	202
3. Low extractivity brain hypoxia after traumatic brain injury. Metabolic profile and <i>in vitro</i> modeling.....	206
3.1. Material and methods	208
3.1.1. Cell culture and hypoxic challenge	208
3.1.2. Cell Viability: Propidium iodide uptake	209
3.1.3. Metabolic analysis.....	210
3.1.4. Western blot (WB)	210
3.1.5. Immunocytochemistry	211
3.1.6. Statistical analysis	212
3.2. Results	212
3.2.1. Effects of hypoxia on cellular proliferation, morphology and viability	212
3.2.1. HIF-1 α protein accumulation and nuclear translocation	214
3.2.2. Expression of glycolytic enzymes in hypoxic cells	215
3.2.3. Effects of hypoxia on astrocytes energy metabolism	217
3.3. Discussion	219
3.4. Study limitations and future research	224
4. References	225

ABBREVIATIONS AND ACRONYMS

4-OHT	4-hydroxytamoxifen
8-iso-PGF2α	8-Iso-Prostaglandin F2 α
[8-IPF2α]_{brain}	Brain 8-Iso-Prostaglandin F2 α concentration
ADP	Adenosine diphosphate
AGS	Astrocyte growth supplement
AIS	Abbreviated injury scale
AM	Astrocyte media
AMPA	α -amino-3-hydroxy-5-methyl-4-isoxazolepropionic acid
ANLS	Astrocyte-neuron lactate shuttle
ATA	Atmospheres absolute
ATP	Adenosine triphosphate
AVDO₂	Arterio-venous difference of oxygen
BBB	Blood brain barrier
BM	Biomarker
BOSS	Biomarkers of Oxidative Stress Study
BTF	Brain trauma foundation
C₀	Matrix concentration of the analyte of interest
CaO₂	Arterial oxygen content
CAT/GPx	Catalase and Glutathione peroxidase
CBF	Cerebral blood flow
CCO	Cytochrome C oxidase
CD68	Cluster of differentiation 68
C_{dial}	Analyte concentration in the dialysate
C_{jvO₂}	Jugular venous oxygen content
[Cl⁻]_o	Extracellular chloride concentration
C_{matrix}	Analyte concentration in the matrix
CMRO₂	Cerebral metabolic rate of oxygen
CNS	Central nervous system
CO₂	Carbon dioxide
COX	Cyclooxygenase
CPP	Cerebral perfusion pressure

CSD	Cortical spreading depression
CSF	Cerebrospinal fluid
CT	Computed tomography
ctHb	Concentration of total hemoglobin
CYP450	Cytochrome P450
DAPI	4',6'-diamino-2-phenylindole
DCX	Doblecortin
DIV	Day <i>in vitro</i>
e-	Electron
ECS	Extracellular space
EEG	Electroencefalography
EGF	Epidermal growth factor
eNOS	Endothelial nitric oxide synthase
ER	Estradiol receptor
ETC	Electron transport chain
FBS	Fetal Bovine serum
FGF	Fibroblast growth factor
FIH1	Factor inhibiting HIF1
FiO₂	Fraction of inspired oxygen
FLAIR	Fluid Attenuated Inversion Recovery
FSC	Forward scatter
FT	Filum terminale
GBM	Glioblastoma Multiforme
GC-MS	Gas chromatography-mass spectrometry
GCS	Glasgow coma scale
GFAP	Glial fibrillary acidic protein
[Glu]_{brain}	Brain glucose concentration
GLUT1	Glucose transporter 1
[Gly]₀	Glycerol interstitial levels
[Gly]_{brain}	Brain glycerol concentration
GOSE	Glasgow Outcome Scale Extended
H⁺	Proton
H₂O₂	Hydrogen peroxide
H&E	Hematoxylin–eosin

Hb	Hemoglobin
HBO	Hyperbaric oxygen therapy
HBSS	Hank's balanced salt solution
HIF-1α	Hypoxia-inducible factor-1 α
HK-2	Hexoquinase 2
hNSC	Human neural stem cells
HO\cdot	Hydroxyl radical
HOCl	Hypochlorous acid
HR	Heart rate
HREs	Hypoxia-response elements
HRP	Horseradish peroxidase
HSP90	Heat-shock protein 90
HTS	Hypertonic saline solutions
IC	Ischemic core
ICC	Immunocytochemistry
ICH	Intracranial hypertension
ICP	Intracranial pressure
ICP-MS	Inductively coupled plasma mass spectrometry
ICS	Intracellular space
ICU	Intensive care unit
IHC	Immunohistochemistry
IL-1β	Interleukin 1 beta
iNOS	Inducible nitric oxide synthase
IP	Ischemic penumbra
IS	Ischemic Stroke
ISS	Injury severity score
[K⁺]_o	Extracellular potassium concentration
KC	Krebs cycle
[Lac]_{brain}	Brain lactate concentration
LC/MS	Liquid chromatography-mass spectrometry
LDH	Lactate dehydrogenase
LDH-A	Lactate dehydrogenase-A
LDH-B	Lactate dehydrogenase-B
LEH	Low extractivity hypoxia

LGR	Lactate-to-glucose ratio
LIF	Leukemia inhibitory factor
LOX	Lipoxygenase
LPR	Lactate-to-pyruvate ratio
MABP	Mean arterial blood pressure
MCA	Middle cerebral artery
MCT	Monocarboxylate transporter
MD	Microdialysis
MMCAI	Malignant middle cerebral artery infarction
MMPs	Matrix metalloproteinases
MNM	Multimodality neuromonitoring
MRI	Magnetic resonance imaging
[Na⁺]_o	Extracellular sodium concentration
NAD⁺	Nicotinamide adenine dinucleotide oxidized form
NADH	Nicotinamide adenine dinucleotide reduced form
NB	Normal injured brain
NBO	Normobaric oxygen therapy
NF200	200-kDa phosphorylated and non-phosphorylated neurofilament
NIRS	Near-infrared spectroscopy
NMDA	<i>N</i> -methyl D-aspartate
NO	Nitric oxide
NO₂	Nitrogen dioxide
NOS	Nitric oxide synthase
ODD	Oxygen-dependent degradation domain
ONOO⁻	Peroxynitrite
OxS	Oxidative stress
P₅₀	Half saturation tension
PaCO₂	Partial pressure of arterial carbon dioxide
PaO₂	Partial pressure of arterial oxygen
PARP-1	Poly-ADP ribose polymerase-1
PBS	Phosphate buffered saline
PC	Pyruvate carboxylase
PDH	Pyruvate dehydrogenase
PET	Positron emission tomography

PFR	PaO ₂ /FiO ₂ ratio
PI	Propidium iodide
PjvCO₂	Partial jugular venous pressure of arterial carbon dioxide
PjvO₂	Partial jugular venous oxygen tension
PO₂	Partial oxygen pressure
PTBCs	Post-traumatic brain contusions
PtiO₂	Brain tissue oxygen pressure
[Pyr]_{brain}	Brain pyruvate concentration
Px	Oxygen extraction tension
REDOX	Reduction-oxidation
RI	Reference interval
RNS	Reactive nitrogen species
ROS	Reactive oxygen species
RR	Relative recovery
RS	Reactive Species
SAH	Subarachnoid hemorrhage
SaO₂	Arterial oxygen saturation
SjvO₂	Jugular venous oxygen saturation
SOD	Superoxide dismutase
SSC	Side scatter
SUR1/TRPM4	Sulfonylurea receptor1/transient receptor potential melastatin 4
SVZ	Subventricular zone
T1W	T1-weighted imaging
T2W	T2-weighted imaging
TBI	Traumatic brain injury
TBS	Tris-buffered saline buffer
TC	Traumatic core
TEM	Transmission electron microscopy
TGF-β	Transforming growth factor-beta
TJs	Tight junctions
TNF-α	Tumor necrosis factor-α
TP	Traumatic penumbra
TSC	Total sodium content
TUJ1	β-tubulin III

ABBREVIATIONS AND ACRONYMS

UHPLC-MS/MS	Ultra-high performance liquid chromatography coupled to tandem mass spectrometry
VEGF	Vascular endothelial growth factor
VEGFR-2	Vascular endothelial growth factor receptor-2
VHL	Hippel Lindau protein
WB	Western blot

SECTION



INTRODUCTION

1

- 1 ISCHEMIC STROKE**
- 2 TRAUMATIC BRAIN INJURY**
- 3 PATHOPHYSIOLOGY OF TRAUMATIC BRAIN INJURY**
- 4 NORMOBARIC BRAIN OXYGEN THERAPY AS A THERAPEUTIC MANEUVER**
- 5 MULTIMODAL MONITORING IN TBI PATIENTS**

INTRODUCTION

Traumatic brain injury (TBI) is the leading cause of death and disability in the world's population under 40 years of age.^{1,2} The pathophysiological mechanisms of TBI are a combination of primary damage, which results from direct tissue disturbance by biomechanical forces at the moment of impact, and secondary damage, which is characterized by the activation of several biochemical cascades in response to mechanical injury with delayed clinical presentation. There are four main categories for these mechanisms: 1) ischemic or non-ischemic brain tissue hypoxia associated with excitotoxicity, energy failure, and cell death; 2) cerebral edema; 3) delayed diffuse axonal injury; and 4) inflammatory cascades triggered by the traumatic insult. The quantitative contribution of each mediator to the outcome and the interplay between them still remains poorly understood. Among these mechanisms, cerebral edema and ischemic and non-ischemic cerebral hypoxia are the most frequent lesions after brain injury. Efforts in the development of neuromonitoring have aimed at designing systems to detect early changes in these lesions and reverse them using early therapeutic maneuvers.

In the past two decades, both clinicians and researchers have considered brain ischemic and non-ischemic cerebral hypoxia, the protagonist of most secondary lesions occurring in patients with severe TBI.^{3,4} Both primary damage and cerebral ischemia trigger the release of neurotransmitters and an energy failure that causes massive ionic fluxes, with subsequent osmotic water movement across the cells followed by brain edema. Brain edema is the major leading cause of death and disability in these patients.

For this reason, the treatment of this type of lesion has traditionally aimed at modulating and reverting the edema and the consequent increase in intracranial pressure (ICP) through the application of hyperosmotic agents. Nevertheless, these treatments have low efficacy and significant systemic side effects. Therefore, it is necessary to search for new therapeutic targets and tools to monitor the ionic profile of the extracellular space (ECS) in the different phases of brain edema. Better understanding of the complex ionic disturbances that cause brain edema would benefit the study and treatment of not only TBI patients but also patients with other acute neurological

injuries, such as malignant middle cerebral artery infarct (MMCAI), one of the most devastating forms of ischemic stroke (IS).

The management of TBI is based on the assumption that most of the brain damage is delayed (secondary damage) and that interventions directed toward preventing and treating secondary damage can make a difference in both survival and functional outcome.⁵ However, despite the many clinical trials targeting patients with moderate or severe TBI in the last decade, there is still no effective therapy for the treatment of these patients. Therapeutic interventions aiming to keep brain tissue oxygenation above certain thresholds might improve mortality and neurological outcomes. Normobaric brain oxygen therapy (NBO) is one strategy that has already tested in a variety of experimental models of TBI and in pilot clinical trials. NBO using a fraction of inspired oxygen (FiO_2) of 1.0 at 1 ATA is easily achieved in mechanically ventilated patients. However, there is still significant controversy regarding the effectiveness and potential secondary effects of this treatment.⁶⁻¹²

The main concern regarding NBO in TBI is the potential toxicity of using supranormal levels of partial pressure of arterial oxygen (PaO_2). The mechanisms by which supranormal O_2 may worsen the outcome in patients with acute brain injuries are not yet clear, but high FiO_2 could induce vasoconstriction, exacerbate oxidative stress (OxS), increase neuroinflammation, or induce excitotoxicity.¹³ Among these proposed mechanisms, the capacity of NBO to induce OxS is the most important because of the ability of O_2 to induce the production of reactive oxygen species (ROS) and therefore damage proteins, lipids, and DNA.¹⁴ Thus, despite the potential benefits in brain metabolism, NBO is still controversial and raises many concerns that need to be addressed before starting clinical trials or using it routinely in patients with acute brain injuries.

In recent years, modern multimodality neuromonitoring (MNM), including brain tissue oxygen pressure (PtiO_2) and cerebral MD monitoring, has provided an unprecedented opportunity to explore the pathophysiology of TBI at the cellular and molecular levels. MD is a powerful tool that can monitor the composition of the interstitial spaces of any organ and allows for quasi-continuous neurochemical sampling of the brain ECS in neurocritical patients. Cerebral MD has primarily been used to study brain-energy metabolism, although any molecule present in the cerebral ECS that is small enough

to cross the semi-permeable dialysis membrane will be collected in the dialysate. Consequently, the ionic and the OxS profile could be determined.

The aim of this doctoral thesis is to expand the knowledge of cerebral edema and cerebral hypoxia, which are two of the most frequent secondary lesions found in TBI patients. Specifically, the work is aimed at defining the role of MNM tools—especially cerebral MD—in the definition of the ionic and metabolic profile of different brain regions of the injured brain. To reflect our experience in multimodal monitoring, we have written a textbook chapter with a methodological and conceptual review of this technique, which has been included in the corpus of the thesis. In addition, we have focused on the study of the ionic profile of different regions of the injured brain in a cohort of patients with TBI and MMCAI. In parallel, we have assessed the metabolic response of the injured brain to 4 hours of NBO treatment and determined whether this therapy may increase the risk of OxS in the brain ECS using the 8-iso-prostaglandin F₂ α (8-iso-PGF₂ α) as a biomarker (BM).

We have also studied the abnormal brain metabolic profiles and the changes in the glycolytic machinery in *low-extractivity* hypoxia, one of the types of hypoxia described by Siggaard-Andersen in 1995,¹⁵ in an *in vitro* model of human cerebral cortex astrocytes. This work is presented in the annexes. To reproduce the abnormal metabolic profiles observed under hypoxia, we first studied the feasibility of obtaining a robust *in vitro* culture model of human brain specimens from surgical operations. The neuropathological hallmarks and the histological characterization of the cultured was determined.

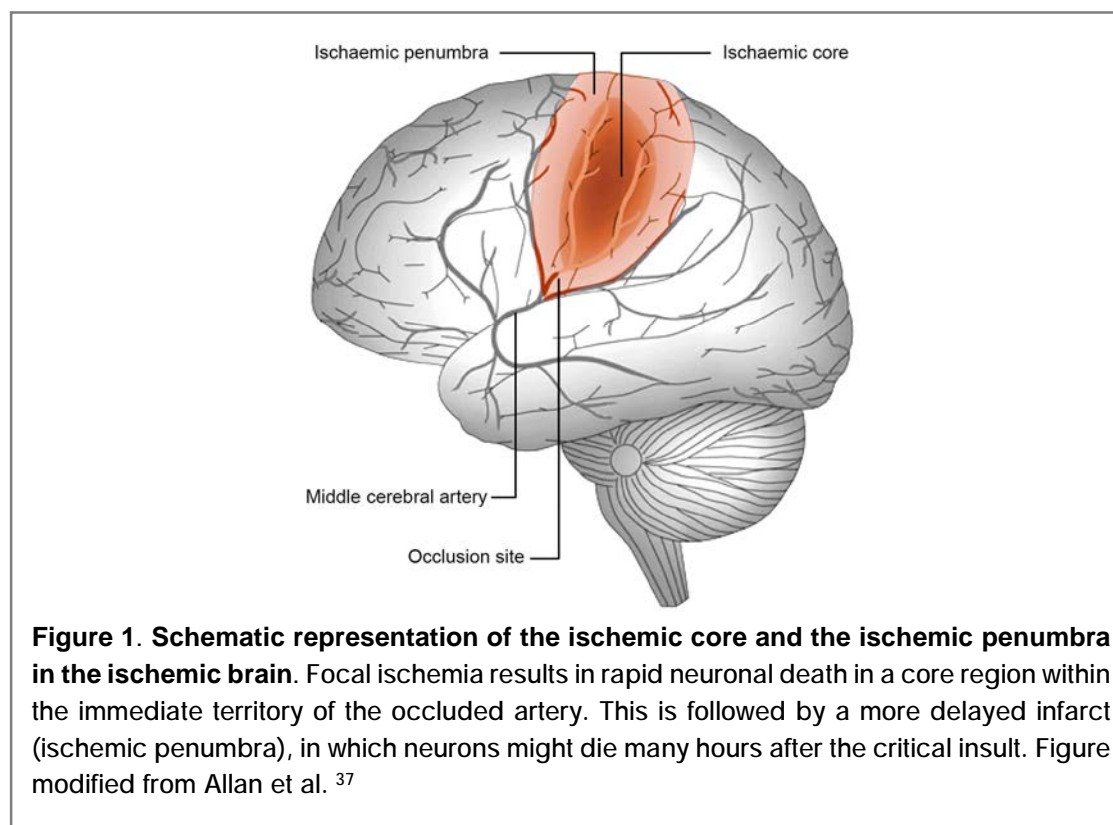
1. Ischemic Stroke

Stroke is defined as an acute neurologic dysfunction of vascular origin with a sudden occurrence of symptoms involving focal areas in the brain.¹⁶ The two main types of stroke are ischemic and hemorrhagic, which are distinguished by the underlying pathological process. Several studies have documented that the ischemic subtype is the most prevalent.^{17,18} IS an acute cerebrovascular event characterized by the sudden loss of blood circulation to an area of the brain, resulting in brain tissue damage and a corresponding loss of neurologic function. IS is considered a serious health problem worldwide. Malignant middle cerebral artery infarction (MMCAI) is a specific subtype of stroke and one of the most devastating forms of IS. The mortality rate is up to 80%, and severe disability can occur when standard medical management is used.¹⁹⁻²¹

Hacke et al. first used the term MMCAI in 1996 to characterize a form of IS that involved at least 50% of the middle cerebral artery (MCA) territory and resulted in transtentorial herniation and death in most patients, despite optimal medical treatment.²¹ The main etiology of MMCAI is thrombosis or embolic occlusion of either the internal carotid artery or the proximal MCA.^{22,23} In addition to the extensive amount of necrotic brain tissue involved in this lesion, other causes of poor neurologic outcome include post-ischemic edema, which leads to cerebral herniations, progressive brainstem dysfunction, and intracranial hypertension (ICH).^{19,24} Space-occupying brain edema is the most important cause of death and disability in MMCAI.²⁴

Experimental data have demonstrated a gradual progression of a reversible degree of ischemia toward infarction.²⁵⁻²⁹ Within the ischemic brain, there are two major well-defined zones: the **ischemic core** and the **ischemic penumbra (Figure 1)**. The core is an area of severe ischemia (severely compromised cerebral blood flow -CBF-), where the loss of oxygen and glucose results in rapid depletion of energy stores. This area rapidly evolves to necrosis through destructive biochemical phenomena, such as lipolysis, proteolysis, and disaggregation of the microtubules.³⁰ A central ischemic core is thought to be surrounded by a rim of moderate ischemic tissue with impaired electrical activity and preserved cellular viability.³¹⁻³³ This area is called the ischemic penumbra, which Astrup et al. originally defined in 1981 as the portion of the ischemic zone with reduced CBF with absent electrical activity but preserved ion homeostasis

and transmembrane electrical potentials.³⁴ This definition has been modified considerably over time, with particular focus on energy metabolism, CBF thresholds, and protein synthesis.³⁵ These areas are at high risk of being irreversibly damaged unless therapeutic measures or prompt reperfusion are rapidly applied.³⁶ With new neuroimaging modalities, penumbral tissue can be identified in patients early after IS.



Despite remarkable advances in the understanding of the pathophysiology of these lesions, until recently, there has been little evidence to guide appropriate treatments for this pathology. Initial assessment of neurologic function and radiologic findings is mandatory to promote the prompt initiation of treatments and ensure the best patient outcomes.²⁴ Treatment options include general measures and pharmacological agents to limit the extent of edema (osmotherapy), as well as surgical decompression to relieve the pressure effects.²² The only currently approved medical stroke therapy is tissue plasminogen activator, which is a thrombolytic agent that targets the thrombus within the blood vessel. Recently, data from randomized trials provided evidence of a substantial decrease in mortality among patients who underwent decompressive craniotomy alone or combined with moderate hypothermia.^{19,38,39}

2. Traumatic brain injury

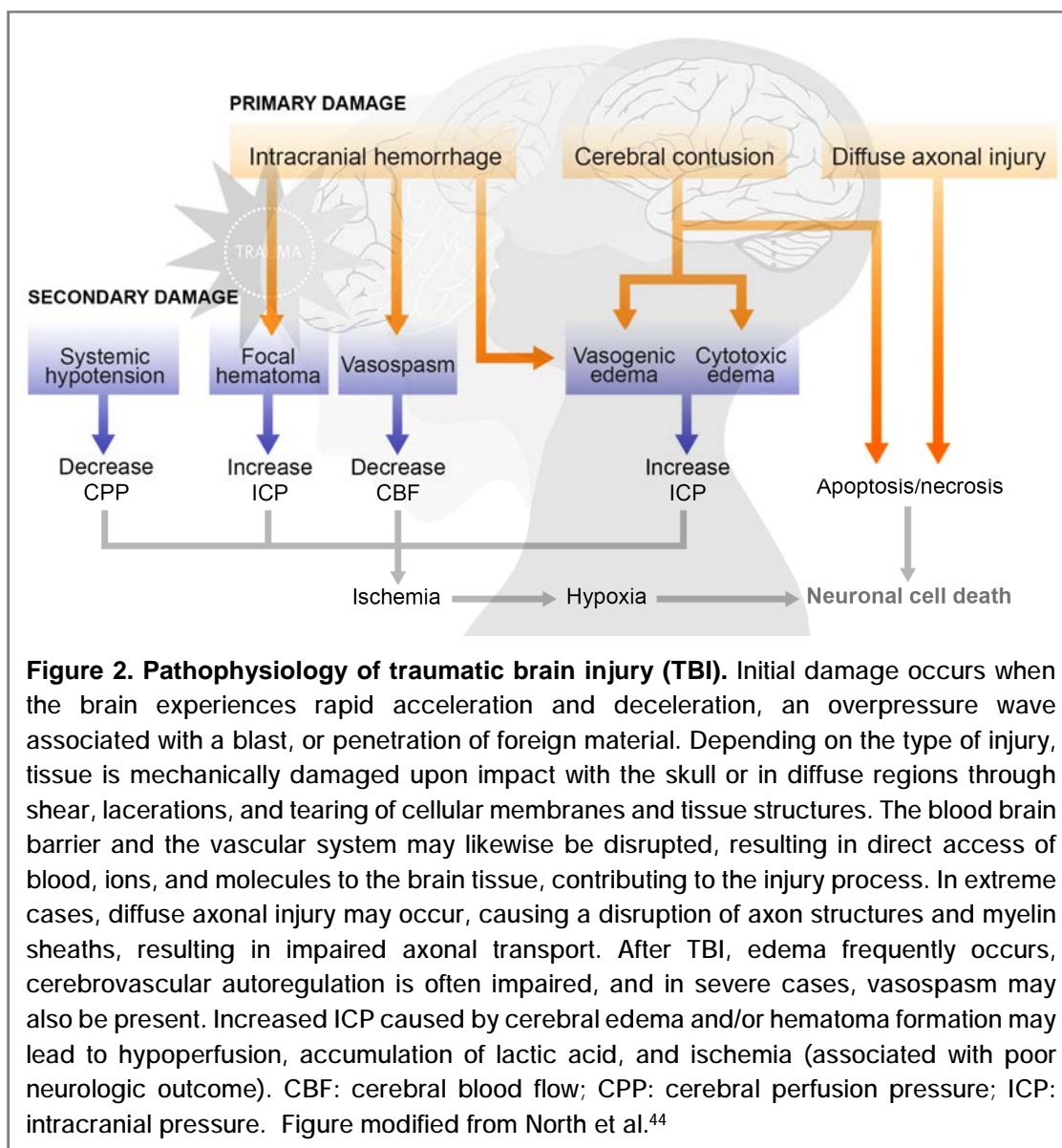
TBI is defined as a non-degenerative, non-congenital insult to the brain as a result of an external mechanical force, which could possibly lead to permanent or temporary impairment of cognitive, physical, and psychosocial functions. TBI is a critical public-health and socioeconomic problem throughout the world, with a high mortality and disability in the world's population under 40 years of age.^{1,2} TBI is considered a "silent epidemic", as society is largely unaware of the magnitude of this problem.¹ Most patients that survive a severe TBI have sequels with major medical, familial, and socioeconomic implications. The incidence of TBI worldwide is rising, but estimates show substantial variation between countries. The annual incidence of severe TBI is estimated to be up to 500/100,000 in the United States and Europe. Country-based incidence estimates for hospitalization following TBI ranges from 100-330 new cases per 100,000 population per year.⁴⁰

The assessment of TBI severity is fundamentally important in clinical management therapies. Traditionally, the TBI classification was based on **1) the clinical indices of severity, 2) the structural damage, and 3) the physical mechanism of injury**. The most commonly used **clinical index** for neurological injury among adults is the Glasgow Coma Scale (GCS), which assesses the level of consciousness after TBI.⁴¹ This scale is based on eye opening in addition to motor and verbal responses.⁴¹ The GCS is scored between 3 (deep unconscious) and 15 (normal conscious level). Mild TBI is defined by GCS scores of 13-15, whereas scores of 9-12 and 3-8 define moderate and severe TBI, respectively. A number of scales are also available to assess extracranial injuries and physiological instability, including the Abbreviated Injury Scale (AIS)⁴² and Injury Severity Score (ISS)⁴³. **Structural damage** is usually assessed by neuroimaging, particularly computer tomography (CT) scans, which are used to determine the location and the anatomical features of the injuries. The Marshall classification of TBI is the most widely used neuroimaging classification system for grading acute TBI. It categorizes patients into six different groups (**Table 1**) using important independent prognostic variables based on CT scan findings, including the state of the basal cisterns, the midline shift, and the presence of local lesions. **The physical mechanisms of injury** include closed, penetrating, crash, and blast mechanisms.⁴⁴

The physiopathological mechanisms of TBI are a combination of primary damage and secondary damage. **Primary damage** results from direct tissue disturbance by biomechanical forces upon impact (lacerations, contusion, fractures, and diffuse axonal injury). **Secondary damage** occurs in response to the primary injury with delayed clinical presentation (e.g., cerebral hematomas and intracranial hemorrhages, post-traumatic swelling, cerebral edema, hypoxic-ischemic lesions, intracranial hypertension and infections).⁴⁵ The timeline involved in these secondary processes extends from several minutes to weeks or even years after the initial insult.⁴⁶ The clinical outcomes of TBI are directly related to the severity of the primary and secondary lesions sustained by the patient.⁴⁷ Primary lesions are considered unavoidable, while secondary injury refers to potentially avoidable damage that occurs at variable times after injury. Among the cellular and biochemical mechanisms that produce secondary brain damage are ischemic or non-ischemic cerebral hypoxia, excitotoxicity, OxS, inflammatory damage, and energy failure and cell death due to the depression of aerobic metabolism and the inability to maintain ionic homeostasis, which can result in further damage to the brain. The mechanisms of this energy failure are not well established, but it is known that both substrate reduction and mitochondrial dysfunction are involved.^{48,49} These secondary lesions may be the origin of cellular and molecular mechanisms ("**tertiary lesions**").⁴⁵ The quantitative contribution of each mediator to the outcome and the interplay between them remains poorly understood (**Figure 2**).

Table 1. The Marshall classification of TBI based on CT.⁵⁰

Category	Definition
Diffuse injury I	No visible intracranial pathology
Diffuse injury II	Cisterns present, midline shift 0–5 mm and/or lesion densities present or no mass lesion >25 mL
Diffuse injury III	Cisterns compressed or absent with midline shift 0–5 mm or no mass lesion >25 mL
Diffuse injury IV	Midline shift >5 mm, no mass lesion >25 mL
Evacuated mass lesion	Evacuated mass lesion: any lesion surgically evacuated
Non-evacuated mass lesion	Non-evacuated mass lesion: High or mixed-density lesion >25 mL, not surgically evacuated



Following TBI, brain tissue that surrounds the regional primary lesion (**traumatic core**) is known as the “**traumatic penumbra**”. The brain traumatic penumbra can be defined as areas of injured but still viable brain tissue, which can either recover or eventually undergo cell death depending on the secondary pathophysiologic events triggered by the trauma. This term was introduced to parallel the well-accepted term of ischemic penumbra. As in ischemia, areas where there is mechanical tissue destruction are usually surrounded by areas of damaged but not dead tissue.⁵¹ Post-mortem studies have shown that ischemic brain damage of the vascular or non-vascular type is highly prevalent in patients who die after head trauma. For that reason, both ischemic and traumatic penumbra may frequently coexist in the same patient.^{3,36} An interesting and

important fact is that biochemical abnormalities are almost identical in both types of penumbra.³⁶

The therapeutic management of intracranial trauma aims to avoid the development of secondary lesions. To this end, the control of physiological parameters such as cerebral perfusion pressure (CPP), ICP, and CBF is crucial to minimize ischemia and tissue damage.⁴⁶ No neuroprotective treatment has been proven to be effective in controlled clinical trials, and neurological sequelae of TBI survivors have not changed significantly in the last 25 years.⁵² The advances in this field have been limited by the lack of knowledge about the biochemical, cellular, and molecular changes involved in the pathophysiology of brain injury.

3. Pathophysiology of traumatic brain injury

Damage from TBI progresses in stages. As mentioned, the first stage (primary injury) is characterized by direct tissue damage, and the second stage (secondary injury) develops as a consequence of the primary injury. The timeline of secondary processes varies from several minutes to weeks or even years after the initial insult,⁵³ and the pathways and processes involved are interrelated and produce a complex mixture of physiological responses and symptoms.

The physiological changes that occur after a TBI are correlated to processes that occur on a cellular and biochemical scale. These mechanisms are not yet fully understood, but they constitute a complex series of interrelated processes that contribute to secondary injury in TBI.⁴⁶ Importantly, many components of these pathways may be present in other neuropathological conditions and are therefore not exclusively associated with TBI. The following sections briefly discuss the biochemical cascades and related cellular processes.

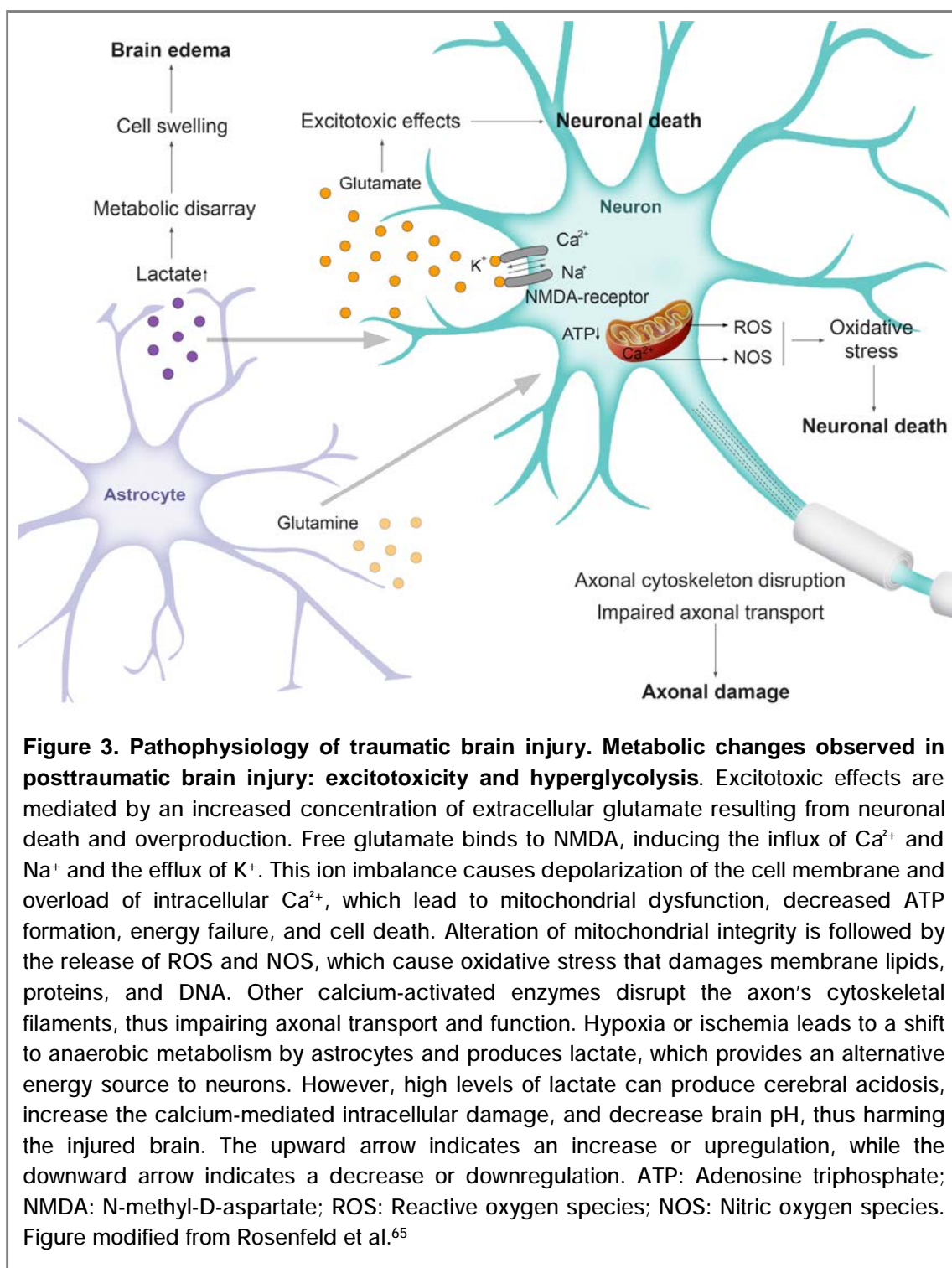
3.1. Excitotoxicity and ionic influx

One of the most significant factors causing secondary brain injury is the excessive release of excitotoxins such as glutamate and aspartate, which occurs during the primary brain injury. There is an increase in metabolic demand related to glutamate uptake due to the excitotoxicity phenomena that frequently occurs in the acute phase of TBI.⁵⁴⁻⁵⁶ Excitotoxicity describes the process by which glutamate and other excitatory amino acids cause neuronal damage.⁵⁷ A rapid, transient increase in extracellular glutamate has been observed within minutes following insult to the brain, and the magnitude and duration have been shown to correlate with injury severity.⁵⁶ This increase in extracellular glutamate levels has been attributed to: 1) the excessive release of glutamate from presynaptic nerve terminals of depolarized neurons; 2) leakage of glutamate from neuronal and glial cells with damaged or perturbed membranes; 3) the extravasation of glutamate through a disrupted blood-brain barrier (BBB);⁵⁸ or 4) alterations in astrocytic glutamate reuptake mechanisms caused by

either the functional impairment of astrocytes resulting from mechanical injury or energy depletion or by the downregulation or decreased activity of astrocytic glutamate transporters.⁵⁹

Under physiological conditions, glutamate is taken up by astrocytes, which convert it into glutamine and deliver it back to neurons as an alternative energy source. However, during the acute phase of TBI, the massive release of glutamate from presynaptic terminals cannot be removed from the ECS. The acute glutamate increase triggers the upregulation and excessive stimulation of glutamate receptors, particularly *N*-methyl-D-aspartate (NMDA), α -amino-3-hydroxy-5-methyl-4-isoxazolepropionic acid (AMPA), and metabotropic receptors, which leads to ionic dysregulation in the form of massive accumulations in extracellular K^+ concentration and the influx of Na^+ and Ca^{2+} .^{56,60} This ion imbalance causes depolarization of the cell membrane and overload of intracellular Ca^{2+} , which lead to mitochondrial dysfunction, decreased adenosine triphosphate (ATP) formation, energy failure, and cell death^{56,61,62} (**Figure 3**). Furthermore, the resultant disruption of ionic homeostasis stimulates energy-dependent pumps, which increases metabolic demand and activates glycolysis. As a result of increased glycolysis, cellular ATP stores are depleted, leading to the accumulation of lactate in brain tissues. Simultaneously, the transport of glutamate into astrocytes and microglia, which is required to maintain correct extracellular glutamate levels under physiological conditions, is inhibited by quinolinic acid, another excitotoxic compound released with glutamate.⁴⁶

The increased intracellular Ca^{2+} concentrations that result from excessive glutamate signaling also induce cellular damage through a variety of additional mechanisms, including: 1) the activation of calcium-dependent proteases (e.g., calpains and caspases), which disrupt the axon's cytoskeletal filaments, thus impairing axonal transport and function;⁶³ 2) generation of ROS and nitric oxygen species (NOS), which result in OxS that damages membrane lipids, proteins, and DNA; and 3) mitochondrial impairment (caused by Ca^{2+} overload) and mitochondrial permeability transition pore formation, leading to apoptotic events.⁶⁴



3.2. Metabolic changes

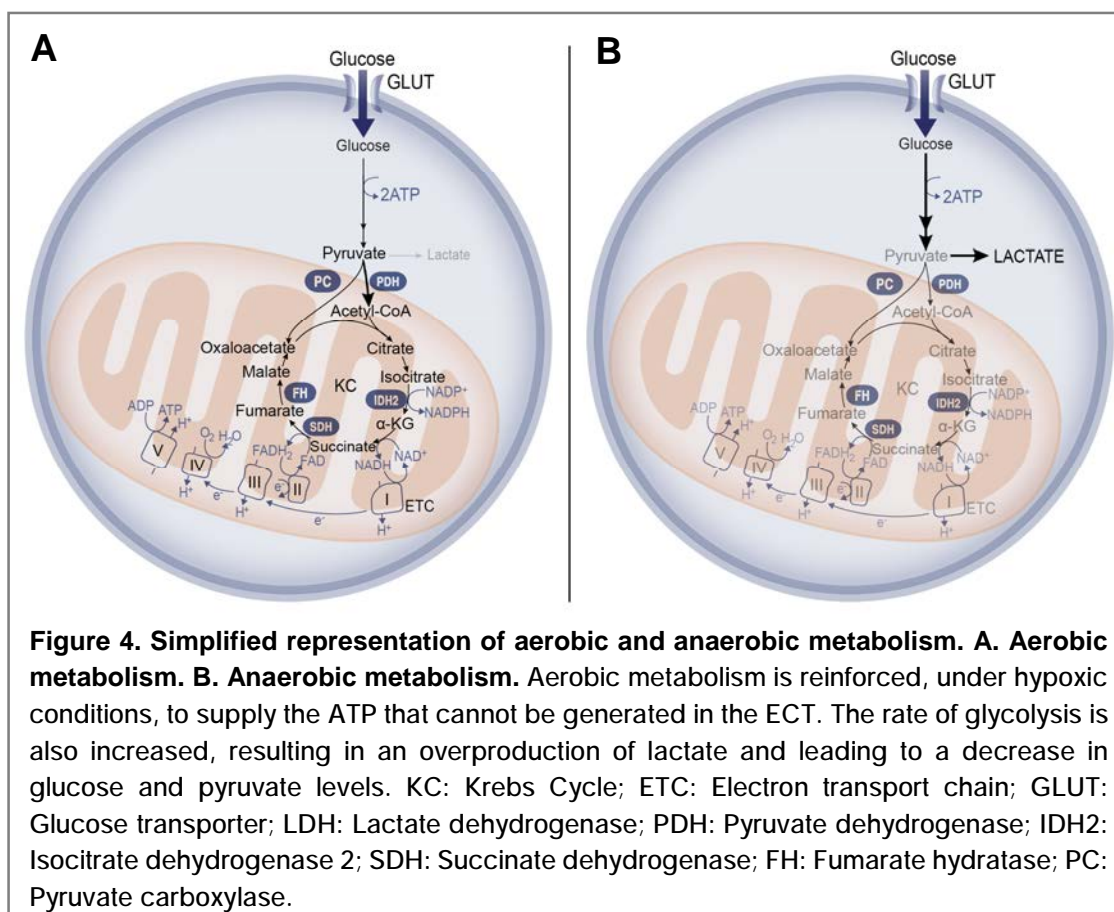
The brain is the organ with the highest energy needs. Although the brain comprises only 2-3% of the whole body weight, it uses up to 20% of the total energy

generated.^{66,67} Glucose is considered the major fuel for both neurons and astrocytes,⁶⁸ leading to higher glucose consumption in the brain compared with other organs of the body. Glucose metabolism supports different pathways with important functions in energy metabolism, such as neurotransmission, reduction-oxidation (redox) reactions, and biosynthesis of essential brain components with non-oxidative (glycolytic) and oxidative components.

In concert with the described changes in excitotoxicity and ionic flux, metabolic change occurs following TBI of all severities.⁶⁹ The energy metabolism of the brain requires a continuous supply of O₂ and glucose as well as normal mitochondrial function to produce sufficient energy (ATP). Under physiological conditions, the major part of the energy production by aerobic respiration takes place in the electron transport chain (ETC) through oxidative phosphorylation. However, after TBI, the energy metabolism can decrease due to ischemia caused by increased ICP and diminished CPP or due to the inability of mitochondria to use the available O₂.⁶⁷ Insufficient ATP synthesis leads to a deterioration of homeostatic mechanisms, an increase of intracellular Ca²⁺ concentration, and cell death.⁶⁷

A crucial event that triggers some metabolic dysfunction is the increase in the release of excitatory amino acids into the ECS following TBI injury, particularly glutamate.⁶⁹ The ionic influx that results from the dramatic rise in extracellular glutamate levels induces a marked increase in cerebral glucose consumption and a consequent accumulation of lactate, presumably to promote the reestablishment of ionic homeostasis. This condition is known as hyperglycolysis. The state of hyperglycolysis is also triggered in conditions of hypoxia, when anaerobic metabolism is reinforced to supply the ATP that cannot be generated in the ETC. In this scenario, pyruvate cannot enter the Krebs cycle (KC) and is diverted to the production of lactate to regenerate NAD⁺ molecules, resulting in a high production of lactate through the enzyme lactate dehydrogenase (LDH) (**Figure 4**). Hyperglycolysis is short-lived and can lead to a decrease in glucose levels in the ECS, a condition associated with poor outcome.^{70,71} Bergsneider et al. first detected post-traumatic hyperglycolysis in humans using positron emission tomography (PET), predominantly within the contusion and pericontusional regions.⁵⁵ This hypothesis is supported by an increased lactate production observed after TBI in animal models and humans, where maintained high lactate levels have been correlated with an unfavorable outcome.⁷⁰⁻⁷²

Increased lactate levels in the brain ECS can produce cerebral acidosis, increase the calcium-mediated intracellular damage, and decrease brain pH, thus harming the injured brain.⁶⁷ However, in the last decades, considerable controversy has emerged about the meaning of elevated ECS lactate levels.⁷³⁻⁷⁵



3.2.1. Brain ischemia Biomarkers: Lactate and the lactate-to-pyruvate ratio

Most clinical research on hypoperfused organs, including the brain, is based on the *"anaerobic threshold"* concept introduced by Wasserman and McIlroy in 1964.⁷⁶ According to this paradigm, increased lactate in any organ or in the blood is a direct consequence of tissue hypoxia. Under conditions of O₂ limitation, the inhibition of the respiratory chain produces insufficient ATP generation via oxidative phosphorylation and increases the mitochondrial and cytosolic pools of nicotinamide adenine dinucleotide (NADH). The increased mitochondrial [NADH]/[NAD] ratio inhibits the KC, leading to the accumulation of pyruvate and thus an increase in lactate production.⁷⁷

According to this theory, an increase in brain extracellular lactate levels (>2.0-4.0 mmol/L) in patients with acute brain injuries has been considered an indicator of increased anaerobic glycolysis and therefore brain hypoxia.^{12,78-80} Nevertheless, the lactate-to-pyruvate ratio (LPR) has been considered a more robust indicator of the anaerobic metabolism and the redox status of the tissue. The LPR has also been found to be an independent predictor of unfavorable outcome and mortality in TBI patients monitored with cerebral microdialysis (MD).⁸⁰ In TBI clinical research, lactate and LPR have been used as equivalent indicators of ischemic and non-ischemic brain hypoxia. However, in a recent study, we found poor agreement between the concentration of lactate and the LPR. We showed that lactate must be interpreted together with LPR to distinguish between anaerobic metabolism and aerobic hyperglycolysis.⁸¹

Metabolic alterations with increased lactate and LPR levels are frequently present in the absence of cerebral ischemia.^{79,80,82} This has confounded the discussion regarding brain metabolism impairment and the potential benefit of some therapies. Different studies offer alternative explanations for increases in lactate production that do not involve O₂ limitation.^{83,84} The conventional interpretation of high brain lactate levels was first challenged by Vespa et al., who showed that increases in lactate in TBI patients may indicate hyperglycolysis or metabolic crisis and not necessarily ischemia.⁸⁵ In severe TBI patients, Sala et al. observed that the increased lactate levels were predominantly associated with glycolysis, normal values of brain PtiO₂, and normal CBF or even a hyperemic brain.⁷¹ Recently, Patet et al. observed increased lactate levels during glucose depletion episodes associated with normal PtiO₂ values.⁸⁶ These studies on acute brain injuries concur with subsequent evidence indicating that lactate is a non-specific BM of increased glycolytic flux, but that the increase in glycolysis can have multiple etiologic factors other than tissue hypoxia.⁸⁷

The classical view of lactate as a waste product has changed toward a more important role as a fuel and signaling molecule. The main findings that lend support to this idea are that lactate accumulation does not correlate with the amount of metabolized glucose and that lactate infusion increases its utilization by the brain and has a glucose-sparing action.⁸⁸ Furthermore, there is growing evidence showing lactate to be a fuel used by neurons under aerobic conditions, which agrees with Pellerin and Magistretti's hypothesis of the astrocyte-neuron lactate shuttle (ANLS).⁸² They hypothesized that the activation of astrocytes by glutamate can convert glucose into

lactate, which is used by neurons via the KC. However, more *in vivo* studies are still needed to define the functional role of the lactate shuttle.

3.2.2. Mitochondrial dysfunction

Mitochondria generate most of their ATP from the transfer of electrons through respiratory complexes containing iron-sulfur (Fe-S), flavin, cytochromes, and ubiquinone centers in cytochrome c oxidase, where O₂ is reduced to H₂O. Mitochondria may play a key role in some of the metabolic alterations that have been observed in TBI. After a TBI, mitochondrial dysfunction can occur and cause a release of excessive ROS and decrease ATP production. Several lines of evidence support that cellular energetics are disturbed in TBI, not because of an inadequate brain O₂ supply, but rather due to an impaired mitochondrial function.

The following evidence suggests that mitochondrial dysfunction may be the cause of most described metabolic disorders: 1) The cerebral metabolic rate of oxygen (CMRO₂) is consistently low after severe TBI, possibly due to mitochondrial inhibition.⁸⁹ The possible impairment of mitochondrial respiration in patients with severe TBI was suggested in the 1980s when Obrist et al. showed that oxidative metabolism (and therefore CMRO₂) is reduced to half the normal levels in severe TBI in proportion to the depth of coma.⁹⁰ 2) Experimental and clinical evidence accumulated in recent years shows that brain energy metabolism is altered in TBI, even when O₂ is available but cells cannot use it. The term "cytopathic hypoxia" was coined to define these changes in mitochondrial respiratory function.⁹¹ This type of hypoxia is equivalent to the "histotoxic hypoxia" defined by Siggaard-Andersen.¹⁵ 3) Some studies have shown that even macroscopically normal brain tissue with normal or high PtiO₂ and no detectable intracranial or systemic insults may present severe metabolic alterations and increased extracellular lactate and LPR levels. Nelson et al. applied data mining techniques to MD data and found a weak relationship between ICP, CPP, and MD data, which did not explain the observed metabolic alterations.⁷⁶ They suggested that factors other than pressure or flow variables were the cause of metabolic dysfunction. 4) Mitochondrial swelling also occurs in the early stages of TBI, and 5) isolated mitochondria from experimental models and TBI patients present a significant decrease in respiratory rate and ATP production.

Experimental evidence confirms that mitochondria play a key role in metabolic dysfunction after TBI and contribute to post-traumatic neuronal death.⁹² However, the causes and consequences of the abnormalities remain poorly understood, and further studies are needed.⁹³ The following are some of the potential causes of mitochondrial failure:

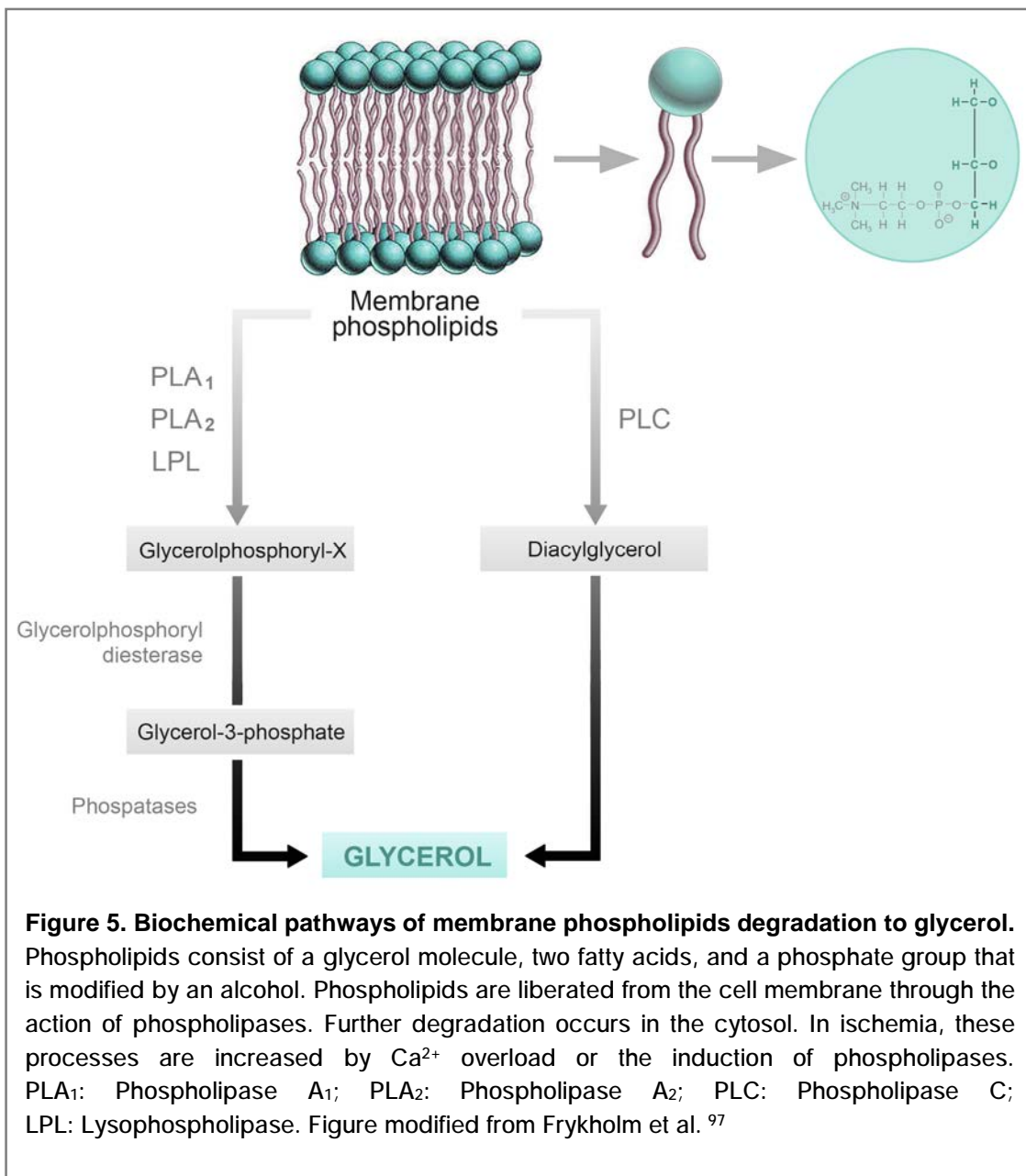
1. The inhibition of key mitochondrial enzymes. TBI is associated with NOS induction and thus increased production of nitric oxide (NO). In addition to its functions as a signal-transducing molecule, NO is implicated in cytotoxic processes due to its ability to interfere in cell energy metabolism by reversibly inhibiting the enzymatic activity of the terminal complex of the mitochondrial ETC Complex IV or cytochrome *a₃-b*.⁹¹ This inhibition is based on the competition between both O₂ and NO for the same binding site on Complex IV. In addition, NO reacts with superoxide radicals (O₂⁻) to form peroxynitrite (ONOO⁻). ONOO⁻ causes an irreversible inhibition of mitochondrial respiration by blocking Complexes I, III, and V⁹¹ and blocking aconitase, the enzyme that converts citrate into isocitrate in the KC.⁹⁴

2. The reduction of pyruvate delivery to the KC due to the inhibition of the pyruvate dehydrogenase (PDH) enzyme. PDH catalyzes the reaction in which pyruvate is converted to acetyl-coenzyme A. This enzyme is tightly regulated by both end-product inhibition and reversible phosphorylation. Inactivation of PDH, even with sufficient O₂, limits the flux of the substrate through the KC and causes pyruvate accumulation, leading to an increased production of lactate.

3. The activation of the enzyme poly-ADP ribose polymerase-1 (PARP-1). PARP-1 is a nuclear enzyme that participates in the repair of breaks in nuclear DNA. ROS can induce breaks in nuclear DNA, thus activating PARP-1. During its activity, it depletes the NAD⁺/NADH content of cells and impairs O₂ utilization to support the synthesis of ATP, causing a type of histotoxic hypoxia. It has been shown that this enzyme activation may be mediated by the presence of inflammatory mediators.⁹⁵ *In vitro* studies showed that incubation of cells with cytomix (a cocktail of 3 pro-inflammatory cytokines) decreased cellular O₂ consumption by >50%. However, if the cytokines are washed away and the cells are incubated in normal culture medium, this phenomenon can be reverted.⁹⁵

3.3. Phospholipid membrane degradation

Failure of cellular metabolism results in the disruption of cell membrane function, which leads to an intracellular influx of Ca^{2+} , activation of phospholipases, and ultimately the degeneration of cell membranes.⁹⁶ This results in the release of phospholipids, free fatty acids, and glycerol (an integral component of the cell membrane) into the brain ECS (**Figure 5**).



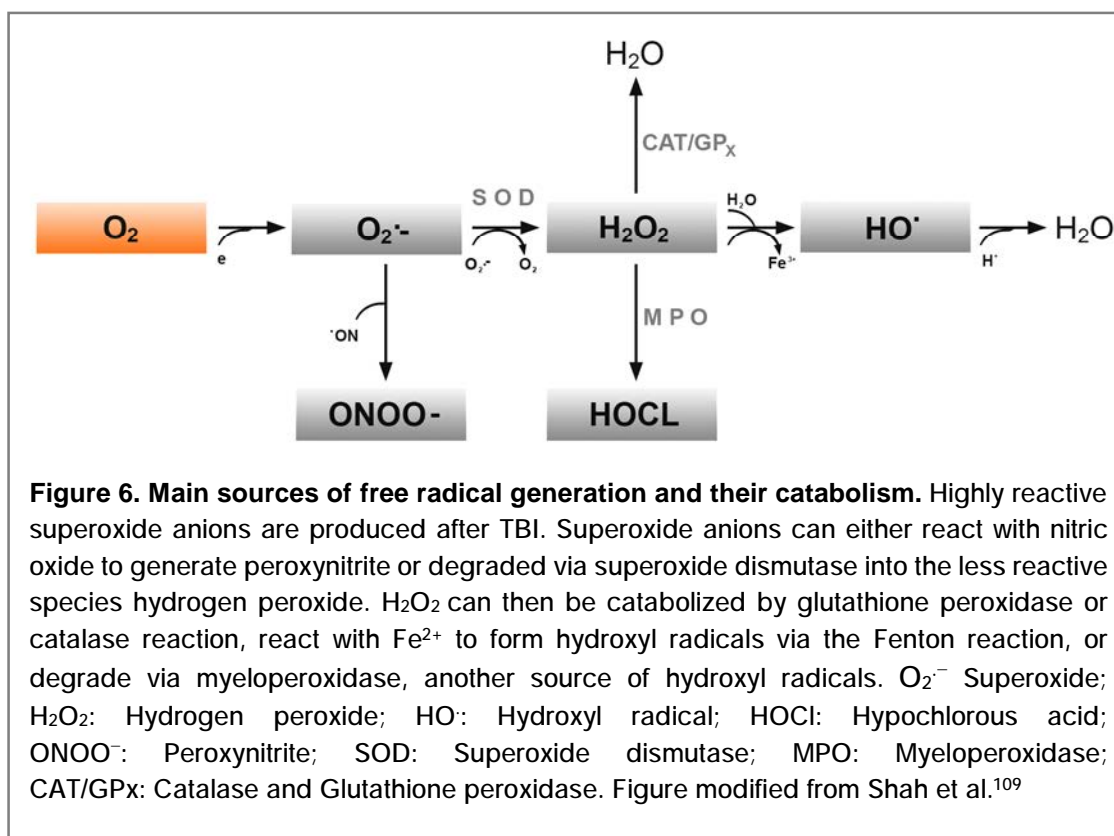
Glycerol has been demonstrated as a sensitive and reliable marker of cell damage in cerebral ischemia.⁹⁸ Several researchers have studied the relationship between glycerol and patient outcomes. Increased levels of ECS glycerol have been found in SAH patients,^{98,99} MMCAI patients,^{98,99} and TBI patients. The role of brain tissue glycerol after TBI is still under debate. Marklund and colleagues monitored the interstitial levels of glycerol ([Gly]_o) in a weight-drop model in rats and found a pronounced increase in [Gly]_o following injury.¹⁰⁰ As a consequence, they proposed using [Gly]_o as a BM of membrane phospholipid degradation after TBI. Stahl et al. observed an increase in cerebral [Gly]_o after severe TBI.¹⁰¹ They later reported the recovery of elevated [Gly]_o in the penumbra of a traumatic subdural hematoma after evacuation.¹⁰² Peerdeman et al. also observed an increase in cerebral [Gly]_o in TBI patients.¹⁰³ However, no correlation was found between glycerol and patient outcomes or adverse secondary episodes (low CPP, high ICP, arterial hypocapnia, low arterial O₂ saturation, and hyperthermia).¹⁰³ Clausen et al. reported similar data.¹⁰⁴ In general, information about [Gly]_o in patients with severe head injury is still rather scarce. Additional studies are needed to shed more light on the pathophysiological role of this parameter after TBI and to make a final assessment regarding the parameter's clinical value.¹⁰⁴

3.4. Oxidative stress and isoprostanes

The term OxS essentially refers to a serious imbalance between the production of reactive species (RS) and the antioxidant defenses that favors RS accumulation.¹⁰⁵ Free radical species contain unpaired electrons in their atoms that are responsible for their reactivity. Numerous experimental reports suggest that a prominent secondary injury mechanism after TBI is the increased production of ROS and reactive nitrogen species (RNS), which overwhelm the endogenous defense systems and lead to OxS and secondary cell damage.¹⁰⁶ ROS and RNS are the main sources of OxS in brain injury. ROS includes O₂⁻, hydroxyl radical (HO·), hydrogen peroxide (H₂O₂), and hypochlorous acid (HOCl). RNS refer to various NO-derived compounds, such as ONOO⁻ and nitrogen dioxide (NO₂). Many enzymes are involved in free radical generation, including the NADPH oxidase family, inducible nitric oxide synthase (iNOS), endothelial nitric oxide synthase (eNOS), cytochrome P450 (CYP450), cyclooxygenase (COX), lipoxygenase (LOX), and xanthine oxidase (XO).

The most common and damaging free radical in TBI is $O_2^{\cdot-}$, which is produced when oxygen molecules gain an electron from other molecules. $O_2^{\cdot-}$ causes tissue damage by promoting hydroxyl radicals from H_2O_2 and peroxynitrite when combined with NO. H_2O_2 is a relatively stable molecule, and it is formed by dismutation of superoxide radicals through the superoxide dismutase (SOD) enzyme. It is generated from nearly all sources of OxS and can diffuse freely in and out of cells and tissues. It impairs cell proliferation and induces cell death by apoptosis or necrosis. H_2O_2 can also be converted to other free radicals through different enzymatic reactions, as shown in **Figure 6**.

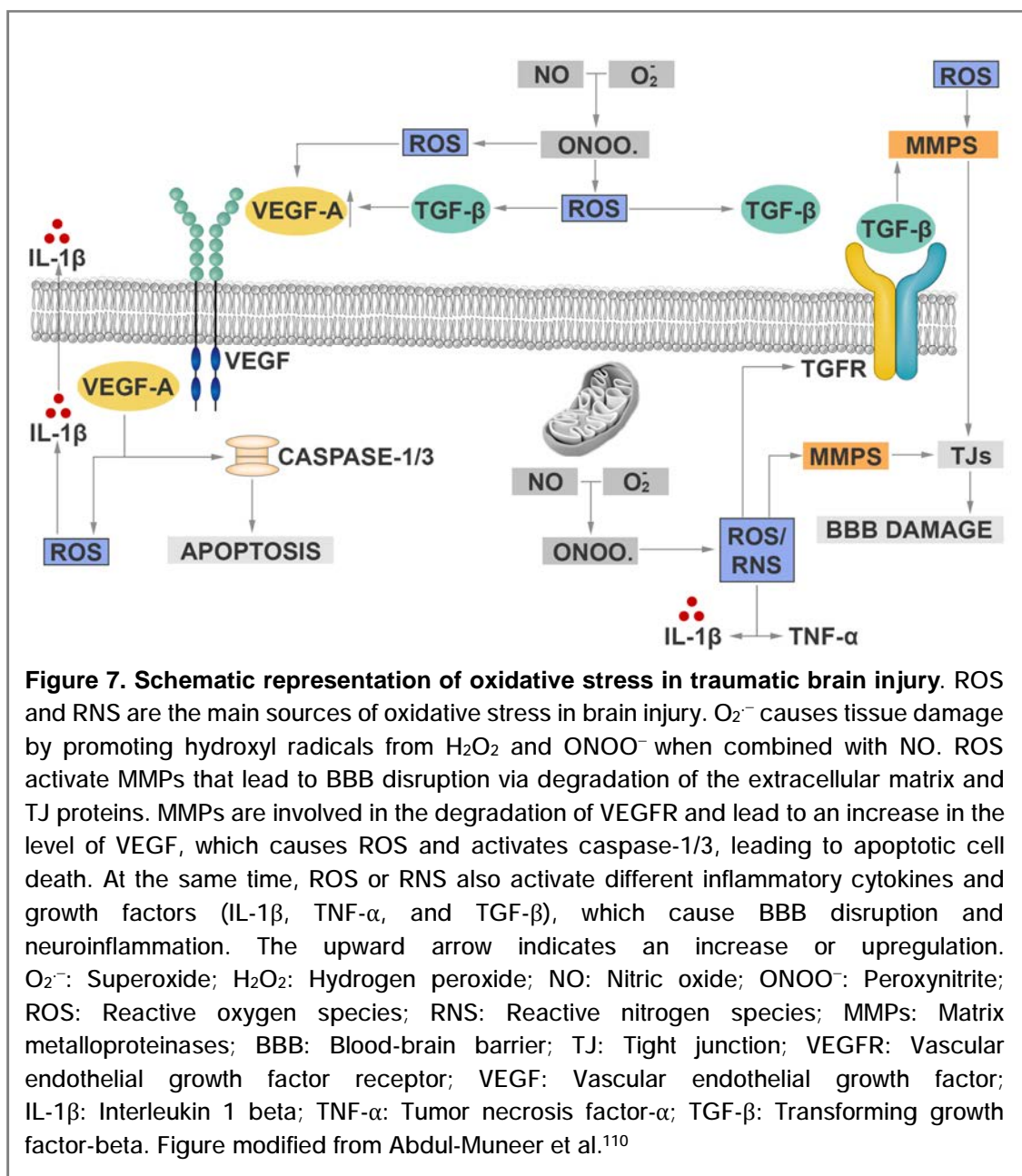
Under physiological conditions, ROS and free radicals are always present at low levels in neuronal cells. There is a considerable increase in their production after a TBI, supporting the idea that OxS plays a decisive role in this pathology.^{107,108} Secondary injury by OxS is related to the destructive actions of high levels of ROS and free radicals following TBI. Both the formation of ROS and free radicals and their injurious effects are closely linked to apoptosis, excitotoxicity, and inflammation, although the full extent of these interactions is still not fully understood.⁴⁶



The production of free radicals can be induced through different pathways: 1) High intracellular Ca^{2+} concentrations resulting from glutamate excitotoxicity upregulate the expression of several enzymes that catalyze the production of free radicals (eg., NOS, XO). 2) Inflammatory cells may release deleterious compounds that exacerbate the oxidative damage to metabolically compromised neurons. Both mechanisms are closely related to mitochondrial dysfunction and thus metabolic disorders. 3) The increase in intracellular Ca^{2+} alters mitochondrial membranes, which disrupts the ETC and allows leakage of electron-reduced oxygen intermediates. 4) Local acidosis and interaction between NO and superoxide radicals releases ONOO^- , which is one of the most damaging free radical species. 5) Apoptotic signaling molecules may further increase ROS generation within mitochondria and participate in permeabilization of the outer mitochondrial membrane.⁴⁶

When levels of these free radicals are sufficient to overwhelm the cellular mechanisms designed to protect against oxidative damage (e.g., SOD, catalase, glutathione peroxidase), the resultant stress causes peroxidation of cell membranes, protein and DNA oxidation/nitration, and inhibition of the mitochondrial ETC.⁴⁶ These mechanisms can contribute to neuroinflammation, early or late apoptotic programs, and immediate cell death.¹¹¹ Specifically, ROS directly downregulates proteins of tight junctions (TJs) and indirectly activates matrix metalloproteinases (MMPs) that further lead to BBB disruption and to amplification of the neuroinflammatory response. In addition, OxS directly activates pro-inflammatory cytokines and growth factors, such as interleukin 1 beta ($\text{IL-1}\beta$), tumor necrosis factor- α ($\text{TNF-}\alpha$), and transforming growth factor-beta ($\text{TGF-}\beta$), or indirectly by activating MMPs. MMPs induced the degradation of endothelial vascular endothelial growth factor receptor-2 (VEGFR-2), which leads to an elevation of cellular/serum vascular endothelial growth factor (VEGF) level inducing apoptosis and neuroinflammation via the activation of caspase-1/3 and $\text{IL-1}\beta$ release¹¹¹ (**Figure 7**).

OxS within injured cells can become self-propagating.⁴⁶ When modified through tyrosine nitration, SOD becomes inactive, leading to further OxS and tissue damage. Additionally, numerous inflammatory mechanisms are activated under OxS, and proinflammatory cytokines activate cyclooxygenase and stimulate the eicosanoid cascades. The net result of these additional processes is increased production of ROS, leading to a cycle of increasing potential for oxidative damage.¹¹²

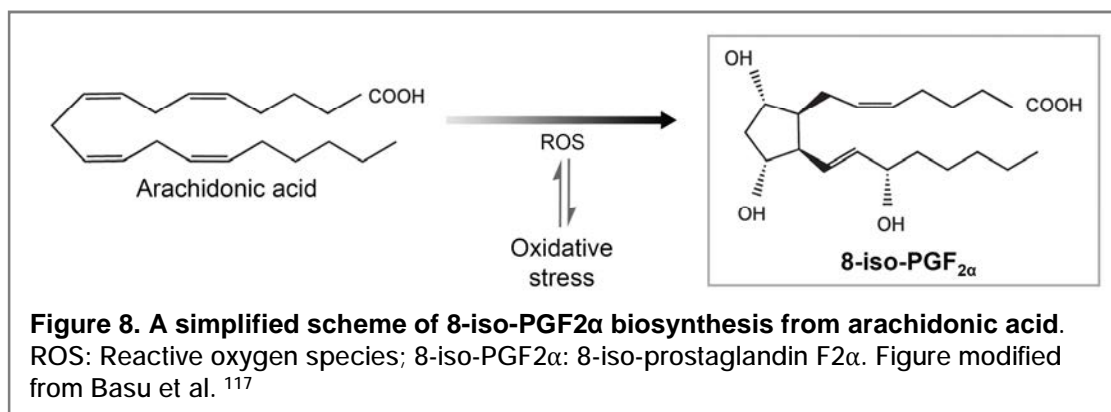


Isoprostanes as biomarkers of oxidative stress

Biochemical BMs can be analyzed from serum, whole blood, cerebrospinal fluid (CSF), and the ECS by MD. They can also reveal structural brain damage and are also markers of secondary injury cascades. The detection of oxidatively modified biomolecules could be used as BMs to indicate the extent of cellular damage or changes in the cascade of secondary brain damage and repair.¹¹³ The short half-life of ROS makes direct measurement virtually impossible in a clinical setting, and therefore, several indirect approaches have been used for estimation. ROS can be

measured either directly or indirectly based on the formation of oxidative by-products of lipids, proteins, or nucleic acids. Mendes-Arent et al. recently reviewed the BMs most commonly used to study the impact of OxS in TBI.¹¹⁴

Isoprostanes are stable products of the peroxidation of arachidonic acid (polyunsaturated omega-6 fatty acid) in both animals and humans. They are regarded as one of the most reliable BMs of OxS *in vivo* and thus provide a valuable tool for exploring the role of OxS in the pathogenesis of human brain injuries. The *Biomarkers of Oxidative Stress Study (BOSS)*, a recent multi-investigatory study sponsored by the National Institute of Health, found that the most accurate method to assess the OxS status *in vivo* is the quantification of F2-isoprostanes.^{115,116} One of the most studied isoprostanes, 8-iso-PGF₂α, is overproduced in diverse disorders such as atherosclerosis, rheumatoid arthritis, hypertension, and Alzheimer's disease, which are pathologies associated with OxS.^{116,117} 8-iso-PGF₂α is considered the gold standard for measuring OxS *in vivo*.^{114,118-120} A simplified schematic formation of 8-Iso-PGF₂α is shown in **Figure 8**.



8-iso-PGF₂α is a stable and robust molecule that is detectable in all human tissues and biological fluids, including plasma, urine, CSF, and MD. Due to their low molecular weight (< 5000 Da), isoprostanes can be analyzed by MD and can therefore be used as BMs of OxS in patients with TBI. Isoprostanes can be measured using different analytical methods, including gas chromatography-mass spectrometry (GC-MS), liquid chromatography-mass spectrometry (LC/MS), radioimmunoassay, and enzyme immunoassays. However, LC/MS is the optimal method, which has advantages of high

sensitivity, specificity, and the possibility of analyzing small volumes of biological fluids.¹²¹

Increased 8-iso-PGF2 α levels have been observed in the interstitial tissue of the brains of TBI patients. This product has been identified as a BM of OxS after severe human TBI,¹¹⁸ suggesting that 8-iso-PGF2 α may represent a BM of neurological injury. 8-iso-PGF2 α in blood or CSF has been used as an indicator of OxS in cerebral ischemia/reperfusion in a porcine cardiac arrest model and in cardiac arrest patients,¹²² as well as in CSF of pediatric and adult TBI patients.^{123,123} Furthermore, recent studies have correlated plasma levels of 8-iso-PGF2 α with the GCS score and showed that it is a good predictor of mortality and outcome with similar sensitivity to the GCS.^{118,119}

3.5. Cerebral edema

3.5.1. Brain volume regulation

In mammals, the central nervous system (CNS) contains four distinct fluid compartments: 1) the blood in the cerebral vasculature, 2) the CSF in the ventricular system and subarachnoid space, 3) the interstitial fluid that bathes cells of the brain parenchyma (ECS), and 4) the intracellular fluid (ICS) contained within neurons and glia.⁵³ Each compartment has a specific volume and a different solute composition. These four compartments are separated from one another by specialized cellular barriers that permit the selective flow of solutes and water from one compartment to another: 1) the BBB, 2) the blood-CSF barrier, and 3) the plasma membranes of glia and neurons.

The brain is contained in an inelastic skull that makes it possible for small changes in total brain volume to increase ICP rapidly. This can lead to brain herniation, irreversible damage of neural structures, neurological injury, and ultimately death. Minor changes in the composition of ions in the brain's extracellular or intracellular fluids can significantly affect the function of neurons, which rely on precise ion gradients across their plasma membranes to induce changes in membrane potential that underlie action potential generation and propagation. Therefore, the transport of water and ions

through the different barriers is tightly regulated by complex regulatory mechanisms, including water channels (aquaporins) and the different families of ion channels integrated into the cell membrane.⁵³

Over 70% of the water in the CNS is contained in the ICS. Compared with the ECS and the CSF, the ICS has a much higher level of K^+ and a much lower level of Na^+ and Ca^{2+} . Under physiological conditions, the maintenance of the ECS-ICS electrochemical gradients can be balanced by energy-dependent ion pumps such as Na^+K^+ -ATPase and Ca^{2+} -ATPase. Na^+K^+ -ATPase prevents the intracellular accumulation of Na^+ ions, thus preventing the influx of solutes and water that would result in cell swelling, the associated loss of cytoskeletal integrity, and oncotic cell death. The activity of the Na^+K^+ -ATPase also generates the electrochemical gradients necessary for secondary active and passive ion transport processes.⁵³

In most cells, water is in thermodynamic equilibrium across the plasma membranes. As a result, the osmotic concentration of cytoplasmic and extracellular fluids is equal under steady-state conditions. Because cell membranes are freely permeable by water, changes in the intracellular or extracellular content of solutes establish transmembrane osmotic gradients that result in the bidirectional flow of water across cells. This movement of water continues until thermodynamic equilibrium is achieved. As a result, transmembrane osmotic gradients trigger the flow of water, which causes cell swelling or shrinkage.

In 1896, Starling formulated the equation that regulates the osmotic movements through the BBB and therefore the basic physiology of cerebral edema. This equation describes the role of hydrostatic and osmotic forces in the movement of water through the capillary endothelial cells: $J_v = K_o(\pi_i - \pi_c) + K_H(P_c - P_i)$.¹²⁴ The flow of fluid (J_v) coming out or entering through the BBB is defined by the factors included. According to this equation, water flow depends on the capillary hydrostatic pressure (P_c), interstitial hydrostatic pressure (P_i), capillary osmotic pressure (π_c), and interstitial osmotic pressure (π_i). Additionally, the equation includes two filtration coefficients that range from 0 to 1 and define the hydraulic conductivity (K_H) and the osmotic conductivity (K_o).¹²⁴

3.5.2. Types of cerebral edema

TBI and IS causes a variable disruption of ionic homeostasis and massive ionic fluxes with subsequent osmotic water movement across the cells. Changes in ionic concentrations induce water accumulation in the intracellular and in the interstitial space, as well as cause brain edema and structural deformation of the damaged brain tissue.¹²⁵ Brain edema is the most frequent cause of neurological worsening and death in patients with severe TBI and malignant IS. It is characterized by an abnormal accumulation of fluid in the parenchyma, which results in a volumetric enlargement of cells or tissue. In these patients, osmotherapy is a first line therapy for managing increased ICP. Osmotic agents (mannitol and hypertonic saline solutions (HTS)) are used because they are maintained within the intravascular compartment and are excluded from the brain ECS via the BBB. However, whether the BBB is tight or leaky can dramatically change the effects of the osmotic solutions on the brain and its effects on ICP.

Since Klatzo proposed the original classification of cerebral edema in 1967, relatively little progress has been made in the molecular basis underlying cerebral edema. Klatzo specified two categories of cerebral edema based on the location of the water increase in the brain and the integrity of the BBB: vasogenic and cytotoxic edema.¹²⁶ In the last decade, Simard et al. has significantly redefined the basics of cerebral edema. In 2007, they introduced a new classification that is applicable to cerebral ischemia and many traumatic brain injuries that behave as ischemia, especially in post-traumatic brain contusions (PTBCs). This classification includes the following types of edema: 1) cytotoxic, 2) ionic, and 3) vasogenic. In this new model, late hemorrhagic reperfusion is considered as a terminal phase of vasogenic edema, in which the BBB is structurally damaged and blood cells pass into the ECS¹²⁷ (**Figure 9**). This change of perspective can help explain the new contributions of molecular biology to the comprehension of the pathophysiology and in the identification of new channels that participate in the water exchange between the different CNS compartments.

Cytotoxic edema

Cytotoxic edema is a premonitory process that involves oncotic cell swelling due to the movement of osmotically active molecules from the ECS to the ICS (principally Na^+ , Cl^- , and water).¹²⁶ The key element in the formation of cytotoxic edema is the intracellular accumulation of Na^+ . This ion is usually more highly concentrated in the ECS than in the ICF due to the selective permeability of the plasma membrane and the activity of the Na^+ - K^+ -ATPase. However, ischemia triggers changes in the permeability of the cell membrane and makes it more permeable to the passage of Na^+ . Cl^- and water passively follow the influx of Na^+ to maintain both electrical and osmotic neutrality. In cytotoxic edema, there is no added component of the intravascular space, and therefore there is no accompanying increase in the total brain volume in the early stages. According to Simard's definition, cytotoxic edema is the *primus movens* that generates the necessary conditions for the formation of ionic and vasogenic edema that causes the increase in brain tissue volume.^{53,127}

Under physiological conditions, the selective impermeability of the membrane to Na^+ and the energy-dependent ion pump Na^+ - K^+ -ATPase prevent the intracellular accumulation of Na^+ ions (**Figure 9A**). However, under pathological conditions, movements of osmotically active molecules into neurons and glial cells can occur by 1) passive transport through ion channels, 2) primary active transport through ionic pump transport (e.g., ATP-dependent, Na^+ - K^+ -ATPase), or 3) secondary active transport through cotransporters (e.g., Na^+ / K^+ / Cl^- cotransporters).¹²⁷

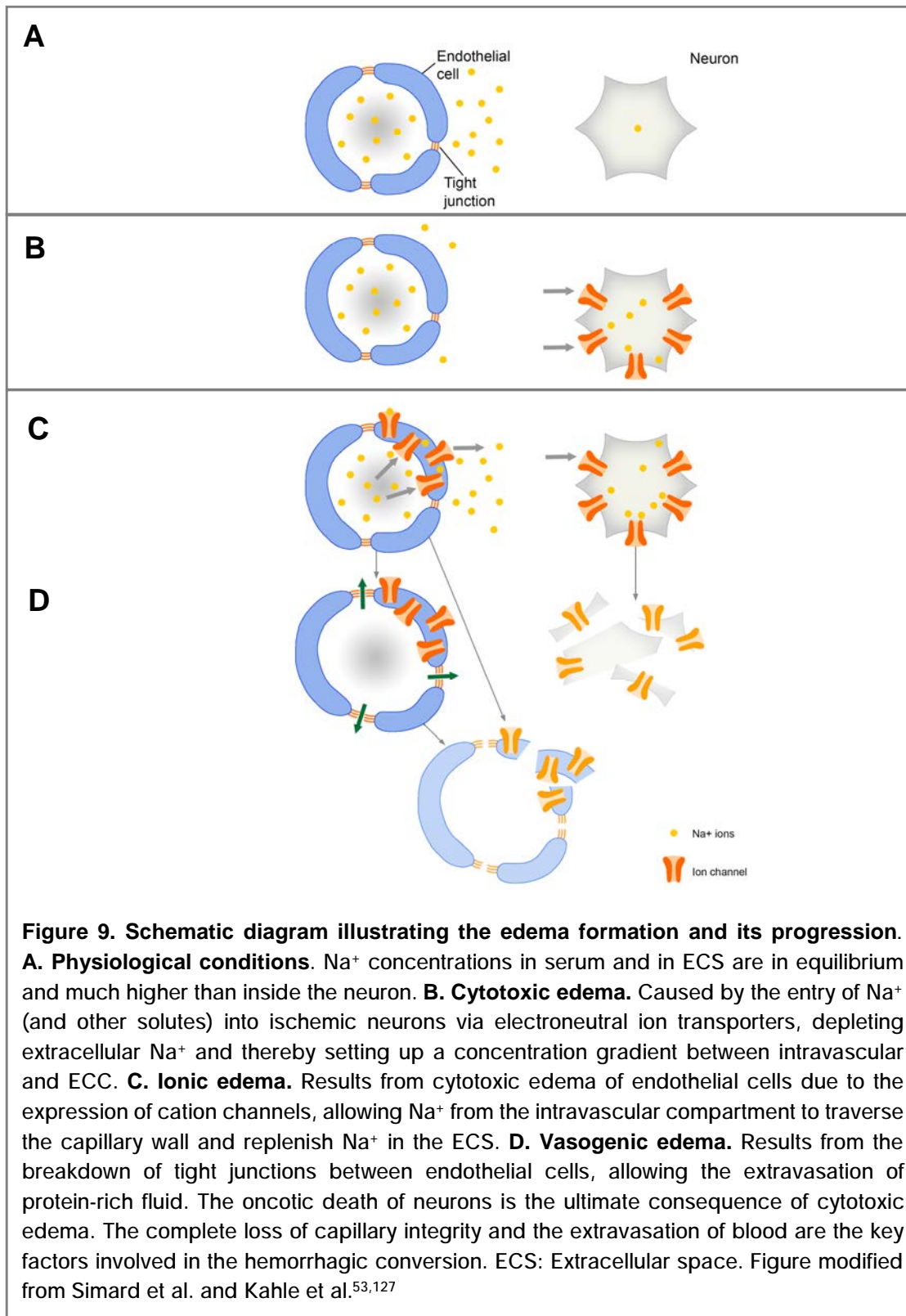
Apart from constitutively expressed pathways usually found in all the cell membranes (aquaporins, Na^+ and K^+ channels, etc.), specific non-selective cation channels that are up-regulated by ischemia or oxidative stress may provide new pathways for Na^+ influx. Transient receptor potential channels¹²⁸ and the sulfonylurea receptor1/transient receptor potential melastatin 4 (SUR1/TRPM4) ion channel^{129,130} can act in this manner. The SUR1-TRPM4 channel is transcriptionally upregulated within the first hours of ischemia. Simard and colleagues identified the crucial role of this ion channel in the formation of brain edema in experimental models of ischemic lesions, spinal cord injuries, and PTBCs.^{127,131} Opening this channel by depletion of ATP allows Na^+ to enter cells and creates an osmotic force that drives the influx of water. This can cause cell depolarization, cell blebbing, cytotoxic edema, and oncotic cell death, all of which are partially or completely prevented by blocking this channel^{127,132} (**Figure 9B**).

Ionic edema

The movement of ions and water into the cells during the stage of cytotoxic edema induces a reduction of Na⁺ concentration in the ECS.^{53,127} This reduction facilitates the passage of ions from the intravascular space to the ECS. Principally, the transport of Na⁺ across the BBB is carried out by 1) the Na⁺/K⁺/Cl⁻ cotransporter located in the luminal part of the capillary endothelium,¹³³ 2) the Na⁺-K⁺ abluminal pump, and 3) the SUR1/TRPM4 channel.^{129,130} The formation of ionic edema involves the transport of Na⁺ across the BBB, which generates an electrical gradient for Cl⁻ and an osmotic gradient for water. The depletion of Na⁺ in the ECS is followed by a replenishing Na⁺, Cl⁻, and water in the extracellular space from the intravascular space¹³⁴ (**Figure 9C**). In this phase, the structural integrity of the BBB is still maintained, capillary TJs are preserved, and macromolecules are excluded from brain parenchyma.¹²⁷

Vasogenic edema

Vasogenic edema is a consequence of the destruction of the TJs and/or the membrane of the endothelial cells (BBB disruption), with leakage of plasma proteins into ECS¹²⁷ (**Figure 9D**). Several mechanisms have been proposed to account for changes in permeability of the BBB, that give rise to vasogenic edema: 1) endothelial cell rounding or retraction with formation of interendothelial gaps; 2) the loss of structure of TJs; 3) enzymatic degradation of basement membrane; 4) reverse pinocytosis; 5) disruption of Ca²⁺ signaling;¹³⁵ and 5) several ischemia-induced factors. Ischemic processes involved in BBB disruption include: thrombin-induced cell retraction,¹³⁶ expression of VEGF and MMPs. VEGF disrupts the physical integrity of endothelial TJs and promotes the formation of vasogenic edema. Furthermore, VEGF promotes the activity of MMP-9 that contributes to the degradation of the basement membrane compromising the structural integrity of the capillaries.^{137,138} Once the integrity of the BBB is lost, capillaries behave like fenestrated capillaries, and the hydrostatic and osmotic pressure gradients contribute to edema formation. Determinants of hydrostatic pressure, including systemic blood pressure and intracranial pressure, now assume an important role, due to secondary changes in the capillary hydrostatic pressure.¹²⁷



Hemorrhagic conversion

The hemorrhagic transformation of edematous brain tissue constitutes the final stage of any type of ischemic edema in which blood flow is restored¹³⁹ or in cases of post-traumatic edema in which there is a disruption of the BBB and an increase in capillary hydrostatic pressure. This phase is marked by the catastrophic failure of capillary integrity, during which all constituents of blood extravasate into the brain parenchyma, including erythrocytes.¹³⁹ The severity of hemorrhage can range from a few petechiae to a large hematoma with a space-occupying effect.¹⁴⁰ Hemorrhagic conversion is probably a multifactorial problem due to reperfusion injury and OxS.¹²⁷ Mechanisms may include plasmin-generated laminin degradation, endothelial cell activation, transmigration of leukocytes through the vessel wall, and other processes related to vasogenic edema.¹²⁷ Of those involved in the previous phase, it is important to highlight those that contribute to the disruption of BBB: VEGF,¹⁴¹ MMP-9,^{137,139} and the SUR1/TRMP4 channel, which mediates the oncotic death of endothelial cells (**Figure 9D**).

3.6. Brain tissue hypoxia

For both clinicians and researchers, brain ischemia has been a primary focus in most secondary lesions occurring in patients with severe TBI. In 1978, Graham et al. raised awareness about the high frequency of ischemic lesions in patients who died from TBI, and in the 1980s, the same group confirmed that ischemic brain damage remained highly prevalent in these patients.^{3,4} Clinical studies published in the 1990s showed that a significant reduction in CBF occurs in many patients during the early stage following TBI, which correlates with early post-traumatic hypoperfusion, ischemia, and a poor neurological outcome. With this evidence, all therapies have been classically directed toward the management of CBF.^{142,143}

In any organ, hypoxia is defined as the reduction of tissue oxygenation to insufficient levels for the maintenance of cellular metabolism and function. The lack of a widely accepted operational definition of "cerebral ischemia" has caused confusion in the debate about the role of ischemic hypoxia. Most studies consider the term "cerebral hypoxia" to be synonymous with "ischemic cerebral hypoxia" or ischemia, a

phenomenon that occurs after a global or regional reduction in partial oxygen pressure (PO_2) or CBF. Sigaard-Andersen introduced the first systematic classification of tissue hypoxia and used the term "ischemic hypoxia" in only situations where there is a reduction in CBF that is uncoupled with a reduction in tissue O_2 consumption.^{15,144}

Although ischemia is a frequent cause of tissue hypoxia, various experimental models and clinical studies have shown that there are multiple causes of non-ischemic tissue hypoxia.^{15,85} The variability in the reported incidence of these phenomena is due in part to the different thresholds used to define the normal range for P_{tiO_2} . Moreover, it is well established that non-ischemic causes of tissue hypoxia are probably more frequent than ischemia induced by reductions in CPP/CBF.

3.6.1. Classes of tissue hypoxia

There are different causes of tissue hypoxia in the brain, and differential diagnosis is essential.¹⁴⁵ The real availability of O_2 in the tissue depends on different variables: PO_2 , the hemoglobin (Hb) concentration, the affinity between Hb and O_2 , the CBF, the number of functioning capillaries and the O_2 diffusion through the cell membrane and the characteristics of the ECS.¹⁴⁶ Apart from all these factors, O_2 metabolism depends on the O_2 reduction in the mitochondria. A failure in one or more of these factors can show similar clinical manifestations, making it difficult to perform a differential diagnosis. Continuous brain P_{tiO_2} monitoring, combined with the information provided by hemometabolic variables, can help to establish the etiology of tissue hypoxia. In **Table 2**, the classes of tissue hypoxia and the monitoring profiles are summarized. This classification is a modification published by our group of the Sigaard-Andersen classification.³⁶

The term, 'oxygen extractivity' was coined by Siggaard-Andersen et al. to define the capacity of the arterial blood that allows the tissues to extract the arbitrary amount of 52 mL/L from the arterial blood without a decrease in arterial oxygen tension below the usual venous tension (~ 38 mmHg).^{15,144} Similarly to the half-saturation tension (P_{50}) the oxygen extraction tension (P_x) is a variable that indicates the extractivity and it's an indicator of the oxygen reserve of the arterial blood.^{15,144} Following this line of thought, 'low extractivity' hypoxia was a new concept introduced by Siggaard-Andersen to

include three potential causes of hypoxia: hypoxic hypoxia, anemic hypoxia and high-affinity hypoxia (low P_{50}). It has been shown that a moderately low alkalosis combined with hypothermia and moderate anemia— that is frequent in ventilated patients with TBI —may contribute significantly to a reduced release of O_2 to the brain.^{15,144,145}

MNM —including P_{tiO_2} and MD monitoring—, are widely used in neurocritical care units, allowing for the quasi-continuous profiling of brain oxygen supply and brain metabolism.^{146,147} Data provided by these tools have cast doubt on the predominant role of brain ischemic hypoxia (reduced CBF uncoupled with $CMRO_2$) in the pathophysiology of TBI.

Table 2. Summary of the main characteristics of types of tissue hypoxia

Hypoxia type	Primary disturbance	Monitoring profile				
		SjvO ₂ (%)	PtiO ₂ (mmHg)	P ₅₀ (mmHg)	P _x (mmHg)	LPR
Ischemic	↓CBF	↓	≤15	24-29	N	↑ (↑L - ↓P)
Low extractability	- Hypoxic Hypoxia	↓	≤15	24-29	↓	↑ (↑L - ↓P)
	- Anemic Hypoxia	↓	≤15	24-29	↓	
	- High affinity hypoxia	↑	≤15	<24	↓	
Shunt	Arterio-venous shunts	N/↑	≤15	24-29	N	↑ (↑L - ↓P)
Dysperfusion	O ₂ diffusion alteration from Hb to the mitochondrion	N/↑	≤15	24-29	N	↑ (↑L - ↓P)
Histotoxic	Inhibition of cytochromes	N/↑	N	24-29	N	↑ (↑L - ↓P)
Uncoupling	Uncoupling between O ₂ reduction and ATP formation	N/↑	N	24-29	N	↑ (↑L ↔ P)
Hypermetabolic	Increase in energy metabolism	↓	≤15	24-29	N	↑ (↑L - ↓P)

Hb: Hemoglobin; N: Within the normal range; SjvO₂: Jugular venous oxygen saturation; PtiO₂: Brain tissue oxygen pressure; P₅₀: O₂ pressure at which Hb is 50% saturated; P_x: O₂ extraction pressure; LPR: Lactate-to-pyruvate ratio; L: Lactate; P: Pyruvate. Table modified from Sahuquillo et al.¹⁴⁶

3.6.2. Molecular adaptation to hypoxia

During short durations of mild hypoxia, the brain develops adaptive mechanisms that allow it to maintain normal physiological conditions. Several molecular pathways have

recently been shown to mediate hypoxia sensing at the cellular and molecular levels. Hypoxia-inducible factor-1 (HIF-1) is the most significant transcription factor that regulates adaptive responses to the lack of oxygen in mammalian cells.¹⁴⁸

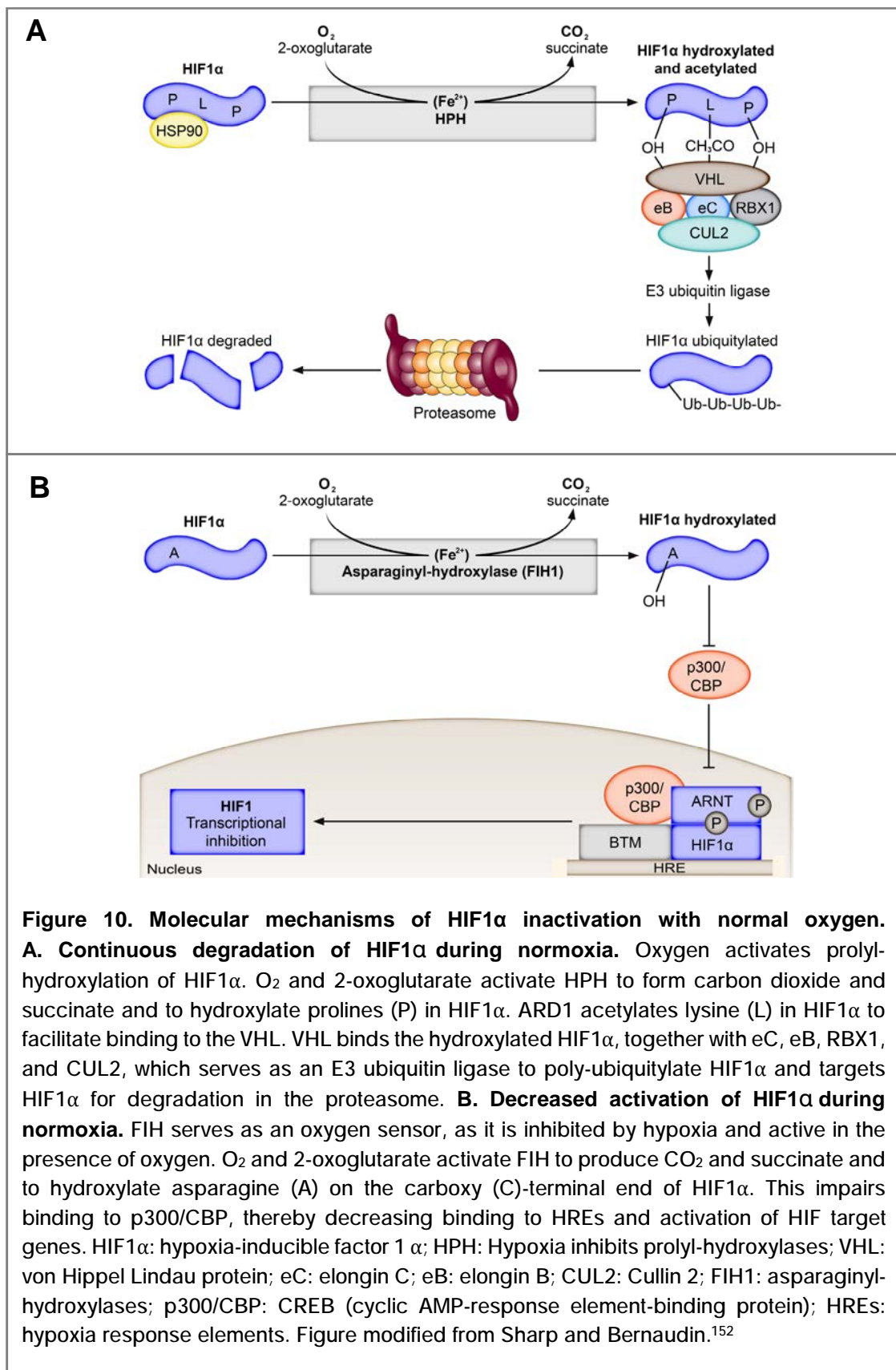
HIF1 consists of two subunits, HIF1 α (120 kDa) and HIF1 β (91–94 kDa), which are basic helix-loop-helix proteins containing a PAS domain (PAS family). HIF1 β (ARNT) is expressed constitutively in all cells and does not respond to changes in oxygen tension. However, it is essential for hypoxia-induced transcriptional changes mediated by the HIF1 heterodimer.^{149,150} In the brain, HIF1 α expression seems to be induced by hypoxia in neurons, astrocytes, ependymal cells, and endothelial cells.^{148,151} HIF1 α includes a bHLH domain near the amino (N) terminal, which is essential for DNA binding to hypoxia-response elements (HREs) in the HIF target genes. There are two transcriptional activation domains in HIF1 α , which are referred to as the N-terminal activation domain and the carboxy (C)-terminal activation domain. Between these two domains is the oxygen-dependent degradation domain (ODD).¹⁵² HIF1 regulates the expression of a broad range of genes that facilitate acclimatization to low oxygen conditions. These genes code for molecules that participate in vasomotor control, angiogenesis, erythropoiesis, iron metabolism, cell proliferation and cell cycle control, cell death, and energy metabolism.¹⁵²

Molecular mechanisms of HIF1 activation

HIF1 α is synthesized continuously but is rapidly degraded and is almost absent in normoxic cells. However, in hypoxic cells, HIF1 α accumulates as a consequence of a delayed degradation. HIF1 α levels increase exponentially *in vitro* after exposure to an oxygen concentration of less than 6%, with a cell-type-dependent maximal response at a concentration of ~0.5%.¹⁵³

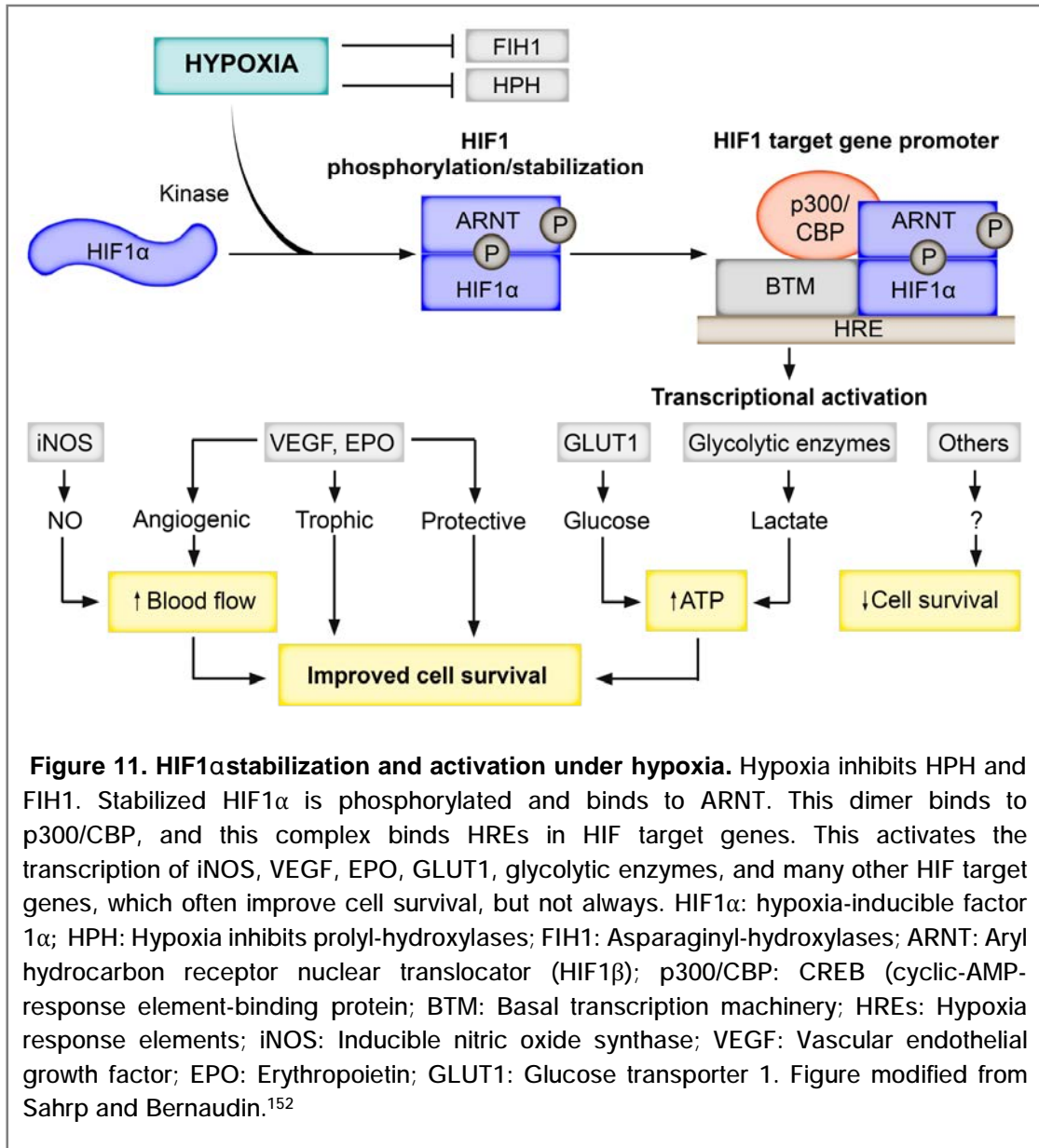
In the presence of O₂, iron, and 2-oxoglutarate, HIF1 α is hydroxylated by prolyl-4-hydroxylases (HPH) in the cytoplasm and nucleus,¹⁵⁴ thereby targeting it for proteasomal degradation. HPH enzymes hydroxylate proline residues (402 and 564) in the ODD of HIF1 α , which changes the conformation of HIF1 α and allows the Hippel Lindau protein (VHL) to recognize and bind to it. Other factors then bind to VHL, including elongin B, elongin C67, Cullin 2,¹⁵⁵ and RBX1. This complex acts as an E3

ubiquitin ligase for HIF1 α poly-ubiquitylation, and the proteasome degrades HIF1 α (Figure 10A).¹⁵⁵



Normoxia also stimulates the binding of ARD1 to HIF1 α , which acetylates lysine 532 in the ODD of HIF1 α . The acetylation increases interaction with VHL and promotes proteasomal degradation of HIF1 α ¹⁵⁶ (**Figure 10B**). By contrast, heat-shock protein 90 (HSP90) seems to stabilize HIF1 α during normoxia through an independent HIF1 α -degradative pathway.¹⁵⁷ Another protein called factor inhibiting HIF1 (FIH1) abrogates the interaction between HIF1 and the transcriptional co-activator p300/CBP.^{158,159} However, under hypoxic conditions, prolyl and asparaginyl-hydroxylases are inhibited, which prevents hydroxylation of HIF1 α . Inhibiting prolyl-hydroxylases decreases the degradation of HIF1 α by the ubiquitin–proteasome system and leads to rapid accumulation.^{160,161} HIF1 α is phosphorylated and dimerizes with HIF1 β . The HIF1 α /HIF1 β dimer binds to p300/CBP and activates HREs in HIF target genes to modulate their transcription.^{162,163}

After focal and global ischemia, several HIF1 target genes are induced in the brain. These include 1) genes that code for factors that participate in vasomotor control (inducible NOS and adrenomedullin),^{164,165} which vasodilate cerebral blood vessels and increase CBF following ischemic stroke;^{166,167} 2) genes involved in angiogenesis (VEGF, FLT1, and PAI1,^{168–170} which might mediate the angiogenesis that occurs around areas of ischemia and infarction); and 3) genes involved in the regulation of energy metabolism and ion transport, including glucose transporter 1 (GLUT1) and several glycolytic enzymes.^{165,171,172} These enzymes increase glucose transport into the brain, as well as increase glucose and lactate metabolism through glycolysis and the KC to increase ATP levels in areas of brain ischemia (**Figure 11**). Interestingly, HPH can be induced by hypoxia, indicating a feedback loop to avoid excessive nuclear HIF1 accumulation.¹⁶² It is now well established that HIF1 can be activated by other conditions than hypoxia. For example, various cytokines and growth factors (e.g., IL-1 β , TNF α , TGF β) have been shown to be capable of stimulating synthesis or stabilization and activation of HIF1 α .¹⁵²



4. Normobaric brain oxygen therapy as a therapeutic maneuver

In the last decade, significant insight has been gained into the underlying pathophysiology of secondary lesions in TBI and the neurochemical cascades that acute injury puts into motion. The absence of suitable BMs to act as surrogates for drug efficacy in humans is a major fundamental problem in translational medicine for TBI. Therefore, strategies to ameliorate post-traumatic cerebral metabolic depression are needed. The interventions currently used related to metabolic dysfunction in TBI are: 1) hypothermia, 2) hyperoxic/hyperbaric oxygen therapy (NBO/HBO), and 3) antioxidant therapy.

Applying therapeutic interventions to keep brain tissue oxygenation above certain thresholds might improve mortality and neurological outcome in TBI patients. As mentioned, it is widely believed that maintaining cerebral metabolism after TBI is vital for the generation of ATP, which in turn is necessary to reestablish the ionic homeostasis of the disturbed neuronal membrane, protect neuronal integrity, and reestablish function. Ischemic and non-ischemic tissue hypoxia has been shown to be highly prevalent after severe TBI. Direct assessment of brain PtiO₂ can be used at the bedside to closely monitor the concentration of free oxygen available in the tissue, which is a surrogate index of the balance between oxygen supply and consumption. Different retrospective studies have shown that low PtiO₂ is associated with high mortality and poor neurological outcome.¹⁷³

In TBI, the oxygen flux from the capillaries to the mitochondria can be altered by diffusion alterations at many different stages.^{174,175} Under normal conditions, the diffusion distance of oxygen molecules from the capillaries to the cell is ~60 μm, but the distance increases after TBI and brain edema.¹⁷⁶ Diffusion barriers to the cellular delivery of O₂ can develop and persist after injury. Thus, some patients may benefit from interventions that increase O₂ pressure and thus the pressure drive that moves oxygen into the brain. Furthermore, a growing body of evidence suggests that mitochondrial dysfunction may play a very important role in the pathophysiology of TBI,⁶⁷ and it might explain the significant reduction in the CMRO₂ found after TBI.⁹⁰ Hypothetically, if mitochondrial function is impaired after TBI, then a steeper capillary-cell O₂ gradient induced by hyperoxia may also improve oxygen utilization.

Potential therapies for this situation have recently been tested. NBO and HBO are strategies that have already been tested in a variety of models of TBI and in pilot clinical trials. NBO is defined as oxygen delivered at FiO_2 of 1.0 and 1 ATA, which may improve CMRO_2 by improving the brain's ability to use the delivered oxygen. According to Fick's law, O_2 delivery is directly proportional to both the O_2 concentration gradient and its diffusivity. It is thus possible to enhance O_2 delivery to tissues through not only hyperoxia but also by enhancing the diffusion of substrates through the plasma boundary layer and the brain tissue. The higher brain tissue PO_2 produced by hyperoxia could improve oxygen metabolism because either impaired mitochondria require a higher PO_2 , or an increased oxygen tension gradient is required to drive oxygen through edematous tissue to reach the mitochondria.

Alternatively, HBO is defined as oxygen delivered at pressures above atmospheric pressure (>1 ATA). HBO has been demonstrated to improve cellular energy metabolism and patient outcomes, and it could be neuroprotective according to animal models.^{177,178} Despite the potential advantages of HBO or combined HBO/NBO treatments, HBO requires expensive hyperbaric chambers and trained and competent personnel to work in this complex environment. These facilities are only available in a few Level 1 trauma centers worldwide, making it difficult to implement this therapeutic strategy. In addition, HBO can only be provided for a short period of time and can significantly disturb conventional critical care management. In this clinical scenario, the simplicity of applying NBO in any institution makes this low-cost option attractive and easy to implement with no modification to the standard of care.

Many experimental and clinical studies indicate that metabolic disorders are common in acute brain injuries. Furthermore, impaired oxygen delivery related to oxygen diffusion anomalies or impaired oxygen utilization in the mitochondria (e.g., mitochondrial dysfunction) may play significant roles in the acute phase of TBI, ischemic stroke, and hemorrhagic stroke.^{79,81,174,179} Clinical non-randomized studies suggest that this therapy could be used as a potential treatment to improve brain oxygenation and some of the metabolic disorders resulting from TBI.¹⁸⁰ However, there is still significant controversy regarding this treatment because the metabolic results are contradictory and vary with the type of injury to which it is applied.⁶⁻¹²

Table 3 summarizes the main results of these clinical studies. In a previous study, our group showed that NBO increased brain PtiO_2 and significantly decreased the LPR in

TBI patients who had increased brain lactate levels at baseline. This suggests that NBO might improve the brain redox state under certain conditions.¹² Furthermore, the baseline metabolic state should be taken into account when applying NBO.

Recently, controversies about the use of NBO have also been raised in the management of IS. The main concern raised by NBO in TBI, stroke, or hypoxic-ischemic encephalopathy is the potential toxicity of using supranormal levels of PaO₂. Some clinical studies have reported that high oxygen levels are associated with worse outcomes after severe TBI.¹⁸¹ These studies raised concerns about using abnormally high FiO₂ levels and questioned the real benefit of maintaining supranormal PaO₂ levels in patients with acute brain injuries. The mechanisms are not yet clear, but high FiO₂ could induce vasoconstriction, exacerbate OxS, increase neuroinflammation, or induce excitotoxicity.¹³ Among these proposed mechanisms, the capacity of NBO to induce OxS is the most important because of the ability of O₂ to induce the production of ROS and therefore damage proteins, lipids, and DNA.¹⁴ Some studies on patients with TBI and cardiac arrest have suggested that arterial hyperoxia is associated with worse outcomes.^{182,183} In patients with aneurysmal subarachnoid hemorrhage (SAH), arterial hyperoxia was associated with a higher incidence of delayed ischemia and poor neurological outcome.^{184,185} Thus, despite the potential benefits in brain metabolism, NBO is still controversial and raises many concerns that need to be clarified before entering clinical trials or using it routinely in patients with brain injuries.

Table 3. Studies assessing the effects of normobaric brain Oxygen therapy (NBO) in patients with traumatic brain injury

Study	Sample Size	Treatment	Time window	Probe location	Harmful
<i>Menzel et al., 1999</i>	22	100% O ₂ (6h)	18h after admission	Not reported	-
<i>Magnoni et al., 2003</i>	8	100% O ₂ (3h)	79h after injury	Normal brain	+
<i>Reinert et al., 2003</i>	20	100% O ₂ (6h)	24h after injury	Normal brain	-
<i>Tolias et al., 2004</i>	52	100% O ₂ (24h)	6h after admission	Frontal lobe	-
<i>Diringer et al., 2007</i>	5	100% O ₂ (1h)	18h after injury	Not reported	+
<i>Tisdall et al., 2008</i>	8	100% O ₂ (1h)	48h after injury	Pericontusional tissue	-
<i>Norije et al., 2008</i>	11	60-80% O ₂ (0.85h)	9 days after injury	Various (normal, abnormal)	-
<i>Rockswold et al., 2010</i>	21	100% O ₂ (3h)	27h after injury	Least injured hemisphere, frontal lobe	-
<i>Vilalta et al., 2011</i>	29	100% O ₂ (2h)	126h after injury	Least injured hemisphere, normal brain	+
<i>Quintard et al., 2014</i>	36	>80 % O ₂	4 days after injury	Normal brain	+
<i>Taher et al.; 2016</i>	34	80% O ₂ (6h)	6h after injury	Not reported	-
<i>Sahoo et al.; 2016</i>	25	40-60-100% O ₂ (0.85h)	24h after injury	Various (normal, abnormal)	-
<i>Gosh et al.; 2016</i>	16	100% O ₂ (2h)	72h after injury	Various (normal, abnormal)	-

+: Study found harm from NBO treatment; -: No harm found from NBO treatment. Table modified from Beynon et al.¹⁸⁶

5. Multimodal monitoring in TBI patients

MNM is a method that aids in understanding real-time brain physiology. Early detection of physiological disturbances is possible with the help of MNM, which allows for identification of the underlying causes of deterioration and the minimization of secondary brain injury.¹⁸⁶ The main objective of monitoring the injured brain is to prevent or detect the occurrence of secondary lesions before they cause irreversible damage to the brain and allow for diagnosis and effective treatment. Therapeutic management in TBI patients is focused on the maintenance of an adequate CBF and energy metabolism guided by cerebral MNM tools. Nevertheless, the high heterogeneity of brain lesions and the different clinical evolutions of TBI patients increase the complexity of analyzing the information provided by these tools, which should be analysed in an individualized and dynamic way.

There are different advanced cerebral techniques involved in the neuromonitoring of neurocritical patients. Cerebral MNM methods can be classified as invasive and non-invasive methods. Invasive methods include ICP, $PTiO_2$, MD, and CBF probes, as well as jugular venous oxygen saturation ($SjvO_2$). Non-invasive methods include transcranial Doppler, continuous electroencephalography (EEG), and near-infrared spectroscopy (NIRS).

5.1. Intracranial Pressure

Continuous ICP monitoring is used as a therapeutic guide for patients with acute neurological lesions and potential ICH. Continuous ICP monitoring is a standard of care in most trauma centers, although there is a wide variability in the indications. Between 50% and 75% of severe TBI patients present ICH at some point in their clinical course, although incidence varies according to the type of brain injury and is dramatically reduced with an aggressive surgical approach to treat focal lesions.¹⁸⁷ With evidence level IIB, the Brain Trauma Foundation (BTF) guidelines suggest that the management of severe TBI patients according to continuous ICP monitoring reduces in-hospital and 2-week post-injury mortality.¹⁸⁸

ICP could be defined as the force that the brain tissue, blood, and CSF exert inside the cranial vault. The Monro-Kellie hypothesis states that the sum of volumes of these components is constant.¹⁸⁹ ICP can be influenced by an increase in brain volume (brain swelling), cerebral blood volume, and a local or diffuse elevated CSF volume due to an increase in its production or a decrease in its clearance. Mass lesions can also increase ICP.¹⁹⁰ The compensatory mechanisms of the intracranial space allow ICP to be maintained within the normal range.¹⁸⁸ If a critical point is reached on the pressure-volume curve (a low compliance point), a small volume increment in any of the mentioned components will generate large increases in ICP levels.¹⁹¹

ICP monitoring enables the following: 1) determining the absolute values of ICP, 2) assessing the presence of pathological waves, 3) obtaining information about brain compliance through the wave amplitude parameter, 4) calculating and managing the CPP, 5) diagnosing the ICH and guiding treatment, 6) helping to obtain information about a patient's prognosis, and 7) recognizing the worsening of intracranial lesions. There are two types of sensors available to measure ICP intraventricular sensors and intraparenchymal sensors. Intraventricular monitoring is the recommended monitoring system in the BTF guidelines because the catheter may be used to perform CSF drainage as a therapeutic technique in addition to measuring ICP. Alternatively, intraparenchymal sensors are implanted easily right in the ICU and allow for the monitoring of patients for whom it is difficult to place a catheter in the ventricle. Brain parenchyma sensors have a very small diameter and are usually not coupled to fluids. These systems are specially designed to be implanted at the bedside and have a very low risk of complications.¹⁹²

In healthy adults at rest in a supine or lateral position, the normal mean ICP is less than 12 mmHg. Normal ICP values in neurocritical patients range from 15 to 20 mmHg. Values above 20 mmHg are associated with increased death and disability in these patients.^{188,193}

5.2. Cerebral microdialysis

Cerebral MD is an extremely sensitive technique that allows for continuous neurochemical monitoring. It also provides the unique opportunity to explore the

disturbances of metabolism in neurocritical patients. Cerebral MD is based on the principle of solute exchange through a semi-permeable membrane located at the distal end of the MD catheter. The main objectives are to monitor 1) the availability of different tissue metabolites, 2) the products released by the cells, and 3) the effects of tissue hypoxia-ischemia on the cells. Analysis of the recovered microdialysate allows for monitoring different tissue metabolites in the ECS and products generated as a result of tissue injury.

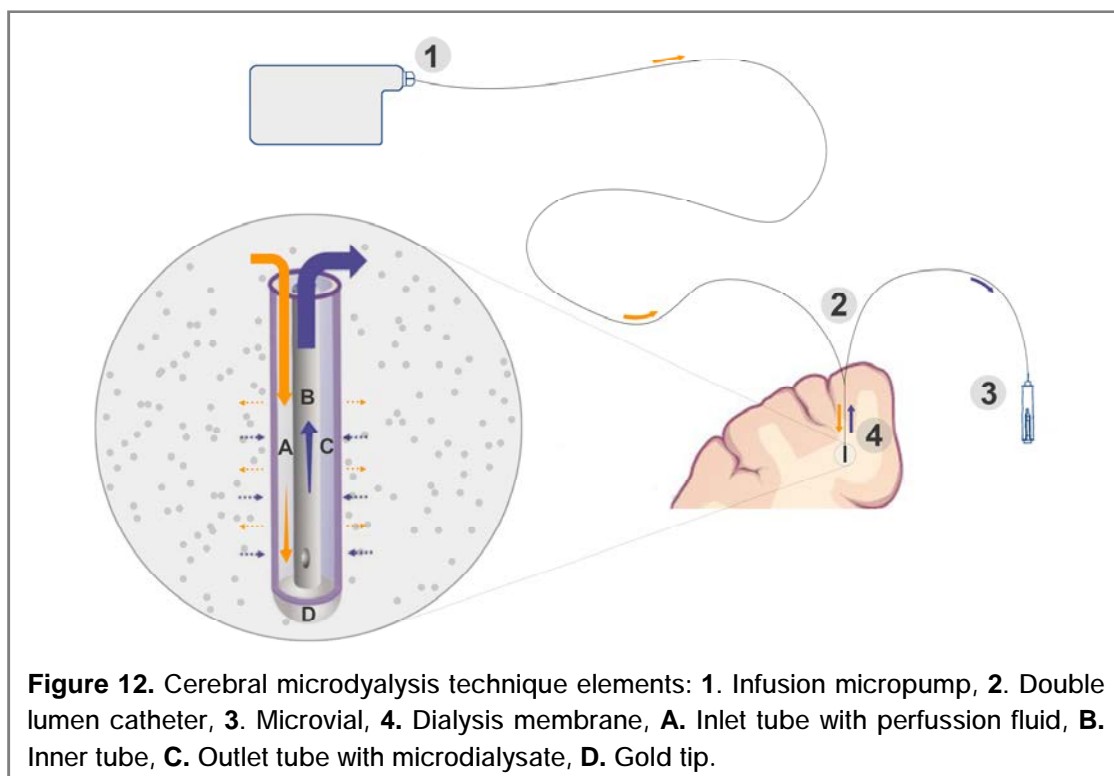
5.2.1. Methodological considerations

MD catheters are flexible probes with a small diameter (< 1 mm) and contain a double lumen with a semi-permeable membrane at their distal end. They function like a blood capillary, and solutes are exchanged through the membrane between a solution of known composition and the ECS surrounding the MD catheter in favor of an osmotic gradient. The internal lumen of the catheter is perfused with a metabolite-free solution, which perfuses the catheter with a constant perfusion flow. Solute exchange occurs at the distal extreme of the membrane. The microdialysate is recovered through a small container (microvial), which contains molecules from the ECS and is changed hourly by a nurse (**Figure 12**).

Once the microvial is replaced, lactate, pyruvate, glucose, glutamate and glycerol are routinely monitored at the bedside through enzyme kinetic methods and colorimetric measurements using an Iscus Flex microdialysis analyzer (e.g., ISCUS Flex analyzer, M Dialysis AB, Stockholm, Sweden). After these hourly measurements, the microvials are placed in a rack (M Dialysis AB) to seal them and prevent evaporation. All racks are stored at 76°C until further analysis of other proteins or molecules of interest. The cerebral values must be compared with the systemic metabolism through an additional catheter placed in the subcutaneous tissue. Metabolic abnormalities detected by MD catheter may help to screen the cause of potential secondary intra- or extra-cranial insults.

There are two types of cerebral MD catheters: the CMA-70 (20-kDa cut-off membrane; MDialysis AB) and CMA-71 (100-kDa cut-off membrane). The 60-mm shaft is made of polyurethane and has an outer diameter of 0.9 mm. The polyarylethersulphone dialysis

membrane is 10 mm long with an outer diameter of 0.6 mm. Cerebral catheters are perfused with a sterile isotonic CNS fluid containing 147 mmol/L of NaCl, 1.2 mmol/L of CaCl₂, 2.7 mmol/L of KCl, and 0.85 mmol/L of MgCl (M Dialysis AB) at a fixed flow rate of 0.3 mL/min using a CMA-106 pump (M Dialysis AB).

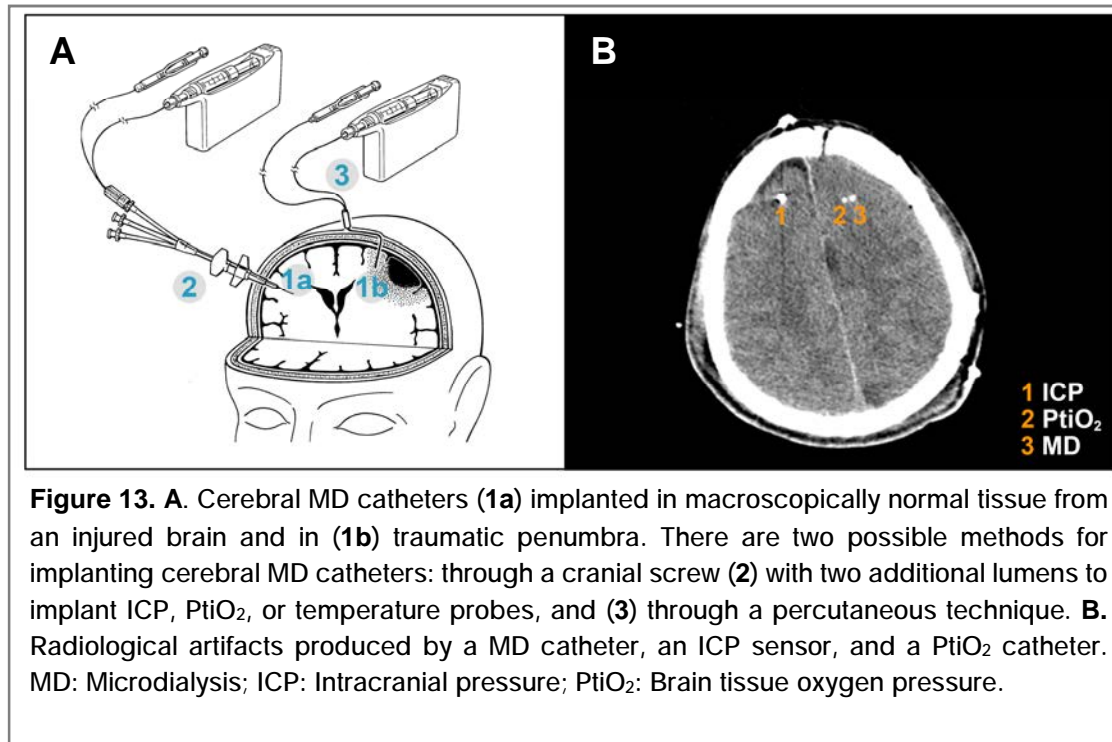


5.2.2. Catheter implantation and tissue classification

Cerebral MD catheters can be surgically implanted through a burr hole or through the cortex after a lesion evacuation. These probes can also be implanted at the bedside through a cranial screw or a percutaneous technique.¹⁹⁴ The MD catheter must be implanted in the brain region that provides the most useful information for patient management. Catheter implantation in healthy tissue provides the possibility of monitoring the tissue with the highest probability of recovery, while implantation in areas of the “penumbra” allows for monitoring brain regions with the greatest risk of ischemia.^{195,196}

In TBI, catheters should be applied according to the type of lesion. In diffuse lesions, the implantation of a single brain catheter in the right frontal region is recommended. In focal lesions, two catheters are recommended: one in the macroscopically non-

lesioned region and the other in the penumbra. The position of the catheter is confirmed by control CT scan, in which the gold tip at the distal end of the catheter is visible (**Figure 13**).



The region of the brain sampled by the probes can be classified in one of the following categories as defined by our group¹⁹⁷: normal injured brain, traumatic penumbra, traumatic core, ischemic penumbra, and ischemic core. **Normal injured brain (NB)** is defined when the probes tips are inserted in a region of the brain without any macroscopically visible abnormality (blood or hypodense lesion). To consider the brain to be “normal,” the closest hemorrhagic/hypodense lesion must be located at least 30 mm from the tip of the probes. **Traumatic penumbra (TP)** defines the position of the probes in the brain parenchyma without any changes in attenuation and at least 20 mm away from any intraparenchymal lesion (contusions, hematomas, etc.). TP is also considered when the probes are located in the brain immediately below any significant extra-cerebral hematoma. The **traumatic core (TC)** is defined when the probes are placed in areas of brain tissue that has macroscopically obvious lesions such as contusions and hemorrhages or when the probes are located in a small hemorrhagic lesion. **Ischemic penumbra (IP)** is defined for patients with a MMCAI in which the tip of the probes is placed in a brain region of normal macroscopic appearance around the core with no changes in brain tissue attenuation in a non-

contrast CT scan. These regions have to be at least 20 mm away from any brain region with parenchymal abnormalities. **Ischemic core (IC)** tissue is defined when the patient has a confirmed diagnosis MMCAI, and the probes are located in a hypodense lesion with or without a hemorrhagic component.¹⁹⁷

5.2.3. Relative recovery and *in vitro* calibration

One inherent problem of the MD is that the concentration of the analyte collected represents only a fraction of the ECS concentration.¹⁹⁸⁻²⁰¹ Relative recovery (RR) is defined as the ratio of the concentration in the dialysate to the true concentration of a given substance *in vitro*.²⁰² The factors determining the RR primarily depend on the physical properties of the membrane, the temperature of the medium, the analyte properties, the perfusion flow rate, the characteristics of the sample matrix, and the diffusion coefficient of the substance of interest.^{198,199,201,202}

The approach most frequently used to evaluate cerebral MD efficiency for any substance involves *in vitro* RR. The determination of *in vitro* RR involves immersing an MD catheter in a matrix with a known concentration of metabolite under controlled conditions. The metabolite levels are analyzed in the dialysate and matrix samples, and the RR is calculated using the following equation:

$$RR = (C_{md}/C_{matrix}) \times 100 \quad (\text{Equation 1})$$

where C_{md} and C_{matrix} are the analyte concentrations in the microdialysate and the matrix, respectively.

During MD, analytes pass through a semipermeable membrane from the ECS into a perfusate. Because the membrane is semipermeable, only some solutes (with low molecular weight) will be recovered. Thus, the concentration of analyte collected by this method will represent only a fraction of the ECS concentration.

The factors determining the amount of analyte recovered during MD can be divided as follows: 1) MD probe membrane properties (e.g., cut-off of the membrane, membrane surface area); 2) perfusion conditions (e.g., composition of the perfusion solution, temperature, flow rate); and 3) analyte properties, which are primarily

determined by the molecular weight of the solute.²⁰³ *In vitro* RR results are difficult to extrapolate to the brain due to the effects of the tissue properties on the diffusion of analytes.^{199,204} There are other biological factors that only influence RR *in vivo* due to the interaction of the dialysis membrane with the tissue biofouling (e.g., tissue tortuosity).

5.2.4. Metabolic thresholds

One of the key problems of the MD technique is establishing reference values for distinct metabolites. The range of reference for brain metabolites is still quite arbitrary because monitoring healthy individuals is ethically impossible. Usually, these values are extrapolated from animal studies, studies on other organs, or from brain MD conducted on patients with intracranial lesions, as well as neurosurgical operations for posterior fossa lesions or epilepsy.^{78,205} **Table 4** summarizes the main results of these clinical studies.

Reinstrup et al. conducted one of the main studies reporting reference interval (RIs) for brain energy metabolites in neurocritical neurosurgical patients under general anesthesia.⁷⁸ Other studies have reported brain metabolite levels in the normal brain of patients with central nervous system tumors,²⁰⁶ in awake epileptic patients,^{205,207} and in patients with spontaneous SAH.^{99,208} However, in most studies, the true ECS concentrations were unknown, and the reference limits were estimated from the concentrations in the dialysate and from the *in vitro* RR for the specific metabolite. This variability remains an important obstacle for adequate interpretation of the metabolic findings in neurocritical patients and for correct patient management.

Recently, our group determined the RI for analytes involved in brain energy metabolism and for glycerol in a cohort of patients who underwent surgical treatment to treat posterior fossa and supratentorial lesions. This group of patients was observed twice: once while anesthetized and once while awake (24 h after surgery and when the patient was extubated and conscious; **Table 4**). The reported RIs provided additional support to the thresholds reported previously. Moreover, our study emphasizes the importance of using different thresholds for awake patients and for patients under anesthesia or deep sedation.²⁰⁹

Table 4. Extracellular concentrations for energy metabolites and glycerol defined in the literature

Study	Condition	Glucose (mmol/L)	Lactate (mmol/L)	Pyruvate (μ mol/L)	LPR	Glycerol	Pathology
<i>Reinstrup et al., 2000</i>	Anesthetized (1 μ L/min)	1.2 \pm 0.6	1.2 \pm 0.6	70 \pm 24	22 \pm 6	28 \pm 16	
	Awake (1 μ L/min)	0.9 \pm 0.6	1.4 \pm 0.9	103 \pm 50	21 \pm 6	42 \pm 29	Posterior fossa tumor
	Awake (0.3 μ L/min)	1.7 \pm 0.9	2.9 \pm 0.9	106 \pm 47	23 \pm 4	82 \pm 44	
<i>Schulz et al., 2000</i>	Anesthetized (0.3 μ L/min)	2.1 \pm 0.2	3.1 \pm 0.3	151 \pm 12	19 \pm 2	82 \pm 12	SAH (nonischemic area)
<i>Abi-Saab et al., 2002</i>	Awake (2.5 μ L/min)	0.8 \pm 0.3	1.4 \pm 1.2	NA	NA	NA	Epilepsy (nonepileptogenic area)
	Awake (ZFM)	1.6 \pm 0.8	5.1 \pm 1.4	NA	NA	NA	
<i>Cavus et al., 2005</i>	Awake (ZFM)	1.6 \pm 0.3	4.7 \pm 0.5	NA	NA	NA	
	ZFM	1.57 (1.12-4.70)	2.01 (1.37-5.44)	80.0 (53.9-223.3)	27.5 (14.9-39.5)	49.9 (21.7-228.7)	Epilepsy (nonepileptogenic area)
<i>Sanchez et al., 2016 *</i>	Anesthetized (0.3 μ L/min)	1.25 (0.64-3.53)	1.40 (1.10-3.84)	73.8 (36.6-149.7)	23.3 (12.8-34.5)	53.8 (24.4-205.1)	Posterior fossa and supratentorial lesions
	Awake (0.3 μ L/min)	1.55 (0.29-3.01)	3.41 (1.56-5.62)	137.1 (85.0-192.0)	24.9 (16.9-35.1)	79.8 (29.3-346.4)	

Values are expressed as mean \pm SD. *Values are expressed as median (min-max). SAH: Subarachnoid hemorrhage; NA: Not applicable;

LPR: Lactate-to-pyruvate ratio; ZFM: Zero-flow method

5.2.5. Clinical applications of microdialysis monitoring

The first known application of MD in humans was reported in 1990 by Meyerson et al., who implanted MD probes in patients with Parkinson's disease.²¹⁰ Since that time, cerebral MD has been increasingly used as a neuromonitoring tool in neurocritical patients with TBI, MMCAI, and SAH to monitor cerebral energy metabolism during the acute phase after injury or stroke onset.²⁰¹ Today, the commercially available equipment is considered to be a well standardized, safe, and powerful research tool that is clinically indicated in the management of neurocritical patients. However, before considering the use of cerebral MD as a clinical monitor after acute brain injury, it is important to understand that there are wide variations in MD variables over time after the injury, not only between different subjects, but also within individuals.²¹¹⁻²¹⁴

There is a large body of literature suggesting that MD monitoring can predict poor outcomes after TBI.²¹¹ There is also some evidence that MD may assist in clinical decision-making, such as in the management of CPP,²¹⁵ guidance of hyperventilation,²¹⁶ and the appropriateness of extensive surgical procedures.²¹⁷ The main aim of MD is the early detection of metabolic changes that suggest the development of tissue ischemia, as well as monitoring the effect of the therapeutic techniques applied to treat the ischemia. Thus, cerebral MD is a highly sensitive technique that can provide early metabolic information about brain energy status (glucose, lactate, and pyruvate), excitatory amino acid (glutamate) levels, and cell membrane integrity (glycerol). The determination of brain energy status can provide information about the relative contribution of the aerobic or anaerobic metabolisms in energy production. A simplified schematic of major energy pathways in the brain is shown in **Figure 14**.

One of the main advantages of cerebral MD monitoring after TBI is the ability to assess the cerebral delivery and utilization of **glucose**.²¹¹ As the primary source of energy to the brain, glucose is an important indicator of changes in brain metabolism. Glucose levels can change for several reasons: 1) ischemia (e.g., insufficient capillary blood flow); 2) hyperemia (e.g., an increase in capillary blood flow); 3) hyper-hypoglycemia (e.g., an increase/decrease in blood glucose concentration); and 4) hypermetabolism or hypometabolism (e.g., an increase or decrease of glucose uptake into cells; a shift from aerobic to anaerobic metabolism). In addition, cerebral MD lactate has been considered for decades to be an excellent BM of oxygen limitation and therefore organ

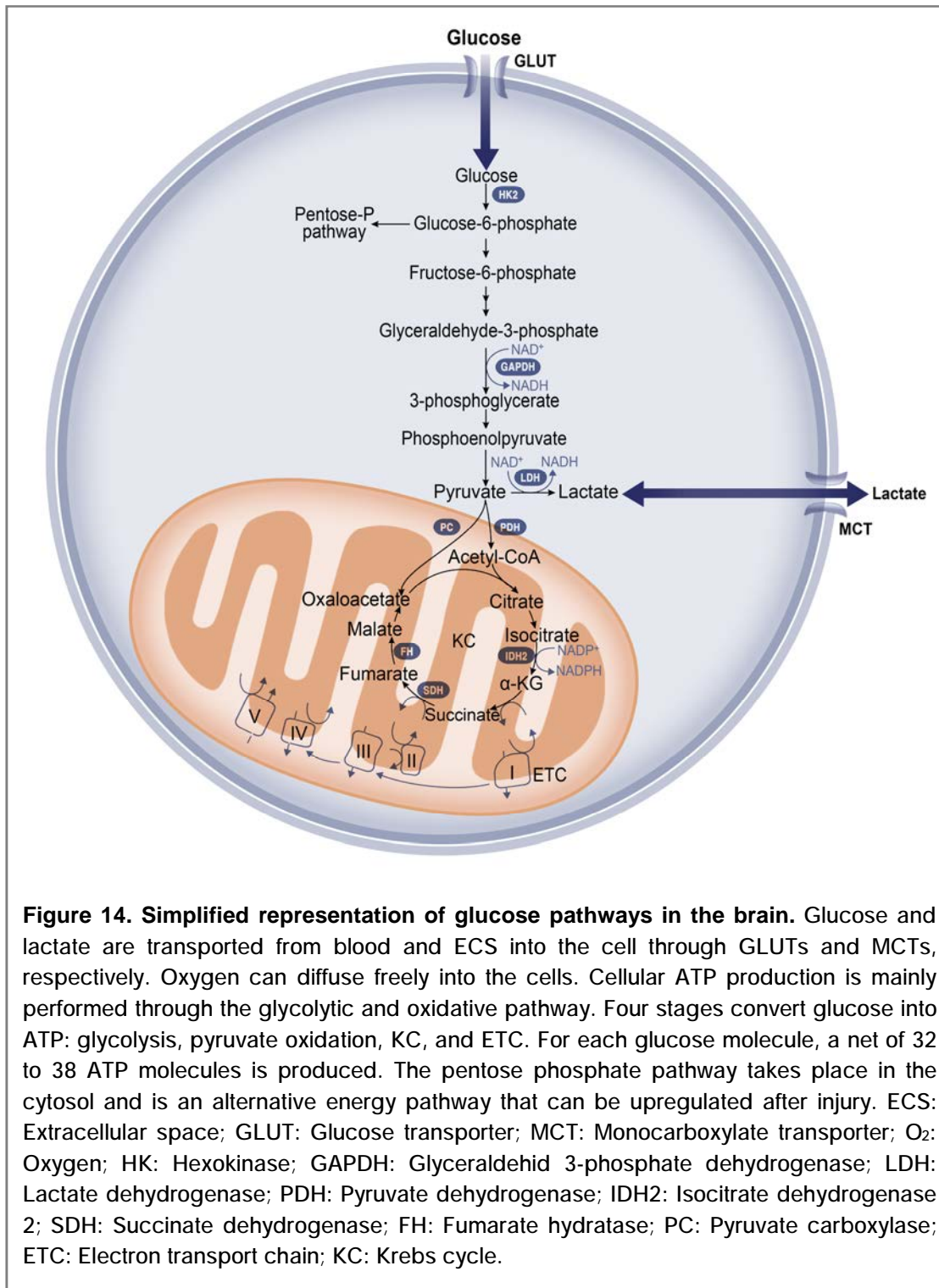
ischemia.⁸¹ **High lactate and LPR levels** indicate an increase in anaerobic metabolism due to impairment in oxidative metabolism. This phenomenon can principally result from two circumstances: 1) a lack of O₂ supply resulting from a hypoxic or ischemic process and 2) a failure in mitochondrial oxidative phosphorylation. The LPR is generally regarded as a more useful clinical marker than lactate concentration alone, although both lactate and pyruvate, along with glucose, must also be reported individually for proper interpretation of bedside microdialysate monitoring.¹⁹⁵ The lactate/glucose ratio (**LGR**) is also a sensitive marker of tissue hypoxia/ischemia and has been interpreted to indicate increased glycolysis.^{99,211} **Glutamate** can give information about the excitatory amino acids released into the extracellular space and about the energetic dysfunction that occurs in certain pathologies. **Glycerol** levels provide information about the membrane state and the level of cellular stress. Briefly, energy loss due to ischemia leads to an influx of calcium into cells, activation of phospholipases, and eventually the decomposition of cell membranes, which liberates glycerol into the ECS.⁹⁸ Glycerol is therefore a useful MD marker of tissue hypoxia and cell damage after TBI.²¹¹

One of the main advantages of using cerebral MD is that it can help in the differential diagnosis of the distinct types of non-ischemic hypoxia. Identification of metabolic patterns can lead to the distinction of ischemia and mitochondrial dysfunction, which helps in the clinical management and therapeutic guidance of TBI patients.^{70,85,218,219} A summary of pathophysiological changes monitored by cerebral MD is shown in **Table 5**.

Table 5. Biochemical markers of secondary injury in TBI

MD marker	Secondary Injury
↓ Glucose	<ul style="list-style-type: none"> • Hypoxia/Ischemia • Reduced glucose supply • Hyperglycolysis
↑ LPR	<ul style="list-style-type: none"> • Hypoxia/Ischemia • Reduction in redox state • Reduced glucose supply • Mitochondrial dysfunction
↑ Glycerol	<ul style="list-style-type: none"> • Hypoxia/Ischemia • Cell membrane degradation
↑ Glutamate	<ul style="list-style-type: none"> • Hypoxia/Ischemia • Excitotoxicity

MD: Microdialysis; LPR: Lactate-to-pyruvate ratio. Table modified from Tisdall and Smith et al.²²⁰



Any molecule present in the cerebral ECS that is small enough to cross the semi-permeable dialysis membrane will also be collected in the dialysate. This opens the door to the investigation of novel BMs of TBI with several applications aimed at increasing knowledge of the physiopathology among patients with acute brain lesions.

The applications include: 1) the recovery of large molecules contained in the ECS (inflammatory molecules and OxS BMs); 2) the use of ^{13}C -labeled substrates to study the fate of specific molecules through metabolic pathways; 3) monitoring the ionic profile of brain tissue in different situations; 4) studying the local effects of drugs on neurochemistry and their penetration across the BBB; and 5) developing on-line analysis systems for continuous monitoring.¹⁹⁵

Combining MD with highly sensitive analytical methods enables the investigation of individual BMs involved in the pathophysiology of acute brain injuries. Several highly sensitive immunochemical analytical methods are used to detect the neuroinflammatory and OxS profile following acute brain injury. In a previous study, our group showed that the *in vivo* ionic concentration can be calculated reliably from the microdialysate concentrations in patients with TBI.²²⁰ However, the main limitation of the methodology used in our proof-of-concept study on this conventional ion-selective electrode-based analyzer was its low temporal resolution. Inductively coupled plasma mass spectrometry (ICP-MS) is the best method available for analyzing metals, including ions at very low concentrations and with extremely low detection limits.²²¹

5.3. Brain oxygenation

In addition to the initial mechanically induced brain tissue injury, the lack of a sufficient oxygen supply to the brain is considered a major cause of secondary brain damage. Cerebral oxygenation can be determined using invasive or non-invasive methods. The most frequently used invasive methods are: 1) the determination of PtiO_2 , a regional method, and 2) the determination of SjvO_2 , a global method. Studies have shown that brain tissue oxygenation closely correlates with several outcome parameters and patient prognosis.^{222,223}

5.3.1. Jugular bulb oxygen saturation

SjvO₂ is an invasive monitoring method that can be used to estimate the balance between global cerebral oxygen delivery and utilization, brain metabolism, and oxygenation. The method also provides information on the relationship between CBF and metabolic O₂ consumption.²²⁴ The clinical application of SjvO₂ determination is mainly in severe TBI patients or other neurocritical patients, including those with SAH or MMCAI. It can also be used during neurosurgical and cardiovascular procedures.

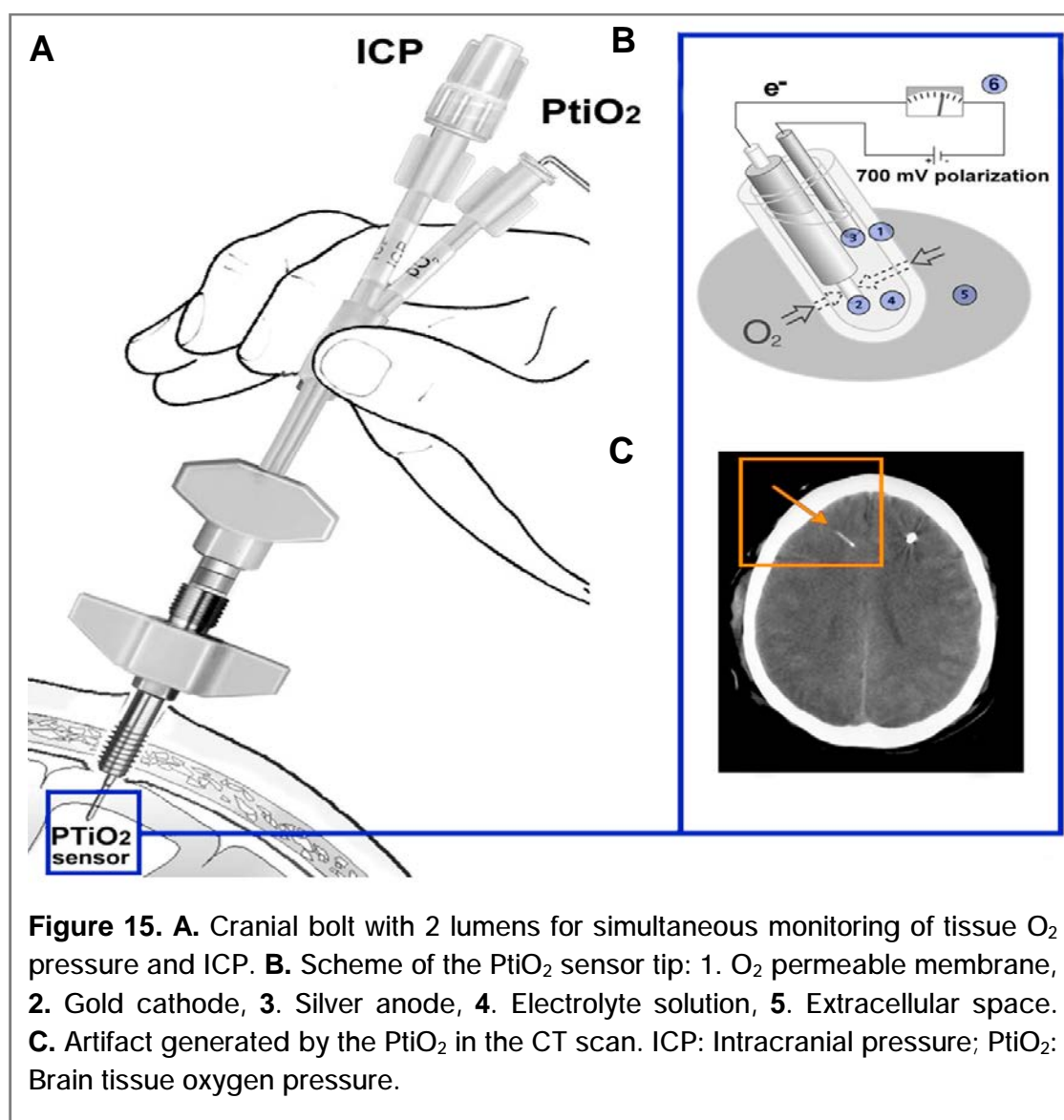
This monitoring system requires the insertion of a catheter using the Seldinger technique at the level of the dominant internal jugular vein bulb. The catheter position must be verified in a lateral cervical spine radiographs. SjvO₂ can be measured made either continuously using a fiber-optic catheter or discontinuously by drawing blood samples and analyzing them with a co-oximeter at the desired frequency. The BTF guidelines for severe TBI recommend maintaining SjvO₂ values above 50% to reduce mortality and improve outcomes.¹⁸⁸ Thus, values below 50% are consistent with brain ischemia, and values above 75% are related to cerebral hyperemia, in which the O₂ supply exceeds the metabolic demands of the brain due to an increase in CBF or a decrease in O₂ consumption.²²⁵

5.3.2. Partial brain tissue oxygen tension

PtiO₂ monitoring is a regional and invasive method that measures brain oxygenation continuously. PtiO₂ reflects the availability of free O₂ in the tissue, which is considered to be equivalent to the O₂ on the venous side of the capillary bed. This method consists of the implantation of an O₂-sensitive catheter in the cerebral parenchyma, which provides the mean O₂ concentration in the area monitored, which comprises three compartments of the cerebral white matter (vascular, intracellular and extracellular).²²⁶

There are two systems available to measure PtiO₂: 1) the Licox® system (Integra Neurosciences, Kiel-Mielkendorf, Germany) and 2) the Neurovent®-PTO sensor (Raumedic Oxygen Measurement System, Rehau, Münchberg, Germany). The Licox® system uses a polarographic method that determines the partial pressure of O₂ through redox reactions produced at the end of the catheter. These reactions generate

an electric current that is transformed to a numerical value (**Figure 15**). The Neurovent-PTO system determines the partial pressure of O_2 by a phenomenon known as O_2 quenching, where fluorescent labeled molecules absorb and emit light of a certain wavelength, depending on the presence or absence of O_2 .²²⁷ Moreover, this system can measure ICP, Pti O_2 , and temperature through the same catheter.



Because of ethical limitations, the range of normality in awake humans has not yet been established. Normal Pti O_2 values measured with a polarographic system range between 15 and 30 mmHg, although some authors believe that the range in TBI patients should be higher. Pti O_2 values <15 mmHg indicate cerebral tissue hypoxia, which can be moderate (10-15 mmHg) or severe (<10 mmHg).²²⁸ Low Pti O_2 values

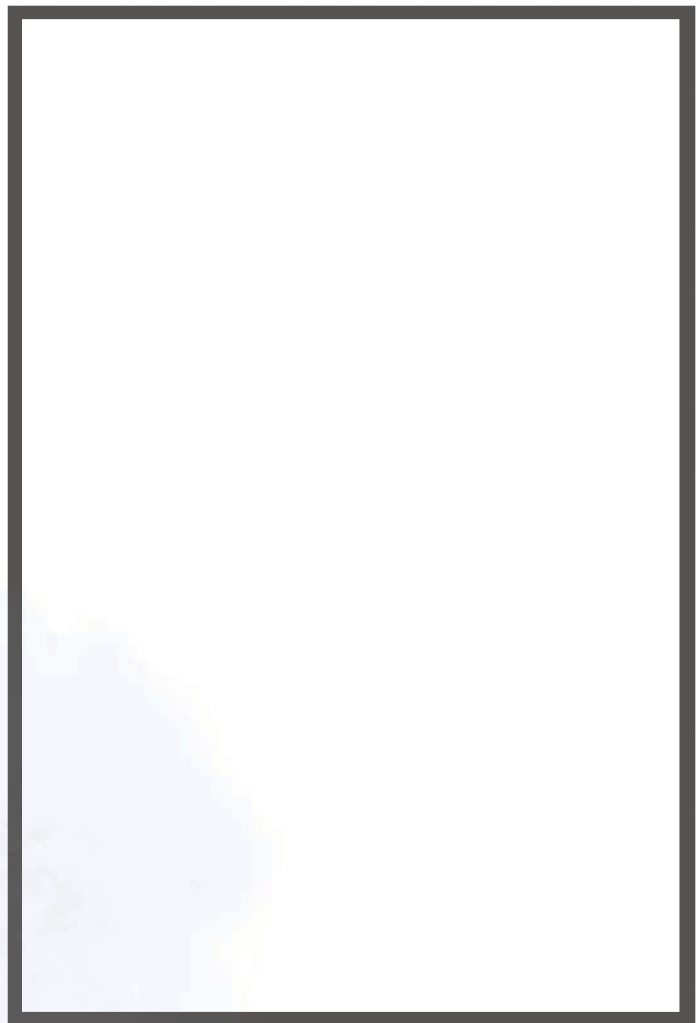
have been related to poor functional outcome.²²⁹ Differential diagnosis is required to define the different causes of hypoxia. Clinicians can establish the etiology of tissue hypoxia with the help of continuous PtiO₂ monitoring combined with hemometabolic variables (Hb concentration, affinity between Hb and O₂, cerebral blood flow, the number of functioning capillaries, O₂ diffusion through the cell membrane, and the characteristics of the extracellular space). Detection of low PtiO₂ can help to 1) identify cerebral ischemia phenomena, 2) establish a differential diagnosis according to the type of tissue hypoxia, 3) individually guide the overall treatment of a patient, and 4) evaluate the effectiveness and repercussions of therapeutic maneuvers.

SECTION



HYPOTHESES & OBJECTIVES

2



HYPOTHESES AND OBJECTIVES

The pathophysiology of TBI includes brain tissue hypoxia, energy failure, and cell death due to the depression of the aerobic metabolism and the inability of the brain tissue to maintain ionic homeostasis, among other mechanisms. The mechanisms of this energy failure are still poorly understood and not well established. Modern MNM, including PtiO₂ and MD monitoring, is widely used in neurocritical care units and allows for the quasi-continuous profiling of brain oxygen supply and brain metabolism.

The working **hypotheses** included the following:

1. Continuous cerebral MD monitoring of the ionic composition of the extracellular space of patients with acute brain lesions (TBI or MMCAI) allows for the definition of the different ionic profiles of brain edema in patients with acute neurological injuries. We hypothesized that the different areas of the injured brain (normal injured brain, traumatic/ischemic penumbra, and traumatic/ischemic core) should present a different ionic profile related to the tissue damage.
2. Normobaric brain oxygen therapy (FiO₂ 1.0, 1 ATA) applied for 4 hours might be an effective therapeutic technique in patients with TBI since this therapy can partially or completely reverse alterations in brain energy metabolism without increasing the risk of oxidative stress.
3. The metabolic profile of hypoxia can be modeled and reproduced *in vitro* in adult human brain cultures. *In vitro* studies allow for a better definition of the abnormal metabolic profiles observed in TBI patients.

Based on these hypotheses, the specific outlined **objectives** include the following:

1. To study the ionic profile of the extracellular space in different regions of the injured brain defined by the area of the brain sampled by the MD catheter in a cohort of patients with TBI and MMCAI.
2. To evaluate the metabolic response of TBI patients to 4 hours of normobaric brain oxygen therapy and to determine whether hyperoxia increases oxidative stress by measuring the changes in the baseline levels of 8-iso-PGF₂ α in MD and plasma samples.
3. To conduct *in vitro* experiments to study the relative recovery of 8-iso-PGF₂ α , one the most reliable biomarkers of oxidative stress *in vivo*, and the feasibility of recovering it in the human brain.
4. To reproduce *in vitro* the abnormal brain metabolic profiles and the changes in the glycolytic machinery described in one of the types of hypoxia by Siggaard-Andersen in 1995 (low-extractivity hypoxia).

SECTION



STUDIES CONDUCTED

3

- 1 **“MICRODIÁLISIS CEREBRAL EN EL PACIENTE NEUROCRÍTICO”**
- 2 **CHARACTERIZATION OF THE IONIC PROFILE OF THE EXTRACELLULAR SPACE OF THE INJURED AND ISCHEMIC BRAIN: A MICRODIALYSIS STUDY**
- 3 **DOES NORMOBARIC HYPEROXIA CAUSE OXIDATIVE STRESS IN THE INJURED BRAIN? A MICRODIALYSIS STUDY USING 8-ISO-PGF₂ α AS A BIOMARKER**

STUDIES CONDUCTED

This doctoral thesis is presented as a compendium of publications with one textbook chapter and two original articles published in peer-reviewed journals:

1. Poca MA, Sahuquillo J, Vidal-Jorge M, Anuncibay V. **Microdiálisis cerebral en el paciente neurocrítico**. In: Rodríguez-Villar S, Amballur D, editors. *Critical Care*. Madrid: Marbán libros S.L.; 2017. p. 656 – 662. [In press]

One of the main aims of the treatment of patients with severe TBI is to prevent secondary lesions. Hence, early detection of brain metabolic dysfunction is important. Cerebral MD is an extremely sensitive technique that can provide metabolic information at bedside in almost real time. The aim of the textbook chapter was to conduct a methodological and conceptual review of cerebral MD for its application in neurocritical patients.

2. T. Martínez-Valverde, A. Sánchez-Guerrero, M. Vidal-Jorge, R. Torné, L. Castro, D. Gandara, F. Munar, M.-A. Poca, and J. Sahuquillo. **Characterization of the Ionic Profile of the Extracellular Space of the Injured and Ischemic Brain: A Microdialysis Study**. *J. Neurotrauma*. Jan. 2017; vol. 34, no. 1, pp. 74–85.

TBI and IS cause a variable disruption of ionic homeostasis and massive ionic fluxes with subsequent osmotic water movement across the cells. Changes in ionic concentrations induce water accumulation in the intracellular and extracellular space and cause brain edema and deformation of the damaged brain tissue. Brain edema is the most frequent cause of neurological worsening and death in patients with severe TBI and MMCAI. In these patients, osmotherapy is a first line therapy for managing increased ICP. Osmotic agents (mannitol and hypertonic saline solutions) are used because they are maintained within the intravascular compartment and are excluded from the brain ECS via the BBB.

However, whether the BBB is tight or leaky can dramatically change the effects of the osmotic solutions on the brain and its effects on ICP.

Cerebral MD has been used extensively to study the neurochemistry of the brain, but the study of ionic profiles in the brain ECS has rarely been reported in experimental models or humans. Notably, a few clinical studies have concentrated on $[K^+]_o$ ²³⁰⁻²³³ as a BM of brain tissue injury severity, brain ischemia, and necrotic death.^{231,234} The ionic profile is severely disrupted in ischemic and injured brain tissue, and it is important to identify the hallmarks of tissue that is at risk and compare them to tissue that is irreversibly damaged and cannot be rescued.

In a previous study, our group showed that the *in vitro* RR for Na^+ , K^+ , and Cl^- was ~100% and that the *in vivo* ionic concentration can be calculated reliably from the microdialysate concentrations in patients with acute brain injuries.²²⁰ However, the main limitation of the methodology used in our proof-of-concept study was its low temporal resolution. ICP-MS is a state-of-the-art instrumental technique for analyzing metals, including ions at very low concentrations. ICP-MS is most accurate for ions in low-volume/low-concentration samples.²²¹ However, because of the high cost of the equipment, it is rarely used in the analysis of ions.²²¹ In this study, we show the first use (to the best of our knowledge) of cerebral MD with ICP-MS to define the human ionic profile of the ECS. We present data on the ionic features of the different regions of the injured brain in a cohort of patients with TBI and MMCAI.

3. M. Vidal-Jorge, A. Sánchez-Guerrero, G. Mur-Bonet, L. Castro, A. Rădoi, M. Riveiro, N. Fernández-Prado, J. Baena, M. A. Poca, and J. Sahuquillo. **Does normobaric hyperoxia cause oxidative stress in the injured brain? A microdialysis study using 8-iso-PGF2 α as a biomarker.** *J. Neurotrauma*. Apr 2017. [Epub ahead of print]

The management of severe TBI is still based on the assumption that most of the brain damage is delayed (secondary injury) and that interventions directed towards prevention and early treatment of secondary injuries make a difference in both survival and functional outcome.⁵ Hypoxemia has been shown to be a secondary brain insult and a strong independent factor of poor neurological outcome in

patients with severe TBI.^{235,236} In the last two decades, significant insight has been gained about the underlying pathophysiology of secondary lesions. Ischemic and non-ischemic tissue hypoxia have been shown to be highly prevalent after severe TBI.³⁶ Direct assessment of brain PtiO₂ can be used at the bedside to closely monitor the concentration of free oxygen available in the tissue that is a surrogate index of the balance between oxygen supply and consumption. Different retrospective studies have shown that low PtiO₂ is associated with high mortality and poor neurological outcome.²³⁷

Potential therapies for this situation have recently been tested. NBO has been tested in a variety of models of TBI and in pilot clinical trials. NBO treatment using 100% FiO₂ at 1 ATA is easily achieved in mechanically ventilated patients. Clinical non-randomized studies suggest that it could be used as a potential treatment to improve brain oxygenation and some of the metabolic disorders resulting from TBI.²³⁸ However, there is still significant controversy regarding this treatment because the metabolic results are contradictory,⁶⁻¹² and the potential clinical benefit of NBO is based on retrospective studies, studies using historical controls, or non-randomized clinical studies.^{11,239} The main concern raised by NBO is the potential toxicity of using supranormal levels of PaO₂.

The mechanisms by which supra-normal O₂ may worsen outcome in patients with acute brain injuries is not yet clear, but high FiO₂ could induce vasoconstriction, exacerbate OxS, increase neuroinflammation, or induce excitotoxicity.¹³ Among these proposed mechanisms, the capacity of NBO to induce OxS is the most important because of the ability of O₂ to induce the production of reactive oxygen species and therefore damage proteins, lipids, and DNA.¹⁴ Thus, despite the potential benefits in brain metabolism, NBO is still controversial and raises many concerns that need to be clarified before entering clinical trials or using it routinely in some patients with brain injuries.

ROS can be measured either directly or indirectly based on the formation of oxidative by-products of lipids, proteins, or nucleic acids. Isoprostanes are stable products of arachidonic acid peroxidation in both animals and humans. They are regarded as the most reliable BMs of OxS *in vivo* and thus provide an important tool for exploring the role of OxS in the pathogenesis of human disease. Isoprostane 8-Iso-prostaglandin F₂α (8-iso-PGF₂α) is considered the gold standard for measuring

OxS *in vivo*.^{27,31} Recent studies have correlated plasma levels of 8-iso-PGF2 α with the Glasgow coma scale (GCS) and shown that it is a good predictor of mortality and outcome with similar sensitivity to GCS.^{31,32} Due to their low molecular weight (< 5000 Da), isoprostanes can be analyzed by MD and can therefore be used as BMs of OxS in patients with TBI. Isoprostanes can be measured using different analytical methods. However, LC/MS is the optimal method and has advantages of high sensitivity, specificity, and the possibility of analyzing small volumes of biological fluids.^{121,122}

The aims of this study were to assess the metabolic response of the injured brain to 4 hours of NBO treatment and to determine whether hyperoxia increases OxS in either the apparently normal brain or in the regions around focal lesions (traumatic penumbra). This assessment was accomplished using 8-iso-PGF2 α as a BM for OxS *in vivo*.²⁴⁰

In addition to the presented articles, additional studies were conducted to study the abnormal brain metabolic profiles and the changes in the glycolytic machinery in low-extractivity hypoxia, using an *in vitro* human model, to confirm or refute the working hypotheses. These studies are detailed in the annex section of this report.



01

MICRODIÁLISIS CEREBRAL EN EL PACIENTE NEUROCRÍTICO

M. A. POCA, J. SAHUQUILLO, M. VIDAL-JORGE, V. ANUNCIBAY
CRITICAL CARE. MADRID: MARBÁN LIBROS S.L.; 2017. P. 656—662. [IN PRESS]

REPRODUCED IN THIS DOCTORAL THESIS WITH PERMISSION. EDITORS. SANCHO RODRÍGUEZ-VILLAR
AND AMBALLUR DAVID JOHN. CRITICAL CARE, THIRD EDITION. MADRID: MARBÁN S.L; 2017

Microdiálisis cerebral en los pacientes neurocríticos

María A. Poca, Juan Sahuquillo, M. Vidal-Jorge y Vanesa Anuncibay

INTRODUCCIÓN

Uno de los objetivos fundamentales del tratamiento de los pacientes con un traumatismo craneoencefálico (TCE) es la prevención de lesiones cerebrales secundarias, de aquí la importancia de poder realizar una detección precoz de la isquemia tisular cerebral. La microdiálisis cerebral permite conocer, en tiempo casi real, los acontecimientos metabólicos que tienen lugar en el encéfalo (disponibilidad de sustratos como la glucosa y producción de diversos metabolitos y neurotransmisores) y realizar, con algunas limitaciones, mediciones continuas de diversos metabolitos a la cabecera del paciente. Además de estas posibilidades, la disponibilidad actual de membranas de diálisis de alta resolución (100 KDa) permite realizar estudios proteómicos que permitirán profundizar en el conocimiento de la fisiopatología de las lesiones neurológicas agudas (ver protocolos 81, 90 y 96).

INDICACIONES

De acuerdo con las conclusiones de un panel de expertos reunido en el Instituto Karolinska de Estocolmo en el año 2002 y publicadas en 2004, los pacientes que más se beneficiarían de incluir la microdiálisis cerebral en su neuromonitorización serían los que han presentado un TCE grave o una HSA. En ambos casos el objetivo de la monitorización con esta técnica sería el mismo: realizar una detección precoz de los cambios metabólicos que sugieran la aparición de isquemia tisular y monitorizar el efecto de las maniobras terapéuticas aplicadas en su tratamiento.



de incluir la microdiálisis cerebral en su neuromonitorización serían los que han presentado un TCE grave o una HSA. En ambos casos el objetivo de la monitorización con esta técnica sería el mismo: realizar una detección precoz de los cambios metabólicos que sugieran la aparición de isquemia tisular y monitorizar el efecto de las maniobras terapéuticas aplicadas en su tratamiento.

- En los TCE deberían colocarse uno o dos catéteres cerebrales en función del tipo de lesión.
- En las lesiones difusas se recomienda la implantación de un único catéter cerebral en la región frontal derecha.
- En las lesiones focales se recomienda la colocación de dos catéteres, uno en una región cerebral macroscópicamente no lesionada y el segundo a nivel de una «zona

de penumbra» (territorio cerebral que rodea a una lesión focal y que se encuentra en una situación de mayor riesgo). En la conferencia de consenso se consideró que la información que puede obtenerse de la implantación de un catéter adicional en el seno de una lesión establecida no ofrece una información relevante para el manejo terapéutico del enfermo.


- En los pacientes con una HSA se recomienda la colocación de un único catéter cerebral, aunque debe implantarse en el territorio vascular de mayor riesgo.

Los analitos recomendados, y la importancia relativa de cada uno de ellos, en ambas patologías es la siguiente:

1. HSA: glutamato e índice lactato/piruvato y
2. TCE: índice lactato/piruvato, glucosa, glicerol y glutamato.

La Tabla 94-1 resume las conclusiones de esta conferencia de consenso.

De forma más reciente, en la conferencia de consenso sobre neuromonitorización en el paciente neurocrítico promovida por la NICEM (*Neuro-Intensive Care and Emergency Medicine*), sección de la ESICM (*European Society of Intensive Care Medicine*), el panel de expertos concluye:

- A pesar del incremento en la aplicación de la microdiálisis cerebral en el manejo clínico de los pacientes con un TCE grave, debemos recordar que no existe evidencia de clase I sobre el uso rutinario de esta técnica. 
- La microdiálisis es la única herramienta que nos permite realizar una monitorización continua de las características

657

Tabla 94-1. Conclusiones de la conferencia de consenso de Estocolmo sobre microdiálisis cerebral en el paciente neurocrítico 

	HSA	TCE
Indicaciones	Paciente graves que requieran monitorización de la PIC y de la PPC	
Catéteres	Un catéter en territorio vascular con riesgo de isquemia	Lesión difusa: 1 catéter Lesión focal: 2 catéteres
Valores	Despreciar los valores de la primera hora	
Metabolitos a determinar	Glutamato Índice lactato-piruvato	Índice lactato-piruvato Glucosa/glicerol/ glutamato

HSA: Hemorragia subaracnoidea. TCE: Traumatismo craneoencefálico. PIC: Presión intracraneal. PPC: Presión de perfusión cerebral.

658

bioquímicas del espacio extracelular del parénquima encefálico. Esta información es mucho más fiable que cualquier otro biomarcador obtenido a nivel de sangre periférica.

- La microdiálisis puede ayudar a realizar un diagnóstico diferencial de las distintas formas de hipoxia tisular de origen no isquémico.
- La microdiálisis cerebral de alta resolución permite recuperar sustancias adicionales contenidas en el espacio extracelular, tales como citocinas, interleucinas y otras moléculas inflamatorias, que van a permitir conocer mejor la fisiopatología de las lesiones neurológicas agudas.
- Esta técnica constituye una herramienta idónea para obtener una información directa sobre el paso de fármacos a través de la barrera hematoencefálica y de su repercusión a nivel metabólico, lo que va a permitir realizar estudios sobre fármacos neuroprotectores de forma más racional y efectiva.

PROCEDIMIENTO

La microdiálisis es una técnica basada en el principio del intercambio de solutos a través de una membrana semipermeable, que emula el funcionamiento de un capilar y cuyos objetivos básicos son: 1) monitorizar la disponibilidad tisular de diferentes metabolitos, 2) monitorizar los elementos liberados por las células y 3) monitorizar las consecuencias celulares de la hipoxia-isquemia tisular. La membrana semipermeable se encuentra en el extremo distal del catéter de microdiálisis y a su través se intercambian solutos entre una solución de composición conocida y el líquido contenido en el espacio extracelular. El análisis del microdializado obtenido permite cuantificar diversos metabolitos derivados de rutas metabólicas fisiológicas o productos que se producen como resultado de una lesión tisular.

Metabolitos a determinar

En el encéfalo, la colocación de un catéter de microdiálisis permite el análisis y cuantificación de los cambios que se producen en diversos metabolitos «energéticos» como: lactato, piruvato, adenosina, inosina o hipoxantina. También permite estudiar la liberación de neurotransmisores y neuromoduladores (glutamato, aspartato, taurina, GABA...) o la liberación de productos de degradación tisular (glicerol). Sin embargo, para que esta información sea válida deben considerarse algunos aspectos metodológicos. Además, la información obte-

nida por los catéteres cerebrales debe contrastarse con la información proporcionada por un catéter adicional colocado en el tejido subcutáneo. Este último aporta información sobre el metabolismo sistémico (extracerebral).

659

Aspectos metodológicos

Los *catéteres de microdiálisis* son elementos flexibles, de pequeño diámetro (menor a 1 mm), que contienen una doble luz y en cuyo extremo se sitúa una membrana semipermeable. A través de esta membrana se produce el paso de pequeñas moléculas, que difunden libremente a favor de un gradiente osmótico. La luz interna del catéter contiene una solución libre de las moléculas a estudiar (solución Ringer sin lactato o suero salino isotónico). El catéter se acopla a una **microbomba de infusión continua**, que infunde la solución a una velocidad constante y predeterminada. En el extremo distal del catéter, y a través de la membrana semipermeable, se produce un intercambio de solutos de un determinado peso molecular (menor a 20 KDa en los catéteres estándar y hasta 100 KDa en los catéteres de alta resolución). El microdializado obtenido contiene moléculas procedentes del espacio extracelular y fluye a través de la luz externa del catéter, recuperándose a través de **microviales** que se sustituyen periódicamente. Un **equipo analizador portátil** analiza el microdializado mediante técnicas enzimáticas y cuantifica los cambios que se han producido en la composición inicial de la solución. Cuando se utilizan catéteres con una membrana de diálisis de 10 mm de longitud y la velocidad de flujo de la perfusión es de 0,3 $\mu\text{l}/\text{min}$, la recuperación de metabolitos es de un 70% de su contenido real en el espacio extracelular cerebral.

En la mayoría de centros el catéter de microdiálisis cerebral se implanta en quirófano, a través de un orificio de trépano o después de haber evacuado una lesión, con introducción del catéter bajo visión directa. Sin embargo, estos catéteres también pueden insertarse a través de un tornillo roscado a la calota craneal o mediante un sistema percutáneo similar al que utilizamos para implantar un sensor de PIC. Al igual que en otros sistemas de monitorización locales, el catéter cerebral debe implantarse en una región que permita obtener la información más útil para el manejo clínico del enfermo. La implantación de un catéter en el tejido «sano» ofrece la posibilidad de monitorizar el tejido con mayores posibilidades de recuperación, mientras que la colocación en las áreas de «penumbra», considerando como tales las zonas adyacentes a las lesiones focales, permiten el seguimiento de regiones cerebrales sometidas a un mayor riesgo de isquemia tisular.

660

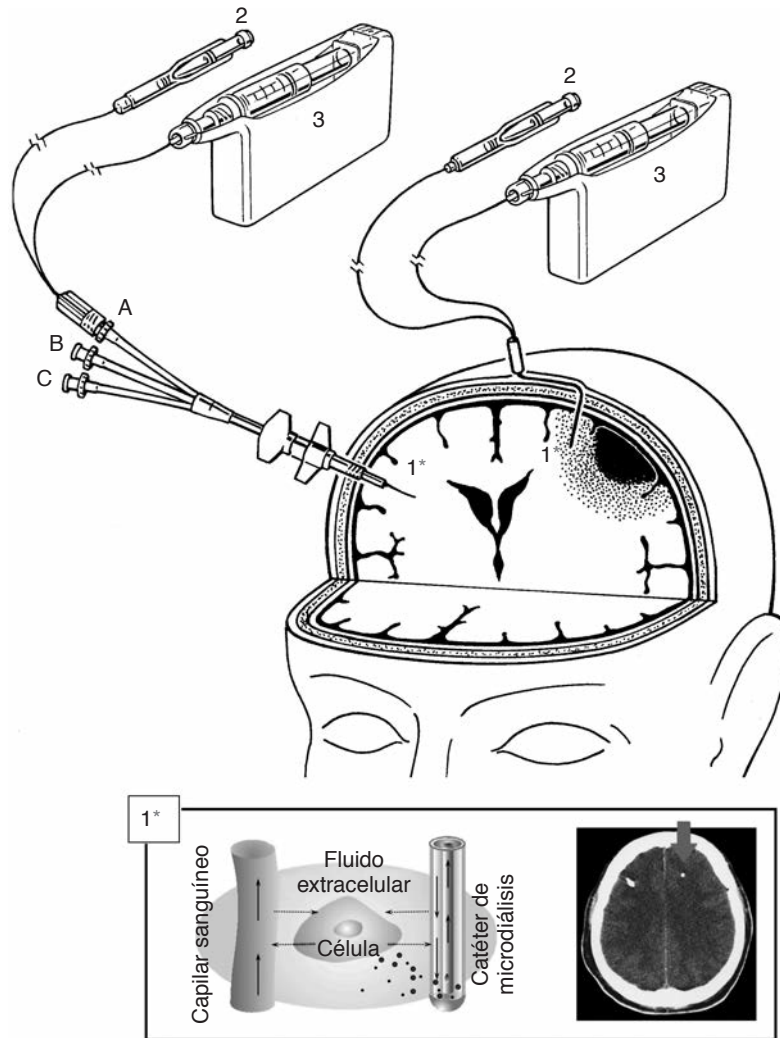


Figura 94-1. Catéteres de microdiálisis cerebral (1*) implantados en tejido aparentemente normal (derecha) y en el área de penumbra traumática (izquierda). El catéter implantado en el hemisferio derecho se ha introducido a través de un tornillo de tres vías (A), quedando disponibles las dos luces restantes (B y C) para implantar catéteres de presión intracraneal, presión tisular de oxígeno o temperatura. El catéter situado en el área de penumbra se ha introducido mediante una técnica percutánea. La imagen muestra un esquema del microdializador (2) y de la microbomba de infusión (3). En el recuadro inferior puede observarse un esquema del extremo dializante del catéter de microdiálisis (1*) y el aspecto del catéter en la TC cerebral (flecha).

Sección VII • Neurología

Valores normales

Uno de los problemas fundamentales de la microdiálisis radica en establecer los valores de normalidad de los diferentes metabolitos. Dada la imposibilidad ética de monitorizar a indi-



02

**CHARACTERIZATION OF THE IONIC PROFILE OF THE
EXTRACELLULAR SPACE OF THE INJURED AND ISCHEMIC BRAIN:
A MICRODIALYSIS STUDY**

**T. MARTÍNEZ-VALVERDE, A. SÁNCHEZ-GUERRERO, M. VIDAL-JORGE, R. TORNÉ,
L. CASTRO, D. GANDARA, F. MUNAR, M. A. POCA, AND J. SAHUQUILLO
J. NEUROTRAUMA. JAN. 2017; VOL. 34, NO. 1, PP. 74–85**

REPRODUCED IN THIS DOCTORAL THESIS WITH PERMISSION.

Characterization of the Ionic Profile of the Extracellular Space of the Injured and Ischemic Brain: A Microdialysis Study

Tamara Martínez-Valverde,¹ Angela Sánchez-Guerrero,¹ Marian Vidal-Jorge,¹ Ramon Torné,^{1,2} Lidia Castro,¹ Dario Gandara,² Francisca Munar,³ Maria-Antonia Poca,^{1,2} and Juan Sahuquillo^{1,2}

Abstract

Traumatic brain injury (TBI) and ischemic stroke cause a variable disruption of ionic homeostasis and massive ionic fluxes with subsequent osmotic water movement across the cells that causes edema, brain swelling, and deformation of the damaged tissue. Although cerebral microdialysis (CMD) has been used to study the brain neurochemistry, the ionic profiles of brain interstitial space fluid have rarely been reported in humans. We studied the ionic profile in injured areas of the brain by using CMD. As a control group, we included seven patients who had undergone surgical treatment of posterior fossa lesions, without abnormalities in the supratentorial compartment. Inductively coupled plasma mass spectrometry (ICP-MS) was used for ion determination. No significant differences were found in the $[Na^+]_o$, $[K^+]_o$, and $[Cl^-]_o$ between normal injured brains and controls. The ionic profile of the ischemic core was characterized by very high $[K^+]_o$ and an increase in $[Na^+]_o$, whereas $[Cl^-]_o$ was linearly related to $[Na^+]_o$. In the traumatic core (TC), significantly higher levels of $[Na^+]_o$, $[Cl^-]_o$, and $[K^+]_o$ were found. The main finding in the penumbra was a completely normal ionic profile for $[Na^+]_o$ and $[K^+]_o$ in 60% of the samples. ICP-MS coupled to ionic assays creates a powerful tool for a better understanding of the complex ionic disturbances that occur after severe TBI and ischemic stroke.

Keywords: brain microdialysis; ischemic stroke; potassium; sodium; TBI

Introduction

IN THE MAMMALIAN CENTRAL NERVOUS SYSTEM (CNS), both glial cells and neurons have a stable internal ionic composition that is not in equilibrium with the interstitial space fluid (ISF). Therefore, ionic gradients across excitable cells in the CNS must be extremely well regulated to maintain the resting membrane potential and the depolarization and repolarization capability that underlies neuronal signaling. Under steady state, the intracellular concentration of potassium ($[K^+]_i$) in the CNS is typically ~ 145 mmol/L, and the extracellular potassium concentration ($[K^+]_o$) is ~ 3 mmol/L.^{1–3} Transmembrane sodium gradients have the opposite orientation, and the extracellular concentration of sodium ($[Na^+]_o$) is much higher than its intracellular concentration ($[Na^+]_i$). The adenosine triphosphate (ATP)-dependent Na^+/K^+ -pump of intact brain cells maintains a concentration gradient between the intracellular and extracellular compartments of $\sim 1:10$. Water and small solutes such as ions, sugars, and amino acids are the main players in the maintenance of the cell volume via complex osmoregulatory phenomena. The neural cell membranes are usually impermeable to

these solutes and, therefore, ion channels, transporters, and a myriad of specialized proteins are needed to move ions in and out of the cell via facilitated or active transport.⁴

Traumatic brain injury (TBI) and ischemic stroke cause a variable disruption of ionic homeostasis and massive ionic fluxes with subsequent osmotic water movement across the cells. Changes in ionic concentrations induce water accumulation in the intracellular and ISF and cause brain edema and deformation of the damaged brain tissue.⁵ Brain edema is the most frequent cause of neurological worsening and death in patients with severe TBI and malignant ischemic stroke. In these patients, osmotherapy is a first line therapy for managing increased intracranial pressure (ICP). Osmotic agents (mannitol and hypertonic saline solutions [HTS]) are used because they are maintained within the intravascular compartment and are excluded from the brain ISF via the blood–brain barrier (BBB). However, whether the BBB is tight or leaky can dramatically change the effects of the osmotic solutions on the brain and its effects on ICP.

Cerebral microdialysis (CMD) is a tool increasingly embraced in neurocritical care units in the management of patients with severe

¹Neurotraumatology and Neurosurgery Research Unit (UNINN), and Departments of ²Neurosurgery and ³Anesthesiology, Vall d'Hebron University Hospital, Universidad Autònoma de Barcelona, Barcelona, Spain.

TBI and aneurysmal subarachnoid hemorrhage who are comatose.⁶ In a report in the International Multidisciplinary Consensus Conference on Multimodality Monitoring in Neurocritical Care, CMD monitoring was recommended in patients with or at risk of cerebral ischemia, hypoxia, energy failure, and glucose deprivation.⁶ CMD has been extensively used to study the neurochemistry of the brain; however, the study of ionic profiles in the brain ISF has rarely been reported in experimental models or humans. It is of note that a few clinical studies have concentrated on $[K^+]_o$,⁷⁻¹⁰ because the increase in $[K^+]_o$ is a biomarker for the severity of the brain tissue injury, brain ischemia, and necrotic death.^{8,11} In addition, some clinical studies in TBI have shown that an increased $[K^+]_o$ is a strong predictor of severe physiological deterioration and a poor outcome.^{8,10,12} The ionic profile is severely disrupted in ischemic and injured brain tissue, and it is important to identify the fingerprints of tissue that is at risk and compare them to tissue that is irreversibly damaged and cannot be rescued. Further, knowledge about the ionic profile of the brain ISF is essential to understanding complex pathophysiological phenomena, such as cortical spreading depolarization (CSD) and brain edema, as well as the effects of drugs used to treat edema, such as HTS.

In a previous study, our group showed that *in vitro*, the relative recovery (RR) for Na^+ , K^+ and Cl^- was ~100% and that the *in vivo* ionic concentration can be reliably calculated from the microdialysate concentrations in patients with acute brain injuries.² However, the main limitation of the methodology used in our proof-of-concept study — conventional ion selective electrode based analyzer — was its low temporal resolution. Inductively coupled plasma mass spectrometry (ICP-MS) is a state-of-the-art instrumental technique for the analysis of metals, including ions at very low concentrations. ICP-MS is most accurate for ions in low-volume/low-concentration samples.¹³ However, because of the high cost of the equipment, it is rarely used in the analysis of ions.¹³ Here we show, to the best of our knowledge, the first use of CMD with ICP-MS to define the human ionic profile of the ISF. We present data on the ionic fingerprints of the different regions of the injured brain in a cohort of patients with TBI and malignant infarction.

Methods

Study design and sample collection

A prospective study was conducted in patients >17 years of age admitted to the Neurotraumatology Intensive Care Unit at Vall d'Hebron University Hospital with moderate/severe TBI (Glasgow Coma Scale score ≤ 13) or malignant stroke (MS). All patients received ICP and CMD monitoring during 48 h post-injury or MS onset between February 2011 and July 2014. Briefly, a CMA-71 CMD catheter with a 100 kDa cutoff membrane (M Dialysis AB, Stockholm, Sweden) was used in all the patients; the position of the probe was confirmed with a computed tomography (CT) scan conducted within the first 12 h after probe implantation as previously described.² The CMD catheters were usually inserted in uninjured brain tissue and/or in regions of interest according to the previously described methodology.¹⁴

Patients who underwent surgical treatment of posterior fossa lesions, and did not present any abnormality in the supratentorial compartment were included as a control group. Patients had an Evans' index ≤ 0.30 and required the implantation of an intraventricular catheter to drain cerebrospinal fluid (CSF) during surgery and at least 24 h postoperatively. During the intraventricular catheter implantation, a CMA-71 probe was also inserted in parallel via the same burr hole in the posterior frontal region 10.5 cm from the

nasion and 3 cm from the midline (Fig. 1A). In both groups cerebral catheters were perfused with a sterile isotonic CNS fluid containing 147 mmol/L NaCl, 1.2 mmol/L $CaCl_2$, 2.7 mmol/L KCl, and 0.85 mmol/L $MgCl_2$ (P000151, M Dialysis AB) at a fixed flow rate of 0.3 $\mu L/min$ using a CMA-106 pump (P000003, M Dialysis AB).

All provisions of the Declaration of Helsinki were followed. The Internal Review Board of Vall d'Hebron University Hospital in Barcelona approved these studies (PR-ATR-286/2013 and PR-AG-140/2011) and written informed consent was obtained from all of the patients or the patient's next-of-kin.

The microdialysis probe, the infusion pump, and the perfusate

The CMA-71 probes used in this study are approved for clinical use in Europe (CE marking approval according to the Medical Device Directive 93/42/EEC). According to the manufacturer's specifications, this probe has a nominal cutoff of “~100 kDa.” The 60 mm shaft is made of polyurethane and has an outer diameter of 0.9 mm. The polyarylethersulphone dialysis membrane is 10 mm long with an outer diameter of 0.6 mm. The inlet and outlet tubes are also made from polyurethane and have a 1 mm outer diameter. Cerebral catheters were perfused with a sterile isotonic CNS fluid containing 147 mmol/L NaCl, 1.2 mmol/L $CaCl_2$, 2.7 mmol/L KCl, and 0.85 mmol/L $MgCl_2$ (P000151, M Dialysis AB) at a fixed flow rate of 0.3 $\mu L/min$ using a CMA-106 pump (P000003, M Dialysis AB). In this routine, the dialysates are collected hourly by the nurse in charge of the patient via capped microvials that are specially designed to collect microvolumetric samples and minimize evaporation. Lactate, pyruvate, glucose, and glycerol (Gly) are routinely monitored at the bedside using an Iscus Flex microdialysis analyzer (8003295, M Dialysis AB). After these hourly measurements were completed, the microvials were placed in a rack to seal them and prevent evaporation (P000028, M Dialysis AB). All racks were stored at $-86^\circ C$ until further analysis.

The extracellular levels of glycerol ($[Gly]_o$) were used in this study as a biomarker for tissue viability. Some studies have shown that $[Gly]_o$ increases as a result of membrane disruption caused by cell injury.^{15,16}

Inductively coupled plasma mass spectrometry analysis

In this study, the determination of all ions was performed on an ICP-MS analyzer (Agilent 7500ce, Agilent Technologies, Santa Clara, CA) with collision cell technology using He as inert gas at 5 mL/min. For CMD samples, the minimum volume needed to perform the ion measurements is 12 μL . The Iscus Flex analyzer consumes 5 μL for routine bedside analysis of glucose, lactate, pyruvate, and Gly and 8 μL if glutamate is included. Because of this, it was necessary to pool the residual content of two microvials to obtain the minimum required volume for assaying TBI and stroke samples. In the control group — in which glutamate was not quantified — the residual volume of one microvial was sufficient for the analysis. For ICP-MS analysis, 15 μL of the pooled or 12 μL of the residual sample was diluted in 1% HNO_3 (v/v) to obtain a final volume of 2.5 mL or 2 mL, respectively. The lower limit of detection for the Agilent 7500ce, on diluted samples, was 5 mmol/L for Na^+ , 1 mmol/L for K^+ and 5 mmol/L for Cl^- . For TBI and MS samples, the microvials corresponding to the first 24 h of monitoring were defrosted on ice to yield 12 determinations per patient. In the control group, the first two microvials collected during the waking state were used to determine the ionic profile as described.

ICP-MS versus ion-selective electrode

To verify whether we could use our previously defined linear model to determine the ionic concentrations in the brain ISF,² we

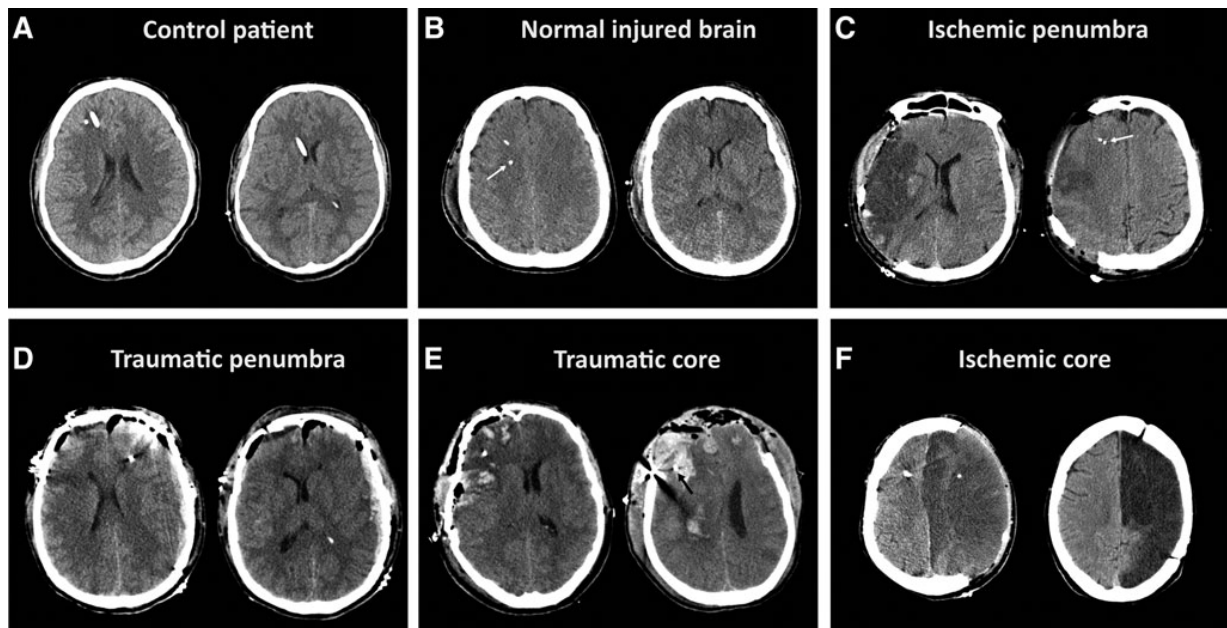


FIG. 1. Examples of the different brain areas defined according to the placement of the cerebral microdialysis (CMD) catheter. For further explanation, see the Material and Methods section. **(A)** Control patient. A 34-year-old male operated on for a right giant vestibular schwannoma. The tip of the cerebral microdialysis probe is shown on the left of the ventricular catheter that is placed in the right frontal horn. **(B)** Normal injured brain. A 46-year-old male admitted to the neurocritical care unit after severe traumatic brain injury (TBI) with an admission Glasgow Coma Scale (GCS) score of 4. The patient was included in the diffuse injury II of the Marshall's classification. The control CT showed that both the CMD probe (arrow) and the brain tissue oxygen (PtiO₂) probe (anterior to the CMD probe) were inserted in the frontal subcortical white matter in a brain region without any observed gross abnormality. **(C)** Ischemic penumbra. A 46-year-old male admitted to our institution 5h after an abrupt onset of left hemiparesis. The National Institute of Health Stroke Scale (NIHSS) score on admission was 13. Because of the clinical and neuroradiological evolution to a malignant stroke, the patient underwent decompressive hemicraniectomy 32 h after the stroke onset. On the left CT scan, the infarction extension is seen with preservation of the anterior cerebral artery territory. On the right CT, the CMD catheter (arrow) is shown 27 mm from the hypodense lesion (ischemic core). **(D)** Traumatic penumbra. A 52-year-old male was injured in a blast. His GCS score on admission was 5. On admission, he was operated on for a left-acute subdural hematoma, left frontal contusion, and right extradural hematoma. A CMD probe was inserted at the end of surgery in the left frontal lobe (left CT scan). **(E)** Traumatic core. A 48-year-old male was admitted because he had sustained a brain injury in his workplace. His GCS score on admission was 7. He was immediately operated on for evacuation of right hemorrhagic contusion and a bifrontal extradural hematoma. A bifrontal decompressive craniectomy was also performed. In the control CT, the PtiO₂ probe is seen on the left, and the CMD is visible on the right slice (arrow). Some metallic artifacts are generated by an eight electrode electrocorticography strip placed on the right frontal lobe. **(F)** Ischemic core. A 52-year-old male who underwent decompressive hemicraniectomy because of a malignant stroke 14 h after stroke onset. The control CT showed the CMD probe inserted in a large area of hypoattenuation corresponding to the core of the infarction. The control CT scan of the same patient 1 year after surgery (right) shows the residual hypodense necrotic brain.

performed a validation study comparing the selective ion electrodes from the AU5400™ analyzer (Diagnostic Systems Group, New York) used previously² and the new ICP-MS analyzer described here. For this validation study, 20 CSF samples were collected during routine analysis from neurosurgical patients who needed either lumbar or ventricular drainage to treat their primary pathologies. The extracted CSF volumes were centrifuged at 4000 rpm for 5 min, and the supernatant was aliquoted into two tubes that were stored at 4°C until analysis. Ion determination was performed both with the AU5400™ analyzer as described previously² and with the ICP-MS.

Brain tissue definitions

All CT scans and magnetic resonance imaging (MRIs) of stroke patients were reviewed by one of the authors (J.S.), who was blinded to the CMD results. The CT scan closest to the hours of the microdialysate analysis was used to determine the position of the CMD probe. The region of the brain sampled by the CMD catheter was categorized in one of the following categories defined opera-

tively for this study: normal injured brain, ischemic core (IC), traumatic core (TC), traumatic penumbra (TP) and ischemic penumbra (IP). *Normal injured brain* was defined as when the CMD tip was inserted in a region of the brain without any macroscopically visible abnormality (blood or hypodense lesion). For the brain to be considered "normal," the closest hemorrhagic/hypodense lesion must be located at least 30 mm from the tip of the CMD catheter (Fig. 1B). *IP* was a term used in patients with a malignant middle cerebral artery infarction (MMCAI) in which the tip of the CMD probe was placed in a brain region of normal macroscopic appearance around the core with no changes in brain tissue attenuation in a noncontrast CT scan; these regions had to be at least 20 mm away from any brain region with parenchymal abnormalities (Fig. 1C). *TP* arbitrarily defines the position of the probe in the brain parenchyma without any changes in attenuation and that is at least 20 mm away from any intraparenchymal lesion (contusions, hematomas). The TP is also considered when the probe was located in the brain immediately below any significant extracerebral hematoma (Fig. 1D). The *TC* was defined in TBI patients when the CMD probe was placed in areas of brain tissue that had

macroscopically obvious lesions such as contusions or hemorrhages, or when the CMD probe had a small hemorrhagic lesion on the tip (Fig. 1E). IC tissue was defined when the patient had a confirmed diagnosis of MMCAI, and the CMD probe was located in a hypodense lesion with or without a hemorrhagic component. In most patients, the probe was inserted after completing a decompressive craniotomy (Fig. 1F).

Reference intervals for Gly

To establish the upper reference range for Gly, we used the data obtained from a prospective study that was conducted among 15 patients >18 years of age who underwent surgical treatment under standard general anesthesia to treat posterior fossa and supratentorial lesions at Vall d'Hebron University Hospital (VHUH) between November 2012 and July 2015. To enroll patients in the study, the inclusion criteria were: 1) posterior fossa or supratentorial lesions requiring the implantation of an external ventricular catheter for the drainage of CSF; 2) no neuroradiological abnormalities in the white/gray matter in the supratentorial compartment, as evaluated based on the following magnetic resonance MRI sequences: T1 weighted (T1W), T2 weighted (T2W), and fluid-attenuated inversion recovery (FLAIR); 3) a normal ventricular size, which was defined as an Evans' index ≤ 0.30 ; ¹⁷ and 4) written informed consent signed by the patient or the next-of-kin. The study was approved by the Institutional Ethics Committee of the Vall d'Hebron University Hospital (protocol number approval PR/AG-140-2011). The upper reference level for Gly calculated using the robust method was 209 $\mu\text{mol/L}$ (unpublished results).

Statistical analysis

Descriptive statistics were obtained for each variable. For continuous variables, the summary statistics were the mean, median, range, and SD. Percentages and sample sizes were used to summarize categorical variables. The Shapiro–Wilk's test and inverse probability plots were used to test whether the data followed a normal distribution. Median, minimum, and maximum values were used to summarize non-normally distributed variables. To compare the ionic profile in the different groups, a one way ANOVA or the nonparametric Kruskal–Wallis one way ANOVA by ranks was used. Multiple pairwise comparisons to identify which group or groups were significantly different were conducted with the Tu-

key's test in ANOVA and with the Nemenyi's test for the non-parametric multiple comparisons of the ranked data. Statistical analyses were performed with R software v3.1.2 (R Foundation for Statistical Computing, Vienna, Austria; <http://www.R-project.org>) and the integrated development environment R Studio v0.98.1103 (RStudio, Inc., Boston, MA; <http://www.rstudio.com>) The *car* package was used for regression analysis. The Bland and Altman method was used to assess the agreement between the two analyzers ¹⁸ and to calculate the limits of agreement and their 95% CI (<http://CRAN.R-project.org/package=BlandAltmanLeh>).

Results

Comparison between the ion-selective electrode and ICP-MS analyzers

The agreement between both methods was excellent and within ± 1.96 SD of the mean difference for all ions, despite to the fact that the AU5400 analyzer slightly overestimated $[\text{Na}^+]_{\text{CSF}}$ (Fig. 2).

Descriptive data of included patients in the microdialysis study

A total of 34 patients were included; 21 patients had a severe TBI, and 13 had an MS. Table 1 lists a summary of the demographic and clinical data. The 34 patient group yielded 374 verified samples. In Table 2 we present a summary of $[\text{Na}^+]_{\text{o}}$, $[\text{K}^+]_{\text{o}}$, and $[\text{Cl}^-]_{\text{o}}$ by primary pathology and the CMD catheter location.

The control group consisted of seven patients that yielded 14 samples (Table 1). The ionic profiles of the awake controls are summarized in Table 2. We used the percentile of 97.5 to define the upper reference limit, which corresponded to 161.6 mmol/L for $[\text{Na}^+]_{\text{o}}$, 4.1 mmol/L for $[\text{K}^+]_{\text{o}}$, and 157.3 mmol/L for $[\text{Cl}^-]_{\text{o}}$. All of the values in Table 2 were corrected with the linear method described elsewhere.² For the $[\text{Na}^+]_{\text{o}}/[\text{Na}^+]_{\text{plasma}}$ and $[\text{K}^+]_{\text{o}}/[\text{K}^+]_{\text{plasma}}$ ratios, the upper reference limits were 1.16 and 0.88, respectively.

Ionic profile in the "normal" injured brain

With the criteria previously noted, five patients (all in the TBI group) had a CMD probe placed in macroscopically normal brain. This group yielded 59 dialysates. The summary statistics

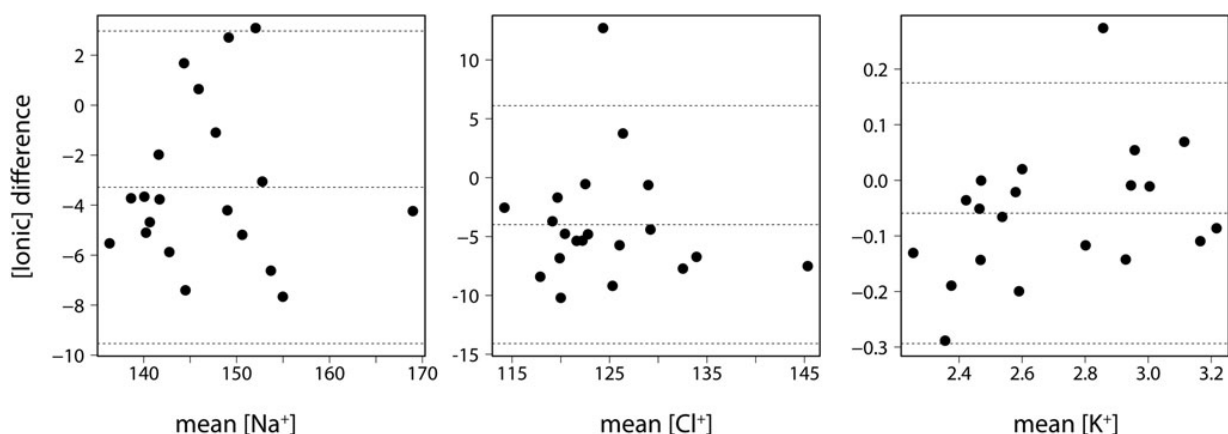


FIG. 2. Bland and Altman's graph evaluating the agreement between the measurements of the ion-selective (IS) and the inductively coupled plasma mass spectrometry (ICP-MS) analyzer. The graph plots the mean of the paired values from each method on the X-axis against the difference of each pair of readings on the Y-axis. The composite plot compares the ICP-MS with the ion selective electrode for each ion (Na+, K+, and Cl-). The difference between the two measurements is on the Y-axis ($[\text{ICP-MS}] - [\text{IS}]$), and the mean of the two measurements for each ion is shown on the X-axis ($([\text{ICP-MS}] + [\text{IS}])/2$). The 95% limits of agreement are shown as two dashed lines.

TABLE 1. SUMMARY OF DEMOGRAPHIC DATA

Group	n	Age	GCS	NIHSS	GOSE	mRS
TBI	21	34 (18 – 57)	5 (3 – 15)	NA	3 (1 – 8)	NA
MMCAI	13	52 (36 – 65)	NA	19 (23 – 14)	NA	4 (3 – 6)
Control	7	38 (22 – 60)	NA	NA	NA	NA

Summary data are presented as median (min–max).

TBI, traumatic brain injury; MMCAI, malignant middle cerebral artery infarction; GCS, Glasgow Coma Scale score; NIHSS, National Institute of Health Stroke Scale; GOSE, Glasgow Outcome Scale Extended; mRS, modified Rankin Scale.

for $[Na^+]_o$, $[K^+]_o$, and $[Cl^-]_o$ are listed in Table 2. Only eight values (all corresponding to the same patient) had a $[Na^+]_o > 162$ mmol/L, both had a $[K^+]_o > 4.1$ mmol/L. Although the difference in mean $[Cl^-]_o$ was 12 mmol/L (141 ± 9.3 in the controls vs. 153.8 ± 11.38 mmol/L in the normal injured brain), the differences between the mean concentrations and the control group were not statistically significant for any of the ions (t test, $p = 0.0574$).

Ionic profile of the ischemic and traumatic core

Twelve patients had the tip of the CMD placed in the hypodense ischemic core. The probe was placed under direct vision at the surgical procedure for all patients (Fig. 1F). This group provided 141 valid microdialysate samples. Summary statistics are listed in Table 2. Thirty-five values (24.8%) had a $[Na^+]_o > 162$ mmol/L, and 88 observations (62.4%) had a $[K^+]_o > 4.1$ mmol/L (Fig. 3). Despite the fact that higher $[Na^+]_o$ values were found in the IC than in the normal tissue in TBI and in the controls, these differences were not statistically significant. However, the $[K^+]_o$ levels were statistically significant when compared with both the controls and the probes placed in the normal brain (Kruskal–Wallis test, $p < 0.001$) (Fig. 3). In all the samples, $[Cl^-]_o$ increased or decreased linearly with $[Na^+]_o$ (Fig. 4B), with a Pearson product-moment correlation coefficient of 0.93 ($p < 0.001$).

According to the definitions noted before, six patients had the CMD probe placed in zones with gross lesions as a result of TBI. These patients yielded 61 samples and the summary statistics are presented in Table 2. Thirty-eight values (52%) had a $[Na^+]_o > 162$ mmol/L, and 49 observations (80%) had a $[K^+]_o > 4.1$ mmol/L (Fig. 3). The differences between the mean concentration and the control group were statistically significant for all of the analyzed ions (Kruskal–Wallis test, $p < 0.001$). The samples with $[Na^+]_o > 162$ mmol/L also had a high $[Cl^-]_o$ (median 182.9 mmol/L, min 151.6, max 276.2) but did not show a significantly higher $[K^+]_o$ (median 6.2 mmol/L, min 2.69, max 11.01), suggesting that a reduction in the volume of the extracellular space, and therefore ionic concentration, was not the main cause of the high $[Na^+]_o$ (Figs. 3 and 4).

The $[Na^+]_o/[Na^+]_{plasma}$ ratio in the traumatic core was significantly higher than that observed in the controls, in the normal-appearing brain and in the IP and TP. However, the IC did not show a significantly increased $[Na^+]_o/[Na^+]_{plasma}$ in comparison with the other damaged or undamaged brain regions. The $[K^+]_o/[K^+]_{plasma}$ ratio was significantly higher in the TC and IC than in the controls, the normal-appearing brain regions, and the IP and TP (ANOVA on ranks, $p < 0.0001$). Therefore, our data suggest that the $[K^+]_o/[K^+]_{plasma}$ ratio is a good biomarker for detecting brain tissue that is at risk or irreversibly damaged.

TABLE 2. IONIC CONCENTRATION AND RATIOS BY PROBE TISSUE LOCATION

Group	$[Na^+]_o$ mmol/L	$[K^+]_o$ mmol/L	$[Cl^-]_o$ mmol/L	$[Na^+]_{plasma}$ mmol/L	$[K^+]_{plasma}$ mmol/L	$[Na^+]_o/[Na^+]_{plasma}$	$[K^+]_o/[K^+]_{plasma}$	Glycerol μ mol/L
Control group	149.9 (144.4 – 161.8)	3.03 (2.78 – 4.08)	140.1 (126.1 – 158.5)	137.4 (134.7 – 142.5)	4.23 (3.39 – 4.60)	1.09 (1.01 – 1.17)	0.79 (0.69 – 0.88)	53.8 (24.4 – 205.0)
Normal brain	145.5 (115.5 – 169.1)	3.08 (2.64 – 6.47)	150.2 (119.6 – 179.9)	139.0 (134.6 – 145.2)	3.59 (3.23 – 4.12)	1.05 (0.82 – 1.19)	0.85 (0.72 – 1.75)	39.3 (10.5 – 150.0)
Penumbra (all)	150.8 (123.9 – 219.9)	3.58 (2.32 – 6.07)	155.7 (117.3 – 224.4)	139.8 (130.7 – 153.2)	4.01 (3.16 – 4.6)	1.06 (0.88 – 1.55)	0.96 (0.55 – 1.50)	71.4 (19.3 – 237.3)
Traumatic penumbra	152.1 (123.9 – 219.9)	3.46 (2.32 – 6.07)	157.8 (125.9 – 224.4)	139.9 (130.7 – 153.2)	4.0 (3.16 – 4.60)	1.06 (0.88 – 1.55)	0.95 (0.55 – 1.50)	76.3 (22.2 – 237.3)
Ischemic penumbra	134.6 (131.2 – 142.8)	4.81 (4.48 – 5.3)	121.7 (117.3 – 132.8)	136.4 (133.5 – 141.6)	136.4 (133.5 – 141.6)	0.99 (0.92 – 1.02)	1.22 (1.04 – 1.32)	26.0 (19.3 – 164.0)
Ischemic core	149.7 (132.7 – 223.1)	5.25 (2.48 – 19.9)	152.0 (136.7 – 228.3)	141.8 (136.9 – 152.0)	3.82 (2.82 – 4.68)	1.05 (0.93 – 1.55)	1.31 (0.63 – 5.08)**	238.0 (17.6 – 1102.0)
Traumatic core	163.0 (143.2 – 264.3)	5.43 (2.56 – 11.0)	166.5 (136.4 – 276.2)	145.7 (138.6 – 166.6)	3.95 (3.16 – 5.08)	1.15 (0.92 – 1.83)**	1.34 (0.72 – 2.25)**	219.5 (36.1 – 5748.0)

For definitions of groups of study, see the text.

The values for glycerol were obtained from a control group of 15 anesthetized patients from another study (for a description, see the text). The $[Na^+]_o/[Na^+]_{plasma}$ was significantly higher in the traumatic core (TC) than in the controls, in the normal brain and in the ischemic core (IC) (ANOVA on ranks, $p < 0.0001$). However, the $[Na^+]_o/[Na^+]_{plasma}$ in the IC was not significantly different from those in the controls or in the perilesional penumbra. The $[K^+]_o/[K^+]_{plasma}$ was significantly higher (***) in the TC and the IC in comparison with the ratios observed in the normal brain, in the controls and in the penumbra (ANOVA on ranks, $p < 0.0001$). The $[K^+]_o/[K^+]_{plasma}$ ratio appears to be much more sensitive than the $[Na^+]_o/[Na^+]_{plasma}$ ratio in detecting brain tissue that is at risk or irreversibly damaged.

Penumbra (all), the 10 patients with the probe in the traumatic penumbra (TP) and the 1 with the probe in the ischemic penumbra (IP) were pooled together; $[Na^+]_o$, extracellular sodium concentration; $[K^+]_o$, extracellular potassium concentration; $[Cl^-]_o$, extracellular chloride concentration; $[Na^+]_{plasma}$, plasma concentration of sodium; and $[K^+]_{plasma}$, plasma concentration of potassium. The values are summarized as the median (min–max).

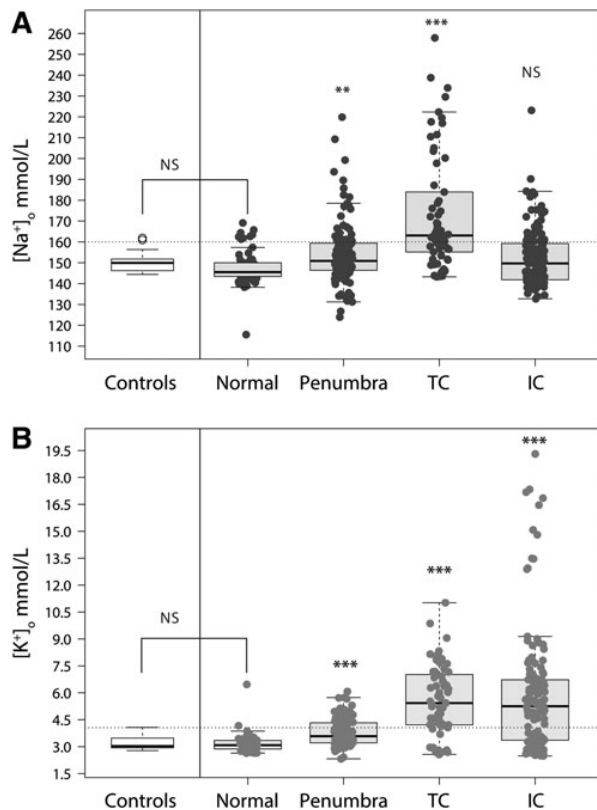


FIG. 3. Box plots showing the $[Na^+]_o$ (A) and $[K^+]_o$ (B) in the different brain tissues and in awake controls. For the sake of clarity, in this figure, samples for both the ischemic penumbra (IP) and traumatic penumbra (TP) were pooled together under the name “penumbra.” The separated data are shown in Table 2.

Ionic profile of the IP and TP

According to our criteria, only 1 patient with an MS had the CMD probe inserted in the IP, and 10 patients had the probe inserted in the TP (perilesional). As a result, the 11 patients were pooled *together* to yield 113 samples for analysis. The summary statistics are presented in Table 2. In the pooled group, 27 samples (23.4%) had a $[Na^+]_o > 162$ mmol/L, and 34 samples (30%) had a $[K^+]_o > 4.1$ mmol/L (Fig. 3). The $[Na^+]_o$, $[K^+]_o$ differences were statistically significant when compared with both controls and the normal injured brain (Fig. 3). $[Cl^-]_o$ differences were statistically significant between penumbra and controls ($p=0.009$) but not when $[Cl^-]_o$ in the penumbra was compared with the $[Cl^-]_o$ in the normal injured brain ($p=0.76$). As occurred in all the other samples, $[Cl^-]_o$ increased or decreased linearly with $[Na^+]_o$ (Fig. 4B).

When the ionic profiles of the IP and the TP were compared, the TP showed more $[Na^+]_o$ than the IP. However, the $[Gly]_o$ appeared to show the fingerprint of viable brain tissue in both regions. However, because of the asymmetry in the number of samples (101 in the TP group vs. 12 in the IP group), these differences may be spurious, and further analysis could not be conducted.

Gly in the normal and injured brain

We have 32 missing values for Gly in the entire patient data set. In the 342 available readings, the median $[Gly]_o$ value was 103.5 $\mu\text{mol/L}$ (min: 10.5, max: 5,748). The summary of the $[Gly]_o$ values observed in the different brain regions is shown in Table 2. In Figure 5, we show the box plots for all of the $[Gly]_o$ data in the different brain regions. All $[Gly]_o$ values were below the 209 $\mu\text{mol/L}$ threshold in the traumatic normal-appearing brain and in all but one reading in the perilesional penumbra. Readings >209 $\mu\text{mol/L}$ were only found in the IC and TC (Fig. 5). However, in 61 of the 128 IC samples (47.6%) and in 28 of the 57 TC samples (49.1%), $[Gly]_o$ was within the normal reference range.

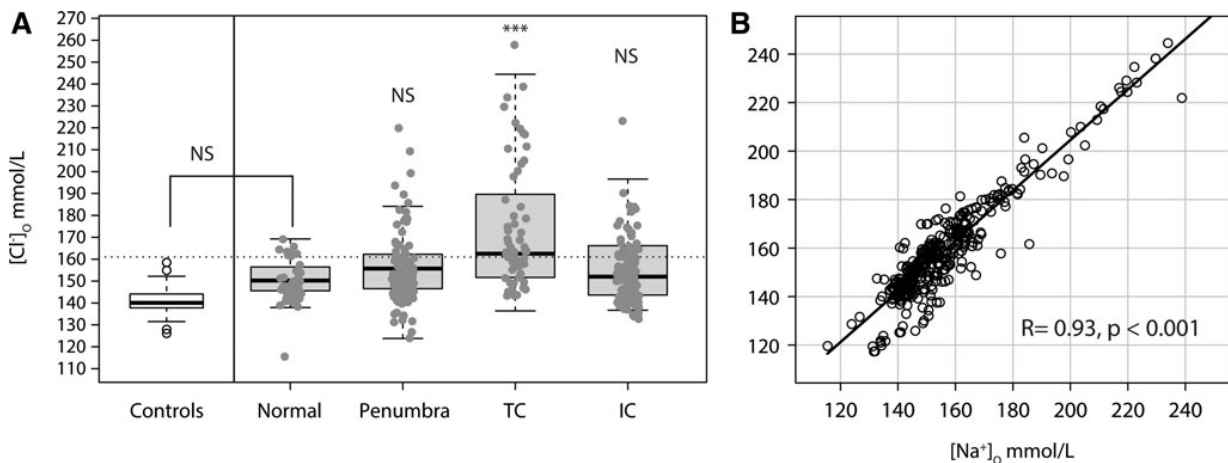


FIG. 4. (A) Box plots showing the $[Cl^-]_o$ in the different brain tissues and also in awake controls. Penumbra, traumatic core (TC), and ischemic core (IC) were compared with the normal brain tissue by Kruskal–Wallis one way analysis of variance. Multiple pairwise comparisons were used to identify which group or groups were significantly different using Nemenyi’s test. (B) Scatter plot in which on the horizontal axis the $[Na^+]_o$ of the whole cohort is shown. The $[Cl^-]_o$ is shown on the Y-axis. Each dot on the scatter plot represents one observation from the whole data set. A linear positive relationship with a Pearson R of 0.93 was found between both variables, showing that, on average, an increase/decrease in $[Na^+]_o$ was followed by an expected coupled increase/decrease in $[Cl^-]_o$. For explanation see text. *** $p < 0.001$. Penumbra, traumatic and ischemic penumbra.

Discussion

Water in the brain is distributed $\sim 80\%$ in the intracellular compartment and $\sim 18\text{--}20\%$ in the interstitial space, with the remaining $1\text{--}3\%$ inside the vascular compartment.¹⁹ The ionic composition of brain ISF previously described has been inferred from measurements taken from the CSF in human controls — assuming that in the steady state, there are no significant concentration gradients between the two compartments — or from animal models ranging from rats to primates.¹⁹ The feasibility of implementing a reliable method to monitor the brain ionic content in neurocritical patients was introduced by our group in a previous study in which we also showed that the ionic concentrations can be reliably calculated from the dialysate by using a least-squares linear regression model; additionally, we showed that RR was close to 100% for all ions of interest.² Recently, Antunes and coworkers have also shown that the *in vitro* RR for K^+ was between 91 and 100% in the same probe that we used.¹² The main limitation of our previous methodology was the poor temporal resolution; this is a drawback intrinsic to most ion-selective analyzers, which in our case required at least $85\ \mu\text{L}$ for the ionic assay and, therefore, pooling at least eight microvials.² A method of dealing with this shortcoming is to increase the infusion speed from the standard $0.3\ \mu\text{L}/\text{min}$ to $0.5\text{--}1.0\ \mu\text{L}/\text{min}$. However, this increase reduces the ionic recovery and, therefore, decreases the lower limit of detection for K^+ in some commercial analyzers; this is clinically relevant because $[K^+]_o$ is the most relevant biomarker to define brain tissue viability.^{11,20} In addition, increasing the infusion speed also reduces the RR of the energy metabolites used at the bedside (lactate, pyruvate, and glucose)^{21–25} and adds excessive complexity to a monitoring system that already increases the workload of the neurointensive care personnel significantly.

ICP-MS is the best method available to improve the temporal resolution of ion assays and allows extremely low detection limits — in the parts per million (ppm) levels — in samples of $<20\ \mu\text{L}$. When we compared ICP-MS with the ion-selective electrode analyzer used in our previous study,² we observed that the correlation between both

methods was excellent, and, consequently, chemistry analyzers used in most hospitals are excellent alternatives to ICP-MS, except for their low temporal resolution. To our knowledge, this is the first report that thoroughly explores the ionic profile in both the human ischemic brain and the human injured brain. We also incorporated a small cohort of awake patients without supratentorial disease that were used as controls.

Ionic profile of the normal brain

For ethical and methodological reasons, the ionic normal range for the human brain ISF has not been published yet. Most studies have instead used the reference levels measured in the CSF as surrogates. In our awake controls, mean $[Na^+]_o$ was $150.6\ \text{mmol/L}$ with an upper reference limit of $162\ \text{mmol/L}$; the sample with $162\ \text{mmol/L}$ had a plasma concentration of $138\ \text{mmol/L}$. However, since our control group was limited to seven patients, we cannot establish a robust upper limit for $[Na^+]_o$ from our data. $[K^+]_o$ never exceeded $4.1\ \text{mmol/L}$ in controls. This upper limit was similar to the upper reference levels of $3.6\text{--}4.1\ \text{mmol/L}$ in the CSF of controls described by others.^{2,3}

Determining whether the ionic profile is normal in the apparently undamaged brain

In our study, we differentiated between controls and CMD probes placed in the macroscopically uninjured brain of TBI patients (Fig. 1). We cannot disregard that in these apparently normal areas, the ionic permeability of the BBB might be increased and that various invisible metabolic, functional, or structural abnormalities in axons, endothelial cells, glial, and neurons might be present.^{26,27} We found a modest increase in $[Na^+]_o$ in some samples, but $[K^+]_o$ always remained within normal limits. Only two patients presented an isolated $[K^+]_o$ reading $>4.1\ \text{mmol/L}$, which reverted spontaneously in the next assay. Reversible increases in $[K^+]_o$ can be found in clinical or subclinical epileptic seizures²⁸ and also in CSD phenomena; this is a frequent finding in TBI that is related to a poor neurological outcome.^{29,30} In all samples, $[Cl^-]_o$ was linearly related to $[Na^+]_o$, as shown in Figure 4B; this demonstrates that, as expected, anions and cations are distributed to achieve electroneutrality.

Ionic profile in the IC and TC

Our CMD samples in MS came from infarcted tissue that was analyzed very late after stroke onset (median time $34.5\ \text{h}$ for the first sample). Therefore, the ionic profile corresponded to necrotic tissue, which on neuroimaging studies always evolved to an encephalomalacic brain (Fig. 1F). It has been shown that high $[K^+]_o$ is a good biomarker for the severity of brain damage both in experimental models and in patients with severe TBI (i.e., those with high ICP or brain hypoxia), aneurysmal subarachnoid hemorrhage, and ischemic or hemorrhagic stroke.^{7–10,12,20} In addition, Antunes and coworkers showed, in aneurysmal subarachnoid hemorrhage, that $[K^+]_o$ does not correlate with the plasma levels.¹²

The ionic profile of the IC was characterized by very high $[K^+]_o$ in 62% of the samples and an increase in $[Na^+]_o$ in only 20% of the samples. Sodium-MRI has been used to study the ionic changes in both experimental models of stroke and in human ischemic stroke.³¹ However, because of the low total sodium concentration (TSC) in the brain ($[Na^+]_{\text{brain}}$) and the low signal-to-noise ratio, clinical applications have been limited to high-field MRI systems.³² Further, sodium-MRI estimates the TSC and not the $[Na^+]_o$ in the

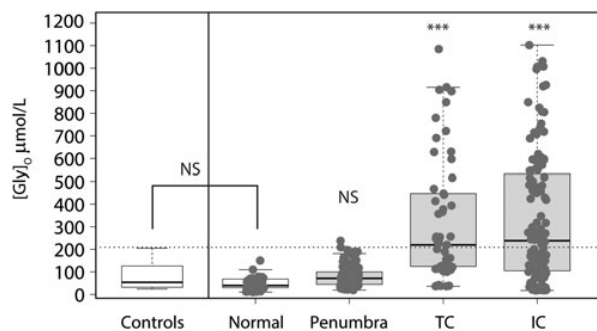


FIG. 5. Box plots showing the interstitial levels of glycerol $[Gly]_o$ in the different brain tissues and in awake controls. In this figure, the samples for both the ischemic penumbra (IP) and the traumatic penumbra (TP) were pooled together under the name “penumbra.” The separated data are shown in Table 2. The data show that all “viable” tissue, as identified according to the CT scan criteria discussed in the text, had $[Gly]_o$ values below the upper reference threshold. Both the traumatic core (TC) and the ischemic core (IC) presented significantly higher $[Gly]_o$ levels than did the controls and to both the IP and TP. $***p < 0.001$.

different brain compartments, and, therefore, $[Na^+]_o$. In a recent study, normal $[Na^+]_{brain}$ was 35.17 ± 3.40 mM and 40.09 ± 4.64 in the normal-appearing white matter and gray matter respectively.³² This approximates the concentrations expected under the assumptions of the theoretical volumes of the intracellular space (75%), the ISF (20%), and the intravascular compartments (5%) in the normal brain with the accepted $[Na^+]_i$: 10 mmol/L inside the cell, 140 mmol/L in the ISF, and 140 mmol/L in plasma. Following a reversible focal ischemic insult in nonhuman primates LaVerde and coworkers showed a linear increase in TSC (intracellular plus extracellular) within ischemic tissue at a rate of $\sim 5\text{--}7\%/h$.³³ However, the $[Na^+]_{brain}$ determined in stroke by sodium-MRI is difficult to compare with the findings we observed when dialyzing the interstitial space.

The fact that $[K^+]_o$ increases in animal models under conditions in which the energy metabolism of the brain has been compromised — regional or global ischemia — is a well-recognized and consistent phenomenon. For a comprehensive review of K^+ movements under experimental models of anoxia until 1985, the reader is referred to the article by Hansen.¹⁹ Mori and coworkers recorded simultaneously $[Na^+]_o$ and $[K^+]_o$ in a 15 min model of global ischemia in rats by using double-barreled ion-selective microelectrodes.¹¹ Their findings were quite consistent with other experimental studies and found that $[K^+]_o$ started to increase moderately immediately after ischemia and that its levels increased abruptly in a second state, reaching a plateau 5 min after ischemia at which values of 65 ± 38 mmol/L were recorded.¹¹ Infarcted brains undergo terminal depolarization at early stages, and later oncotic destruction of the brain cells if ischemia persists. Oncotic cell death releases huge amounts of K^+ into the ISF from the intracellular pool, and if the infarcted tissue has a hemorrhagic component, the hemolysis contributes to the increase of the total K^+ content.

In experimental models of permanent MCA occlusion, the changes in $[K^+]_o$ are explosive in nature, and $[K^+]_o$ increases suddenly from ~ 3 mmol/L to >50 mmol/L in the few seconds after the onset of ischemia.²⁰ In the same model, the ischemic core showed little $[K^+]_o$ dissipation within 3 h after artery occlusion.^{11,19,20} Although we find very high $[K^+]_o$ in the IC, the levels never reached the concentrations found in the acute phase of experimental ischemic stroke. Our findings are difficult to compare with those from animal models because long-term recordings of $[K^+]_o$ have not been made thus far in any experimental model. Therefore, we cannot compare our data with the findings of any experimental model of ischemia that have mostly evaluated the few minutes or hours after the ischemic insult. Released K^+ is usually cleared by the glial cells of the penumbra and by bulk flow to the CSF; however, both mechanisms become inoperative at the ischemic core and are dysfunctional in the ischemic penumbra that may also have an increased $[K^+]_o$. Infarcted tissue maintains high levels of K^+ that if unbuffered may affect the viability of the penumbra tissue or even the normal brain. Our hypothesis to explain the lower levels of $[K^+]_o$ found in our patients is that the infarcted tissue behaves as a tissue homogenate, and because of its high osmolarity, attracts massive amounts of water that dilute the extremely high concentrations that occur initially.

The cause of death in patients with MS left to their natural evolution is severe brain swelling. Natti and coworkers found a total concentration of K^+ of 170 mmol/L and 32 mmol/L for Na^+ in tissue homogenates of normal rat brain cortex.³⁴ Therefore, the expected $[K^+]_i$ in a completely necrotic tissue is still higher than that found in acute models of ischemia, and again a dilutional effect is suggested. As shown in Table 2, the $[K^+]_o/[K^+]_{plasma}$ ratio was significantly higher both in TC and IC than in controls, in normal-appearing brain regions

and in the IP and TP (ANOVA on ranks, $p < 0.0001$). Therefore, our data suggest that the $[K^+]_o/[K^+]_{plasma}$ ratio is a good biomarker in detecting brain tissue at risk or that is irreversibly damaged.

Paradoxically, in the IC, $[Na^+]_o$, $[Cl^-]_o$ and $[K^+]_o$ were within the reference limits in 32.6% of the analyzed samples. This was the reason why, on average, the differences between the ionic content for $[Na^+]_o$ and $[Cl^-]_o$ were not significantly different than the values found in the uninjured brain (Figs. 3 and 4). As already discussed, our hypothesis to explain this phenomenon is that necrotic tissue at the IC is a powerful attractor for water and that the initial increase in ions is apparently normalized by the considerable amount of water that enters the IC and dilutes them. This phenomenon has not been reported previously, because of the relatively short recording time in experimental models of ischemic stroke that usually does not exceed a follow-up of 6–8 h.^{20,35} Therefore, in brain monitoring, the hallmark of irreversibly damaged tissue needs to be defined taking into consideration the temporal evolution of the ionic profile. Isolated measurements can be misleading when ionic concentrations are within the normal range if previous values are unknown. This theory is highly speculative and needs verification in animal models.

An in-depth discussion of the mechanisms involved in the strong attraction of water by the core is beyond the aim of this study. In brief, the main characteristic in any type of severe brain damage is that cell membranes lose their integrity, and the fixed charge density (FCD) inside the cells, which are generated by proteins, DNA, and proteoglycans, are exposed to the extracellular medium.⁵ According to Lang and coworkers, necrotic tissue can be modeled as a mixture of solid components with FCD, water, and ions.⁵ In this situation, the FCD is a powerful attractor for water via the Gibbs–Donnan effect. Blood is also a component, in some cases, of ischemic infarction and is almost constantly found in brain contusions; also increasing the protein content of the necrotic brain. Similarly to ischemia, the contusional core is characterized by rapid pannecrosis, disintegration, and homogenization of the brain tissue,^{36,37} which creates an osmotic sink that attracts water.^{38–40} The large amount of edema that accumulates in the contusion core is caused by a significant increase in tissue osmolality that does not depend only of the changes in ionic concentrations.⁴¹ Kawamata and coworkers raised the hypothesis that injured tissue induces an accumulation of metabolic intermediate osmoles or the formation of idiogenic osmoles from the pathological degradation of lipids, proteins, DNA, and other catabolic processes that occur in the damaged tissue.⁴¹

TC is a much more heterogeneous tissue than IC, and zones of injured but with still intact membranes may coexist with necrotic unviable tissue. The main finding in TC was the significant higher levels of $[Na^+]_o$, $[Cl^-]_o$, and $[K^+]_o$ compared with controls and uninjured brain. As in IC, the leakage of $[K^+]_i$ from the intracellular compartment occurs because of the rupture of cellular membranes associated with mechanically induced or ischemic cell death.^{7,8} However, the main difference between IC and TC was the significantly higher $[Na^+]_o$ in the TC group (Fig. 3). This finding was counterintuitive and difficult to explain. For thermodynamic reasons, $[Na^+]_o$ should not exceed $[Na^+]_{serum}$ except if active transport of Na^+ was involved; however, this cannot occur in dead brain tissue. The core is surrounded by brain tissue with a BBB that is leaky and behaves more like a fenestrated endothelium. Under these circumstances, a set of possible speculative options to explain these findings is: 1) patients could be treated with HTS and have an increase in $[Na^+]_o$ as a consequence of high plasma Na^+ levels (this was not the case in our series where patients with $[Na^+]_o > 162$ mmol/L had $[Na^+]_{serum}$ within the normal range); 2) proteins released from dying cells and particularly DNA-histone complexes

might release Na^+ ;⁴² 3) an increase in the negatively charged protein concentration in the TC attracts positively charged Na^+ ions into the core, thereby leading to an increase in the $[\text{Na}^+]_o$; 4) the preload of cells with Na^+ in the early phases of injury caused by cytotoxic edema can release a higher $[\text{Na}^+]_i$ into the necrotic tissue; and 5) the increased activity of Na^+/H^+ exchangers in the TP may release Na^+ into the core, which will act as an inert sink. The role of Na^+/H^+ exchangers and other sodium transporters in ischemia has been discussed by O'Donnell in a recent review.⁴³ However, these hypotheses are speculative and only have the purpose of framing the issue of a significantly increased Na^+ in the TC. Any further clarification of this counterintuitive paradox requires further experimental studies in animal models in which experimental conditions can be well controlled, and the ionic profile together with the temporal evolution of the ionic profile, brain tissue osmolarity, protein content, and the total content of idiogenic osmoles should be measured.

Determining whether Gly is a good biomarker for determining brain tissue viability

Gly is an end product of phospholipid degradation, and some studies have used it as a biomarker for cell membrane deterioration and, therefore, cell destruction both in TBI injury and in other acute brain injuries.^{15,16} Peerdeman and coworkers, in a small cohort of TBI patients, found that although the extracellular concentration of glycerol $[\text{Gly}]_o$ was not useful for early detection of secondary adverse events,¹⁵ values of $[\text{Gly}]_o > 150 \mu\text{mol/L}$ in the normal-appearing regions of the brain had a positive predictive value of 100% for an unfavorable outcome.¹⁵

We found a significant increase in $[\text{Gly}]_o$ in both the IC and the TC, but the $[\text{Gly}]_o$ levels were always below the upper reference threshold in the normal-appearing brain and in the penumbra (Fig. 5). However, in many IC and TC samples, $[\text{Gly}]_o$ was within the reference range. This finding indicates that a $[\text{Gly}]_o < 209 \mu\text{mol/L}$ is a good predictor for tissue viability, with high sensitivity (99.4%) but modest specificity (52%). The reason why some dead brain tissue shows $[\text{Gly}]_o$ levels within the reference range may be because Gly has a low molecular weight (MW) (92 Da); therefore, once Gly is released, it can be washed out from the damaged brain by simple diffusion and osmotic gradients. However, we did not find any linear or nonlinear relationship between $[\text{Gly}]_o$ and $[\text{K}^+]_o$. The fact that many MD samples in the TC and IC had normal $[\text{Gly}]_o$ values might justify this lack of relationship. Taken together, our data suggest that when they are within their reference ranges, both $[\text{Gly}]_o$ and $[\text{K}^+]_o$ are highly sensitive but not very specific for detecting viable brain tissue, and could, therefore, be good candidates for incorporation into a future panel of biomarkers to evaluate the viability of brain tissue.

The BBB is highly permeable to sodium in the penumbra

The accurate identification of brain penumbra in TBI is clinically relevant because it can identify patients who could benefit from changing their management and in designing future clinical trials of potential neuroprotective drugs. Our main finding in the TP was a completely normal ionic profile for $[\text{Na}^+]_o$ and $[\text{K}^+]_o$ in 60% of the samples. Our study confirms the findings of Wetterling and coworkers who showed that the IP may be defined as a region of reduced blood supply in which the sodium concentration gradient is still maintained.³¹

Of the 40% of the samples in which abnormal ionic profiles were found, an isolated increase in $[\text{Na}^+]_o$ accompanied with an increased $[\text{Cl}^-]_o$ to preserve electroneutrality was the most frequent abnormality found; however, in most cases $[\text{K}^+]_o$ was within the normal range (22 of 27 samples). The normal or moderately increased $[\text{K}^+]_o$ was the main difference with the ionic profile found in the TC/IC, suggesting that the perilesional brain is still able to buffer $[\text{K}^+]_o$ overloading. Moderate increases in $[\text{K}^+]_o$ can be observed in the presence of both CSD and epileptic seizures; this phenomena occurs both in the IP and the TP. Another explanation for the increase in $[\text{K}^+]_o$ found in penumbral tissue is its diffusion from the adjacent ischemic core from focal hemorrhagic brain lesions found in TBI.¹² Hubschmann and Kornhauser, in experimental models of intracerebral hemorrhage in cats, showed that acute injection of blood in the brain induces an acute depolarization of the cortex with a significant increase in $[\text{K}^+]_o$ to values of 18–28 mmol/L. However, this transient peak was rapidly buffered and returned to baseline 2–4 min after the injection.⁴⁴

One possible explanation for these 40% abnormalities is that our definition of penumbra was inaccurate; actually “penumbra” meant, as we discussed, perilesional macroscopically normally appearing brain in the CT scan. Therefore, MRI in these patients might have shown diffusion-perfusion abnormalities and would have been included by other neuroimaging techniques in the category of “core.” In addition, most of our findings reflect the ionic findings in the brain tissue around brain contusions in TBI, and it should be more accurately defined as “perilesional tissue.” However, we decided to preserve the term ischemic/traumatic “penumbra” to be consistent with the literature and because, in many samples, the ionic profile was normal; therefore, it was theoretical functional tissue that could be recruited into the core of the lesion.

The isolated increase of $[\text{Na}^+]_o$ in some the penumbra may suggest an increased permeability of the BBB to Na^+ . The fact that $[\text{Na}^+]_o$ accumulates in ISF might indicate early stages of ionic or vasogenic edema that have been described in the ischemic and injured brain.^{45–47} Simard and coworkers have shown that the sulfonylurea receptor 1 - transient receptor potential melastatin 4 (SUR1-TRPM4) ion channel is overexpressed in the endothelial and neural cells of the ischemic and injured brain and that this channel is the main driver of the increase in $[\text{Na}^+]_o$.^{48,49} Recently, we have shown that SUR1, the regulatory unit of this channel, is significantly overexpressed in the perilesional brain around human brain contusions, and that upregulation of SUR1 is an important molecular player in the pathophysiology of these lesions.⁵⁰ In addition, as shown in ischemia, Na-K-Cl cotransporters and Na^+/H^+ exchangers in endothelial cells and also in glia and neurons are actively involved in ischemic edema and in the fluxes of Na^+ .⁴³ However, in our study, we did not evaluate the permeability of the BBB and, therefore, our suggestions need to be considered as working hypothesis for new studies.

Osmotherapy is the most important first-line tool in the management of intracranial hypertension after TBI and stroke. The beneficial effects of osmotherapy on ICP are the result of the brain shrinkage induced by the shift of water out of the brain tissue.⁵¹ The ideal osmotic agent should establish a strong osmotic gradient across the BBB by remaining largely in the intravascular compartment. Mannitol is the osmotic drug of choice and is the recommended option in the Brain Trauma Foundation guidelines (level II recommendation).⁵² However, HTS is a widely used alternative to mannitol, although it is being used in a wide range of formulations. In a comprehensive review of the literature, White and coworkers showed that HTS is used at sodium chloride concentrations ranging from 1.7% to 29.2%.⁵¹ In

clinical practice, this range means a difference in the administered Na^+ concentration from 291 to 5000 mmol/L.⁵¹ As for mannitol, the main assumption behind the use of HTS is that the permeability of the intact BBB to Na^+ is very low and the reflection coefficient for Na^+ is very high. Therefore, HTS administration produces an osmotic gradient between the intravascular and interstitial compartments, leading to shrinkage of the brain tissue and to a consequent reduction in ICP.⁵¹ However, despite the increased enthusiasm about the use of HTS after TBI, the number of human studies remains limited and the evidence justifying their routine clinical use remains scarce.^{51,53}

We found an increase in $[\text{Na}^+]_o$ in the damaged brain, suggesting that the permeability of the BBB to Na^+ is significantly increased in many damaged brain regions. Our findings raise some concerns about the use of HTS in TBI patients with significant brain damage and in patients with MS, in whom massive destruction of the brain tissue is consistently found. In experimental post-traumatic contusions, Kurland and coworkers showed that the permeability of the surrounding brain tissue (the penumbra and parapenumbra in Simard's terms) has a very low reflection coefficient for Na^+ because of the overexpression of the SUR1-TRPM4 ion channel, which facilitates the movement of large amounts of sodium to the damaged brain.⁴⁷ From the data obtained in animal models, it is quite clear that the type of cerebral edema (vasogenic or cytotoxic) and the degree of BBB disruption depends upon the mode of injury; therefore, traditional neuromonitoring tools cannot predict the degree of BBB disruption.

We believe that the use of HTS in patients with significant areas of damaged brain — in which the BBB may have an increased permeability to Na^+ — should be at least reconsidered. To obtain a clear understanding of the Na^+ fluxes in and out of the brain that occur when using these solutions, the ionic profiles should be studied before and after HTS boluses; we believe that CMD is a powerful tool for monitoring the ionic content of the ISF and for improving our understanding of the pathophysiology of the BBB.

Limitations of the study and future directions

Our study presents some limitations that merit discussion. The most important one is that our methodology only calculated the ionic concentration corresponding to an average of the final 2h of monitoring. Therefore, the rapid fluxes in extracellular $[\text{K}^+]_o$, $[\text{Na}^+]_o$, and $[\text{Cl}^-]_o$ could not be studied. However, hourly trends are still very useful as a method for identifying brain tissue at risk and the abnormal permeability of the BBB, and, probably, to define therapeutic windows for recoverable tissue. We have been not able to explain the counterintuitive finding of increased $[\text{Na}^+]_o$ in patients in whom the CMD was placed inside the core of a traumatic lesion. We could only raise some hypotheses that need verification in additional studies in large animal models that allows monitoring by CMD different brain areas of the same animal.

Conclusion

To conclude, we believe that ICP-MS coupled to ionic assays is a powerful tool for improving our understanding of the complex ionic disturbances that occur after severe TBI and ischemic and hemorrhagic stroke. Despite some of its intrinsic limitations, CMD is the only monitoring method that allows, with an acceptable risk, repeated measurements of ionic concentrations in combination with other analyses in humans. In addition, unlike ion-selective sensors, CMD allows for many physiological and biochemical processes to be studied simultaneously in the living brain and is, therefore, a powerful tool for better understanding the complex

pathophysiology of BBB disruption, and a good method for monitoring brain edema and for rationalizing the use of hyperosmolar solutions. We believe that the routine use of CMD in the exploration of the ionic profiles of different regions in the injured brain opens up an exciting avenue to explore the complexities of ionic disturbances, the classification of the different types of brain edema, and the design of a viability index that can be used to explore the effects of therapeutic strategies in patients with acute brain injuries.

Acknowledgments

We are grateful to J. Marc Simard from the Department of Neurosurgery, University of Maryland for critically reviewing the manuscript and providing relevant scientific input. The Neurotraumatology and Neurosurgery Research Unit is supported by a grant from the Departament d'Universitats, Recerca i Societat de la Informació de la Generalitat de Catalunya (SGR 2014-844). This work has been supported in part by the Fondo de Investigación Sanitaria (Instituto de Salud Carlos III) with grants PI10/00302 and FIS PI11/00700, which were co-financed by the European Regional Development Fund (ERDF) and awarded to Drs. Poca and Sahuquillo, respectively. T. Martínez-Valverde and A. Sánchez-Guerrero are the recipients of personal pre-doctoral grants from the Instituto de Salud Carlos III (grants number FI11/00195 and FI12/00074, respectively).

Author Disclosure Statement

No competing financial interests exist.

References

1. Somjen, G.G. (2004). *Ions in the Brain: Normal Function, Seizures, and Stroke*. Oxford University Press: Oxford; New York.
2. Martínez-Valverde, T., Vidal-Jorge, M., Montoya, N., Sánchez-Guerrero, A., Manrique, S., Munar, F., Pellegrini, M.D., Poca, M.A., and Sahuquillo, J. (2015). Brain microdialysis as a tool to explore the ionic profile of the brain extracellular space in neurocritical patients: a methodological approach and feasibility study. *J. Neurotrauma* 32, 7–16.
3. Harrington, M.G., Fonteh, A.N., Cowan, R.P., Perrine, K., Pogoda, J.M., Biringer, R.G., and Huhmer, A.F. (2006). Cerebrospinal fluid sodium increases in migraine. *Headache* 46, 1128–1135.
4. Purves, W.K. (2004). Cellular membranes, in: *Life, the Science of Biology*. W.K. Purves (ed.). W.H. Freeman & Co.: Gordonsville, VA, pps. 87–105.
5. Lang, G.E., Stewart, P.S., Vella, D., Waters, S.L., and Goriely, A. (2014). Is the Donnan effect sufficient to explain swelling in brain tissue slices? *J. R. Soc. Interface* 11, 20140123.
6. Le Roux, P., Menon, D.K., Citerio, G., Vespa, P., Bader, M.K., Brophy, G., Diring, M.N., Stocchetti, N., Videtta, W., Armonda, R., Badjatia, N., Bosel, J., Chesnut, R., Chou, S., Claassen, J., Czornyka, M., De Georgia, M., Figaji, A., Fugate, J., Helbok, R., Horowitz, D., Hutchinson, P., Kumar, M., McNett, M., Miller, C., Naidech, A., Oddo, M., Olson, D., O'Phelan, K., Provencio, J.J., Puppo, C., Riker, R., Roberson, C., Schmidt, M., and Taccone, F. (2014). The International Multidisciplinary Consensus Conference on Multimodality Monitoring in Neurocritical Care: evidentiary tables: a statement for healthcare professionals from the Neurocritical Care Society and the European Society of Intensive Care Medicine. *Neurocrit. Care* 21 Suppl. 2, S297–361.
7. Doppenberg, E.M., Reinert, M., Zauner, A., Massie, T.S., and Bullock, R. (1999). Determinants of cerebral extracellular potassium after severe human head injury. *Acta Neurochir. (Wien) Suppl.* 75, 31–34.
8. Reinert, M., Khaldi, A., Zauner, A., Doppenberg, E., Choi, S., and Bullock, R. (2000). High level of extracellular potassium and its correlates after severe head injury: relationship to high intracranial pressure. *J. Neurosurg.* 93, 800–807.

9. Valadka, A.B., Goodman, J.C., Gopinath, S.P., Uzura, M., and Robertson, C.S. (1998). Comparison of brain tissue oxygen tension to microdialysis-based measures of cerebral ischemia in fatally head-injured humans. *J. Neurotrauma* 15, 509–519.
10. Goodman, J.C., Valadka, A.B., Gopinath, S.P., Uzura, M., Grossman, R.G., and Robertson, C.S. (1999). Simultaneous measurement of cortical potassium, calcium, and magnesium levels measured in head injured patients using microdialysis with ion chromatography. *Acta Neurochir. Suppl.* 75, 35–37.
11. Mori, K., Miyazaki, M., Iwase, H., and Maeda, M. (2002). Temporal profile of changes in brain tissue extracellular space and extracellular ion (Na⁺), K⁺) concentrations after cerebral ischemia and the effects of mild cerebral hypothermia. *J. Neurotrauma* 19, 1261–1270.
12. Antunes, A.P., Schiefecker, A.J., Beer, R., Pfaußler, B., Sohm, F., Fischer, M., Dietmann, A., Lackner, P., Hackl, W.O., Ndayisaba, J.P., Thome, C., Schmutzhard, E., and Helbok, R. (2014). Higher brain extracellular potassium is associated with brain metabolic distress and poor outcome after aneurysmal subarachnoid hemorrhage. *Crit. Care* 18, R119.
13. Ehling, S., Tefera, S., Earl, R., and Cole, S. (2010). Comparison of analytical methods to determine sodium content of low-sodium foods. *J. AOAC Int.* 93, 628–637.
14. Poca, M.A., Sahuquillo, J., Vilalta, A., de los Rios, J., Robles, A., and Exposito, L. (2006). Percutaneous implantation of cerebral microdialysis catheters by twist-drill craniostomy in neurocritical patients: description of the technique and results of a feasibility study in 97 patients. *J. Neurotrauma* 23, 1510–1517.
15. Peerdeman, S.M., Girbes, A.R., Polderman, K.H., and Vandertop, W.P. (2003). Changes in cerebral interstitial glycerol concentration in head-injured patients: correlation with secondary events. *Intensive Care Med.* 29, 1825–1828.
16. Merenda, A., Gugliotta, M., Holloway, R., Levasseur, J.E., Alessandri, B., Sun, D., and Bullock, M.R. (2008). Validation of brain extracellular glycerol as an indicator of cellular membrane damage due to free radical activity after traumatic brain injury. *J. Neurotrauma* 25, 527–537.
17. Evans, J.W.A. (1942). An encephalographic ratio for estimating ventricular enlargement and cerebral atrophy. *Arch. Neurol. Psychiatry* 47, 931–937.
18. Bland, J.M., and Altman, D.G. (1986). Statistical methods for assessing agreement between two methods of clinical measurement. *Lancet* 1, 307–310.
19. Hansen, A.J. (1985). Effect of anoxia on ion distribution in the brain. *Physiol. Rev.* 65, 101–148.
20. Sick, T.J., Feng, Z.-C., and Rosenthal, M. (1998). Spatial stability of extracellular potassium ion and blood flow distribution in rat cerebral cortex after permanent middle cerebral artery occlusion. *J. Cereb. Blood Flow Metab.* 18, 1114–1120.
21. Torto, N. (2009). A review of microdialysis sampling systems. *Chromatographia* 70, 1305–1309.
22. Lieutaud, T., Dailler, F., Artru, F., and Renaud, B. (2007). Neurochemical monitoring in neurointensive care using intracerebral microdialysis, in: *Handbook of Microdialysis: Methods, Applications and Perspectives*. B.H.C. Westerink, and T.I.F.H. Cremers (eds.). Elsevier Academic Press: Amsterdam; Boston, pps. xiv, 697.
23. Kitagawa, R., Yokobori, S., Mazzeo, A.T., and Bullock, R. (2013). Microdialysis in the neurocritical care unit. *Neurosurg. Clin. N. Am.* 24, 417–426.
24. Hutchinson, P.J., Oconnell, M.T., AlRawi, P.G., Maskell, L.B., Kett-White, R., Gupta, A.K., Richards, H.K., Hutchinson, D.B., Kirkpatrick, P.J., and Pickard, J.D. (2000). Clinical cerebral microdialysis: a methodological study. *J. Neurosurg.* 93, 37–43.
25. Elmquist, W.F., and Sawchuk, R.J. (1997). Application of microdialysis in pharmacokinetic studies. *Pharm. Res.* 14, 267–288.
26. Sahuquillo, J., Poca, M.A., and Amoros, S. (2001). Current aspects of pathophysiology and cell dysfunction after severe head injury. *Curr. Pharm. Des.* 7, 1475–1503.
27. Sahuquillo, J., Merino, M.A., Sánchez-Guerrero, A., Arkan, F., Vidal-Jorge, M., Martínez-Valverde, T., Rey, A., Riveiro, M., and Poca, M.A. (2014). Lactate and the lactate-to-pyruvate molar ratio cannot be used as independent biomarkers for monitoring brain energetic metabolism: a microdialysis study in patients with traumatic brain injuries. *PLoS One* 9, e102540.
28. Gorji, A., Stemmer, N., Rambeck, B., Jürgens, U., May, T., Pannek, H.W., Behne, F., Ebner, A., Straub, H., and Speckmann, E.-J. (2006). Neocortical microenvironment in patients with intractable epilepsy: potassium and chloride concentrations. *Epilepsia* 47, 297–310.
29. Hartings, J.A., Watanabe, T., Bullock, M.R., Okonkwo, D.O., Fabricius, M., Woitzik, J., Dreier, J.P., Puccio, A., Shutter, L.A., Pahl, C., and Strong, A.J. (2011). Spreading depolarizations have prolonged direct current shifts and are associated with poor outcome in brain trauma. *Brain* 134, 1529–1540.
30. Strong, A.J., and Dardis, R. (2005). Depolarisation phenomena in traumatic and ischaemic brain injury. *Adv. Tech. Stand. Neurosurg.* 30, 3–49.
31. Wetterling, F., Gallagher, L., Mullin, J., Holmes, W.M., McCabe, C., Macrae, I.M., and Fagan, A.J. (2015). Sodium-23 magnetic resonance imaging has potential for improving penumbra detection but not for estimating stroke onset time. *J. Cereb. Blood Flow Metab.* 35, 103–110.
32. Eisele, P., Konstandin, S., Griebel, M., Szabo, K., Wolf, M.E., Alonso, A., Ebert, A., Serwane, J., Rossmanith, C., Hennerici, M.G., Schad, L.R., and Gass, A. (2015). Heterogeneity of acute multiple sclerosis lesions on sodium (²³Na) MRI. *Mult. Scler.* [Epub ahead of print].
33. LaVerde, G.C., Jungreis, C.A., Nemoto, E., and Boada, F.E. (2009). Sodium time course using ²³Na MRI in reversible focal brain ischemia in the monkey. *J. Magn. Reson. Imaging* 30, 219–223.
34. Nattie, E.E., Bergin, M.B., Daley, J., and Melton, J. (1980). CSF and brain ions, acid-base balance, and ventilation in acute hyponatremia. *J. Appl. Physiol.* 49, 95–101.
35. Betz, A.L., Keep, R.F., Beer, M.E., and Ren, X.D. (1994). Blood-brain barrier permeability and brain concentration of sodium, potassium, and chloride during focal ischemia. *J. Cereb. Blood Flow Metab.* 14, 29–37.
36. Kawamata, T., and Katayama, Y. (2007). Cerebral contusion: a role model for lesion progression. *Prog. Brain Res.* 161, 235–241.
37. Lindenberg, R., and Freytag, E. (1957). Morphology of cortical contusions. *AMA Arch. Pathol.* 63, 23–42.
38. Katayama, Y., and Kawamata, T. (2003). Edema fluid accumulation within necrotic brain tissue as a cause of the mass effect of cerebral contusion in head trauma patients. *Acta Neurochir. (Wien) Suppl.* 86, 323–327.
39. Maeda, T., Katayama, Y., Kawamata, T., Koyama, S., and Sasaki, J. (2003). Ultra-early study of edema formation in cerebral contusion using diffusion MRI and ADC mapping. *Acta Neurochir. (Wien) Suppl.* 86, 329–331.
40. Katayama, Y., Mori, T., Maeda, T., and Kawamata, T. (1998). Pathogenesis of the mass effect of cerebral contusions: rapid increase in osmolality within the contusion necrosis. *Acta Neurochir. (Wien) Suppl.* 71, 289–292.
41. Kawamata, T., Mori, T., Sato, S., and Katayama, Y. (2007). Tissue hyperosmolality and brain edema in cerebral contusion. *Neurosurg. Focus* 22, E5.
42. Nguyen, M.K., and Kurtz, I. (2006). Quantitative interrelationship between Gibbs–Donnan equilibrium, osmolality of body fluid compartments, and plasma water sodium concentration. *J. Appl. Physiol.* (1985) 100, 1293–1300.
43. O'Donnell, M.E. (2014). Blood–brain barrier Na transporters in ischemic stroke, in: *Advances in Pharmacology*. P.D. Thomas (ed.). Academic Press, San Diego, CA, pps. 113–146.
44. Hubschmann, O.R., and Kornhauser, D. (1983). Effects of intraparenchymal hemorrhage on extracellular cortical potassium in experimental head trauma. *J. Neurosurg.* 59, 289–293.
45. Simard, J.M., Kent, T.A., Chen, M., Tarasov, K.V., and Gerzanich, V. (2007). Brain oedema in focal ischaemia: molecular pathophysiology and theoretical implications. *Lancet Neurol.* 6, 258–268.
46. Simard, J.M., Kahle, K.T., and Gerzanich, V. (2010). Molecular mechanisms of microvascular failure in central nervous system injury: synergistic roles of NKCC1 and SUR1/TRPM4. *J. Neurosurg.* 113, 622–629.
47. Kurland, D., Hong, C., Aarabi, B., Gerzanich, V., and Simard, J.M. (2012). Hemorrhagic progression of a contusion after traumatic brain injury: a review. *J. Neurotrauma* 29, 19–31.
48. Simard, J.M., Chen, M., Tarasov, K.V., Bhatta, S., Ivanova, S., Melnitchenko, L., Tsybalyuk, N., West, G.A., and Gerzanich, V. (2006). Newly expressed SUR1-regulated NC(Ca-ATP) channel mediates cerebral edema after ischemic stroke. *Nat Med* 12, 433–440.
49. Simard, J.M., and Chen, M. (2004). Regulation by sulfanylurea receptor type 1 of a non-selective cation channel involved in cytotoxic edema of reactive astrocytes. *J. Neurosurg. Anesthesiol.* 16, 98–99.

IONIC PROFILE OF THE INJURED AND ISCHEMIC BRAIN

85

50. Martínez-Valverde, T., Vidal-Jorge, M., Martínez-Saez, E., Castro, L., Arikian, F., Cordero, E., Rádoi, A., Poca, M.A., Simard, J.M., and Sahuquillo, J. (2015). Sulfonylurea receptor 1 in humans with post-traumatic brain contusions. *J. Neurotrauma* 32, 1478–1487.
51. White, H., Cook, D., and Venkatesh, B. (2006). The use of hypertonic saline for treating intracranial hypertension after traumatic brain injury. *Anesth. Analg.* 102, 1836–1846.
52. Brain Trauma Foundation, American Association of Neurological Surgeons, Congress of Neurological Surgeons, Joint Section on Neurotrauma and Critical Care, AANS/CNS, Bratton, S.L., Chestnut, R.M., Ghajar, J., McConnell Hammond, F.F., Harris, O.A., Hartl, R., Manley, G.T., Nemecek, A., Newell, D.W., Rosenthal, G., Schouten, J., Shutter, L., Timmons, S.D., Ullman, J.S., Videtta, W., Wilberger, J.E., and Wright, D.W. (2007). Guidelines for the management of severe traumatic brain injury. II. Hyperosmolar therapy. *J. Neurotrauma* 24 Suppl. 1, S14–20.
53. Prabhakar, H., Singh, G.P., Anand, V., and Kalaivani, M. (2014). Mannitol versus hypertonic saline for brain relaxation in patients undergoing craniotomy. *Cochrane Database Syst. Rev.* 7, Cd010026.

Address correspondence to:

Juan Sahuquillo, MD, PhD

Department of Neurosurgery and Neurotraumatology

and Neurosurgery Research Unit (UNINN)

Vall d'Hebron University Hospital

Universitat Autònoma de Barcelona

Paseo Vall d'Hebron 119-129

08035 Barcelona

Spain

E-mail: sahuquillo@neurotrauma.net



03

**DOES NORMOBARIC HYPEROXIA CAUSE OXIDATIVE STRESS IN
THE INJURED BRAIN? A MICRODIALYSIS STUDY USING
8-ISO-PGF₂ α AS A BIOMARKER**

**M. VIDAL-JORGE, A. SÁNCHEZ-GUERRERO, G. MUR-BONET, L. CASTRO, A. RĂDOI,
M. RIVEIRO, N. FERNÁNDEZ-PRADO, J. BAENA, M. A. POCA, AND J. SAHUQUILLO
J. NEUROTRAUMA. APR. 2017. [EPUB AHEAD OF PRINT]**

REPRODUCED IN THIS DOCTORAL THESIS WITH PERMISSION.

Does Normobaric Hyperoxia Cause Oxidative Stress in the Injured Brain? A Microdialysis Study Using 8-Iso-Prostaglandin F_{2α} as a Biomarker

Marian Vidal-Jorge,^{1,*} Angela Sánchez-Guerrero,^{1,*} Gemma Mur-Bonet,¹ Lidia Castro,¹ Andreea Rădoi,¹ Marilyn Riveiro,² Natalia Fernández-Prado,² Jacinto Baena,² Maria-Antonia Poca,^{1,3} and Juan Sahuquillo^{1,3}

Abstract

Significant controversy exists regarding the potential clinical benefit of normobaric hyperoxia (NBO) in patients with traumatic brain injury (TBI). This study consisted of two aims: 1) to assess whether NBO improves brain oxygenation and metabolism and 2) to determine whether this therapy may increase the risk of oxidative stress (OxS), using 8-iso-Prostaglandin F_{2α} (PGF_{2α}) as a biomarker. Thirty-one patients with a median admission Glasgow Coma Scale score of 4 (min: 3, max: 12) were monitored with cerebral microdialysis and brain tissue oxygen sensors and treated with fraction of inspired oxygen (FiO₂) of 1.0 for 4 h. Patients were divided into two groups according to the area monitored by the probes: normal injured brain and traumatic penumbra/traumatic core. NBO maintained for 4 h did not induce OxS in patients without preOxS at baseline, except in one case. However, for patients in whom OxS was detected at baseline, NBO induced a significant increase in 8-iso-PGF_{2α}. The results of our study showed that NBO did not change energy metabolism in the whole group of patients. In the five patients with brain lactate concentration ([Lac]_{brain}) > 3.5 mmol/L at baseline, NBO induced a marked reduction in both [Lac]_{brain} and lactate-to-pyruvate ratio. Although these differences were not statistically significant, together with the results of our previous study, they suggest that TBI patients would benefit from receiving NBO when they show indications of disturbed brain metabolism. These findings, in combination with increasing evidence that TBI metabolic crises are common without brain ischemia, open new possibilities for the use of this accessible therapeutic strategy in TBI patients.

Keywords: 8-iso-PGF_{2α}; microdialysis; NBO; oxidative stress, TBI

Introduction

THE MANAGEMENT OF severe traumatic brain injury (TBI) is still based on the assumption that most of the brain damage is delayed (secondary injury) and that interventions directed toward preventing and early treatment of secondary injuries make a difference in both survival and functional outcome.¹ Hypoxemia has been shown to be a secondary brain insult and a strong independent factor of poor neurological outcome in patients with severe TBI.² In the past two decades, significant insight has been gained about the underlying pathophysiology of secondary lesions and the neurochemical cascades that TBI puts into motion. Ischemic and non-ischemic tissue hypoxia have been shown to be highly prevalent after severe TBI.³ Direct assessment of brain tissue oxygen partial pressure (PtiO₂) can be used at the bedside to closely monitor the concentration of free oxygen available in the tissue, which is a surrogate

index of the balance between oxygen supply and consumption. Different retrospective studies have shown that low PtiO₂ is associated with high mortality and poor neurological outcome.^{4,5}

Normobaric oxygen (NBO) treatment using FiO₂ of 1.0 at 1 ata is easily achieved in mechanically ventilated patients. Clinical nonrandomized studies suggest that it could be used as a potential treatment to improve brain oxygenation and some of the metabolic disorders resulting from TBI.⁶ However, there is still significant ongoing controversy regarding this treatment, because the metabolic results are contradictory,^{7–12} and the potential clinical benefit of NBO is based on retrospective studies, studies using historical controls, or nonrandomized clinical studies.^{10,13} In a previous study, our group showed that NBO increased brain PtiO₂ and significantly decreased the lactate-to-pyruvate ratio (LPR) in TBI patients who had increased brain lactate levels at baseline, suggesting that NBO might improve the brain redox state under certain

¹Neurotraumatology and Neurosurgery Research Unit (UNINN), Vall d'Hebron Research Institute (VHIR), Barcelona, Spain.

²Neurotraumatology Intensive Care Unit, and ³Department of Neurosurgery, Vall d'Hebron University Hospital, Universitat Autònoma de Barcelona, Barcelona, Spain.

*The first two authors contributed equally.

conditions.¹¹ Taher and coworkers showed, in a single-center randomized clinical trial, that in patients with severe TBI, NBO administered within the first 6 h after an accident could improve the 6 month neurological outcome.¹⁴

The main concern raised by NBO in TBI, stroke, or hypoxic-ischemic encephalopathy is the potential toxicity of using supranormal levels of partial pressure of oxygen (PaO₂). The mechanisms by which supranormal O₂ may worsen outcome in patients with acute brain injuries is not yet clear; however, it is possible that high FiO₂ could induce vasoconstriction, exacerbate oxidative stress (OxS), increase neuroinflammation, or induce excitotoxicity.¹⁵ Among these proposed mechanisms, the capacity of NBO to induce OxS is the most important, because of the ability of O₂ to induce the production of reactive oxygen species (ROS) and therefore damage proteins, lipids, and DNA.¹⁶ Further, some studies on patients with TBI and cardiac arrest have suggested that arterial hyperoxia is associated with worse outcomes,^{17,18} and that hyperoxia in patients with aneurysmal subarachnoid hemorrhage (aSAH) was associated with a higher incidence of delayed ischemia and poor neurological outcome.^{19,20} Therefore, despite the potential benefits in brain metabolism, NBO is still controversial and its use raises many concerns that need to be clarified before it is entered in clinical trials or is used routinely in some patients with brain injuries.

The short half-life of ROS makes direct measurement virtually impossible in a clinical setting, and therefore, several indirect approaches have been used for estimation. Isoprostanes are stable products of arachidonic acid peroxidation in both animals and humans and are regarded as the most reliable biomarkers (BMs) of OxS *in vivo*, thus providing an important tool for exploring the role of OxS in the pathogenesis of human disease.^{21,22} Isoprostane 8-iso-Prostaglandin F_{2α} (8-iso-PGF_{2α}) is considered one of many reliable BMs for measuring OxS *in vivo*.^{23,24} Recent studies have correlated plasma levels of 8-iso-PGF_{2α} with the Glasgow Coma Scale (GCS) score, and found them to be a good predictor of mortality and outcome with similar sensitivity to GCS.^{23,25} Because of their low molecular weight (< 5000 Da), isoprostanes can be analyzed by microdialysis (MD) and can therefore be used as BMs of OxS in patients with TBI. Isoprostanes can be measured using different analytical methods: gas chromatography-mass spectrometry (GC-MS), liquid chromatography-mass spectrometry (LC/MS), radioimmunoassay, and enzyme immunoassays. However, LC/MS is the optimal method, as it has the advantages of high sensitivity, specificity, and the possibility of analyzing small volumes of biological fluids.²⁶ The aims of this study were to assess the metabolic response of the injured brain to 4 h of NBO treatment and to determine whether hyperoxia increases OxS in either the apparently normal brain or in the regions around focal lesions (traumatic penumbra [TP]). This assessment was accomplished using 8-iso-PGF_{2α} as a BM for OxS *in vivo*.

Methods

Study design and sample collection

A prospective study was conducted from a cohort of adult patients (aged ≥18 years) who had sustained a severe or moderate TBI, had an abnormal CT scan on admission, and required intracranial pressure (ICP) monitoring. Moderate or severe TBI was defined as an admission GCS score ≤13 after resuscitation, which was evaluated when no effects from paralytic agents or sedation were present. The Traumatic Coma Data Bank (TCDB) classification²⁷ was used to stratify patients. This study was approved by the institutional ethics committee of Vall d'Hebron University Hospital (Barcelona, Spain;

protocol PR-AG-140/2011), and written informed consent was obtained from the patients' next of kin. Outcome was assessed by an independent evaluator at 6 months after injury using the Extended Glasgow Outcome Scale (GOSE). The scores obtained were dichotomized into two categories: unfavorable outcome (GOSE: 1–4) and favorable outcome (GOSE: 5–8).

ICP monitoring

Continuous ICP monitoring was performed for all patients using a Camino 110-4B intraparenchymatous ICP sensor (Integra Neurosciences, Plainsboro, NJ). Our complete ICP monitoring protocol for neurocritical patients has been published elsewhere.²⁸ Because of the significant interhemispheric ICP gradients in patients with focal lesions,²⁹ the ICP sensor was always implanted in the pre-coronal region, 11 cm from the nasion, and 3 cm from the midline in the "worst" hemisphere, which was defined as the hemisphere with the most evident lesion. All patients received standard treatment based on the Brain Trauma Foundation guidelines, which aim to maintain the following therapeutic targets: a cerebral perfusion pressure (CPP) >60 mm Hg and an ICP <20 mm Hg.³⁰

Brain tissue oxygen monitoring

All included patients were monitored with a Licox[®] CMP system (Integra Neurocare, Plainsboro, NJ). A CC1.SB sensor (Integra Neurocare) was used in 30 patients, and a CC1.P1 sensor (Integra Neurocare) was used in 4 patients. The brain tissue O₂ probe was implanted close to the MD catheter. Probes were allowed to stabilize for ≥3 h after insertion before any oxygen challenge was performed. End-hour ICP and PtiO₂ readings were recorded either manually by the patients' nurses or by a custom-built system, PowerLab (ADInstruments Ltd, Oxford, United Kingdom), running LabChart software v7.0.3 (ADInstruments Ltd). Data were exported to a flat file for statistical analysis.

Microdialysis probe, infusion pump, and perfusate

A CMA-71 probe (M Dialysis AB, Solna, Sweden) was implanted close to the PtiO₂ probe in all patients. According to the manufacturer's specifications, this probe has a nominal cutoff of ~100 kDa. The 60 mm shaft is made of polyurethane and has an outer diameter of 0.9 mm. The polyarylethersulphone dialysis membrane is 10 mm long, with an outer diameter of 0.6 mm. Cerebral catheters were perfused with a sterile isotonic CNS fluid containing 147 mmol/L NaCl, 1.2 mmol/L CaCl₂, 2.7 mmol/L KCl, and 0.85 mmol/L MgCl₂ (M Dialysis AB) at a fixed flow rate of 0.3 μL/min using a CMA-106 pump (M Dialysis AB). The dialysates were collected hourly by the nurse in charge of the patient via capped microvials. Lactate, pyruvate, glucose, and glycerol were routinely monitored at the bedside using an Iscus Flex microdialysis analyzer (M Dialysis AB). No clinical decisions were based on MD data except for decisions to screen for potential secondary intra- or extracranial insults.

Brain tissue definitions

The CT scan closest to the time of the hyperoxic challenge was used to determine the position of the MD and PtiO₂ probes. All CT scans were reviewed by one of the authors (J.S.), who was blinded to the MD results. The region of the brain sampled by the probes was assigned to one of the following previously described categories: apparently normal injured brain (NB), traumatic penumbra (TP), and traumatic core (TC).³¹ NB was defined as when the probe tips were inserted in a region of the brain without any macroscopically visible abnormality (blood or hypodense lesion) (Fig. 1A). For the brain to be considered "normal," the closest hemorrhagic/hypodense lesion must be located ≥30 mm from the tip of the cerebral MD catheter. TP is arbitrarily defined by the

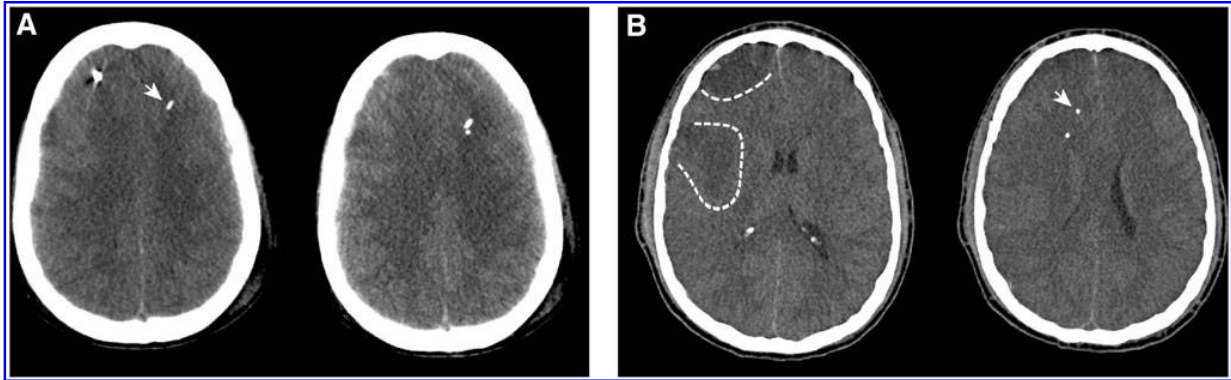


FIG. 1. Images showing the different definitions used in this study for normal injured brain and traumatic penumbra. **(A)** Normal injured brain. This 18-year-old female was admitted to our institution (Vall d'Hebron University Hospital) 1 h after sustaining a severe TBI in a traffic accident. The Glasgow Coma Score (GCS) upon admission was 6 (1-5-T). The admission CT scan indicated findings compatible with a diffuse brain injury type III of Marshall's classification (right hemispheric swelling). In the slice shown on the left, the intraparenchymal intracranial pressure (ICP) probe is seen in the right frontal lobe. In the right slice (left hemisphere), both the oxygen partial pressure (PtiO₂) (white arrow) and the tip of the cerebral microdialysis (MD) probe are implanted in the macroscopically normal brain. **(B)** Traumatic penumbra (TP). This 22-year-old male was admitted to our institution 0.5 h after sustaining a severe TBI in an 8 m fall. GCS at admission was 6 (1-5-T). The CT scan was classified as a diffuse injury type III. In the right slice, both the PtiO₂ (white arrow) and the tip of the cerebral MD probe are placed in the apparently normal brain. However, the slice on the left taken 7 mm below the previous slice showed two frontal hypodense contusions (dashed outline). Because the probes were <20 mm away from the contusions, both were considered to be placed in a zone of TP.

position of the probes in the brain parenchyma without any changes in attenuation, and is located ≥ 20 mm away from any intraparenchymal lesion (e.g., contusions, hematomas). TP was also considered when the probe was located in the brain immediately below any significant extracerebral hematoma (Fig. 1B). TC was defined as when the cerebral MD probe was placed in areas of brain tissue that had macroscopically obvious lesions such as contusions or hemorrhages, or when the MD probe had a small hemorrhagic lesion on the tip.

NBO

Hyperoxic challenge was performed as soon as possible after implanting the MD and PtiO₂ probes. All patients received continuous sedation and analgesia by continuous infusion of midazolam and morphine. Patients had to be hemodynamically stable and correctly sedated at the beginning of the hyperoxic test, as previously described.¹¹ Care was taken to maintain stable CPP, temperature, and partial pressure of arterial carbon dioxide (PaCO₂) to avoid confounding factors that could influence the cerebral metabolism. As a first step, we extracted a baseline arterial blood sample to determine the oxygenation status of the patient. If PaO₂ was >170 mm Hg, the ventilator or FiO₂ settings were modified to obtain a basal PaO₂ between 100 and 150 mm Hg and a PaCO₂ between 35 and 40 mm Hg. After these changes, at least 1 h was allowed to pass before conducting the hyperoxic challenge.

Before hyperoxia was induced, systemic variables (systolic and diastolic blood pressure, heart rate), ICP, CPP, brain microdialysates, and brain PtiO₂ values were recorded. Baseline blood samples were taken, and the total hemoglobin content (ctHb), PaO₂, and PaCO₂ were recorded. As a second step, FiO₂ was increased to 1.0 and maintained at this level for 4 h. Arterial blood samples were extracted again 2 h after starting hyperoxia and at the end of the test, and the same physiological variables mentioned were recorded. Immediately after completing the NBO challenge, FiO₂ was modified again to maintain a PaO₂ of ~ 100 mm Hg. In patients with a catheter in the jugular bulb, a jugular venous blood sample was extracted at the same time as the arterial blood sample (Fig. 2). After microvials were analyzed at the bedside, 0.005% butylated hydroxytoluene (BHT, Sigma, St. Louis, MO) was added in the microdialysate as an antioxidant to prevent *ex vivo* oxidation.³²⁻³⁴

Blood samples were centrifuged and the resultant plasma was aliquoted into tubes with the addition of 0.005% BHT. All samples were stored at -76°C until analysis. The baseline values recorded for both systemic and cerebral parameters correspond to the mean of the 3 h prior to the hyperoxic challenge, and the parameters recorded during the hyperoxic challenge are the mean values obtained during the 4 h of hyperoxia. The pulmonary function at baseline and after the NBO challenge was evaluated using the PaO₂/FiO₂ ratio (PFR) suggested by Rosenthal and coworkers in hyperoxic challenges.³⁵

Monitoring brain oxygen and hypoxic thresholds

A hypoxic pattern was considered when PtiO₂ was <15 mm Hg,³⁶ or when the PtiO₂/PaO₂ ratio was <0.10.³⁷ In the absence of hypoxemia (low PaO₂) and at a constant cerebral metabolic rate of oxygen (CMRO₂), ratios <0.10 indicate covert hypoxia and a deficient delivery of oxygen to the brain. A PtiO₂/PaO₂ ratio >0.35 indicates a relative hyperoxic status.³⁷

Control group for 8-iso-PGF2 α levels

Patients who underwent surgical treatment of posterior fossa or supratentorial lesions and required the implantation of an intraventricular catheter to drain cerebrospinal fluid (CSF) were included as controls. A CMA-71 probe was also inserted in parallel via the same burr hole in the posterior frontal region 11 cm from the nasion and 3 cm from the midline. This cohort was part of a different study, to define the range of reference for brain metabolites.³⁸ The control group for plasma 8-iso-PGF2 α levels was obtained from the plasma of healthy volunteers recruited for a different study. These studies were also approved by the Institutional Ethics Committee of Vall d'Hebron University Hospital (protocols PR-AG-140/2011 and PR-AG-47-2013). Written informed consent was obtained from all of the participants.

In vitro determination of relative recovery for 8-iso-PGF2 α

Experiments were conducted to confirm the *in vitro* recovery characteristics of the CMA-71 probes for 8-iso-PGF2 α in an *in vitro*

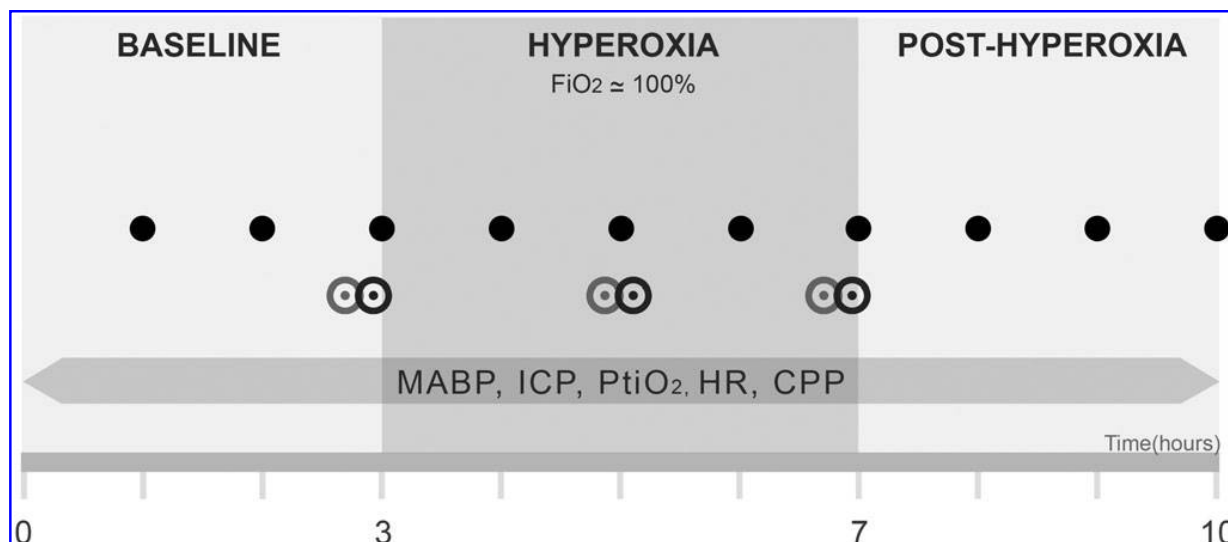


FIG. 2. Schematic diagram showing the normobaric hyperoxia protocol and the measured variables. Dots indicate arterial blood gas extraction, jugular blood gas extraction, and microdialysis sampling. FiO_2 , fraction of inspired oxygen; MABP, mean arterial blood pressure; ICP, intracranial pressure; $PtiO_2$, brain tissue oxygen partial pressure; HR, heart rate; CPP, cerebral perfusion pressure.

setting, as described elsewhere by our group.³⁹ For this study, four commercial CMA-71 probes were used (M Dialysis AB). In brief, the experiments involved placing each CMA-71 catheter into a matrix solution with a known concentration of the study molecule (Cayman Chemical, Ann Arbor, MI). Study matrices were prepared with: 1) Milli-Q water, 2) the CNS fluid used as a perfusate in patients (CNS fluid, M Dialysis AB) containing 147 mmol/L NaCl, 1.2 mmol/L $CaCl_2$, 2.7 mmol/L KCl, and 0.85 mmol/L $MgCl_2$, 3) a constant concentration of 200 pg/mL of 8-iso-PGF_{2 α} (Cayman Chemical), and 4) 200 mg/L of albumin (Grifols[®], Barcelona, Spain), which is within the reference range for the albumin concentration in the normal human CSF.⁴⁰ The matrix solution was placed in a 5 mL glass tube (BD Vacutainer[®], BD Diagnostics[®], Oxford, UK) on an unstirred dry bath (Labnet International, NJ, USA) set at 37°C. The CMA-71 probes were placed in the glass tube containing the matrix, connected to a CMA-402 pump (M Dialysis AB), and perfused at 0.3 μ L/min (18 μ L/h) with an isotonic solution whose ionic composition was identical to that of the matrix solution. To compensate for the osmotic pressure difference between the matrix and the dialysate, 3% albumin was added.

At the start of each experiment and during the first 1–3 h, minor adjustments were made to correct for small differences in hydrostatic pressures, as well as to obtain zero fluid loss and fluid recovery close to the expected theoretical volume (18 μ L/h). The recovery experiment was only conducted when a steady state was achieved. The experiment consisted of a perfusion of the MD probes at a constant flow rate of 0.3 μ L/min and the collection of one microvial every 2 h; a total of 12 microvials were obtained during 3 consecutive days for each catheter (four microvials/day). A sample of the matrix solution was collected and analyzed before and after each microvial change, to control for the variables that can modify the matrix's analyte concentration in the medium, such as evaporation or solute depletion by the dialysis procedure. At the end of the 8 h experiment, a total volume of 200 μ L was removed from the matrix. Both the container and the matrix were replaced daily to avoid volume loss by evaporation and the consequent variations in hydrostatic pressure and analyte concentration. The relative recovery (RR) was calculated using the following equation: $RR = (C_{md}/C_{matrix}) \times 100$ (Eq. 1), where C_{md} and C_{matrix} are the

isoprostane concentrations in the microdialysate and in the matrix, respectively.

Sample preparation and analysis of 8-iso-PGF_{2 α}

Ultra-high performance liquid chromatography coupled to tandem mass spectrometry (UHPLC-MS/MS) was used to analyze 8-iso-PGF_{2 α} in both the brain microdialysate and plasma. To achieve a sample volume sufficient for analyzing the 8-iso-PGF_{2 α} (~30 μ L), MD samples from at least 3 consecutive h were pooled before, during, and after the hyperoxic challenge for baseline, hyperoxia, and post-hyperoxia determinations, respectively. To extract 8-iso-PGF_{2 α} , a modified version of the method described by Taylor and coworkers was used.⁴¹ Ten microliters of a BHT solution (1% in ethanol) was added to the samples and brought up to 200 μ L with Milli-Q H₂O. Then, 200 μ L of hydrolysis solution (1 mL of 50% [w/w] NaOH, 1 mL Milli-Q H₂O, and 10 mL methanol) were added. After vortexing, the mixture was incubated at 37°C for 60 min under nitrogen atmosphere. When the mixture reached room temperature, 300 μ L of Milli-Q H₂O was added and the solution was acidified to pH=3 with HCl (3N). The sample was extracted with 1 mL of hexane and the organic phase was discarded. Then, the aqueous phase was extracted with 3:1 ethyl acetate:hexane and the organic phase was collected and evaporated to dryness and reconstituted with 100 μ L of 1:1 Milli-Q H₂O:MeOH (250 pg/mL of 8-iso-PGF_{2 α} -d4).

The determination of 8-iso-PGF_{2 α} was conducted on an Agilent 1290 UHPLC chromatograph coupled to a triple quadrupole (QqQ) 6495 Series with an ESI interface (Agilent Technologies, Waldbronn, Germany). The chromatographic column used was Kinetex EVO C18 (2.1 mm \times 100 mm, 2.6 μ m, Phenomenex (Torrance, CA). Chromatographic separation was performed in gradient elution using ultrapure water with acetic acid (0.05%) and with acetonitrile (Sigma) (B) as the mobile phases, at a flow rate of 0.3 mL/min. The gradient was as follows: 0.0–0.5 min, 0% B, isocratic; 0.5–1.0 min, 10% B, linear gradient; 1.0–15 min, 50% B, linear gradient; 15.0–16.0 min, 100% B, linear gradient; 16.0–17.5 min, 100% B, isocratic; 17.5–18.0 min, 0% B, linear gradient; and 18.0–20.0 min, 0% B, isocratic. Mass spectrometric detection was performed by multiple reaction monitoring (MRM) in negative ESI

mode, and three transitions for each compound were acquired. In accordance with the guidelines established in the Commission Decision 2002/657/EC,⁴² the transitions monitored were: 353.2 > 291.1, 353.2 > 247.2, and 353.2 > 193.1 for 8-iso-PGF2 α ; and 357.2 > 295.1, 357.2 > 313.1, and 357.2 > 197.2 for 8-iso-PGF2 α -d4. The ESI parameters were as follows: gas temperature (230°C), gas flow rate (11 L/min), nebulizer pressure (20 psi), sheath gas temperature (400°C), sheath gas flow (11 L/min), and capillary voltage (2000 V). All assays were conducted by expert personnel at the Metabolomics Service of the Center for Omics Sciences; personnel were blinded to the clinical results or the results of the hyperoxia challenge (COS, Reus, Spain).

Statistical analysis

Statistical analyses were conducted with R v3.2.0 (R Foundation for Statistical Computing, Vienna, Austria; <http://www.R-project.org>) and the integrated development environment R Studio v0.99.902 (RStudio, Inc., Boston, MA; <http://www.rstudio.com>). Statistical significance was set at $p \leq 0.05$. To define whether or not NBO changed the metabolic profile, all patients were first analyzed and then divided into two groups according to baseline brain lactate levels: patients with baseline brain lactate concentrations ≤ 3.5 mmol/L and patients with brain lactate concentrations > 3.5 mmol/L (protocol described previously¹¹). The lactate thresholds used in our present study were selected based on the range of normality in anesthetized patients, which was published recently.³⁸ To calculate the reference intervals (RIs) for 8-iso-PGF2 α levels in plasma, as well as their upper and lower values, the first step was to apply Horn's algorithm⁴³ (implemented in the package "referenceIntervals") to detect outliers. Each detected outlier was reviewed, and if the patient or the data were considered doubtful, the case was eliminated from the RI calculations. To calculate the upper plasma RI limit, we used the distribution-free nonparametric method described in the Clinical and Laboratory Standards Institute (CLSI) guidelines C28-A3 for estimating percentile intervals^{44,45} by using the R package "referenceIntervals."⁴⁶ In our data, we had many readings that were under the detection limit for 8-iso-PGF2 α in microdialysis samples. Our procedure for managing nondetects was conducted according to the recommendations of Helsel.⁴⁷

Results

Thirty-four patients were included in the study, and a total of 35 hyperoxic tests were performed. In one patient, the test was repeated twice with an interval period of 3 days. Three tests were excluded from analyses: two were excluded because a significant increase in PaO₂ (270.6 and 309.1 mm Hg) did not induce any increase in PtiO₂, and an additional case was excluded because PaO₂ levels did not increase after the hyperoxic challenge. The remaining 31 patients (32 tests) were included in the analysis. The median time from injury until hyperoxic challenge was 57 h (min: 22, max: 96). Table 1 shows a summary of the demographic and clinical data of the included patients. According to the described criteria, 17 patients had the cerebral MD probe inserted in the NB, 12 patients had the cerebral MD probe inserted in the TP, and in 2 patients, the probe was inserted in the TC. Patients in whom the probe was inserted in the TP and TC were grouped together (TP/Core group).

Systemic and intracranial changes after the hyperoxic challenge

Summary measures of the systemic and cerebral parameters at baseline and during the hyperoxic challenge are summarized in Table 2. Jugular blood gas variables were only available in 15 tests (nine in the NB and six in the TP/Core). Five patients (two in the

TABLE 1. DEMOGRAPHIC AND CLINICAL CHARACTERISTICS OF THE PATIENTS

Sex	
Male	24 (77%)
Female	7 (23%)
Age	36 (18–63)
Initial GCS	4 (3–12)
Initial CT scan classification	
Diffuse injury II	10 (32%)
Diffuse injury III	4 (13%)
Diffuse injury IV	0 (0%)
Evacuated mass lesion	10 (32%)
Unevacuated mass lesion	7 (23%)
Neurological outcome (GOSE)	
Good outcome	8 (26%)
Bad outcome	21 (68%)
Dead at discharge	4 (13%)
Lost for 6 month follow-up	2 (6%)
Probe location	
Normal injured brain	17 (55%)
Traumatic penumbra	12 (39%)
Traumatic core	2 (6%)

Sex, initial CT classification, GOSE, and probe location are expressed as number of cases and percentage. Age and Initial GCS are expressed as median (min-max).

GCS, Glasgow Coma Scale; GOSE: Glasgow Outcome Scale Extended.

NB and three in the TP/Core) presented with brain hypoxia at baseline (PtiO₂ < 15 mm Hg and/or a PtiO₂/PaO₂ ratio < 0.10). As expected and compared with baseline, most O₂-related arterial and venous parameters (PtiO₂, PaO₂, arterial oxygen saturation [SaO₂], and arterial oxygen content [CaO₂]) changed significantly in both groups during hyperoxia, as shown in Table 2. Some of the increases in jugular venous oxygen saturation [SjvO₂] and jugular venous oxygen content [CjvO₂] that were observed on both groups were not statistically significant because of the small sample size. Statistically significant—but clinically irrelevant—changes were found in arterial pH in the NB group.

At baseline, seven patients (23%) presented with poor pulmonary function, defined as PFR ≤ 250 . The median PFR at baseline was 317 (min: 165, max: 470) and did not change significantly at the end of NBO (median 320, min: 124, max: 483), indicating that pulmonary function was not affected by 4 h of NBO. Median PaO₂ after hyperoxia increased from 115 mm Hg to 445 mm Hg in the NB group and from 127 mm Hg to 435 mm Hg in the TP/Core group. This produced a modest but statistically significant increase in CaO₂ in both groups. Hyperoxia induced a median Δ PtiO₂ of 54.4 mm Hg (min: 11.9, max: 180 mm Hg) in the NB group and a similar median Δ PtiO₂ of 56.2 mm Hg (min: 16.2, max: 179 mm Hg) in the TP/Core group (Fig. 3). Statistically nonsignificant differences were observed in ICP levels in both groups, and a statistically significant but clinically irrelevant increase in mean arterial blood pressure (MABP) was also observed (Table 2).

Metabolic response to hyperoxia in the normal and injured brain

Baseline and hyperoxia values for both groups (NB and TP/Core) and for each metabolite are shown in Table 3. In the NB group, NBO induced a statistically significant moderate decrease in brain lactate concentration ([Lac]_{brain}) from 1.98 mmol/L (min:

TABLE 2. INTRACRANIAL AND LABORATORY PARAMETERS BEFORE AND AFTER THE HYPEROXIC CHALLENGE

Variable	Normal injured brain (n=17)			Traumatic penumbra-traumatic core (n=15)		
	Baseline	Hyperoxia	p*	Baseline	Hyperoxia	p*
FiO ₂	0.35 (0.24, 0.67)	1.00 (0.95, 1.00)	0.0003	0.40 (0.30, 0.60)	1.00 (0.90, 1.00)	0.0007
PtiO ₂ (mmHg)	25.6 (7.5, 40.7)	74.9 (35.7, 218)	<0.0001	24.8 (4.90, 44.3)	79.3 (21.1, 204)	<0.0001
Brain hypoxia (n,%)	2 (12%)	2 (12%)	NS	3 (20%)	2 (13%)	NS
PFR ≤250 (n,%)	5 (29%)	5 (29%)	NS	3 (13%)	3 (20%)	NS
HR (mmHg)	81 (49, 109)	77 (51, 102)	NS	71 (47, 121)	69 (46, 109)	0.008
MABP (mmHg)	76 (68, 95)	78 (67, 98)	0.035	80 (69, 103)	84 (67, 105)	0.008
ICP (mmHg)	10 (2, 19)	11 (3, 21)	NS	11 (6, 25)	13 (2, 27)	NS
CPP (mmHg)	68 (58, 83)	69 (53, 92)	NS	69 (57, 72)	71 (57, 91)	0.027
Arterial blood gases						
ctHb (g/dL)	10.1 (7.8, 14.9)	10.1 (7.0, 15.6)	NS	10.2 (8.6, 12)	10.0 (8.6, 11.5)	NS
pH	7.45 (7.34, 7.48)	7.42 (7.31, 7.46)	0.033	7.45 (7.38, 7.50)	7.45 (7.28, 7.49)	NS
PaCO ₂ (mmHg)	37.2 (31.4, 48.9)	38.5 (33.5, 49.1)	0.036	37.5 (32.1, 42.2)	37.5 (30.5, 56.5)	NS
PaO ₂ (mmHg)	115 (81.0, 171)	445 (253, 615)	<0.0001	127 (89.0, 204)	435 (266, 621)	<0.0001
SaO ₂ (%)	98.5 (96.2, 99.2)	99.8 (99.1, 99.9)	0.0003	98.9 (97.3, 99.5)	99.7 (99.4, 100.1)	0.001
CaO ₂ (mL/100mL)	14 (11, 20)	15 (11, 22)	0.0007	14 (12, 16)	15 (13, 17)	0.002
Jugular blood gases						
PjvCO ₂ (mmHg)	42.5 (38.1, 46.0)	45.5 (41.5, 50.1)	0.004	43.9 (38.4, 42.4)	45.5 (39.2, 60.0)	NS
PjvO ₂ (mmHg)	42.4 (34.2, 52.6)	56.0 (40.0, 103.6)	0.004	44.1 (38.8, 56.4)	50.9 (48.2, 84.5)	NS
SjvO ₂ (%)	80.0 (65.5, 95.8)	90.9 (73.10, 97.6)	0.008	81.0 (76.2, 88.6)	86.9 (81.9, 97.9)	NS
CjvO ₂ (mL/100mL)	11.5 (8.5, 17.3)	13.2 (9.2, 19.2)	NS	11.3 (10.5, 14.2)	12.7 (10.8, 13.92)	NS
AVDO ₂ (mL/100mL)	3.17 (0.50, 4.54)	2.74 (1.49, 4.73)	NS	2.37 (1.82, 3.61)	2.92 (1.16, 3.40)	NS

Jugular blood gas variables were determined in 15 tests ($n=9$, normal injured brain; $n=6$, traumatic penumbra-traumatic core). Results are expressed as median (min, max).

*Comparisons between variables were made using the two tailed paired t test or the Wilcoxon signed rank test depending on the normality of the variables' distribution.

PFR, PaO₂/FiO₂ ratio; HR, heart rate; MABP, mean arterial blood pressure; ICP, intracranial pressure; CPP, cerebral perfusion pressure; NS, not significant.

1.06, max: 7.42 mmol/L) at baseline to 1.79 mmol/L (min: 0.90, max: 5.72 mmol/L) at hyperoxia nadir (Wilcoxon test, $p=0.0351$). A statistically nonsignificant reduction in the LPR was found in the entire cohort. In the TP/Core group, statistically nonsignificant differences were observed in brain tissue metabolites during hy-

peroxia. Only five patients in the entire cohort (15.6%) presented with a [Lac]_{brain} > 3.5 mmol/L before the hyperoxic challenge. In this subgroup, the median baseline [Lac]_{brain} was 6.4 mmol/L (min: 6.1, max: 7.4 mmol/L), with a median LPR of 25.9 (min: 19.2, max: 217). NBO induced a statistically nonsignificant reduction in both [Lac]_{brain} (median 5.7 mmol/L, min: 4.8, max: 6.4; Wilcoxon test, $p=0.063$) and LPR (median 22.7, min: 19.3, max: 243; Wilcoxon test, $p=0.81$).

In vitro relative recovery and reference range for 8-iso-PGF₂α

Four catheters that yielded a total of 43 samples were used for these experiments. The mean RR calculated using Equation 1 was $117 \pm 38\%$ (min: 55%, max: 222%). We did not find any statistically significant difference among the samples collected on different days (Kruskal–Wallis test, $p=0.919$), which demonstrated stability in the *in vitro* RR during the 3 days that the experiment lasted.

The control group for 8-iso-prostaglandin F₂α concentration (8-IPF₂α) in the microdialysate consisted of 12 patients (8 women and 4 men) with a median age of 43 years (min: 22, max: 69 years). Eleven patients presented with a posterior fossa lesion. Only one patient presented with a supratentorial lesion (meningioma). All patients except one had an Evans index score ≤0.30. This cohort of 12 patients yielded 36 samples that resulted in 12 determinations (the lower number of determinations was because of the need to pool microvials). The minimum detection level for 8-IPF₂α was 55 pg/mL. In our control group ($n=12$), all but one patient presented values under the detection level (< 55 pg/mL). Only one patient presented brain 8-iso-prostaglandin F₂α concentration

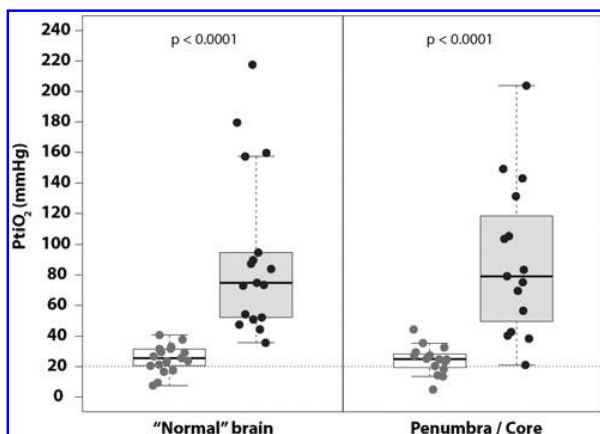


FIG. 3. Box plots showing changes in brain oxygen levels at baseline and after hyperoxic challenge in both groups. Median PaO₂ after hyperoxia increased from 115 mm Hg to 445 mm Hg in the normal brain (NB) group and from 117 mm Hg to 435 mm Hg in the traumatic penumbra (TP)/Core group (see text). This increase in PaO₂ produced a significant increase in PtiO₂ in both brain regions with no macroscopic lesions and in brain regions classified as TP/core. The dashed line marks the 20 mm Hg threshold.

NORMOBARIC HYPEROXIA AND OXIDATIVE STRESS

TABLE 3. BRAIN AND SUBCUTANEOUS MICRODIALYSIS DATA BEFORE AND AFTER THE HYPEROXIC CHALLENGE

Metabolites	Normal injured brain (n=17)			Traumatic penumbra-traumatic core (n=15)		
	Baseline	Hyperoxia	p*	Baseline	Hyperoxia	p*
Brain tissue						
Glucose (mmol/L)	1.33 (0.29, 3.55)	1.38 (0.27, 3.75)	NS	1.40 (0.11, 4.58)	1.44 (0.16, 5.30)	NS
Lactate (mmol/L)	1.98 (1.06, 7.42)	1.79 (0.90, 5.72)	0.0351	2.30 (0.84, 6.64)	2.43 (0.79, 6.37)	NS
Pyruvate (μ mol/L)	77.8 (55.5, 387)	77.3 (45.3, 295)	NS	96.7 (29.9, 273)	82.6 (26.4, 221)	NS
Glycerol (μ mol/L)	69.7 (24.2, 378)	63.5 (31.2, 421)	NS	69.1 (18.8, 585)	63.0 (17.7, 549)	NS
LPR	23.5 (9.93, 38.0)	22.3 (10.3, 39.2)	NS	22.4 (11.4, 217)	21.6 (12.8, 243)	NS
LGR	1.43 (0.40, 8.86)	1.44 (0.36, 9.09)	0.0312	1.33 (0.50, 58.6)	1.20 (0.54, 49.3)	NS
Subcutaneous tissue						
Glucose (mmol/L)	3.18 (0.94, 9.55)	3.56 (0.50, 10.3)	NS	3.65 (1.07, 7.72)	3.73 (0.90, 7.42)	NS
Lactate (mmol/L)	0.92 (0.27, 2.76)	0.84 (0.25, 2.73)	NS	0.89 (0.21, 3.65)	0.72 (0.24, 3.10)	0.0184
Pyruvate (μ mol/L)	64.6 (7.98, 231)	60.2 (9.55, 211)	NS	62.1 (11.5, 232)	66.8 (8.43, 162)	NS
Glycerol (μ mol/L)	274 (85.0, 1364)	240 (67.5, 1341)	NS	199 (76.1, 535)	231 (88.2, 1184)	NS
LPR	13.4 (9.63, 38.7)	14.8 (9.81, 26.7)	NS	12.0 (9.99, 37.3)	13.0 (8.77, 41.7)	NS
LGR	0.29 (0.16, 0.54)	0.28 (0.15, 0.60)	NS	0.28 (0.13, 0.82)	0.27 (0.14, 0.57)	NS

Results are expressed as median (min, max).

*Comparisons between variables were made using the two tailed paired *t* test or the Wilcoxon signed rank test, depending on the normality of the variables' distribution.

LPR, lactate-to-pyruvate ratio; LGR, lactate-to-glucose ratio; NS, not significant.

([8-IPF2 α]_{brain}) = 83.2 pg/mL. This patient was a 31-year-old male who had undergone operation for a vestibular schwannoma without hydrocephalus, in whom ventricular drainage was inserted at the time of surgery. This patient recovered uneventfully and both the ventricular drainage and the MD catheter were removed 72 h after surgery. For the purposes of this article, we considered [8-IPF2 α]_{brain} < 84 pg/mL to be the normal range. Because of the difficulties associated with representing so many censored data in box plots, we summarized these data in Table 4.

The control group for plasma 8-IPF2 α levels consisted of 21 patients (7 women and 15 men), with a median age of 30 years (min: 18, max: 64 years). We obtained only one value under the detection limit that was assigned a value of 12.5 pg/mL and one outlier detected by the Horn's method that was excluded from analysis (2172.7 pg/mL). The median plasma for healthy controls was 115 pg/mL (min: <25, max: 186.2 pg/mL) (Fig. 4). The upper reference limit calculated by the robust method was 186.2 pg/mL.

Plasma and cerebral 8-iso-PGF2 α levels at baseline and after hyperoxia

At baseline, the median plasma level for 8-IPF2 α in TBI patients was 89.1 pg/mL (min: <25, max: 401.7 pg/mL). In three

patients, the levels were above the upper RI. NBO did not increase the plasma levels of 8-IPF2 α . During the 4 h of NBO, the median level in the entire cohort was 77.1 pg/mL (min: <25, max: 470.5 pg/mL), and the same three patients had values that were above the upper RI (Wilcoxon test, *p* = 0.59) (Fig. 4). A total of five patients presented evidence of brain OxS at baseline: two patients in whom the MD probe was placed in NB (14.1%) and three in whom the MD probe was placed in TP/Core (23.1%) (Table 4). Of those patients who showed no evidence of OxS at baseline (both NB and TP/Core groups), only one developed hyperoxia-induced OxS. In this single patient—included in the NB group—8-IPF2 α levels rose from <55 pg/mL at baseline to 612 pg/mL during hyperoxia, and reverted to baseline values 3 h after aborting NBO. Of the two patients who had the MD probe in NB and who showed evidence of OxS at baseline, one had a 8-IPGF2 α value that rose from 390 pg/mL at baseline to 1078 pg/mL during NBO, and then decreased below baseline value 3 h after NBO therapy (98.6 pg/mL). In the second case, the 8-IPGF2 α level decreased from 117 pg/mL at baseline to <55 pg/mL during hyperoxia. Of the three patients who had the MD probe in the TP/Core with evidence of OxS at baseline, two showed a significant increase in tissue 8-IPGF2 α levels during NBO (2342–3153 pg/mL in one patient and 352–1139 pg/mL in one patient). Both patients

TABLE 4. 8-ISO-PGF2 α LEVELS BEFORE, DURING, AND AFTER THE HYPEROXIC CHALLENGE

8-iso-PGF2 α levels	Normal injured brain			Traumatic penumbra-traumatic core		
	Baseline	Hyperoxia (4h)	Post-Hyperoxia	Baseline	Hyperoxia (4h)	Post-Hyperoxia
N (%)	14 (100%)	14 (100%)	14 (100%)	13 (100%)	13 (100%)	13 (100%)
Censored (<55 pg/mL)	11 (78.6%)	11 (78.6%)	11 (78.6%)	10 (76.9%)	10 (76.9%)	7 (53.8%)
Min-Max (pg/mL)	<55–389	<55–1078	<55–98.6	<55–2342	<55–3153	<55–1023
N above upper RI	2 (14.3%)	2 (14.3%)	1 (7.14%)	3 (23.1%)	3 (23.1%)	4 (30.8%)

The minimum detection level for 8-IPF2 α was 55 pg/mL; values <55 pg/mL were considered to be censored data. [8-IPF2 α]_{brain} < 84 pg/mL was defined as the reference range. Values at baseline and post-hyperoxia correspond to 3 h before and after the hyperoxic challenge, respectively.

RI, reference interval.

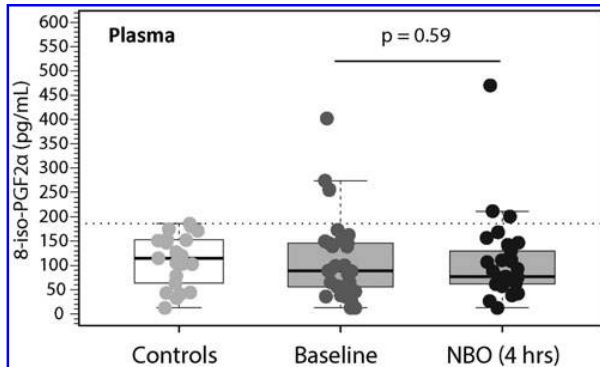


FIG. 4. Box plots showing baseline plasmatic levels for 8-IPGF2 α in controls and in patients, at baseline and after 4 h of hyperoxia. At baseline, three patients showed elevated levels that were above the upper reference interval (RI). Normobaric hyperoxia maintained for 4 h did not increase the plasmatic levels of 8-isoprostaglandin F2 α concentration (8-IPGF2 α) (Wilcoxon test, $p=0.59$). The dotted line is the upper reference limit, as calculated using the robust method (186.2 pg/mL).

reverted to values that were below baseline 8-IPGF2 α levels 3 h after NBO (1023 and 122 pg/mL, respectively). In the third patient, hyperoxia improved OxS, gradually reducing 8-IPGF2 α levels during and after NBO, from 314 to 121 pg/mL.

Discussion

The rationale used to justify that hyperoxia—either normobaric or hyperbaric oxygen (HBO)—is beneficial for patients with severe TBI rests on the robust evidence supporting the notion that ischemic and nonischemic brain hypoxia plays a relevant role in the pathophysiology of the injured brain.⁴⁸ In addition, many experimental and clinical studies indicate that metabolic disorders are common in acute brain injuries and that impaired oxygen delivery—related to oxygen diffusion anomalies—or impaired oxygen utilization in the mitochondria (i.e., mitochondrial dysfunction) may play a significant role in the acute phase of TBI, ischemic and hemorrhagic stroke.^{49–52} In TBI, the oxygen flux from the capillaries to the mitochondria can be altered by diffusion alterations at many different stages.^{52,53} Because diffusion barriers to the cellular delivery of O₂ can develop and persist after injury, some patients may benefit from interventions that increase O₂ pressure and, consequently, the pressure drive that moves oxygen into the brain. Further, a growing body of evidence suggests that mitochondrial dysfunction may play a very important role in the pathophysiology of TBI,⁵⁴ and might explain the significant reduction in the CMRO₂ found after TBI.⁵⁵ Hypothetically, if mitochondrial function is impaired after TBI, then the steeper capillary-cell O₂ gradient induced by hyperoxia may also improve oxygen utilization.

The use of therapeutic O₂ in TBI has focused primarily on hyperbaric hyperoxia (HBO), which has been demonstrated to improve cellular energy metabolism and outcome and which can be neuroprotective in animal models.^{56,57} A few clinical trials have also shown that HBO has short-term neuroprotective effects in both mild and severe TBI,⁵⁸ and produces a significant reduction in the risk of death in TBI patients.⁵⁹ Despite its potential advantages, HBO requires expensive hyperbaric chambers and trained and competent personnel to work in this complex environment. In addition, HBO can be only provided for a short period of time and can significantly disturb conventional critical care management. In this clinical scenario, the simplicity with which NBO can

be applied in any institution makes this low-cost option attractive and easy to implement with no modification to standard of care.

Effects of NBO on brain oxygenation and metabolism

NBO has been shown to induce neuroprotection in multiple models of neurological injury, in particular in several models of focal ischemia in rodents in which NBO was found to extend the salvaging reperfusion time window.⁶⁰ However, the evidence regarding the potential clinical benefits of NBO is still controversial, and varies by the type of brain injury in which it has been applied (i.e., ischemic stroke, aSAH, cardiac arrest). The NBO-induced metabolic effects and changes in brain hemodynamic variables are heterogeneous and sometimes contradictory. Diring and coworkers used positron emission tomography (PET) to show that using NBO in patients with severe TBI for 1 h induced no significant change in the CMRO₂.⁶¹ However, Nortje and coworkers showed that NBO improved cerebral metabolism in brain tissue (defined in our study as TP), with a significant reduction in the LPR but with no significant global changes in the brain.⁶² The same inconsistent results and contradictory findings have been reported for the effects of NBO in brain energy metabolism.^{7–11,63} In the present study, NBO induced a significantly increase in PaO₂ and a statistically significant but clinically irrelevant increase in CaO₂ of ~1 mL/100 mL (Table 2). NBO induced a median increase in PtiO₂ of ~50 mm Hg in both the normal brain and regions defined as TP/Core (Fig. 3). On average, this represented an ~215% increase from PtiO₂ baseline levels, significantly lower than the increase (~600%) achieved by Rockswold and coworkers in the uninjured brain when using HBO.⁶⁴ An interesting finding we observed was that the increase in PtiO₂ was similar for both the normal and the injured brain, suggesting that when the gradient is high enough, O₂ can even diffuse across injured and edematous tissue and can reach the target—the mitochondria—even in the damaged and edematous brain.

A few studies have found that brain metabolism improves after hyperoxic challenge, but with heterogeneous results. The initial studies showed a decrease of [Lac]_{brain} in TBI patients treated with short-lasting hyperoxia.^{8–10,63} However, two subsequent studies did not show a significant decrease in the LPR ratio,^{7,10} and an additional study only observed a decrease in the LPR for patients with an increased baseline [Lac]_{brain}.¹¹ Vilalta and coworkers showed that NBO did not induce any significant change in brain energy metabolism in patients with normal [Lac]_{brain}, but that it significantly decreased the LPR in patients with elevated baseline [Lac]_{brain}.¹¹ Tisdall and coworkers incorporated the study of changes in oxidized cytochrome C oxidase (CCO) concentration by near-infrared spectroscopy (NIRS), and observed a decrease in lactate and LPR levels and an increase in CCO oxidized concentration, that correlated with changes in PtiO₂ and indicated an increased aerobic metabolism.⁶⁵ Similar results have been reported recently by Ghosh and coworkers.¹²

Our study replicates our previous findings that NBO does not change energy metabolism in the whole group of patients.¹¹ Statistically significant—but clinically irrelevant—changes were observed in [Lac]_{brain} and brain pyruvate concentration ([Pyr]_{brain}) in the macroscopically normal brain; however, no significant change in the LPR was observed (Table 3). However, in the five patients (15.6%) who presented with [Lac]_{brain} > 3.5 mmol/L at baseline, NBO induced a statistically nonsignificant reduction both in the [Lac]_{brain} and the LPR. The LPR changed from a median of 25.9 at baseline to a median of 22.7.

Does NBO induce OxS?

Some clinical studies have reported that high oxygen levels are associated with worse outcomes after severe TBI.⁶⁶ These studies raised concerns about using abnormally high FiO_2 levels, and questioned the real benefit of maintaining supranormal PaO_2 levels in patients with acute brain injuries. Tight regulatory control over tissue O_2 levels is an evolutionary mechanism that developed in mammals so as to avoid high levels of O_2 and protect the organs from OxS.⁶⁷ In a recent study, we showed that, in a control group of 16 patients who underwent surgical clipping of incidentally found aneurysms, a 45 min hyperoxic challenge raised PtiO_2 in the normal brain, with a linear relationship between $\text{PaO}_2/\text{PtiO}_2$, but that PtiO_2 never exceeded 120 mm Hg, suggesting that hyperoxia-induced increases in PtiO_2 eventually plateau in the normal brain.³⁷ Therefore, the significant increases we observed in PtiO_2 (PtiO_2 levels were as high as 218 mm Hg in some patients) suggest an impaired or lost oxygen regulatory mechanism.

OxS is a deleterious process that damages proteins, DNA, and lipids, and it induces brain inflammation and necrosis. The brain is highly sensitive to OxS because it consumes 20–30% of inspired oxygen and contains high levels of both polyunsaturated fatty acids and metals, making it an ideal target for a free radical attack.²⁴ Although some studies have demonstrated that hyperoxia increases OxS, others have not. Several factors may account for the conflicting results; however the key factors are likely the type of injury and the pre-existence of OxS in the tissue, as well as the timing and duration of hyperoxia. In experimental models of TBI (i.e., cortical impact, weight drop, and blast injury models), OxS has been shown to play a critical role in the secondary injury process.⁶⁸

The production of ROS by brain cells is closely related to neuroinflammatory cascades. Inflammatory cells may release deleterious compounds or cytokines that exacerbate oxidative damage to metabolically compromised neurons. Both mechanisms are closely related to mitochondrial dysfunction. The production of ROS and its potential deleterious effects are directly related to the amount of dissolved oxygen that increases in NBO and HBO. In our study, NBO maintained for 4 h did not induce OxS, a finding that was true for both the plasma and the uninjured brain, as shown by stable levels of 8-iso-PGF2 α before and after NBO in most patients. Our findings are in agreement with those of Puccio and coworkers, which showed that NBO for 2 h did not increase the CSF levels of P_2 -isoprostane, nor did it reduce the total antioxidant reserves.⁶⁹ We showed the same findings and with longer NBO, supporting the notion that NBO does not induce OxS in macroscopically uninjured brains without pre-existing OxS. In the few cases of elevated baseline OxS, NBO increased the levels of 8-iso-PGF2 α . However, OxS normalized after reverting to normoxia for these patients, indicating a direct effect of NBO on BMs of cell damage.

Alternative mechanisms for NBO-induced adverse effects

An alternative/synergic mechanistic option to justify the potential deleterious effect observed with HBO/NBO is the powerful vasoconstriction effect that the dissolved oxygen has on the brain, and the reduction in CBF it induces.^{70,71} Hyperoxia can directly induce vasoconstriction, or indirectly induce it because of hyperoxia-associated hypocapnia.⁷² Experimental and clinical studies have suggested that excitotoxicity may be an alternative or a synergic factor together with OxS for oxygen-induced tissue

damage.¹⁵ In a retrospective analysis of 36 patients with severe TBI, Quintard and coworkers showed that hyperoxia was associated with a threefold increase in extracellular glutamate.¹⁵ We did not systematically monitor glutamate in our patients, and, therefore, we do not have data to verify or refute this hypothesis.

Study limitations

Because our study was not designed or powered to assess clinical outcomes, we are unable to comment on whether or not NBO had any effect on clinical outcomes. In addition, the clinical relevance of our finding that NBO may worsen OxS in patients with pre-existing OxS cannot be clarified from our data. Additionally, we cannot disregard the fact that longer exposures to hyperoxia (> 4 h) can induce OxS. In some studies, the presence of OxS has been observed in prolonged (> 24 h) NBO or HBO but has not been found in shorter periods of hyperoxia. Only a few patients in our study had lactate levels >3.5 at baseline, and although there was a positive trend toward improving energy metabolism in this subgroup, our study lacked sufficient power to replicate the metabolic findings reported by our group previously.¹¹

An important step in defining potential subgroups of patients who can benefit from NBO will be to use both MD and PtiO_2 monitoring to detect such patients. Patients with either low PtiO_2 —once other causes of brain hypoxia have been ruled out—or in whom $[\text{Lac}]_{\text{brain}}$ and the LP ratio are increased—suggesting mitochondrial dysfunction—may be potential targets for NBO. Future studies should investigate this question more closely.

Conclusions and Future Directions

Our study shows that NBO increased PtiO_2 in both macroscopically NB and in traumatic regions at risk (TP), suggesting that pressurized oxygen may be delivered to the target and offered to the mitochondria in regions with brain edema and impaired oxygen diffusion. By using a robust indicator of OxS, namely 8-iso-PGF2 α , which was analyzed directly from the brain extracellular fluid, we showed that 4 h of NBO only induced OxS in the injured brains of patients with pre-existing OxS. Only one patient who showed no signs of OxS at baseline demonstrated an increase in 8-iso-PGF2 α levels. These findings, combined with the increasing evidence that in TBI metabolic crises are common without brain ischemia,^{73–75} open new avenues for the use of this accessible therapeutic strategy in patients with TBI. However, our study was not designed to evaluate the impact of NBO on short- or long-term outcomes in these patients, nor was it designed to define the best way to optimize NBO treatment in terms of frequency, dose, and length. In addition, whether or not longer NBO times (< 4 h) or repetitive doses of NBO in the same day may induce OxS and/or lung injury has not been defined thus far, despite the fact some experimental studies suggest that OxS might be related to longer exposure to hyperoxia.¹⁶

In light of our data, it can be hypothesized that TBI patients would benefit from receiving NBO when they show indications of brain hypoxia, objective indicators of metabolic stress, or evidence of increased anaerobic metabolism. In the era of personalized medicine and precision medicine, new clinical trials should focus on these subgroups of patients to see whether or not NBO may be a useful tool in patients in whom oxygen delivery, metabolic crisis, or mitochondrial dysfunction (either in isolation or in combination) play a role in the pathophysiology of brain damage. Using longer periods of NBO (24 h) may be the next step; however, such an investigation requires proof of safety, and, ideally, the use of robust biomarkers of brain OxS and metabolic impairment.

Acknowledgments

We gratefully acknowledge the contribution of the nursing staff, and the technical and research staff of the Neurotraumatology Intensive Care Unit. We greatly appreciate the help of Dennis R. Helsel of Practical Stats (Denver, CO) for orienting us in the nondetect management of the 8-iso-PGF_{2α} data. The Neurotraumatology and Neurosurgery Research Unit is supported by a grant from the Departament d'Universitats, Recerca i Societat de la Informació de la Generalitat de Catalunya (SGR 2014-844). This work has been supported in part by the Fondo de Investigación Sanitaria (Instituto de Salud Carlos III) with grants FIS PI11/00700 (J. Sahuquillo) and grant FIS PI13/02397 (M.A. Poca), which were co-financed by the European Regional Development Fund (ERDF). A. Sánchez-Guerrero and A. Rádoi are recipients of pre-doctoral grants from the ISCIII (FI12/00074) and from Fundació Institut de Recerca HUVH (PRED-VHIR-2012-26), respectively.

Author Disclosure Statement

No competing financial interests exist.

References

- Park, E., Bell, J.D., and Baker, A.J. (2008). Traumatic brain injury: can the consequences be stopped? *CMAJ* 178, 1163–1170.
- Stahel, P.F., Wade, R.S., and Moore, E.F. (2007). Hypoxia and hypotension, the “lethal duo” in traumatic brain injury: implications for prehospital care. *Intensive Care Med.* 34, 402–404.
- Sahuquillo, J., Poca, M.A., and Amorós, S. (2001). Current aspects of pathophysiology and cell dysfunction after severe head injury. *Curr. Pharm. Des.* 7, 1475–1503.
- Meixensberger, J., Renner, C., Simanowski, R., Schmidtke, A., Dings, J., and Roosen, K. (2004). Influence of cerebral oxygenation following severe head injury on neuropsychological testing. *Neurol. Res.* 26, 414–417.
- Valadka, A.B., Gopinath, S.P., Contant, C.F., Uzura, M., and Robertson, C.S. (1998). Relationship of brain tissue PO₂ to outcome after severe head injury. *Crit. Care Med.* 26, 1576–1581.
- Stiefel, M.F., Spiotta, A., Gracias, V.H., Garuffe, A.M., Guillaumondegui, O., Maloney-Wilensky, E., Bloom, S., Grady, M.S., and LeRoux, P.D. (2005). Reduced mortality rate in patients with severe traumatic brain injury treated with brain tissue oxygen monitoring. *J. Neurosurg.* 103, 805–811.
- Magnoni, S., Ghisoni, L., Locatelli, M., Caimi, M., Colombo, A., Valeriani, V., and Stocchetti, N. (2003). Lack of improvement in cerebral metabolism after hyperoxia in severe head injury: a microdialysis study. *J. Neurosurg.* 98, 952–958.
- Menzel, M., Doppenberg, E.M., Zauner, A., Soukup, J., Reinert, M.M., Clausen, T., Brockenbrough, P.B., and Bullock, R. (1999). Cerebral oxygenation in patients after severe head injury: monitoring and effects of arterial hyperoxia on cerebral blood flow, metabolism and intracranial pressure. *J. Neurosurg. Anesthesiol.* 11, 240–251.
- Reinert, M., Barth, A., Rothen, H.U., Schaller, B., Takala, J., and Seiler, R.W. (2003). Effects of cerebral perfusion pressure and increased fraction of inspired oxygen on brain tissue oxygen, lactate and glucose in patients with severe head injury. *Acta Neurochir. (Wien)* 145, 341–349.
- Tolias, C.M., Reinert, M., Seiler, R., Gilman, C., Scharf, A., and Bullock, M.R. (2004). Normobaric hyperoxia-induced improvement in cerebral metabolism and reduction in intracranial pressure in patients with severe head injury: a prospective historical cohort-matched study. *J. Neurosurg.* 101, 435–444.
- Vilalta, A., Sahuquillo, J., Merino, M.A., Poca, M.A., Garnacho, A., Martínez-Valverde, T., and Dronavalli, M. (2011). Normobaric hyperoxia in traumatic brain injury. Does brain metabolic state influence the response to hyperoxic challenge? *J. Neurotrauma* 28, 1139–1148.
- Ghosh, A., Highton, D., Kolyva, C., Tachtsidis, I., Elwell, C.E., and Smith, M. (2016). Hyperoxia results in increased aerobic metabolism following acute brain injury. *J. Cereb. Blood Flow Metab.* [Epub ahead of print. DOI: 10.1177/0271678X16674222].
- Narotam, P.K., Morrison, J.F., and Nathoo, N. (2009). Brain tissue oxygen monitoring in traumatic brain injury and major trauma: outcome analysis of a brain tissue oxygen-directed therapy. *J. Neurosurg.* 111, 672–682.
- Taher, A., Pilehvari, Z., Poorolajal, J., and Aghajani, M. (2016). Effects of normobaric hyperoxia in traumatic brain injury: a randomized controlled clinical trial. *Trauma Mon* 21, e26772.
- Quintard, H., Patet, C., Suys, T., Marques-Vidal, P., and Oddo, M. (2015). Normobaric hyperoxia is associated with increased cerebral excitotoxicity after severe traumatic brain injury. *Neurocrit. Care* 22, 243–250.
- Tatarkova, Z., Engler, I., Calkovska, A., Mokra, D., Drgova, A., Hodas, P., Lehotsky, J., Dobrota, D., and Kaplan, P. (2011). Effect of long-term normobaric hyperoxia on oxidative stress in mitochondria of the guinea pig brain. *Neurochem. Res.* 36, 1475–1481.
- Litjós, J.-F., Mira, J.-P., Duranteau, J., and Cariou, A. (2016). Hyperoxia toxicity after cardiac arrest: What is the evidence? *Ann. Intens. Care* 6, 23.
- Helmerhorst, H.J., Roos-Blom, M.J., van Westerloo, D.J., and de Jonge, E. (2015). Association between arterial hyperoxia and outcome in subsets of critical illness: a systematic review, meta-analysis, and meta-regression of cohort studies. *Crit. Care Med.* 43, 1508–1519.
- Jeon, S.B., Choi, H.A., Badjatia, N., Schmidt, J.M., Lantigua, H., Claassen, J., Connolly, E.S., Mayer, S.A., and Lee, K. (2014). Hyperoxia may be related to delayed cerebral ischemia and poor outcome after subarachnoid haemorrhage. *J. Neurol. Neurosurg. Psychiatry* 85, 1301–1307.
- Starke, R.M., and Kassell, N.F. (2014). The link between hyperoxia, delayed cerebral ischaemia and poor outcome after aneurysmal SAH: association or therapeutic endeavour. *J. Neurol. Neurosurg. Psychiatry* 85, 1292.
- Basu, S. (2008). F₂-isoprostanes in human health and diseases: from molecular mechanisms to clinical implications. *Antioxid. Redox Signal.* 10, 1405–1434.
- Pryor, W.A. (2000). Forum on Oxidative Stress Status (OSS) and its measurement. *Free Radic. Biol. Med.* 29, 387.
- Clausen, F., Marklund, N., Lewné, A., Enblad, P., Basu, S., and Hillered, L. (2011). Interstitial F₂-isoprostane 8-iso-PGF_{2α} as a biomarker of oxidative stress after severe human traumatic brain injury. *J. Neurotrauma* 29, 766–775.
- Mendes Arent, A., de Souza, L.F., Walz, R., and Dafre, A.L. (2014). Perspectives on molecular biomarkers of oxidative stress and antioxidant strategies in traumatic brain injury. *BioMed Res. Int.* 2014, 723060.
- Yu, G.-F., Jie, Y.-Q., Wu, A., Huang, Q., Dai, W.-M., and Fan, X.-F. (2013). Increased plasma 8-iso-Prostaglandin F_{2α} concentration in severe human traumatic brain injury. *Clin. Chim. Acta* 421, 7–11.
- Janicka, M., Kot-Wasik, A., Paradzziej-Lukowicz, J., Sularz-Peszynska, G., Bartoszek, A., and Namiesnik, J. (2013). LC-MS/MS determination of isoprostanes in plasma samples collected from mice exposed to doxorubicin or tert-butyl hydroperoxide. *Int. J. Mol. Sci.* 14, 6157–6169.
- Marshall, S.B., Klauber, M.R., Van Berkum Clark, M., Eisenberg, H.M., Jane, J., Luerssen, T.G., Marmarou, A., Marshall, L.F., and Foulkes, M.A. (1991). A new classification of head injury based on computerized tomography. *J. Neurosurg. (Suppl.)* 75, 14–20.
- Poca, M.A., Sahuquillo, J., Arribas, M., Bagueña, M., Amorós, S., and Rubio, E. (2002). Fiberoptic intraparenchymal brain pressure monitoring with the Camino V420 monitor: reflections on our experience in 163 severely head-injured patients. *J. Neurotrauma* 19, 439–448.
- Sahuquillo, J., Poca, M.A., Arribas, M., Garnacho, A., and Rubio, E. (1999). Interhemispheric supratentorial intracranial pressure gradients in head-injured patients: are they clinically important? *J. Neurosurg.* 90, 16–26.
- Brain Trauma Foundation, American Association of Neurological Surgeons, Congress of Neurological Surgeons, Joint Section on Neurotrauma Critical Care, AANC and CNS (2007). Guidelines for the management of severe traumatic brain injury (3rd Edition). *J. Neurotrauma* 24, Suppl. 1, S1–106.
- Martínez-Valverde, T., Sánchez-Guerrero, A., Vidal-Jorge, M., Torne, R., Castro, L., Gandara, D., Munar, F., Poca, M.A., and Sahuquillo, J. (2016). Characterization of the ionic profile of the extracellular space of the injured and ischemic brain: a microdialysis study. *J. Neurotrauma*.

32. Liu, W., Morrow, J.D., and Yin, H. (2009). Quantification of F2-isoprostanes as a reliable index of oxidative stress in vivo using gas chromatography–mass spectrometry (GC-MS) method. *Free Radic. Biol. Med.* 47, 1101–1107.
33. Milne, G.L., Sanchez, S.C., Musiek, E.S., and Morrow, J.D. (2007). Quantification of F2-isoprostanes as a biomarker of oxidative stress. *Nat. Protoc.* 2, 221–226.
34. Spickett, C.M., Wiswedel, I., Siems, W., Zarkovic, K., and Zarkovic, N. (2010). Advances in methods for the determination of biologically relevant lipid peroxidation products. *Free Radic. Res.* 44, 1172–1202.
35. Rosenthal, G., Hemphill, J.C., Sorani, M., Martin, C., Morabito, D., Meeker, M., Wang, V., and Manley, G.T. (2008). The role of lung function in brain tissue oxygenation following traumatic brain injury. *J. Neurosurg.* 108, 59–65.
36. Jodicke, A., Hubner, F., and Boker, D.K. (2003). Monitoring of brain tissue oxygenation during aneurysm surgery: prediction of procedure-related ischemic events. *J. Neurosurg.* 98, 515–523.
37. Arikian, F., Vilalta, J., Noguer, M., Olive, M., Vidal-Jorge, M., and Sahuquillo, J. (2014). Intraoperative monitoring of brain tissue oxygenation during arteriovenous malformation resection. *J. Neurosurg. Anesthesiol.* 26, 328–341.
38. Sanchez-Guerrero, A., Mur-Bonet, G., Vidal-Jorge, M., Gandara-Sabatini, D., Chocron, I., Cordero, E., Poca, M.A., Mullen, K., and Sahuquillo, J. (2016). Reappraisal of the reference levels for energy metabolites in the extracellular fluid of the human brain. *J. Cereb. Blood Flow Metab.* [Epub ahead of print. DOI: 10.1177/0271678X16674222].
39. Martínez-Valverde, T., Vidal-Jorge, M., Montoya, N., Sánchez-Guerrero, A., Manrique, S., Munar, F., Pellegrini, M.D., Poca, M.A., and Sahuquillo, J. (2015). Brain microdialysis as a tool to explore the ionic profile of the brain extracellular space in neurocritical patients: a methodological approach and feasibility study. *J. Neurotrauma* 32, 7–16.
40. Reiber, H., Thompson, E.J., Grimsley, G., Bernardi, G., Adam, P., Monteiro de Almeida, S., Fredman, P., Keir, G., Lammers, M., Liblau, R., Menna-Barreto, M., Sa, M.J., Seres, E., Sindić, C.J., Teelken, A., Trendelenburg, C., Trojano, M., van Antwerpen, M.P., and Verbeek, M.M. (2003). Quality assurance for cerebrospinal fluid protein analysis: international consensus by an Internet-based group discussion. *Clin. Chem. Lab. Med.* 41, 331–337.
41. Taylor, A.W., Bruno, R.S., Frei, B., and Traber, M.G. (2006). Benefits of prolonged gradient separation for high-performance liquid chromatography–tandem mass spectrometry quantitation of plasma total 15-series F-isoprostanes. *Anal. Biochem.* 350, 41–51.
42. Directive 96/23/EC (2002). COMMISSION DECISION of 12 August 2002 implementing Council Directive 96/23/EC concerning the performance of analytical methods and the interpretation of results. *Official Journal of the European Communities*, 8–36.
43. Horn, P.S., Feng, L., Li, Y., and Pesce, A.J. (2001). Effect of outliers and nonhealthy individuals on reference interval estimation. *Clin. Chem.* 47, 2137–2145.
44. Horn, P.S., Pesce, A.J., and Copeland, B.E. (1998). A robust approach to reference interval estimation and evaluation. *Clin. Chem.* 44, 622–631.
45. Horn, P.S., and Pesce, A.J. (2003). Reference intervals: an update. *Clin. Chim. Acta* 334, 5–23.
46. Finnegan, D. (2014). referenceIntervals: Reference Intervals. R package version 1.1.1. <http://CRAN-R-project.org/package=referenceIntervals> (last accessed April 10, 2017).
47. Helsel, D.R. (2012). *Statistics for Censored Environmental Data Using Minitab and R*, 2nd ed. Wiley: Hoboken, NJ.
48. Sala, N., Suys, T., Zerlauth, J.B., Bouzat, P., Messerer, M., Bloch, J., Levivier, M., Magistretti, P.J., Meuli, R., and Oddo, M. (2013). Cerebral extracellular lactate increase is predominantly nonischemic in patients with severe traumatic brain injury. *J. Cereb. Blood Flow Metab.* 33, 1815–1822.
49. Patet, C., Suys, T., Carteron, L., and Oddo, M. (2016). Cerebral lactate metabolism after traumatic brain injury. *Curr. Neurol. Neurosci. Rep.* 16, 31.
50. Oddo, M., Levine, J.M., Frangos, S., Maloney-Wilensky, E., Carrera, E., Daniel, R.T., Levivier, M., Magistretti, P.J., and Leroux, P.D. (2012). Brain lactate metabolism in humans with subarachnoid hemorrhage. *Stroke* 43, 1418–1421.
51. Sahuquillo, J., Merino, M.-A., Sánchez-Guerrero, A., Arikian Abello, F., Vidal-Jorge, M., Martínez-Valverde, T., Rey, A., Riveiro, M., and Poca, M.-A. (2014). Lactate and the lactate-to-pyruvate molar ratio cannot be used as independent biomarkers for monitoring brain energetic metabolism: a microdialysis study in patients with traumatic brain injuries. *PLoS One* 9, e102540.
52. Veenith, T.V., Carter, E.L., Geeraerts, T. and et al. (2016). Pathophysiologic mechanisms of cerebral ischemia and diffusion hypoxia in traumatic brain injury. *JAMA Neurol.* 73, 542–550.
53. Menon, D.K., Coles, J.P., Gupta, A.K., Fryer, T.D., Smielewski, P., Chatfield, D.A., Aigbirhio, F., Skepper, J.N., Minhas, P.S., Hutchinson, P.J., Carpenter, T.A., Clark, J.C., and Pickard, J.D. (2004). Diffusion limited oxygen delivery following head injury. *Crit. Care Med.* 32, 1384–1390.
54. Verweij, B.H., Muizelaar, J.P., Vinas, F.C., Peterson, P.L., Xiong, Y., and Lee, C.P. (2000). Impaired cerebral mitochondrial function after traumatic brain injury in humans. *J. Neurosurg.* 93, 815–820.
55. Obrist, W.D., Langfitt, T.W., Jaggi, J.L., Cruz, J., and Gennarelli, T.A. (1984). Cerebral blood flow and metabolism in comatose patients with acute head injury. Relationship to intracranial hypertension. *J. Neurosurg.* 61, 241–253.
56. Wang, G.H., Zhang, X.G., Jiang, Z.L., Li, X., Peng, L.L., Li, Y.C., and Wang, Y. (2010). Neuroprotective effects of hyperbaric oxygen treatment on traumatic brain injury in the rat. *J. Neurotrauma* 27, 1733–1743.
57. Lin, K.C., Niu, K.C., Tsai, K.J., Kuo, J.R., Wang, L.C., Chio, C.C., and Chang, C.P. (2012). Attenuating inflammation but stimulating both angiogenesis and neurogenesis using hyperbaric oxygen in rats with traumatic brain injury. *J. Trauma* 72, 650–659.
58. Huang, L., and Obenaus, A. (2011). Hyperbaric oxygen therapy for traumatic brain injury. *Med. Gas Res.* 1, 21.
59. Bennett, M.H., Trytko, B., and Jonker, B. (2012). Hyperbaric oxygen therapy for the adjunctive treatment of traumatic brain injury. *Cochrane Database Syst. Rev.* 12, CD004609.
60. Deng, J., Lei, C., Chen, Y., Fang, Z., Yang, Q., Zhang, H., Cai, M., Shi, L., Dong, H., and Xiong, L. (2014). Neuroprotective gases – Fantasy or reality for clinical use? *Prog. Neurobiol.* 115, 210–245.
61. Diring, M.N., Aiyagari, V., Zazulia, A.R., Videen, T.O., and Powers, W.J. (2007). Effect of hyperoxia on cerebral metabolic rate for oxygen measured using positron emission tomography in patients with acute severe head injury. *J. Neurosurg.* 106, 526–529.
62. Nortje, J., Coles, J.P., Timofeev, I., Fryer, T.D., Aigbirhio, F.I., Smielewski, P., Outtrim, J.G., Chatfield, D.A., Pickard, J.D., Hutchinson, P.J., Gupta, A.K., and Menon, D.K. (2008). Effect of hyperoxia on regional oxygenation and metabolism after severe traumatic brain injury: Preliminary findings. *Crit. Care Med.* 36, 273–281.
63. Menzel, M., Doppenberg, E.M., Zauner, A., Soukup, J., Reinert, M.M., and Bullock, R. (1999). Increased inspired oxygen concentration as a factor in improved brain tissue oxygenation and tissue lactate levels after severe human head injury. *J. Neurosurg.* 91, 1–10.
64. Rockswold, S.B., Rockswold, G.L., Zaun, D.A., and Liu, J. (2013). A prospective, randomized Phase II clinical trial to evaluate the effect of combined hyperbaric and normobaric hyperoxia on cerebral metabolism, intracranial pressure, oxygen toxicity, and clinical outcome in severe traumatic brain injury. *J. Neurosurg.* 118, 1317–1328.
65. Tisdall, M.M., Tachtsidis, I., Leung, T.S., Elwell, C.E., and Smith, M. (2008). Increase in cerebral aerobic metabolism by normobaric hyperoxia after traumatic brain injury. *J. Neurosurg.* 109, 424–432.
66. Brenner, M., Stein, D., Hu, P., Kufera, J., Woodford, M., and Scalea, T. (2012). Association between early hyperoxia and worse outcomes after traumatic brain injury. *Arch. Surg.* 147, 1042–1046.
67. Massabau, J.C. (2001). From low arterial- to low tissue-oxygenation strategy. An evolutionary theory. *Respir. Physiol.* 128, 249–261.
68. Readnower, R.D., Chavko, M., Adeeb, S., Conroy, M.D., Pauly, J.R., McCarron, R.M., and Sullivan, P.G. (2010). Increase in blood–brain barrier permeability, oxidative stress, and activated microglia in a rat model of blast-induced traumatic brain injury. *J. Neurosci. Res.* 88, 3530–3539.
69. Puccio, A.M., Hoffman, L.A., Bayir, H., Zullo, T.G., Fischer, M., Darby, J., Alexander, S., Dixon, C.E., Okonkwo, D.O., and Kochanek, P.M. (2009). Effect of short periods of normobaric hyperoxia on local brain tissue oxygenation and cerebrospinal fluid oxidative stress markers in severe traumatic brain injury. *J. Neurotrauma* 26, 1241–1249.
70. Kety, S.S., and Schmidt, C.F. (1948). Effects of altered arterial tensions of carbon dioxide and oxygen on cerebral blood flow and cerebral oxygen consumption of normal young men. *J. Clin. Invest.* 27, 484–492.

71. Johnston, A.J., Steiner, L.A., Gupta, A.K., and Menon, D.K. (2003). Cerebral oxygen vasoreactivity and cerebral tissue oxygen reactivity. *Br. J. Anaesth.* 90, 774–786.
72. Jacobson, I., Harper, A.M., and McDowall, D.G. (1964). The effects of oxygen at 1 and 2 atmospheres on the blood flow and oxygen uptake of the cerebral cortex. *Surg. Gynecol. Obstet.* 119, 737–742.
73. Vespa, P., Bergsneider, M., Hattori, N., Wu, H.M., Huang, S.C., Martin, N.A., Glenn, T.C., McArthur, D.L., and Hovda, D.A. (2005). Metabolic crisis without brain ischemia is common after traumatic brain injury: a combined microdialysis and positron emission tomography study. *J. Cereb. Blood Flow Metab.* 25, 763–774.
74. Wu, H.M., Huang, S.C., Vespa, P., Hovda, D.A., and Bergsneider, M. (2013). Redefining the pericontusional penumbra following traumatic brain injury: evidence of deteriorating metabolic derangements based on positron emission tomography. *J. Neurotrauma* 30, 352–360.
75. Coles, J.P., Fryer, T.D., Smielewski, P., Rice, K., Clark, J.C., Pickard, J.D., and Menon, D.K. (2004). Defining ischemic burden after traumatic brain injury using 15O PET imaging of cerebral physiology. *J. Cereb. Blood Flow Metab.* 24, 191–201.

Address correspondence to:

Juan Sahuquillo, MD, PhD

Department of Neurosurgery and Neurotraumatology

and Neurosurgery Research Unit

Vall d'Hebron University Hospital

Universitat Autònoma de Barcelona

Paseo Vall d'Hebron 119-129

08035 Barcelona

Spain

E-mail: sahuquillo@neurotrauma.net

SECTION



RESULTS & DISCUSSION

4

- 1 CHARACTERIZATION OF THE IONIC PROFILE OF THE EXTRACELLULAR SPACE OF THE INJURED AND ISCHEMIC BRAIN
- 2 NORMOBARIC HYPEROXIA AND OXIDATIVE STRESS IN THE INJURED BRAIN

RESULTS AND DISCUSSION

In this section, the results and the discussion of the 2 published articles are explained in the first 2 separated sub-sections. Study limitations and future directions, of each study, are detailed in the last sub-section.

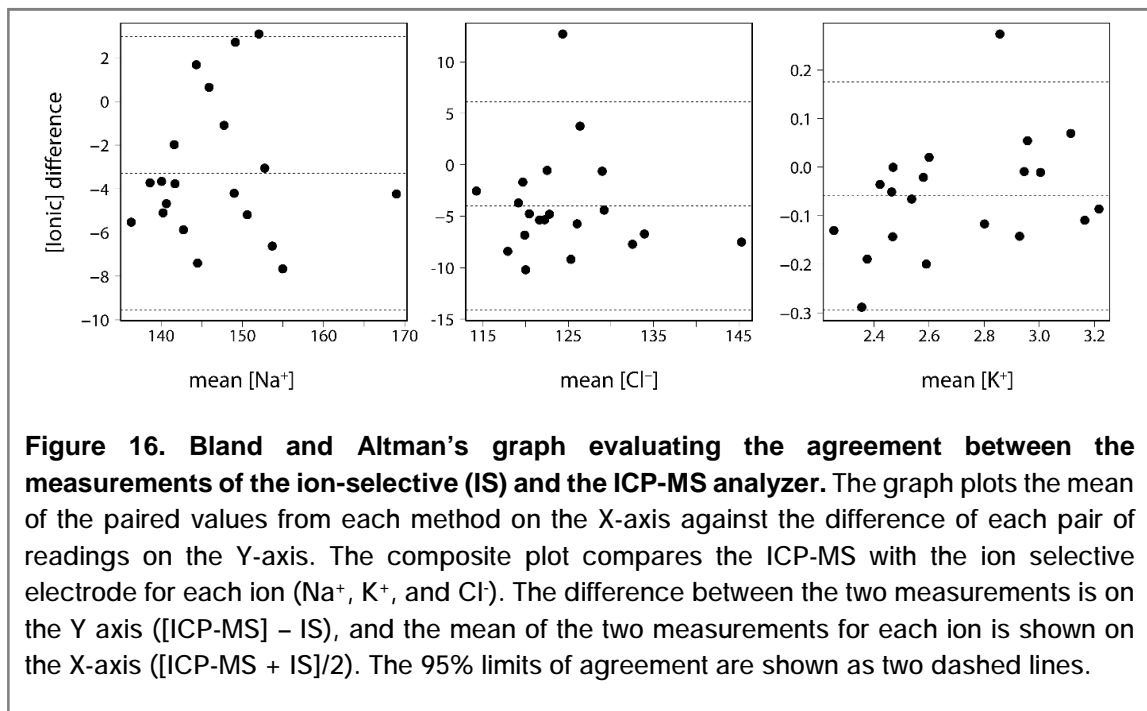
1. Characterization of the ionic profile of the extracellular space of the injured and ischemic brain

TBI and IS cause a variable disruption of ionic homeostasis and massive ionic fluxes with subsequent osmotic water movement across the cells. Changes in ionic concentrations induce water accumulation in the ICS and the ECS and cause brain edema, brain swelling and deformation of the damaged tissue.¹²⁵ Brain edema is the most frequent cause of neurological worsening and death in these patients. Osmotherapy (mannitol and HTS) is a first line therapy for managing increased ICP.

Cerebral MD is a tool increasingly embraced in neurocritical intensive care units (ICU) in the management of patients with severe TBI and aneurysmal subarachnoid hemorrhage who are comatose.²⁴¹ In a previous study, our group showed that *in vitro*, the RR for Na⁺, K⁺, and Cl⁻ was ~100% and that the *in vivo* ionic concentration can be reliably calculated from the MD concentrations in patients with acute brain injuries.²²¹ However, the main limitation of the methodology used in our proof-of-concept study —conventional ion selective electrode-based analyzer— was its low temporal resolution. ICP-MS is a state-of-the-art instrumental technique for the analysis of metals including ions at very low concentrations.²²² In the present study, we show, to the best of our knowledge, the first use of MD with ICP-MS to define the human ionic profile of the ECS. We present data on the ionic fingerprints (Na⁺, K⁺, and Cl⁻) of the different regions of the injured brain (normal brain, ischemic/traumatic penumbra and traumatic/ ischemic core) in a cohort of patients with TBI and MMCAI.

1.1. Ion-selective electrode versus ICP-MS analyzer

To verify whether we can use our previously defined linear model to determine the ionic concentrations in the brain ECS²²¹ we performed a validation study comparing the selective ion electrodes from the AU5400™ analyzer (Diagnostic Systems Group, New York, USA) used in our previous study, and the new ICP-MS analyzer (Agilent 7500ce, Agilent Technologies, Santa Clara, CA, USA). For this validation, 20 CSF samples were collected during routine analysis from neurosurgical patients who needed either lumbar or ventricular drainage to treat their primary pathologies. Ion determination was performed both with the AU5400™ analyzer, as described previously²²¹, and with the ICP-MS. The agreement between both methods was excellent and within ± 1.96 SD of the mean difference for all ions, despite the fact the AU5400 analyzer slightly overestimated $[\text{Na}^+]_{\text{CSF}}$ (**Figure 16**).



1.2. Study Group

A prospective study was conducted in patients aged above 17 years old admitted to the Neurotraumatology ICU at Vall d'Hebron University Hospital between February 2011 and July 2014, with moderate/severe TBI (GCS score ≤ 13) or MMCAI. All patients received ICP and MD monitoring during 48 h post-trauma or malignant stroke onset. A total of 34

patients were included; 21 patients had a severe TBI, and 13 had a MMCAI. **Table 6** summarizes the demographic and clinical data.

For this study, the determination of extracellular potassium concentration ($[K^+]_o$), sodium concentration ($[Na^+]_o$) and chloride concentration ($[Cl^-]_o$) was performed on the ICP-MS. For cerebral MD samples, the minimum volume needed to carry out the ion measurements is 12 μ L. For routine metabolic bedside analysis in neurocritical patients, the Iscus Flex analyzer consumes 5 μ L to measure glucose, lactate, pyruvate and glycerol and 8 μ L if glutamate is included. Because of this, it was necessary to pool the residual content of 2 microvials to obtain the minimum required volume for assaying the ionic content in TBI and stroke samples. In the control group (next section) —in which glutamate was not quantified— the residual volume of one microvial was sufficient for the analysis.

Table 6. Summary of demographic and clinical data

Group	N	Age	GCS	NIHSS	GOSE	mRS
TBI	21	34 (18 - 57)	5 (3 - 15)	NA	3 (1 - 8)	NA
MMCAI	13	52 (36 - 65)	NA	19 (23- 14)	NA	4 (3 - 6)
Control	7	38 (22 - 60)	NA	NA	NA	NA

Summary data are presented as median (min - max).

TBI: Traumatic brain injury; MMCAI: Malignant middle cerebral artery infarction; GCS: Glasgow Coma Scale; NIHSS: National institute of health stroke scale; GOSE: Glasgow Outcome Scale Extended; mRS: Modified Rankin Scale; NA: Not applicable.

1.3. Control group

Patients who underwent surgical treatment to treat posterior fossa and supratentorial lesions, and did not present any neurological abnormalities in the supratentorial compartment were included as a control group for ion profile determination and for establishing the upper reference range for $[Gly]_o$. The inclusion criteria to enroll patients in the study were: 1) posterior fossa or supratentorial lesions requiring the implantation of an external ventricular catheter for the drainage of CSF during surgery and at least 24 h postoperatively; 2) no neuroradiological abnormalities in the white/gray matter in the supratentorial compartment, as evaluated based on the following MRI (Magnetic Resonance Imaging) sequences: T1-weighted (T1W), T2-weighted (T2W), or Fluid Attenuated Inversion Recovery (FLAIR) images, 3) a normal ventricular size, which was defined as an Evan Index below or equal to 0.30,²⁴² and 4) written informed consent signed by the patient or the next-of-kin. During the intraventricular catheter implantation,

a CMA-71 MD probe was also inserted in parallel via the same burr hole in the posterior frontal region 10.5 cm from the nasion and 3 cm from the midline (**Figure 17A**). Under these criteria, seven patients were included as controls for the ionic profile (**Table 6**). The $[Gly]_o$ threshold was selected based on the range of normality of 15 anesthetized patients who underwent surgical treatment to treat posterior fossa and supratentorial lesions where the upper reference level was 209 $\mu\text{mol/L}$.

1.4. Ionic content related to cerebral pathology and microdialysis catheter insertion zone

The CT scan closest in time to the microdialysate analysis was used to determine the position of the cerebral MD probe. The cerebral MD catheters were usually inserted in non-injured brain tissue and/or in regions of interest according to the previously described methodology.¹⁹⁴ The region of the brain sampled by the MD catheter was categorized in one of the following categories defined operatively for this study: normal injured brain, ischemic core, traumatic core, traumatic penumbra and ischemic penumbra. All probes were inserted into the subcortical white matter.

Normal injured brain (NB) was defined when the MD tip was inserted in a region of the brain without any macroscopically visible abnormality (blood or hypodense lesion). To consider the brain to be "normal", the closest hemorrhagic/hypodense lesion must be located at least 30 mm from the tip of the MD catheter (**Figure 17B**). **Ischemic penumbra (IP)** was defined for patients with a MMCAI in which the tip of the MD probe was placed in a brain region of normal macroscopic appearance around the core with no changes in brain tissue attenuation in a non-contrast CT scan; these regions had to be at least 20 mm away from any brain region with parenchymal abnormalities (**Figure 17C**). **Traumatic penumbra (TP)** arbitrarily defines the position of the probe in the brain parenchyma without any changes in attenuation and that is at least 20 mm away from any intraparenchymal lesion (e.g., contusions, hematomas). The traumatic penumbra is also considered when the probe was located in the brain immediately below any significant extracerebral hematoma (**Figure 17D**). The **traumatic core (TC)** was defined in TBI patients when the MD probe was placed in areas of brain tissue that had macroscopically obvious lesions such as contusions, hemorrhages or when the MD probe had a small hemorrhagic lesion on the tip (**Figure 17E**). **Ischemic core (IC)** tissue was defined when

the patient had a confirmed diagnosis MMCAI, and the MD probe was in a hypodense lesion with or without a hemorrhagic component. In most patients, the probe was inserted after completing a decompressive craniotomy (**Figure 17F**).

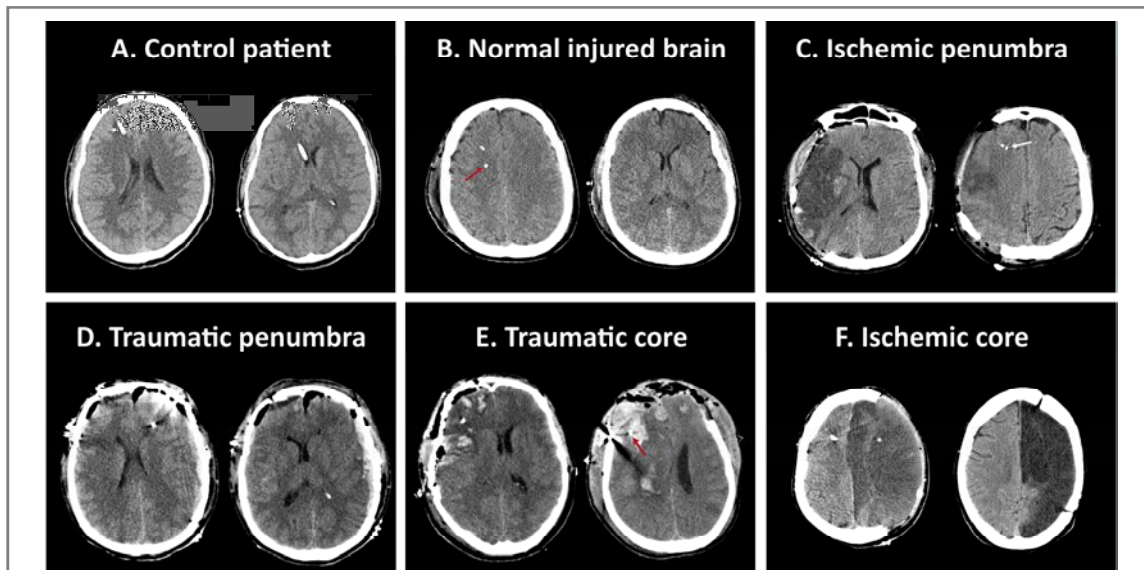


Figure 17. Examples of computed tomography (CT) images for the categories of brain tissue defined according to the placement of the cerebral microdialysis (MD) catheter.

A. Control patient. A 34-year-old male operated of a right giant vestibular schwannoma. The tip of the cerebral MD probe is shown on the left of the ventricular catheter that is placed in the right frontal horn. **B. Normal injured brain.** A 46-year-old male admitted to the neurocritical care unit after severe TBI with an admission Glasgow coma scale (GCS) score of 4. The patient was included in the diffuse injury II of the Marshall's classification. The control CT scan showed that both the MD probe (arrow) and the brain tissue oxygen pressure (PtiO₂) probe were inserted in the frontal subcortical white matter, in a brain region without any gross abnormality. **C. Ischemic penumbra.** A 46-year-old male admitted to our institution 5 h after an abrupt onset of left hemiparesis. The National Institute of Health Stroke Scale (NIHSS) score on admission was 13. Because of the clinical and neuroradiological evolution to a malignant stroke, the patient underwent decompressive hemicraniectomy 32 h after stroke onset. On the left CT scan, the infarction extension is seen with preservation of the anterior cerebral artery territory. On the right CT, the MD catheter (arrow) is shown 27 mm from the hypodense lesion (ischemic core). **D. Traumatic penumbra.** A 52-year-old male was injured in a blast. His GCS score on admission was 5. The patient was operated on admission of a left-acute subdural hematoma, left frontal contusion, and a right extradural hematoma. A MD probe was inserted at the end of surgery in the left frontal lobe (left CT scan). **E. Traumatic core.** A 48-year-old male was admitted because he suffered a head injury at his workplace. His GCS score on admission was 7. The patient was immediately operated on for evacuation of right hemorrhagic contusion and a bifrontal extradural hematoma. A bifrontal decompressive craniectomy was also conducted. In the control CT scan, the PtiO₂ probe is seen on the left, and the MD is visible on the right slice (arrow). Some metallic artifacts are generated by a 8-electrode electrocorticography strip placed on the right frontal lobe. **F. Ischemic core.** A 52-year-old male underwent decompressive hemicraniectomy because of a malignant evolution at 14 h after stroke onset; probe inserted in the core of the infarction. The control CT scan of the same patient one year after surgery (right) shows the residual hypodense necrotic brain.

According to these criteria, 5 patients (all in the TBI group) had the MD probe placed in macroscopically normal brain (yielding 59 dialysates), 10 patients in traumatic penumbra (yielding 101 dialysates), one patient in the ischemic penumbra (yielding 12 dialysates), 12 patients in the hypodense ischemic core (yielding 141 dialysates) and 6 patients in zones with gross lesions (traumatic core) (yielding 61 dialysates). The statistics of interstitial levels of each ion ($[\text{Na}^+]_o$, $[\text{K}^+]_o$ and $[\text{Cl}^-]_o$) are summarized in **Table 7**.

Ionic profile in the 'normal' injured brain

The ions thresholds used in the present study were selected based on the data obtained from the control group (**Table 7**). The upper limits for each ion were: 162 mmol/L for $[\text{Na}^+]_o$, 4.1 mmol/L for $[\text{K}^+]_o$, and 159mmol/L for $[\text{Cl}^-]_o$. Although 8 values (all corresponding to the same patient) had a $[\text{Na}^+]_o$ concentration above 162 mmol/L, and 2 determinations had a $[\text{K}^+]_o$ concentration above 4.1mmol/L, the differences between the mean concentrations of the control group and the normal injured brain were not statistically significant for any of the ions studied.

Ionic profile of the ischemic core

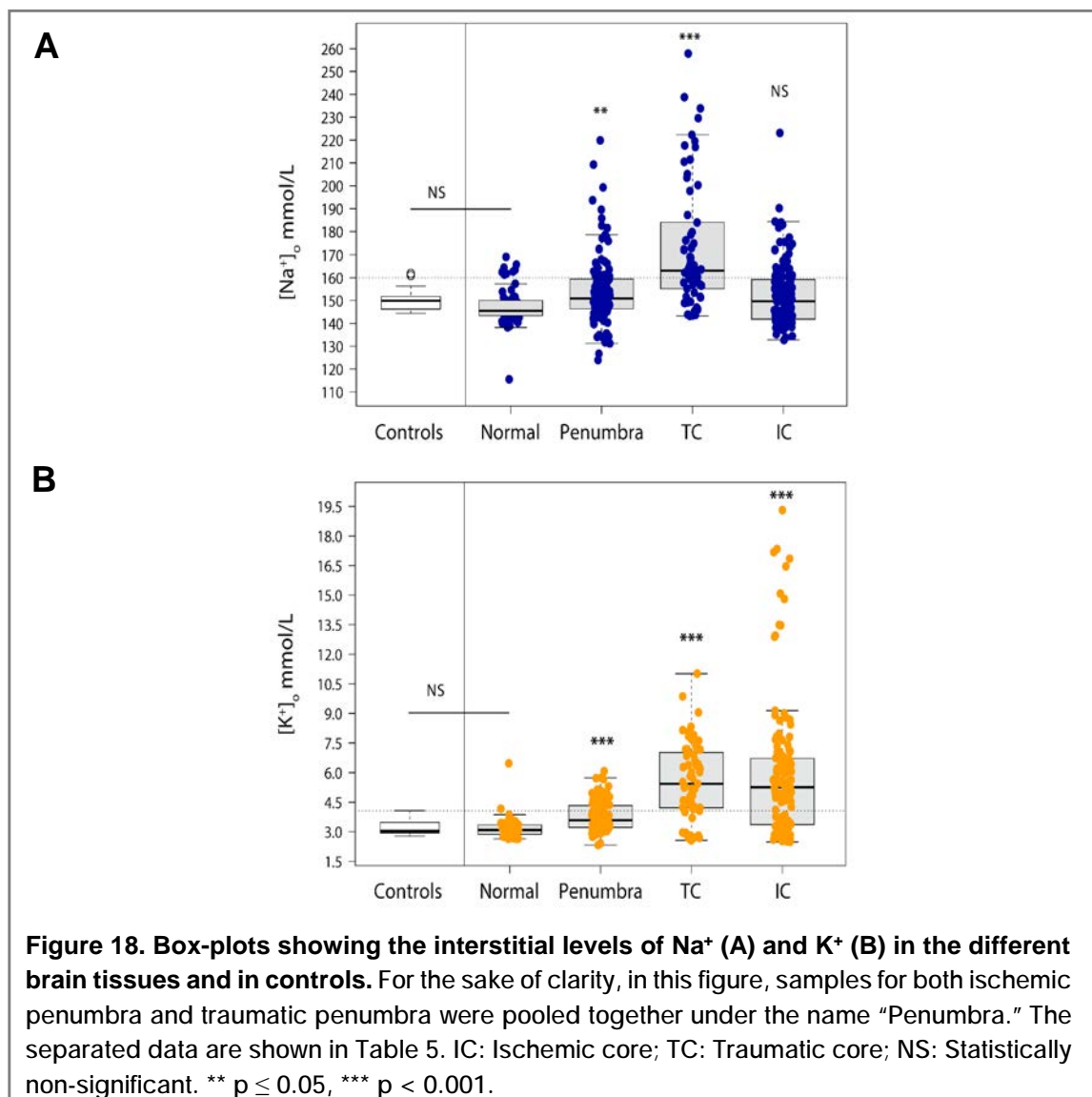
The IC was characterized by a statistically significant increase in the $[\text{K}^+]_o$ levels, when compared with both controls and probes placed in the normal injured brain (Kruskal-Wallis test, $p < 0.001$) (**Figure 18**). Despite the fact that higher $[\text{Na}^+]_o$ concentrations were found in the IC compared with the normal tissue (NB and controls), these differences were not statistically significant. In all the samples $[\text{Cl}^-]_o$ increased or decreased linearly with $[\text{Na}^+]_o$ (**Figure 19B**) with a Pearson product-moment correlation coefficient of 0.93 ($p < 0.001$).

Ionic profile of the traumatic core

In the TC, it was observed that 52% of the measures had $[\text{Na}^+]_o$ above the upper threshold of this ion (162 mmol/L), and for K^+ 80% of the measures were above 4.1

mmol/L (**Figure 18**). The differences between the mean concentration in the TC and the control group were statistically significant for all of the analyzed ions (Kruskal-Wallis test, $p < 0.001$). The samples with $[Na^+]_o$ above 162 mmol/L also had a high $[Cl^-]_o$ but did not show a significantly higher $[K^+]_o$ (**Figures 18 and 19**).

The $[Na^+]_o/[Na^+]_{plasma}$ ratio in the TC was significantly higher than that observed in controls, in the normal-appearing brain and in the ischemic and traumatic penumbra. However, the IC did not show a significantly increased $[Na^+]_o/[Na^+]_{plasma}$ in comparison to the other damaged or non-damaged brain regions. The $[K^+]_o/[K^+]_{plasma}$ ratio was significantly higher in the TC and IC than in the controls, the normal-appearing brain regions and the ischemic and traumatic penumbra (ANOVA on ranks, $p < 0.0001$). Therefore, our data suggest that the $[K^+]_o/[K^+]_{plasma}$ ratio is a good biomarker for detecting brain tissue that is at risk for irreversibly damage.



Ionic profile of the ischemic and traumatic penumbra

According to our criteria, only one patient with MMCAI had the cerebral MD probe inserted in the IP, and 10 patients in the traumatic penumbra. As a result, the 11 patients were pooled together to yield 113 samples for the analysis. In the pooled group, 23.4% of the determinations had a $[\text{Na}^+]_o$ concentration above the upper threshold of 162 mmol/L and 30% had a $[\text{K}^+]_o$ concentration above 4.1 mmol/L (**Figure 18**). The differences observed for both ions were statistically significant when compared with controls and the normal injured brain (Kruskal-Wallis test, $p < 0.05$ and Kruskal-Wallis test, $p < 0.001$, respectively) (**Figure 18**). However, for $[\text{Cl}^-]_o$, differences were only statistically significant when compared to the control group (Kruskal-Wallis test, $p = 0.009$) (**Figure 19**).

When comparing the ionic profiles of the IP and TP, TP showed more $[\text{Na}^+]_o$ than IP. However, due to the asymmetry in the number of samples (101 in the TP group vs. 12 in the IP group), these differences may be spurious, and further analysis could not be conducted.

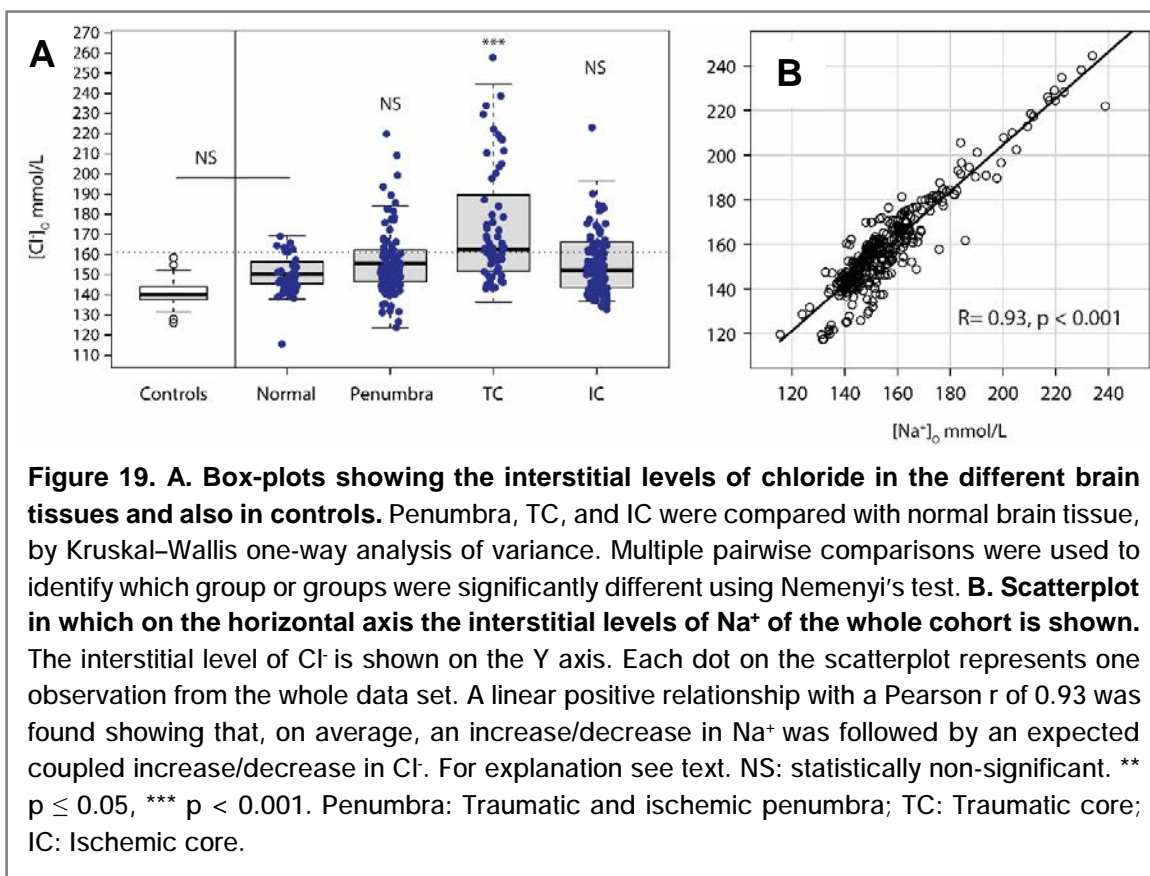


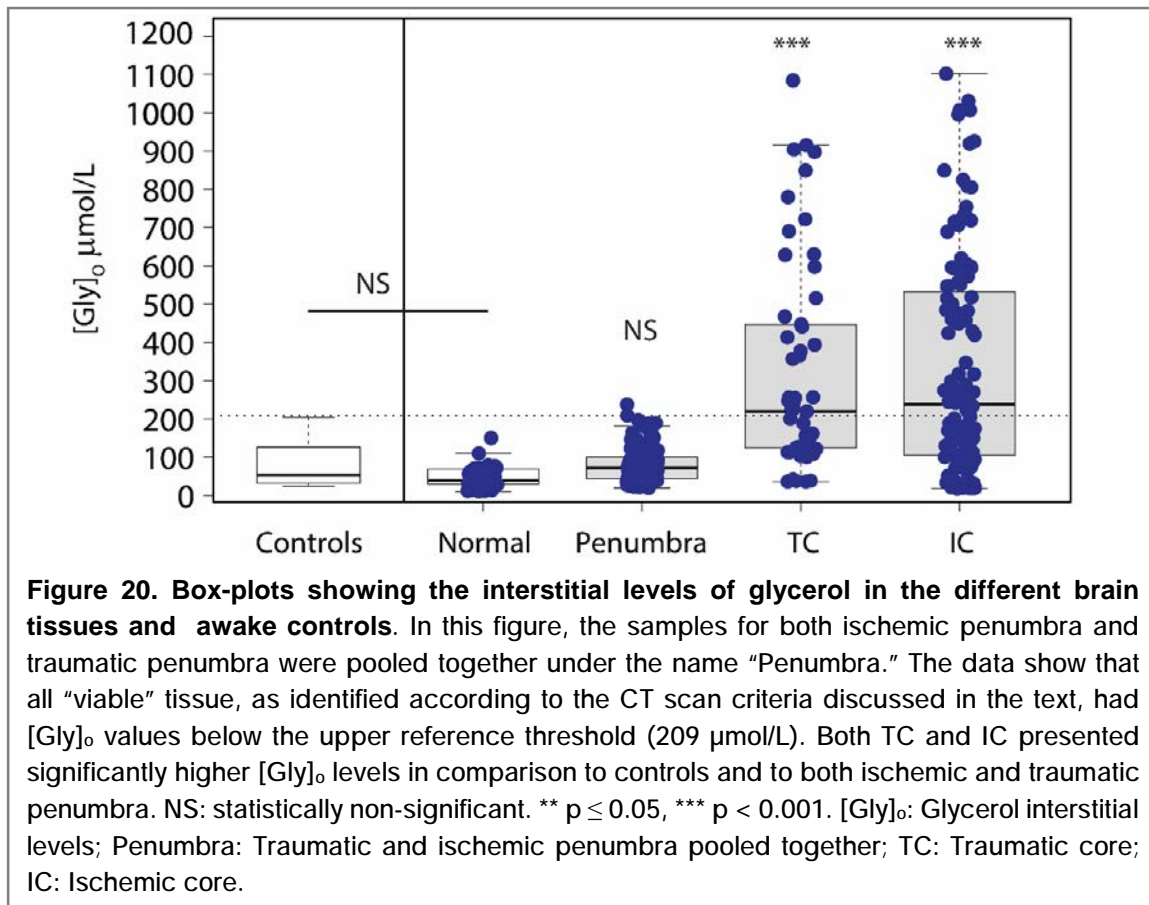
Table 7. Ionic concentration and ratios by probe tissue location

Group	[Na ⁺] _o mmol/L	[K ⁺] _o mmol/L	[Cl ⁻] _o mmol/L	[Na ⁺] _{plasma} mmol/L	[K ⁺] _{plasma} mmol/L	[Na ⁺] _o /[Na ⁺] _{plasma}	[K ⁺] _o /[K ⁺] _{plasma}	Glycerol μmol/L
Control	149.9 (144.4 – 161.8)	3.03 (2.78 – 4.08)	140.1 (126.1 – 158.5)	137.4 (134.7 – 142.5)	4.23 (3.39 – 4.60)	1.09 (1.01 – 1.17)	0.79 (0.69 – 0.88)	53.8 (24.4 – 205.0)*
Normal brain	145.5 (115.5 – 169.1)	3.08 (2.64 – 6.47)	150.2 (119.6 – 179.9)	139.0 (134.6 – 145.2)	3.59 (3.23 – 4.12)	1.05 (0.82 – 1.19)	0.85 (0.72 – 1.75)	39.3 (10.5 – 150.0)
Penumbra	150.8 (123.9 – 219.9)	3.58 (2.32 – 6.07)	155.7 (117.3 – 224.4)	139.8 (130.7 – 153.2)	4.01 (3.16 – 4.6)	1.06 (0.88 – 1.55)	0.96 (0.55 – 1.50)	71.4 (19.3 – 237.3)
Traumatic penumbra	152.1 (123.9 – 219.9)	3.46 (2.32 – 6.07)	157.8 (125.9 – 224.4)	139.9 (130.7 – 153.2)	4.0 (3.16 – 4.60)	1.06 (0.88 – 1.55)	0.95 (0.55 – 1.50)	76.3 (22.2 – 237.3)
Ischemic penumbra	134.6 (131.2 – 142.8)	4.81 (4.48 – 5.3)	121.7 (117.3 – 132.8)	136.4 (133.5 – 141.6)	136.4 (133.5 – 141.6)	0.99 (0.92 – 1.02)	1.22 (1.04 – 1.32)	26.0 (19.3 – 164.0)
Ischemic core	149.7 (132.7 – 223.1)	5.25 (2.48 – 19.9)	152.0 (136.7 – 228.3)	141.8 (136.9 – 152.0)	3.82 (2.82 – 4.68)	1.05 (0.93 – 1.55)	1.31 (0.63 – 5.08)**	238.0 (17.6 – 1102.0)
Traumatic core	163.0 (143.2 – 264.3)	5.43 (2.56 – 11.0)	166.5 (136.4 – 276.2)	145.7 (138.6 – 166.6)	3.95 (3.16 – 5.08)	1.15 (0.92 – 1.83)**	1.34 (0.72 – 2.25)**	219.5 (36.1 – 5748.0)

The values are summarized as the median (min – max). *The control values for glycerol were obtained from another study (15 anesthetized patients). The [Na⁺]_o/[Na⁺]_{plasma} was significantly higher in the traumatic core (TC) than in the controls, in the normal brain and in the ischemic core (IC) (Anova on ranks, p < 0.0001). However, the [Na⁺]_o/[Na⁺]_{plasma} in the IC was not significantly different from those in the controls or in the perilesional penumbra. The [K⁺]_o/[K⁺]_{plasma} was significantly higher (**) in the TC and the IC in comparison to the ratios observed in the normal brain, in the controls and in the penumbra (Anova on ranks, p < 0.0001). Penumbra: Traumatic penumbra and Traumatic core; [Na⁺]_o: extracellular sodium concentration; [Na⁺]_{plasma}: plasma concentration of sodium; [K⁺]_o: extracellular potassium concentration; [Cl⁻]_o: extracellular chloride concentration; [Na⁺]_{plasma}: plasma concentration of sodium; and [K⁺]_{plasma}: plasma concentration of potassium.

1.5. Glycerol in the normal and injured brain

[Gly]_o was used as a biochemical marker of cell tissue viability. The summary of the [Gly]_o observed in the different brain tissue categories is shown in **Table 7**. In **Figure 20**, we show the boxplots for all of the [Gly]_o data in the different brain regions. Of the entire patient dataset, there are 32 missing values for glycerol. In the traumatic normal-appearing brain and in all but one reading in the perilesional penumbra, all [Gly]_o values were below the 209 $\mu\text{mol/L}$ threshold that was established in an independent study in the control group described above. Readings above 209 $\mu\text{mol/L}$ were only found in the IC and TC (**Figure 20**). Nevertheless, in 47.6% of the IC samples and 49.1% of the TC, [Gly]_o was within the normal reference range (**Figure 20**).



1.6. Discussion

Despite the fact that Reinert and coworkers²³¹ determined the concentration of $[K^+]_o$ in a cohort of 85 patients with severe TBI, this is; to our knowledge, the first study to explore

the ionic profile (Na^+ , K^+ and Cl^-) of different areas of the injured brain in both the human ischemic brain and the human traumatically injured brain. In addition, we incorporated a small cohort of patients without supratentorial disease that were used as controls. The ionic composition of brain ECS has been inferred from measurements taken from the CSF in human controls —assuming that in the steady state, there are no significant concentration gradients between the two compartments— and from animal models, ranging from rats to primates.²⁴³

The feasibility of implementing a reliable method to monitor the brain ionic content in neurocritical patients was introduced by our group in a previous study.²²¹ In that study, we showed that the ionic concentrations can be reliably calculated from the dialysate by using a least-squares linear regression model and that the RR was close to 100% for all ions of interest.²²¹ Recently, Antunes et al. have also shown that the *in vitro* RR for K^+ was between 91 and 100% with the same MD probe used in our study.²⁴⁴ The main limitation of our previous methodology was the poor temporal resolution; this is a drawback intrinsic to most ion-selective analyzers, that in our case required at least 85 μL for the ionic assay and therefore pooling at least 8 microvials.²²¹ For this reason, in the present study we used the best analytical method available to improve the temporal resolution for determination of ions in small sample volumes, the ICP-MS.²⁴⁵

ICP-MS allows extremely low detection limits —in the parts per million (ppm) levels— in samples of less than 20 μL .²⁴⁵ Therefore, we could study the ionic concentrations hourly, at the same frequency that is used routinely at the bedside for monitoring brain energy metabolism. When we compared ICP-MS with the ion-selective electrode analyzer used in our previous study,²²¹ we observed that the correlation between both methods was excellent, and, consequently, the chemistry analyzers available in most hospitals are excellent alternatives to ICP-MS, except for their low temporal resolution.

The ionic profile of the normal brain

For ethical and methodological reasons, the normal ionic range for the human brain ECS has not been published until now. For this reason, most studies have used the reference levels measured in the CSF instead. Since our control group was limited to 7 patients, we could not establish a robust upper limit for all the ions studied from our data.

Nevertheless, we observed that $[K^+]_o$ never exceeded 4.1 mmol/L in controls. This upper limit was similar to the upper reference levels of 3.6 - 4.1 mmol/L in the CSF of control patients described by others.^{221,246}

The ionic profile of the normal injured brain

In the present study, we differentiated between controls (patients with no neuroradiological abnormalities in the supratentorial compartment) and MD probes placed in the macroscopically non-injured brain tissue/areas of TBI patients (**Figure 17**). We cannot disregard that in these apparently normal areas, the ionic permeability of the BBB might be increased and that various non-visible metabolic, functional, or structural abnormalities in axons, endothelial cells, glial, and neurons might be present.^{36,81} In this group of patients, we found a modest statistically not significant increase in $[Na^+]_o$ and $[Cl^-]_o$ in some samples, but $[K^+]_o$ always remained within normal limits. Only two patients presented an isolated $[K^+]_o$ reading above 4.1 mmol/L that reverted spontaneously in the next assay. Reversible increases in $[K^+]_o$ can be found in clinical or subclinical epileptic seizures²⁴⁷ and also in CSD (cortical spreading depression) phenomena; this is a frequent finding in TBI that is related to a poor neurological outcome.^{248,249} However, the differences between the mean concentrations of the control group and the normal injured brain were statistically not significant for any of the ions studied. In all samples, $[Cl^-]_o$ was linearly related to $[Na^+]_o$, as shown in **Figure 19B**; this demonstrates that, as expected, anions and cations are distributed to achieve electroneutrality.

Ionic profile of the penumbra

Our most significant finding in the group of patients that had the MD placed in the penumbra zone was a completely normal ionic profile for $[Na^+]_o$ and $[K^+]_o$ in 60% of the samples. Our study confirms the findings of Wetterling et al., who showed that the ischemic penumbra may be defined as a region of reduced blood supply in which the sodium concentration gradient is still maintained.²⁵⁰

Of the 40% of the samples in which abnormal ionic profiles were found, an isolated increase in $[Na^+]_o$ accompanied by an increased $[Cl^-]_o$ —to preserve electroneutrality—

was the most frequent abnormality, but in most cases with a $[K^+]_o$ within the normal range (81%). The normal or moderately increased $[K^+]_o$ was the main difference with the ionic profile found in the TC/IC, suggesting that the perilesional brain is still able to buffer $[K^+]_o$ overloading. As previously described, moderate increases in $[K^+]_o$ can be observed in the presence of both CSD and epileptic seizures; this phenomenon occurs both in IP and TP. Another explanation for the increase in $[K^+]_o$ found in penumbral tissue is its diffusion from the adjacent ischemic core from focal hemorrhagic brain lesions found in TBI.²⁴⁴ Hubschmann and Kornhauser, in experimental models of intracerebral hemorrhage in cats, showed that acute injection of blood in the brain induces an acute depolarization of the cortex with a significant increase in $[K^+]_o$ to values of 18-28 mmol/L. However, this transient peak was rapidly buffered and returned to baseline 2-4 minutes after the injection.²⁵¹

The isolated increase of $[Na^+]_o$ in the penumbra may suggest an increased permeability of the BBB to Na^+ . The fact that $[Na^+]_o$ accumulates in ECS might indicate early stages of ionic or vasogenic edema that have already been described in the ischemic and traumatically injured brain.^{127,252} Simard et al. have shown that the SUR1/TRPM4 ion channel is overexpressed in the endothelial and neural cells of the ischemic and injured brain and that this channel is the main driver of the increase in $[Na^+]_o$.^{129,253} Moreover, we recently have shown that SUR1, the regulatory unit of this channel, is significantly overexpressed in the perilesional brain around human brain contusions and that upregulation of SUR1 is an important molecular player in the pathophysiology of these lesions.²⁵⁴ In addition, as shown in ischemia, Na-K-Cl cotransporters and Na^+/H^+ exchangers in endothelial cells and also in glia and neurons are actively involved in ischemic edema and in the fluxes of Na^+ .²⁵⁵ However, in our study, we did not evaluate the permeability of the BBB, and therefore our suggestions need to be considered as working hypothesis for new research projects.

Another possible explanation for the 40% abnormalities is that our definition of penumbra could have been inaccurate; "penumbra" was considered, as we discussed, perilesional macroscopically normally-appearing brain in the CT scan. Therefore, using MRI in these patients might have shown diffusion-perfusion abnormalities and their results would have transitioned to the TC group. In addition, most of our results reflect the ionic findings in the brain tissue around brain contusions in TBI and it is more accurately described as perilesional tissue. However, we decided to preserve the term ischemic/traumatic "penumbra" to be consistent with the literature and because, in many

samples, the ionic profile was normal so it was theoretical functional tissue that could be recruited into the core of the lesion. The accurate identification of brain penumbra in TBI is clinically relevant because it can aid in selecting patients who could benefit from changing their management and in designing future clinical trials of potential neuroprotective drugs.

Ionic profile in the ischemic and traumatic core

To our knowledge, this is the first report that explores the complete ionic profile in the human ischemic brain. An important issue of our study is that the cerebral MD samples obtained in MMCAI came from infarcted tissue that was analyzed very late after stroke onset (median time 34.5 hours for the first sample). Therefore, the ionic profile corresponded to necrotic tissue that on neuroimaging studies always evolved to an encephalomalacic brain (**Figure 17F**).

Our study shows that the ionic profile of the IC was characterized by very high $[K^+]_o$ in 62% of the samples and an apparently normal profile for $[Na^+]_o$ and $[Cl^-]_o$; alterations were found only in 20% of the samples for $[Na^+]_o$ and 38% for $[Cl^-]_o$. The brain total sodium content (TSC) has been studied extensively in both experimental models of infarction and human IS. Following a reversible focal ischemic insult in non-human primates, LaVerde et al. showed a linear increase in TSC within ischemic tissue at a rate of ~5-7%/hour.²⁵⁶ In various animal models of MCAI occlusion, it has been shown that $[Na^+]_{brain}$ rises continuously during the first eight hours after stroke onset.²⁵⁷ This principle is the rationale to estimate the time after stroke onset and the brain tissue viability by sodium MRI.²⁵⁸ Sodium-MRI has been used to study the ionic changes in both experimental models of stroke and in human IS.²⁵⁹ However, sodium-MRI estimates the TSC and not the $[Na^+]$ in the different brain compartments and therefore $[Na^+]_o$. Consequently, it needs to be emphasized that the TSC does not necessarily correlate with $[Na^+]_o$ measured by MD in the ECS.

The brain has a precise mechanism to buffer the excess of $[K^+]_o$. Astrocytes play a critical role in brain K^+ homeostasis and are responsible for potassium buffering by redistributing locally elevated $[K^+]_o$ through astrocyte cytoplasm and the gap junctions.²⁶⁰ Under physiological conditions, released K^+ is usually cleared by the glial cells of the penumbra

and by bulk flow to the CSF. However, both mechanisms become inoperative at the ischemic core and are dysfunctional in the ischemic penumbra that may have also increased $[K^+]_o$. Infarcted tissue maintains high levels of K^+ , which, if unbuffered, may affect the penumbral tissue or even the normal brain. A significant increase in $[K^+]_o$ was the fingerprint of the irreversible damaged brain and the extreme high values for $[K^+]_o$, observed in some cases, were never found in controls, in the 'normal brain' or in the perilesional tissue.

It has been shown that high $[K^+]_o$ is a good BM for the severity of brain damage both in experimental models and in patients with severe TBI (e.g., those with high ICP or brain hypoxia), aneurysmal subarachnoid hemorrhage, and ischemic or hemorrhagic stroke.^{231-233,244,261} The fact that $[K^+]_o$ increases in animal models under conditions in which the energy metabolism of the brain has been compromised—regional or global ischemia—is a well-recognized and consistent phenomenon. Mori et al. recorded simultaneously $[Na^+]_o$ and $[K^+]_o$ in a model of global ischemia in rats by using double-barrelled ion-selective microelectrodes.²³⁴ Their findings were quite consistent with other experimental studies and found that $[K^+]_o$ started to increase moderately immediately after ischemia and that its levels increased abruptly in a second state, reaching a plateau 5 min after ischemia at which values of 65 ± 38 mmol/L were recorded.²³⁴ Infarcted brains suffer terminal depolarization at early stages and later oncotic destruction of the brain cells if ischemia persists. In experimental models of permanent MCA occlusion, the changes in $[K^+]_o$ are explosive in nature, and $[K^+]_o$ increases suddenly from approximately 3 mmol/L to more than 50 mmol/L in the few seconds after the onset of ischemia.²⁶¹ In the same model, the ischemic core showed little $[K^+]_o$ dissipation within 3-hours after artery occlusion.^{234,243,261} Although in our study we find very high $[K^+]_o$ in the IC, the levels never reached the concentrations found in the acute phase of experimental IS. Our findings are difficult to compare with those from animal models because long-term recordings of $[K^+]_o$ has not been conducted thus far in any experimental model. Therefore, we cannot compare our data with the findings of any experimental model of ischemia that have mostly evaluated the few minutes or hours after the ischemic insult.

Paradoxically, in the IC, $[Na^+]_o$, $[Cl^-]_o$ and $[K^+]_o$ were within the reference limits in 32.6% of the analyzed samples. Our hypothesis to explain the lower levels of $[Na^+]_o$, $[Cl^-]_o$ and $[K^+]_o$ found in some of our patients is that the infarcted tissue behaves as a tissue homogenate and, due to its high osmolarity, attracts massive amounts of water that

dilutes the extremely high concentrations that occur initially. This was the reason why, on average, the differences between the ionic content for $[\text{Na}^+]_o$ and $[\text{Cl}^-]_o$ were not significantly different from the values found in the non-injured brain. The high affinity of necrotic tissue by water has been studied extensively in posttraumatic brain contusions by Katayama's group.^{262,263} This phenomenon has not been reported before because of the relatively short recording time in experimental models of ischemic stroke that usually do not exceed a follow-up of 6 - 8 hours.^{257,261} In tissue homogenates of normal rat brain cortex, Nattie et al. found a total concentration of K^+ of 170 mmol/L and 32 mmol/L for Na^+ .²⁶⁴ Therefore, the expected $[\text{K}^+]_o$ in a completely necrotic tissue is still higher than those found in acute models of ischemia, and again a dilutional effect is suggested. Therefore, in brain monitoring, the hallmark of irreversible damaged tissue needs to be defined taking into consideration the temporal evolution of the ionic profile. Isolated measurements can be misleading when ionic concentrations are within the normal range if previous values are unknown. Needless to say, this theory is highly speculative and needs verification in animal models.

Similarly to ischemia, the contusional core is characterized by rapid pannecrosis, disintegration, and homogenization of the brain tissue,²⁶⁵ which creates a powerful osmotic sink that attracts water.²⁶³ The large amount of edema that accumulates in the contusion core is due to a significant increase in tissue osmolality that does not only depend on the changes in ionic concentrations.²⁶² Kawamata et al. raised the hypothesis that injured tissue induces an accumulation of metabolic intermediate products of the pathological degradation of lipids, proteins, DNA and other catabolic processes that occur in the damaged tissue²⁶² that would also attract water generating edema.

Unlike the IC, the TC is a much more heterogeneous tissue, and zones of injured but with still intact membranes may coexist with necrotic non-viable tissue. The main finding in TC was the significant higher levels of $[\text{Na}^+]_o$, $[\text{Cl}^-]_o$, and $[\text{K}^+]_o$ compared with controls and non-injured brain. As in IC, the leakage of $[\text{K}^+]_i$ from the intracellular compartment occurs because of the rupture of cellular membranes associated with mechanically-induced or ischemic cell death.^{230,231} However, the main difference between IC and TC was the significantly higher $[\text{Na}^+]_o$ in the TC group (**Figure 18A**). In the absence of active transport, the $[\text{Na}^+]_o$ should not exceed $[\text{Na}^+]_{\text{plasma}}$. Theoretically, in the core of the traumatic injury, the decreased ATP levels and the dysfunction of the necrotic tissue

make this transport impossible. Therefore, these findings are counterintuitive and difficult to explain.

The traumatic core is surrounded by brain tissue with a BBB that is leaky and behaves more like a fenestrated endothelium. Under these circumstances, a set of possible speculative theoretical ideas that may explain the increase in $[Na^+]_o$: 1) patients could be treated with HTS and have an increase in $[Na^+]_o$ as a consequence of high plasma Na^+ levels. This was not the case in our series where patients with $[Na^+]_o > 162$ mmol/L had $[Na^+]_{plasma}$ within the normal range; 2) proteins released from dying cells and particularly DNA-histone complexes might release Na^+ ;²⁶⁶ 3) an increase in the negatively charged protein concentration in the TC attracts positively charged Na^+ ions into the core, thereby leading to an increase in the $[Na^+]_o$. 4) the preload of cells with Na^+ in the early phases of injury due to cytotoxic edema can release a higher Na^+ intracellular concentration into the necrotic tissue. 5) the increased activity of Na^+/H^+ exchangers in the traumatic penumbra may release Na^+ to the core that will act as an inert sink. However, these suppositions have only the purpose to frame the issue of a significantly increased Na^+ in the TC. Any further clarification of this counterintuitive paradox requires further experimental studies in animal models in which experimental conditions can be well controlled.

Glycerol as a biomarker of brain tissue viability

Glycerol is an end product of phospholipid degradation, and some studies have used it as a BM for cell membrane deterioration and therefore cell destruction, both in TBI injury and in other acute brain injuries.^{102,267} Peerdeman et al. found in a small cohort of TBI patients that values of extracellular $[Gly]_o > 150$ μ mol/L in the normal-appearing regions of the brain had a positive predictive value of 100% for an unfavorable outcome, although the $[Gly]_o$ was not useful for early detection of secondary adverse events.¹⁰²

We found a significant increase in $[Gly]_o$ in both the IC and the TC, but the $[Gly]_o$ levels were always below the upper reference threshold in the normal-appearing brain and the penumbra (47.6% in the IC and 49.1% in the TC) (**Figure 20**). However, in many IC and TC samples, $[Gly]_o$ was within the reference range (this finding indicates that a $[Gly]_o < 209$ μ mol/L (upper threshold in the control group) is a good predictor for tissue viability, with high sensitivity (99.4%) but modest specificity (52%). The reason why some dead

brain tissue shows $[\text{Gly}]_o$ levels within the reference range may that glycerol has a low molecular weight (MW; 92 Da); therefore, once glycerol is released, it can be washed out from the damaged brain by simple diffusion and osmotic gradients. However, we did not find any linear or non-linear relationship between $[\text{Gly}]_o$ and $[\text{K}^+]_o$. The fact that many MD samples in the TC and IC had normal $[\text{Gly}]_o$ values might justify this lack of relationship. Taken together, our data suggest that when $[\text{Gly}]_o$ and $[\text{K}^+]_o$ are within their reference ranges, both are highly sensitive but not very specific for detecting viable brain tissue, and could, therefore, be good candidates for incorporation into a future panel of biomarkers to evaluate the viability of brain tissue.

Clinical application of the study of the ionic profile of the extracellular space of the traumatic injured and ischemic brain

Osmotherapy is the most important first-line tool in the management of high ICP after TBI and stroke. The beneficial effect of osmotherapy on ICP is the brain shrinkage induced by the shift of water out of the brain tissue.²⁵⁶ The ideal osmotic agent should establish a strong osmotic gradient across the BBB by remaining largely in the intravascular compartment. Mannitol is the osmotic drug of choice and is the recommended option by the Brain Trauma Foundation guidelines (Level II recommendation). However, HTS is a widely used alternative to mannitol, although it is being used in a variety of formulations. In a comprehensive review of the literature, White et al. showed that HTS is used at sodium chloride concentrations ranging from 1.7% to 29.2%.²⁵⁶ In clinical practice, this range means a difference in the administered Na^+ concentration from 291 to 5,000 mmol/L.²⁵⁶ As for mannitol, the main assumption behind the use of HTS is that the permeability of the intact BBB to Na^+ is very low and therefore its reflection coefficient is very high. Therefore, HTS administration produces an osmotic gradient between the intravascular and interstitial compartments, leading to shrinkage of the brain tissue and to a consequent reduction in ICP.²⁵⁶ However, despite the increased enthusiasm about the use of HTS after TBI, the number of human studies remains limited, and the evidence justifying their routine clinical use remains scarce.^{256,268}

In our study, we found an increase in $[\text{Na}^+]_o$ in the damaged brain, suggesting that the permeability of the BBB to Na^+ is significantly increased in many damaged brain regions. Our findings raise some concerns about the use of HTS in TBI patients with significant

brain damage and in patients with MS, where massive destruction of the brain tissue is consistently found. In experimental post-traumatic contusions, Kurland et al. showed that the BBB permeability of the surrounding brain tissue (penumbra) has a very low reflection coefficient for Na^+ due to the overexpression of the SUR1-TRPM4 ion channel, which facilitates the movement of large amounts of sodium to the damaged brain.²⁵² From the data obtained in animal models, it is quite clear that the type of cerebral edema (vasogenic or cytotoxic) and the degree of BBB disruption depends on the mode of injury; therefore, traditional neuromonitoring tools cannot predict the degree of BBB disruption.

We consider that the use of HTS in patients with significant areas of damaged brain—in which the BBB may have an increased permeability to Na^+ —should be at least reconsidered. To obtain a clear understanding of the Na^+ fluxes that occur when using these solutions, the ionic profiles should be studied before and after HTS boluses. We believe that cerebral MD is a powerful tool for monitoring the ionic content of the ECS and for improving our understanding of the pathophysiology of the BBB.

1.7. Limitations of the study and future directions

Our study presents some limitations that merit discussion. The most important one is that our methodology only calculated the ionic concentration corresponding to an average of the final 2 hours of monitoring. Therefore, the rapid fluxes in extracellular $[\text{K}^+]_o$, $[\text{Na}^+]_o$, and $[\text{Cl}^-]_o$ could not be studied. However, hourly trends are still very useful as a method for identifying brain tissue at risk, the abnormal permeability of the BBB and probably for defining therapeutic windows for recoverable tissue. We have been not able to explain the counterintuitive finding of increased $[\text{Na}^+]_o$ in patients in which the MD was placed inside the core of a traumatic lesion. We could only raise some hypotheses that need verification in additional studies of a different design and in large animal models which conduct MD in the same way it is monitored in neurocritical patients.

We consider that the routine use of MD in the exploration of the ionic profiles of different regions in the injured brain opens up an exciting avenue to explore the complexities of ionic disturbances, the classification of the different types of brain edema, and the design of a viability index that can be used to prospect the effects of therapeutic strategies.

2. Normobaric hyperoxia and oxidative stress in the injured brain

The management of severe TBI is still based on the assumption that most of the brain damage is delayed (secondary injury) and that preventive interventions and early treatment of secondary injuries make a difference in both survival and functional outcome.⁵ Hypoxemia has been shown to be a secondary brain insult and a strong independent factor of poor neurological outcome in patients with severe TBI.^{235,236} Potential therapies for this situation have recently been tested. One strategy already tested in a variety of models of TBI and in pilot clinical trials is NBO. Recently, controversies about the use of NBO have also been raised in the management of TBI and IS.⁶⁻¹² The mechanisms by which supra-normal O₂ may worsen outcome in patients with acute brain injuries is not yet clear, but high FiO₂ could induce vasoconstriction, OxS, increase neuroinflammation and excitotoxicity.¹³ Among these proposed mechanisms, the capacity of NBO to induce OxS is the most important adverse consequence because of the ability of O₂ to induce the production of ROS and therefore damage proteins, lipids, and DNA.¹⁴ The aims of this study were to assess the metabolic response of the injured brain to 4 h of NBO treatment and to determine whether hyperoxia increases OxS in either the apparently normal brain or in the regions around focal lesions. This assessment was accomplished using 8-iso-PGF₂ α as a BM for OxS *in vivo*.²⁶⁹

2.1. Study Group

A prospective study was conducted of a cohort of adult patients (aged ≥ 18 years) who had sustained a severe or moderate TBI, had an abnormal CT scan upon admission and required ICP monitoring. Moderate or severe TBI was defined as an admission GCS score ≤ 13 after resuscitation, which was evaluated when no effects from paralytic agents or sedation were present. The Traumatic Coma Data Bank (TCDB) classification⁵⁰ was used to stratify patients.

Thirty-four patients were included in the study, and a total of 35 hyperoxic tests were performed. In one patient, the test was repeated twice with an interval period of 3 days. Three tests were excluded from analyses: two were excluded because a significant increase in PaO₂ (270.6 and 309.1 mmHg) did not induce any increase in PtiO₂, and an

additional case was excluded because PaO₂ levels did not increase after the hyperoxic challenge. The remaining 31 patients (32 tests) were included in the analysis. The median time from injury until the hyperoxic challenge was 57 h (min: 22, max: 96). **Table 8** shows a summary of the demographic and clinical data of the patients.

Table 8. Demographic and clinical characteristics of the patients

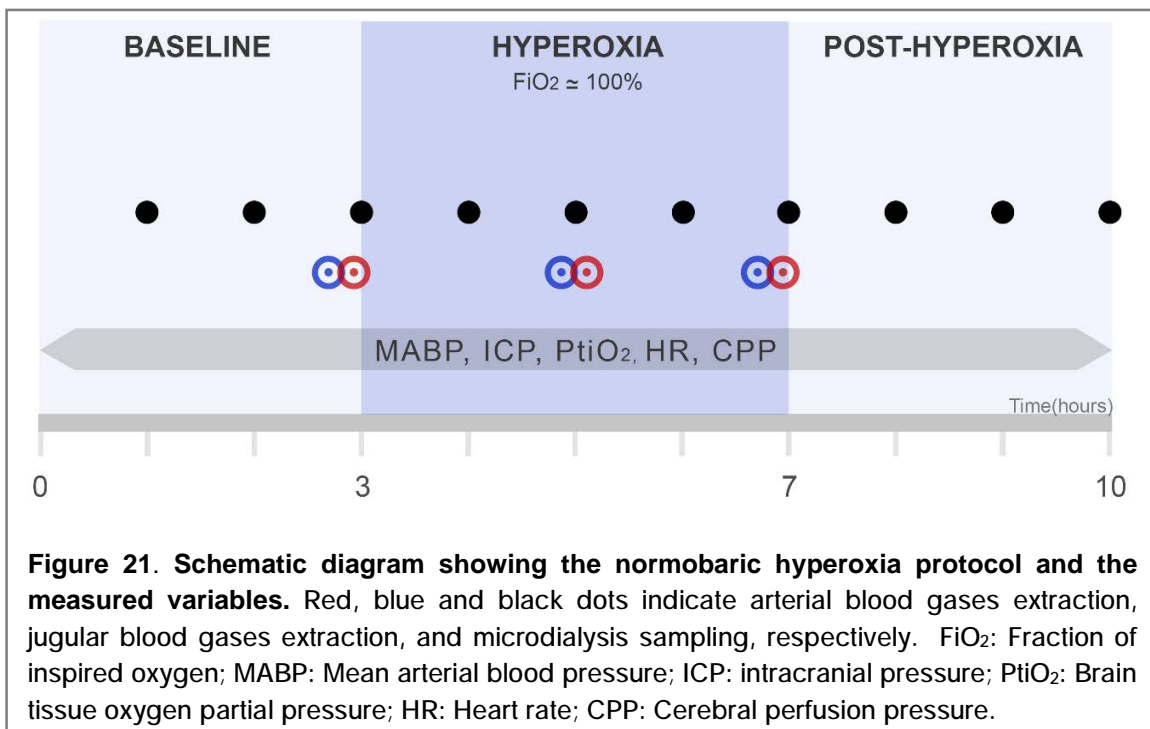
Sex	
Man	24 (77%)
Woman	7 (23%)
Age	36 (18-63)
Initial GCS	4 (3-12)
Initial CT scan classification	
Diffuse injury II	10 (32%)
Diffuse injury III	4 (13%)
Diffuse injury IV	0 (0%)
Evacuated mass lesion	10 (32%)
Non-evacuated mass lesion	7 (23%)
Neurological outcome (GOSE)	
Favorable outcome	8 (26%)
Unfavorable outcome	21 (68%)
Dead at discharge	4 (13%)
Lost to 6 month follow up	2 (6%)
Probe location	
Normal injured brain	17 (55%)
Traumatic penumbra	12 (39%)
Traumatic core	2 (6%)

Sex, initial CT classification, GOSE and probe location are expressed as number of cases and percentage. Age and Initial GCS are expressed as median (min-max). GCS: Glasgow Coma Scale; GOSE: Glasgow Outcome Scale Extended.

The CT scan closest in time to the hyperoxic challenge was used to determine the position of the MD and PtiO₂ probes. The region of the brain sampled by the probes was assigned to one of the previously described categories: apparently **normal injured brain (NB)**, **traumatic penumbra (TP)**, and **traumatic core (TC)**. According to the described criteria, 17 patients had the cerebral MD probe inserted in the apparently **NB**, 12 patients in the **TP**, and two patients in the **TC**. Patients where the probe was inserted in the TP and TC were grouped together (**TP/Core group**).

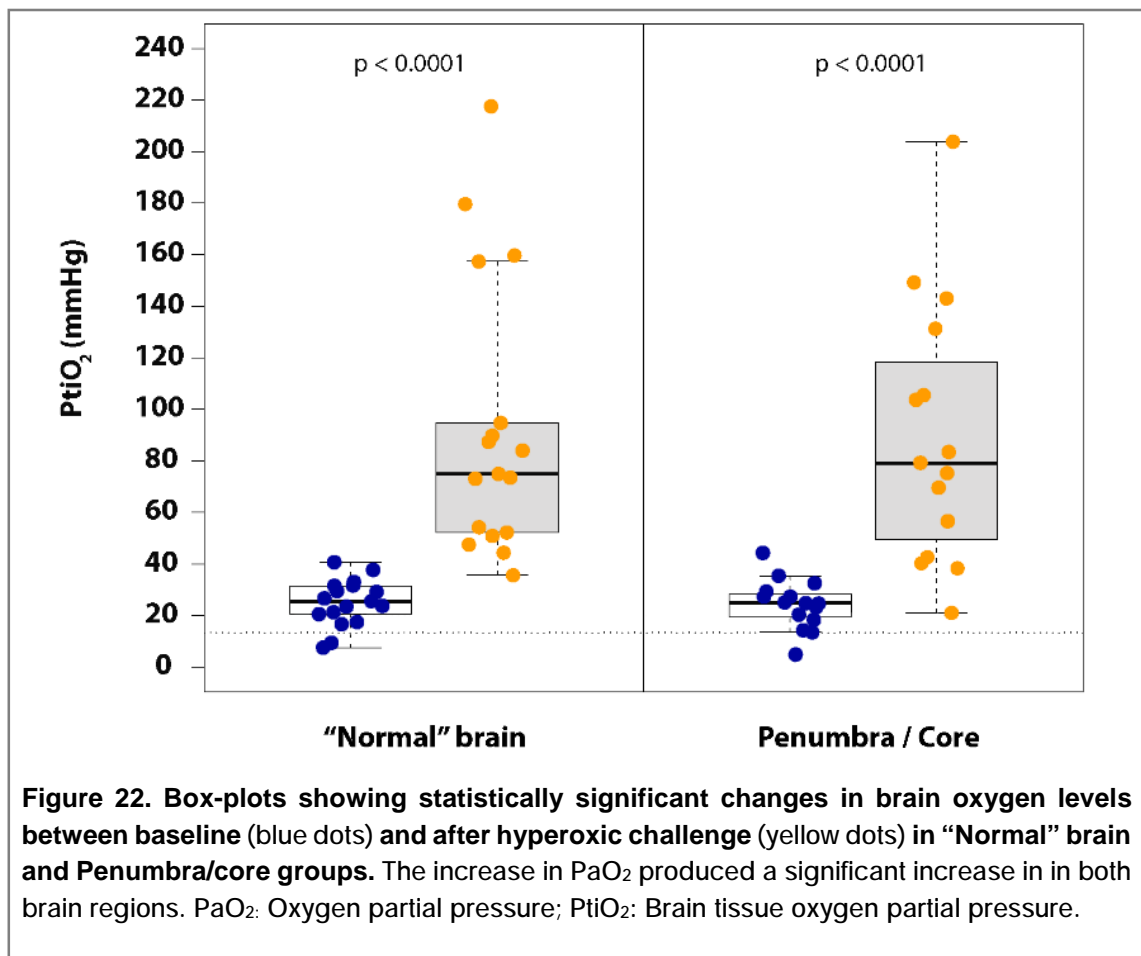
2.2. Normobaric hyperoxia

Hyperoxic challenge was performed as soon as possible after implanting the MD and PtiO₂ probes. Before hyperoxia was induced, systemic variables (systolic and diastolic blood pressure, heart rate), ICP, CPP, brain MD, and brain PtiO₂ values were recorded. Baseline blood samples were taken, and the total hemoglobin content (ctHb), PaO₂, and carbon dioxide partial pressure (PaCO₂) were recorded. As a second step, FiO₂ was increased to 100% and maintained at this level for 4 h. Arterial blood samples were extracted again 2 h after starting hyperoxia and at the end of the test, and the same physiological variables mentioned above were recorded. Immediately after completing the NBO challenge, FiO₂ was modified again to maintain a PaO₂ of ~100 mmHg. In patients with a catheter in the jugular bulb, a jugular venous blood sample was extracted at the same time as the arterial blood sample (**Figure 21**). Plasma and microdialysate samples were stored at -76°C until analysis by ultra-high performance liquid chromatography coupled to tandem mass spectrometry (UHPLC-MS/MS), to determine the 8-iso-PGF₂α levels. The pulmonary function at baseline and after the NBO challenge was evaluated using the PaO₂/FiO₂ ratio (PFR) suggested by Rosenthal et al.²⁷⁰



2.3. Systemic and intracranial changes after the hyperoxic challenge

Summary measures of the systemic and cerebral parameters at baseline and during the hyperoxic challenge are summarized in **Table 9**. At baseline, seven patients (23 %) presented poor pulmonary function, defined as PFR ratio ≤ 250 . The median PFR at baseline was 317 (min: 165, max: 470) and did not change significantly at the end of NBO (median 320, min: 124, max: 483), indicating that pulmonary function was not affected by 4 h of NBO. Median PaO₂ after hyperoxia increased from 115 mmHg to 445 mmHg in the NB group and from 127 mmHg to 435 mmHg in the TP/Core group. This produced a modest but statistically significant increase in arterial oxygen content (CaO₂) in both groups. Hyperoxia induced a median Δ PtiO₂ of 54.4 mmHg (min: 11.9, max: 180 mmHg) in the NB group and a similar median Δ PtiO₂ of 56.2 mmHg (min: 16.2, max: 179 mmHg) in the TP/Core group (**Figure 22**). Non-statistically significant differences were observed in ICP levels in both groups, and a statistically significant but clinically irrelevant increase in mean arterial blood pressure (MABP) was also observed (**Table 9**).



Jugular blood gas variables were only available in 15 tests (nine in the NB and six in the TP/Core). Five patients (two in the NB and three in the TP/Core) presented with brain hypoxia at baseline ($P_{tiO_2} < 15$ mmHg and/or a P_{tiO_2}/P_{aO_2} ratio < 0.10). As expected, compared to baseline, most O_2 -related arterial and venous parameters (P_{tiO_2} , P_{aO_2} , arterial oxygen saturation - SaO_2 , and CaO_2) changed significantly in both groups during hyperoxia, as shown in **Table 7**. Some of the increases in internal $SjvO_2$ and jugular venous O_2 content (C_{jvO_2}) that were observed in both groups were not statistically significant because of the small sample size. Statistically significant—but clinically irrelevant—changes were found in arterial pH in the NB group.

2.4. Metabolic response to hyperoxia in the normal and injured brain

Baseline and hyperoxia values for both groups (NB and TP/Core) and for each metabolite are shown in **Table 10**. In the NB group, NBO induced a statistically significant moderate decrease in $[Lac]_{brain}$ (lactate) from 1.98 mmol/L (min: 1.06, max: 7.42 mmol/L) at baseline to 1.79 mmol/L (min: 0.90, max: 5.72 mmol/L) at hyperoxia nadir (Wilcoxon test, $p=0.035$). A modest reduction in $[Pyr]_{brain}$ (pyruvate) was also observed, from 77.8 μ mol/L at baseline (min: 55.5, max: 387 μ mol/L) to 77.3 μ mol/L (min: 45.3, max: 295 μ mol/L) during NBO treatment (Wilcoxon test, $p=0.030$). A statistically non-significant reduction in the LPR was found in the entire cohort. In the TP/Core group, non-statistically significant differences were observed in brain tissue metabolites during hyperoxia. Only five patients in the entire cohort (15.6%) presented with a $[Lac]_{brain} > 3.5$ mmol/L before the hyperoxic challenge. In this subgroup, the median baseline $[Lac]_{brain}$ was 6.4 mmol/L (min: 6.1, max: 7.4 mmol/L), with a median LPR of 25.9 (min: 19.2, max: 217). In both groups NBO induced a non-statistically significant reduction in both $[Lac]_{brain}$ (median 5.7 mmol/L, min: 4.8, max: 6.4; Wilcoxon Test, $p= 0.063$) and LPR (median 22.7, min: 19.3, max: 243; Wilcoxon test, $p= 0.81$).

TABLE 9. Intracranial and laboratory parameters before and after the hyperoxic challenge

Variable	Normal Injured Brain (n=17)		Traumatic Penumbra-Traumatic Core (n=15)	
	Baseline	Hyperoxia	Baseline	Hyperoxia
FiO ₂	0.35 (0.24 - 0.67)	1 (0.95 - 1.00)	0.40 (0.30 - 0.60)	1.00 (0.90 - 1.00)
PtiO ₂ (mmHg)	25.6 (7.5 - 40.7)	74.9 (35.7 - 218)	24.8 (4.90 - 44.3)	79.3 (21.1 - 204)
Brain hypoxia (n,%)	2 (12%)	2 (12%)	3 (20%)	2 (13%)
PFR ≤ 250 (n,%)	5 (29%)	5 (29%)	2 (13%)	3 (20%)
HR (mmHg)	81 (49 - 109)	77 (51 - 102)	71 (47 - 121)	69 (46 - 109)
MABP (mmHg)	76 (68 - 95)	78 (67 - 98)	80 (69 - 103)	84 (67 - 105)
ICP (mmHg)	10 (2 - 19)	11 (3 - 21)	11 (6 - 25)	13 (2 - 27)
CPP (mmHg)	68 (58 - 83)	69 (53 - 92)	69 (57 - 72)	71 (57 - 91)
Arterial blood gases				
ctHb (g/dl)	10.1 (7.8 - 14.9)	10.1 (7.0 - 15.6)	10.2 (8.6 - 12)	10.0 (8.6 - 11.5)
pH	7.45 (7.34 - 7.48)	7.42 (7.31 - 7.46)	7.45 (7.38 - 7.50)	7.45 (7.28 - 7.49)
PaCO ₂ (mmHg)	37.2 (31.4 - 48.9)	38.5 (33.5 - 49.1)	37.5 (32.1 - 42.2)	37.5 (30.5 - 56.5)
PaO ₂ (mmHg)	115 (81.0 - 171)	445 (253 - 615)	127 (89.0 - 204)	435 (266 - 621)
SaO ₂ (%)	98.5 (96.2 - 99.2)	99.8 (99.1 - 99.9)	98.9 (97.3 - 99.5)	99.7 (99.4 - 100.1)
CaO ₂ (mL/100mL)	14 (11 - 20)	15 (11 - 22)	14 (12 - 16)	15 (13 - 17)
Jugular blood gases				
PjvCO ₂ (mmHg)	42.5 (38.1 - 46.0)	45.5 (41.5 - 50.1)	43.9 (38.4 - 42.4)	45.5 (39.2 - 60.0)
PjvO ₂ (mmHg)	42.4 (34.2 - 52.6)	56.0 (40.0 - 103.6)	44.1 (38.8 - 56.4)	50.9 (48.2 - 84.5)
SjvO ₂ (%)	80.0 (65.5 - 95.8)	90.9 (73.10 - 97.6)	81.0 (76.2 - 88.6)	86.9 (81.9 - 97.9)
CjvO ₂ (mL/100mL)	11.5 (8.5 - 17.3)	13.2 (9.2 - 19.2)	11.3 (10.5 - 14.2)	12.7 (10.8 - 13.92)
AVDO ₂ (mL/100mL)	3.17 (0.50 - 4.54)	2.74 (1.49 - 4.73)	2.37 (1.82 - 3.61)	2.92 (1.16 - 3.40)

Results are expressed as median (min - max). *Comparisons between variables were made using the two-tailed paired t-test or the Wilcoxon signed rank test depending on the normality of the variables' distribution. Jugular blood gases variables were determined in 15 tests (n=9, normal injured brain; n=6, traumatic penumbra-traumatic core).

FiO₂: Fraction of inspired oxygen; PtiO₂: Brain tissue oxygen pressure; PFR: PaO₂/FiO₂ ratio; HR: Heart rate; MABP: Mean arterial blood pressure; ICP: Intracranial pressure; CPP: Cerebral perfusion pressure; ctHb: Concentration of total hemoglobin; PaCO₂: Partial pressure of arterial carbon dioxide; PaO₂: Partial oxygen pressure; SaO₂: Arterial oxygen saturation; CaO₂: Arterial oxygen content; PjvCO₂: Arterial jugular venous pressure of carbon dioxide; PjvO₂: Partial jugular venous oxygen tension; SjvO₂: Jugular venous oxygen saturation; CjvO₂: Jugular venous oxygen content; AVDO₂: Arterio-venous difference of oxygen; NS: Not significant (p < 0.05).

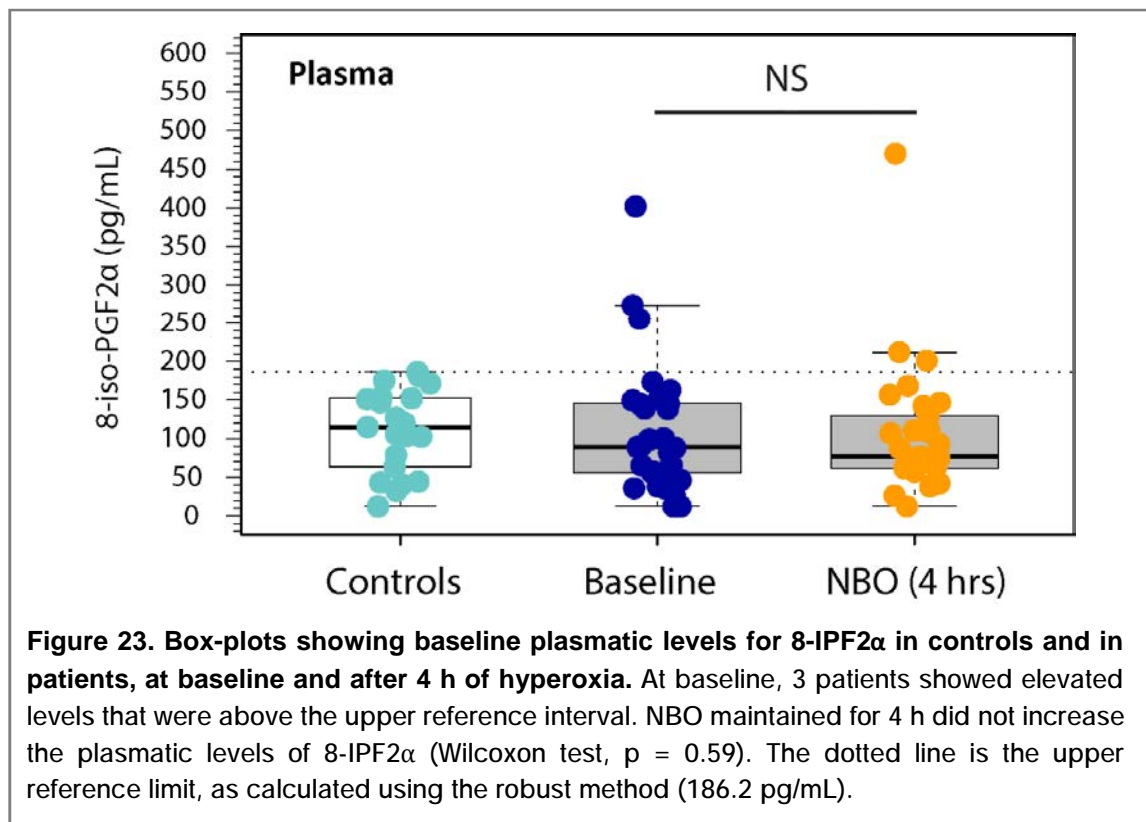
Table 10. Brain and subcutaneous microdialysis data before and after the hyperoxic challenge

Metabolites	Normal Injured Brain (n=17)			Traumatic Penumbra-Core (n=15)		
	Baseline	Hyperoxia	p*	Baseline	Hyperoxia	p*
Brain						
Glucose (mmol/L)	1.33 (0.29 - 3.55)	1.38 (0.27 - 3.75)	NS	1.40 (0.11 - 4.58)	1.44 (0.16 - 5.30)	NS
Lactate (mmol/L)	1.98 (1.06 - 7.42)	1.79 (0.90 - 5.72)	0.035	2.30 (0.84 - 6.64)	2.43 (0.79 - 6.37)	NS
Pyruvate (µmol/L)	77.8 (55.5 - 387)	77.3 (45.3 - 295)	NS	96.7 (29.9 - 273)	82.6 (26.4 - 221)	NS
Glycerol (µmol/L)	69.7 (24.2 - 378)	63.5 (31.2 - 421)	NS	69.1 (18.8 - 585)	63.0 (17.7 - 549)	NS
LPR	23.5 (9.93 - 38.0)	22.3 (10.3 - 39.2)	NS	22.4 (11.4 - 217)	21.6 (12.8 - 243)	NS
LGR	1.43 (0.40 - 8.86)	1.44 (0.36 - 9.09)	0.031	1.33 (0.50 - 58.6)	1.20 (0.54 - 49.3)	NS
Subcutaneous						
Glucose (mmol/L)	3.18 (0.94 - 9.55)	3.56 (0.50 - 10.3)	NS	3.65 (1.07 - 7.72)	3.73 (0.90 - 7.42)	NS
Lactate (mmol/L)	0.92 (0.27 - 2.76)	0.84 (0.25 - 2.73)	NS	0.89 (0.21 - 3.65)	0.72 (0.24 - 3.10)	0.018
Pyruvate (µmol/L)	64.6 (7.98 - 231)	60.2 (9.55 - 211)	NS	62.1 (11.5 - 232)	66.8 (8.43 - 162)	NS
Glycerol (µmol/L)	274 (85.0 - 1364)	240 (67.5 - 1341)	NS	199 (76.1 - 535)	231 (88.2 - 1184)	NS
LPR	13.4 (9.63 - 38.7)	14.8 (9.81 - 26.7)	NS	12.0 (9.99 - 37.3)	13.0 (8.77 - 41.7)	NS
LGR	0.29 (0.16 - 0.54)	0.28 (0.15 - 0.60)	NS	0.28 (0.13 - 0.82)	0.27 (0.14 - 0.57)	NS

Results are expressed as median (min - max). * Comparisons between variables were made using the two-tailed paired t-test or the Wilcoxon signed rank test depending on the normality of the variables' distribution.
LPR: Lactate-to-pyruvate ratio; LGR: Lactate-to-glucose ratio. NS: Not significant (p < 0.05).

2.5. Reference range for 8-Iso-Prostaglandin F2 α

The control group for plasma 8-iso-PGF2 α levels was obtained from healthy volunteers recruited for a different study, and consisted of 21 patients (7 women and 15 men), with a median age of 30 years (min: 18, max: 64 years). One value under the detection limit (25 pg/mL) was assigned a value of 12.5 pg/mL and one outlier detected by the Horn's method was excluded from analysis (2172.7 pg/mL). The median plasma for healthy controls was 115 pg/mL (min: <25, max: 186.2 pg/mL) (**Figure 23**). The upper RI calculated by the robust method was 186.2 pg/mL.



The control group for microdialysate 8-iso-PGF2 α levels was obtained from patients who underwent surgical treatment of posterior fossa or supratentorial lesions and required the implantation of an intraventricular catheter to drain CSF. A CMA-71 MD probe was also inserted in parallel via the same burr hole in the posterior frontal region, 11 cm from the nasion and 3 cm from the midline. This control group consisted of 12 patients (eight women and four men) with a median age of 43 years (min: 22, max: 69 years). Eleven patients presented with a posterior fossa lesion. Only one patient presented with a supratentorial lesion (meningioma). All patients except one had an Evans index score

≤ 0.30 . This cohort of 12 patients yielded 36 samples that resulted in 12 determinations (the low number of determinations was due to the need to pool microvials). The minimum detection level for 8-IPF2 α was 55 pg/mL. In our control group (n=12), all but 1 patient presented values under the detection level (<55pg/mL). Only one case presented [8-IPF2 α]_{brain} = 83.2 pg/mL. This patient was a 31-year-old male who underwent operation for a vestibular schwannoma without hydrocephalus, in whom ventricular drainage was inserted at the time of surgery. This patient recovered uneventfully and both the ventricular drainage and the MD catheter were removed 72 h after surgery. For the purposes of this paper, we considered [8-IPF2 α]_{brain} < 84 pg/mL to be the normal range.

2.6. *In vitro* relative recovery of 8-iso-PGF2 α

One inherent problem of the MD is the fact that the concentration of the analyte collected by MD represents only a fraction of the ECF concentration.¹⁹⁸⁻²⁰¹ RR is defined as the ratio of the concentration in the dialysate to the true *in vitro* concentration of a given substance.²⁰² Experiments were conducted to confirm the *in vitro* recovery characteristics of the CMA-71 probes for 8-iso-PGF2 α in an *in vitro* setting, as described elsewhere by our group²²¹. Four catheters that yielded a total of 43 samples were used for these experiments. In brief, the experiments involved placing each CMA-71 catheter into a matrix solution with a known concentration of the study molecule (Cayman Chemical, Ann Arbor, MI, USA). Study matrix was prepared with: 1) Milli-Q water, 2) the CNS fluid used as a perfusate in patients (CNS fluid, M Dialysis AB) containing 147 mmol/L NaCl, 1.2 mmol/L CaCl₂, 2.7 mmol/L KCl, and 0.85 mmol/L MgCl₂, 3) a constant concentration of 200 pg/mL of 8-iso-PGF2 α (Cayman Chemical), and 4) 200 mg/L of albumin (Grifols[®], Barcelona, Spain), which is within the reference range for the albumin concentration in the normal human CSF²⁷¹. The catheter was perfused at 0.3 μ L/min (18 μ L/hr) with an isotonic solution that had the same ionic composition as the matrix but contained an additional 3% albumin. Albumin was added to the perfusate as an osmotic agent to compensate for the osmotic pressure difference between the matrix and the dialysate and to facilitate fluid recovery.

In each experiment, minor adjustments were made during the initial phase to correct for small differences in hydrostatic pressures and to obtain a zero-fluid loss and a fluid recovery close to the expected theoretical volume (18 μ L/h). The recovery experiment

was only conducted when a steady state was achieved. In summary, 12 microvials were obtained during 3 consecutive days for each catheter (4 microvials/day). Both dialysate and matrix samples were analyzed by UHPLC-MS/MS. The relative recovery (RR) was calculated using the following equation: $RR = (C_{md}/C_{matrix}) \times 100$ (**Equation 1**), where C_{md} and C_{matrix} are the analyte concentrations in the microdialysate and the matrix, respectively.

In this experiment, the mean RR calculated using **Equation 1** was $117 \pm 38\%$ (min: 55%, max: 222%). We did not find any statistically significant difference between the samples collected on different days (Kruskal Wallis test, $p = 0.919$), which demonstrated stability (maintained RR) in the *in vitro* RR during the 3 days the experiment lasted.

2.7. Plasma and cerebral 8-iso-PGF2 α levels at baseline and after hyperoxia

At baseline, the median plasma level for 8-IPF2 α in TBI patients was 89.1 pg/mL (min: <25, max: 401.7 pg/mL). In three patients, the levels were above the upper RI. NBO did not increase the plasma levels of 8-IPF2 α . During the 4 h of NBO, the median level in the entire cohort was 77.1 pg/mL (min: <25, max: 470.5 pg/mL), and the same three patients had values that were above the upper RI (Wilcoxon test, $p = 0.59$) (**Figure 23**). A total of five patients presented evidence of brain OxS at baseline: two patients in whom the MD probe was placed in NB (14.1%) and three in whom the MD probe was placed in TP/Core (23.1%) (**Table 11**). Of those patients who showed no evidence of OxS at baseline (both NB and TP/Core groups), only one developed hyperoxia-induced OxS. In this single patient—included in the NB group— 8-IPF2 α levels rose from < 55 pg/mL at baseline to 612 pg/mL during hyperoxia and reverted to baseline values 3 h after aborting NBO. Of the two patients who had the MD probe in NB and who showed evidence of OxS at baseline, one had a 8-IPGF2 α value that rose from 390 pg/mL at baseline to 1,078 pg/mL during NBO, and then decreased below baseline value 3 h after NBO therapy (98.6 pg/mL). In the second case, the 8-IPGF2 α level decreased from 117 pg/mL at baseline to <55 pg/mL during hyperoxia. Of the three patients who had the MD probe in the TP/core with evidence of OxS at baseline, two showed a significant increase in tissue 8-IPGF2 α levels during NBO (2,342 to 3,153 pg/mL in one patient and 352 to 1,139 pg/mL in 1 patient). Both patients reverted to values that were below baseline 8-IPGF2 α levels

3 h after NBO (1,023 and 122 pg/mL, respectively). In the third patient, hyperoxia improved OxS, gradually reducing 8-IPGF2 α levels during and after NBO, from 314 to 121 pg/mL.

Table 11. 8-iso-PGF2 α microdialysis levels before, during and after the hyperoxic challenge

8-iso-PGF2 α levels	Baseline	Hyperoxia	Post-Hyperoxia
Normal Injured Brain			
N (%)	14 (100%)	14 (100%)	14 (100%)
Censored (<55 pg/mL)	11 (78.6%)	11 (78.6%)	11 (78.6%)
Min-Max (pg/mL)	<55 - 389	<55 - 1078	<55 - 98.6
N above upper RI	2 (14.3%)	2 (14.3%)	1 (7.14%)
Traumatic Penumbra-Traumatic Core			
N (%)	13 (100%)	13 (100%)	13 (100%)
Censored (<55 pg/mL)	10 (76.9%)	10 (76.9%)	7 (53.8%)
Min-Max (pg/mL)	<55 - 2342	<55 - 3153	<55 - 1023
N above upper RI	3 (23.1%)	3 (23.1%)	4 (30.8%)

The minimum detection level for 8-iso-PGF2 α was 55 pg/mL; values under 55 pg/mL were considered as censored data. [8-IPF2 α]_{brain} < 84 pg/mL was defined to be the reference range. Values at baseline and post-hyperoxia correspond to 3 hours before and after the hyperoxic challenge, respectively. N: Cases; NA: Not applicable; RI: Reference interval.

2.8. Discussion

Ischemic and non-ischemic brain hypoxia play a relevant role in the pathophysiology of the injured brain.⁷¹ Therefore, NBO is considered a potential therapy that could be beneficial to TBI patients. In addition, many experimental and clinical studies indicate that metabolic disorders are common in acute brain injuries and that impaired oxygen delivery—related to oxygen diffusion anomalies—or impaired oxygen utilization in the mitochondria (e.g., mitochondrial dysfunction) may play a significant role in the acute phase of TBI, ischemic, and hemorrhagic stroke.^{79,81,86,174} In TBI, the oxygen flux from the capillaries to the mitochondria can be changed by diffusion alterations at many different stages.¹⁷⁴ Because diffusion barriers to the cellular delivery of O₂ can develop and persist after injury, some patients may benefit from interventions that increase O₂ pressure and consequently the pressure drive that moves oxygen into the brain. Furthermore, a growing body of evidence suggests that mitochondrial dysfunction may play a crucial role in the pathophysiology of TBI,⁶⁷ and might explain the significant reduction in the

CMRO₂ found after TBI.⁹⁰ Hypothetically, if mitochondrial function is impaired after TBI, then the steeper capillary-cell O₂ gradient induced by hyperoxia may also improve O₂ utilization.

The use of therapeutic O₂ in TBI has focused primarily on HBO, which it has been demonstrated that improves cellular energy metabolism and outcome and that can be neuroprotective in animal models.^{177,272} A few clinical trials have also shown that HBO has short-term neuroprotective effects in both mild and severe TBI²⁷³ and a significant reduction in the risk of death in TBI patients.²⁷⁴ A randomized phase II study in a single-center study compared combined HBO/NBO treatment (FiO₂ 1.0 delivered for 60 minutes at 1.5 atmospheres absolute -ATA- followed by 3 h of NBO) with standard of care in severe TBI and showed a significant 36% increase in the absolute risk of a favorable outcome in the HBO/NBO arm.²⁷⁵ Despite its potential advantages, HBO requires expensive hyperbaric chambers and trained and competent personnel to work in this complex environment. These facilities are only available in a few Level 1 trauma centers worldwide, making this therapeutic strategy difficult to implement. In addition, HBO can be only provided for a short period of time and can significantly disturb conventional critical care management. In this clinical scenario, the simplicity with which NBO can be applied in any institution makes this low-cost option attractive and easy to implement with no modification to standard of care.

NBO-induced changes in brain oxygenation and metabolism

NBO has been shown to induce neuroprotection in multiple models of neurological injury, in particular in several models of focal ischemia in rodents where NBO was found to extend the salvaging reperfusion time window.²⁷⁶ However, the evidence regarding the potential clinical benefits of NBO is still controversial and varies by the type of brain injury in which it has been applied (i.e., ischemic stroke, SAH, cardiac arrest, etc.). The NBO-induced metabolic effects and changes in brain hemodynamic variables are heterogeneous and sometimes contradictory. Diringier et al. used PET to show that using NBO in patients with severe TBI for 1-hr induced no significant change in the CMRO₂.²⁷⁷ However, Nortje et al. showed that NBO improved cerebral metabolism in brain tissue (defined in our study as traumatic penumbra), with a significant reduction in the LPR but with no significant global changes in the brain.²⁷⁸ The same inconsistent results and

contradictory findings have been reported for the effects of NBO in brain energy metabolism.⁷⁻¹² In the present study, NBO induced a significantly increase in PaO₂ and a statistically significant but clinically irrelevant increase in CaO₂ of ~1mL/100 mL (**Table 9**). NBO induced a median increase in PtiO₂ of ~50 mmHg in both the normal brain and regions defined as TP/Core (**Figure 22**). On average, this represented ~215% increase from PtiO₂ baseline levels, significantly lower than the increase (~600%) achieved by Rockswold et al. in the non-injured brain when using HBO.²⁷⁹ An interesting finding we observed was that the increase in PtiO₂ was similar for both the normal and the injured brain, suggesting that when the gradient is high enough, O₂ can even diffuse across injured and edematous tissue and can reach the target—the mitochondria—even in the damaged and edematous brain.

A few studies have found that brain metabolism improves after hyperoxic challenge, but with heterogeneous results. The initial studies showed a decrease of [Lac]_{brain} in TBI patients treated with short-lasting hyperoxia.⁸⁻¹¹ However, two subsequent studies did not show a significant reduction in the LPR ratio,^{7,11} and an additional study only observed a decrease in the LPR for patients with an increased baseline [Lac]_{brain}.¹² Vilalta et al. showed that NBO did not induce any significant change in brain energy metabolism in patients with normal [Lac]_{brain} but that it significantly decreased the LPR in patients with elevated baseline [Lac]_{brain}.¹² Tisdall et al. incorporated the study of changes in oxidized cytochrome C oxidase (CCO) concentration by NIRS, and observed a decrease in lactate and LPR levels and an increase in COO oxidized concentration, that correlated with changes in PtiO₂ and indicated an increased aerobic metabolism.²⁸⁰ Similar results have been reported recently by Ghosh et al.⁶

Our study replicates our previous findings that NBO does not change energy metabolism in the whole group of patients. Statistically significant—but clinically irrelevant—changes were observed in [Lac]_{brain} and [Pyr]_{brain} in the macroscopically normal brain, but no significant change in the LPR was observed (**Table 10**). However, in the five patients (15.6%) that presented with [Lac]_{brain} >3.5 mmol/L at baseline, NBO induced a non-statistically significant reduction both in the [Lac]_{brain} and in the LPR. The LPR changed from a median of 25.9 at baseline to a median of 22.7. Although these differences were not statistically significant due to the limited number of cases, this trend was similar to what we have reported in our previous study and suggests that NBO can improve metabolism in the subgroup of patients with objective findings of disturbed brain metabolism.¹²

NBO and oxidative stress

Some clinical studies have reported that high O₂ levels are associated with worse outcomes after severe TBI.¹⁸¹ These studies raised concerns about using abnormally high FiO₂ levels and questioned the real benefit of maintaining supranormal PaO₂ levels in patients with acute brain injuries. Tight regulatory control over tissue O₂ levels is an evolutionary mechanism that developed in mammals so as to avoid high levels of O₂ and protect the organs from OxS.²⁸¹ In a recent study, we showed that, in a control group of 16 patients who underwent surgical clipping of incidentally found aneurysms, a 45 min hyperoxic challenge raised PtiO₂ in the normal brain, with a linear relationship between PaO₂/PtiO₂, but that PtiO₂ never exceeded 120 mmHg, suggesting that hyperoxia-induced increases in PtiO₂ eventually plateau in the normal brain.²⁸² Therefore, the significant increases we observed in PtiO₂ (PtiO₂ levels were as high as 218 mmHg in some patients) suggest an impaired or lost oxygen regulatory mechanism.

OxS is a deleterious process that damages proteins, DNA, and lipids, and it induces brain inflammation and necrosis. The brain is highly sensitive to OxS because it consumes 20–30% of inspired oxygen and contains high levels of both polyunsaturated fatty acids and metals, making it an ideal target for a free radical attack.⁴⁷ About 1-2% of the oxygen reduced by mitochondria is converted to superoxide anion in the mitochondria's complex I, and this amount increases when the ETC is altered or blocked.⁴⁷ Another source of ROS is activated microglia. Both microglia-derived ROS and its subsequent reaction products, hydrogen peroxide and peroxynitrite, have the potential to harm cells, and an experimental model of blast injury implicated both in contributing to OxS.²⁸³ Hyperoxia toxicity has long been recognized as a problem in divers exposed to HBO. The high levels of PaO₂ experienced by these divers (>1200 mmHg) lead to seizures and loss of consciousness. However, the data supporting hyperoxia as a cause of OxS is conflicting. While some studies have demonstrated that hyperoxia increases OxS, others have not. Several factors may account for the conflicting results, but the key factors are likely the type of injury, the pre-existence of OxS in the tissue, as well as the timing and duration of hyperoxia. In experimental models of TBI (e.g., cortical impact, weight drop, and blast injury models), OxS has been shown to play a critical role in the secondary injury process.²⁸³ Finally, the role of ROS-induced oxidative in damaging lipids (e.g., lipid peroxidation), DNA, proteins, and free amino acids has strong experimental support.¹⁴

Many BMs of OxS and their capacity to damage lipids and proteins have been used in the literature, including 4-hydroxynonenal (4-HNE) as a marker of lipid peroxidation and 3-nitrotyrosine (3-NT) as a biomarker of protein nitration.²⁸³ The production of ROS by brain cells is closely related to neuroinflammatory cascades. Inflammatory cells may release deleterious compounds or cytokines that exacerbate oxidative damage to metabolically compromised neurons. Both mechanisms are closely related to mitochondrial dysfunction. The production of ROS and its potentially deleterious effects are directly related to the amount of dissolved oxygen that increases in NBO and HBO. In our study, NBO maintained for 4 h did not induce OxS, a finding that was true for both the plasma and the non-injured brain, as shown by stable levels of 8-iso-PGF2 α before and after NBO in most patients. Our findings are in agreement with those of Puccio et al., which showed that NBO for 2 h did not increase the CSF levels of P₂-isoprostane in the CSF, nor did it reduce the total antioxidant reserves.²⁸⁴ We showed the same findings and with longer NBO, supporting the notion that NBO does not induce OxS in macroscopically non-injured brains without preexisting OxS. In the few cases of elevated baseline OxS, NBO increased the levels of 8-iso-PGF2 α . However, OxS normalized after reverting to normoxia for these patients, indicating a direct effect of NBO on BMs of cell damage.

Potential NBO-induced adverse effects

An alternative/synergic mechanistic option to justify the potential deleterious effect observed with HBO/NBO is the powerful vasoconstriction effect the dissolved oxygen has on the brain and the reduction it induces in CBF.^{285,286} Hyperoxia can induce vasoconstriction directly, and indirectly due to hyperoxia-associated hypocapnia (reduced carbon dioxide in the blood).²⁸⁷ Furthermore, studies in humans have demonstrated that NBO produces a consistent and variable reduction of CBF, a reduction whose magnitude was nearly 27% in some cases.²⁸⁶ Experimental and clinical studies have suggested that excitotoxicity may be an alternative or a synergic factor together with OxS for oxygen-induced tissue damage.^{13,288} In a retrospective analysis of 36 patients with severe TBI, Quintard et al. showed that hyperoxia (defined as a PaO₂ >150 mmHg) was associated with a threefold increase in extracellular glutamate.¹³ We did not systematically monitor glutamate in our patients, and therefore we do not have data to verify or refute this hypothesis. Thus, despite the potential benefits in brain

metabolism, NBO is still controversial and raises many concerns that need to be clarified before entering clinical trials or being used routinely in patients with brain injuries.

2.9. Future directions and study limitations

Our study shows that 4 h of NBO only induced OxS in the injured brains of patients with pre-existing OxS. These findings, combined with the increasing evidence that in TBI metabolic crises are common without brain ischemia,^{85,289} open new avenues for the use of this accessible therapeutic strategy in patients with TBI.

Our study was not designed to evaluate the impact of NBO on short- or long-term outcomes in these patients, nor was it designed to define the best way to optimize NBO treatment in terms of frequency, dose, and length. Additionally, we cannot disregard the fact that longer exposures to hyperoxia (> 4 h) or repetitive doses of NBO in the same day can induce OxS. In some experimental studies, the presence of OxS has been observed in prolonged (> 24 h) NBO or HBO, but have not been found in shorter periods of hyperoxia.¹⁴ Using longer periods of NBO (24 h) may be the next step, but such an investigation requires proof of safety, and ideally the use of robust biomarkers of brain OxS and metabolic impairment. Furthermore, only a few patients in our study had lactate levels >3.5 mmol/L at baseline, and although there was a positive trend toward improving energy metabolism in this subgroup, our study lacked sufficient power to replicate the metabolic findings reported by our group previously.¹²

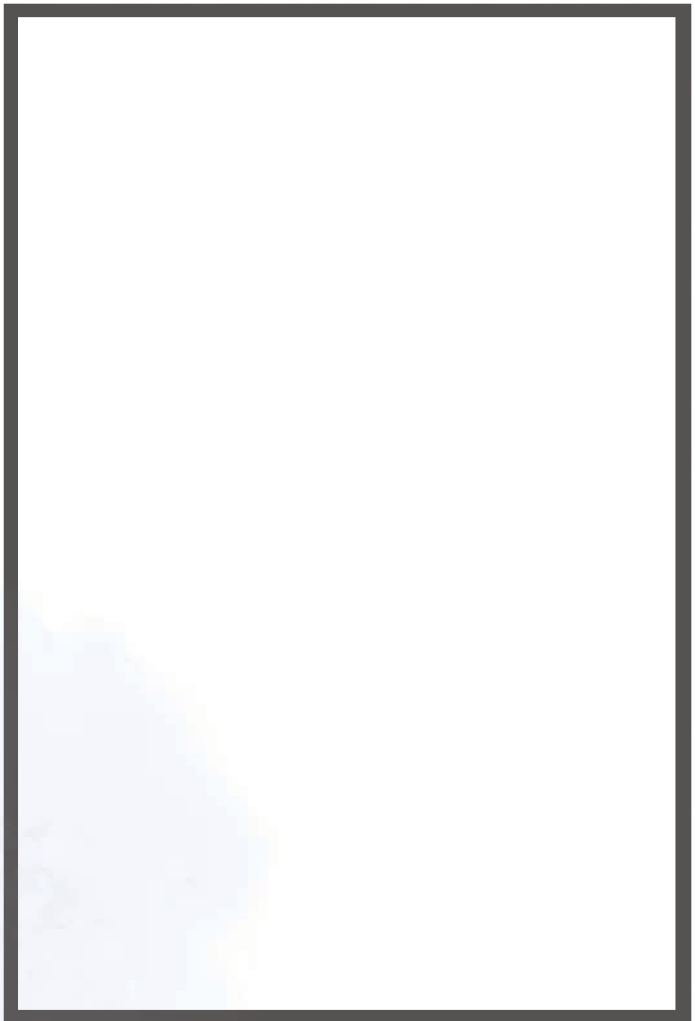
In light of our data, it can be hypothesized that TBI patients would benefit from receiving NBO when they show indications of brain hypoxia, objective indicators of metabolic stress, or evidence of increased anaerobic metabolism. An important step in defining potential subgroups of patients who can benefit from NBO will be to use both MD and PtiO₂ monitoring to detect such patients. Patients with either low PtiO₂—once other causes of brain hypoxia have been ruled out—or in whom [Lac]_{brain} and the LP ratio are increased—suggesting mitochondrial dysfunction— may be potential targets for NBO. In the era of personalized treatment and precision medicine, new clinical trials should focus on these subgroups of patients to determine whether or not NBO may be a useful tool in patients in whom oxygen delivery, metabolic crisis, or mitochondrial dysfunction (either in isolation or in combination) play a role in the pathophysiology of brain damage.

SECTION



CONCLUSIONS

5



CONCLUSIONS

1. Cerebral MD combined with ICP-MS is a powerful tool for better understanding of the complex ionic disturbances that occur after severe TBI as well as ischemic and hemorrhagic stroke. Furthermore, the correlation between this method and the ion-selective electrode analyzer used in our previous study was excellent for Na^+ , K^+ , and Cl^- . Thus, chemistry analyzers used in most hospitals are excellent alternatives to ICP-MS, except for their low temporal resolution.
2. The ionic composition of the brain ECS differs according to the severity of the tissue disturbance. Thus, the results should be interpreted according to the region of the brain sampled by the cerebral MD catheter. The ionic profile of the ischemic tissue is characterized by very high $[\text{K}^+]_o$ and pseudonormal levels of $[\text{Na}^+]_o$ and $[\text{Cl}^-]_o$. In contrast, the core of the traumatic tissue following a TBI presents high levels of $[\text{Na}^+]_o$, $[\text{Cl}^-]_o$, and $[\text{K}^+]_o$. Finally, in the regions bordering both types of lesions (the penumbra), there is a slight increase in all of the ions analyzed.
3. Glycerol is a good biomarker for determining brain tissue viability. Together with the $[\text{K}^+]_o$ in the ECS, these findings could be used as a BM to define brain tissue viability, and the increase of $[\text{Na}^+]_o$ may suggest an increased permeability of the BBB.
4. NBO increased PtIO_2 in both macroscopically normal injured brain and in traumatic regions at risk (traumatic penumbra). This suggests that pressurized oxygen may be delivered to the target and offered to the mitochondria in regions with brain edema and impaired oxygen diffusion. NBO did not change energy metabolism in the whole group of patients. In the five patients with $[\text{Lac}]_{\text{brain}} > 3.5$ mmol/L at baseline, NBO induced a marked reduction in both $[\text{Lac}]_{\text{brain}}$ and the lactate-to-pyruvate ratio. Although these differences were not statistically significant, together

with the results of our previous study, they suggest that TBI patients would benefit from receiving NBO when they show indications of disturbed brain metabolism.

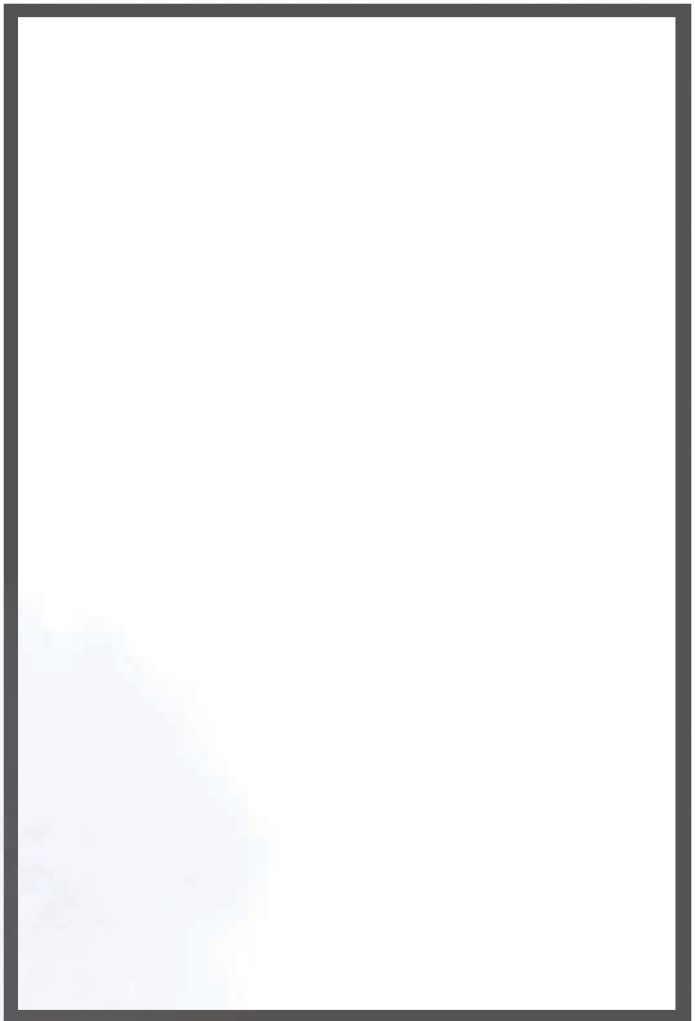
5. NBO maintained for 4 hours did not induce OxS in patients without pre-existing OxS at baseline, except in one case. OxS was measured using a robust indicator (8-iso-PGF₂α) and directly analyzed from the brain extracellular fluid. However, for patients in whom OxS was detected at baseline, NBO induced a significant increase in 8-iso-PGF₂α. Combined with the increasing evidence that metabolic crises are common in TBI without brain ischemia, these findings open new avenues for the use of this accessible therapeutic strategy in patients with TBI.

SECTION



REFERENCES

6



REFERENCES

1. Stenberg, M. *Severe traumatic brain injury - clinical course and prognostic factors*. (2016).
2. Ownsworth, T. & McKenna, K. Investigation of factors related to employment outcome following traumatic brain injury: a critical review and conceptual model. *Disabil. Rehabil.* 26, 765–783 (2004).
3. Graham, D. I., Adams, J. H. & Doyle, D. Ischaemic brain damage in fatal non-missile head injuries. *J. Neurol. Sci.* 39, 213–234 (1978).
4. Graham, D. I. *et al.* Ischaemic brain damage is still common in fatal non-missile head injury. *J. Neurol. Neurosurg. Psychiatry* 52, 346–50 (1989).
5. Park, E., Bell, J. D. & Baker, A. J. R review. 178, (2008).
6. Ghosh, A. *et al.* Hyperoxia results in increased aerobic metabolism following acute brain injury. *J. Cereb. Blood Flow Metab.* 0271678X16679171 (2016). doi:10.1177/0271678X16679171
7. Magnoni, S. *et al.* Lack of improvement in cerebral metabolism after hyperoxia in severe head injury: a microdialysis study. *J. Neurosurg.* 98, 952–958 (2003).
8. Menzel, M. *et al.* Increased inspired oxygen concentration as a factor in improved brain tissue oxygenation and tissue lactate levels after severe human head injury. *J. Neurosurg.* 91, 1–10 (1999).
9. Menzel, M. *et al.* Cerebral oxygenation in patients after severe head injury: monitoring and effects of arterial hyperoxia on cerebral blood flow, metabolism and intracranial pressure. *J. Neurosurg. Anesthesiol.* 11, 240–51 (1999).
10. Reinert, M. *et al.* Effects of cerebral perfusion pressure and increased fraction of inspired oxygen on brain tissue oxygen, lactate and glucose in patients with severe head injury. *Acta Neurochir. (Wien)*. 145, 341-349-350 (2003).
11. Tolia, C. M. *et al.* Normobaric hyperoxia--induced improvement in cerebral metabolism and reduction in intracranial pressure in patients with severe head injury: a prospective historical cohort-matched study. *J. Neurosurg.* 101, 435–444 (2004).
12. Vilalta, A. *et al.* Normobaric hyperoxia in traumatic brain injury: does brain metabolic state influence the response to hyperoxic challenge? *J. Neurotrauma* 28, 1139–1148 (2011).

13. Quintard, H., Patet, C., Suys, T., Marques-Vidal, P. & Oddo, M. Normobaric hyperoxia is associated with increased cerebral excitotoxicity after severe traumatic brain injury. *Neurocrit. Care* 22, 243–50 (2015).
14. Tatarkova, Z. *et al.* Effect of long-term normobaric hyperoxia on oxidative stress in mitochondria of the guinea pig brain. *Neurochem. Res.* 36, 1475–1481 (2011).
15. Siggaard-Andersen, O., Ulrich, a & Gøthgen, I. H. Classes of tissue hypoxia. *Acta Anaesthesiol. Scand. Suppl.* 107, 137–42 (1995).
16. Hinkle, J. L. & Guanci, M. M. Acute ischemic stroke review. *J. Neurosci. Nurs.* 39, 285–293, 310 (2007).
17. Osuntokun BO, Bademosi O, Akinkugbe OO, Oyediran AB, C. R. *et al.* Incidence of stroke in an African City: results from the Stroke Registry at Ibadan, Nigeria, 1973–1975. *Stroke* 10, 205–207 (1979).
18. Bamford, J., Sandercock, P., Dennis, M., Burn, J. & Warlow, C. A prospective study of acute cerebrovascular disease in the community: the Oxfordshire Community Stroke Project--1981-86. *J Neurol Neurosurg Psychiatry* 53, 16–22 (1990).
19. Poca, M. A. *et al.* Monitoring intracranial pressure in patients with malignant middle cerebral artery infarction: is it useful? *J Neurosurg* 112, 648–657 (2010).
20. Berrouschot, J., Sterker, M., Bettin, S., Köster, J. & Schneider, D. Mortality of space-occupying ('malignant') middle cerebral artery infarction under conservative intensive care. *Intensive Care Med.* 24, 620–623 (1998).
21. Hacke W, Schwab S, Horn M, Spragner M, De Georgia M, von K. R. 'Malignant' Middle Cerebral Artery Territory Infarction: Clinical Course and Prognostic Signs. *Arch Neurol* 53, 309–15 (1996).
22. Treadwell, S. D. & Thanvi, B. Malignant middle cerebral artery (MCA) infarction: pathophysiology, diagnosis and management. *Postgrad. Med. J.* 86, 235–242 (2010).
23. Huttner, H. B. & Schwab, S. Malignant middle cerebral artery infarction: clinical characteristics, treatment strategies, and future perspectives. *Lancet Neurol.* 8, 949–958 (2009).
24. Simard, J. M., Sahuquillo, J., Sheth, K. N., Kahle, K. T. & Walcott, B. P. Managing Malignant Cerebral Infarction. *Curr. Treat. Options Neurol.* 13, 217–229 (2011).
25. Kaufmann, A. M. *et al.* Ischemic Core and Penumbra in Human Stroke. *Stroke* 30, 93–99 (1999).

26. Heiss, W. D. *et al.* Progressive derangement of periinfarct viable tissue in ischemic stroke. *J. Cereb. Blood Flow Metab.* 12, 193–203 (1992).
27. Weinstein, P. R., Anderson, G. G. & Telles, D. a. Neurological deficit and cerebral infarction after temporary middle cerebral artery occlusion in unanesthetized cats. *Stroke.* 17, 318–24 (2009).
28. DeGirolami, U., Crowell, R. M. & Marcoux, F. W. Selective necrosis and total necrosis in focal cerebral ischemia. Neuropathologic observations on experimental middle cerebral artery occlusion in the macaque monkey. *J Neuropathol Exp Neurol* 43, 57–71 (1984).
29. Jones, T. H. *et al.* Thresholds of focal cerebral ischemia in awake monkeys. *J. Neurosurg.* 54, 773–782 (1981).
30. Dirnagl, U., Iadecola, C. & Moskowitz, M. A. Pathobiology of ischaemic stroke: An integrated view. *Trends Neurosci.* 22, 391–397 (1999).
31. Ginsberg, M. D. & Pulsinelli, W. A. The ischemic penumbra, injury thresholds, and the therapeutic window for acute stroke. *Ann. Neurol.* 36, 553–554 (1994).
32. Astrup, J., Symon, L., Branston, N. M. & Lassen, N. A. Cortical Evoked Potential and Extracellular K⁺ and H⁺ at Critical Levels of Brain Ischemia. *Stroke* 8, 51–57 (1977).
33. Importance, T. A Journal of Cerebral Circulation. *Fed. Proc.* 5, 425–428 (1974).
34. Astrup, J., Siesjö, B. K. & Symon, L. Thresholds in cerebral ischemia - the ischemic penumbra. *Stroke.* 12, 723–725 (1979).
35. Fisher, M. The ischemic penumbra: Identification, evolution and treatment concepts. *Cerebrovasc. Dis.* 17, 1–6 (2004).
36. Sahuquillo, J., Poca, M. A. & Amorós, S. Current aspects of pathophysiology and cell dysfunction after severe head injury. *Curr. Pharm. Des.* 7, 1475–1503 (2001).
37. Allan, S. M. & Rothwell, N. J. Cytokines and acute neurodegeneration. *Nat. Rev. Neurosci.* 2, 734–44 (2001).
38. Els, T. *et al.* Safety and therapeutical benefit of hemicraniectomy combined with mild hypothermia in comparison with hemicraniectomy alone in patients with malignant ischemic stroke. *Cerebrovasc. Dis.* 21, 79–85 (2006).
39. Mori, K., Nakao, Y., Yamamoto, T. & Maeda, M. Early external decompressive craniectomy with duroplasty improves functional recovery in patients with massive hemispheric embolic infarction: Timing and indication of decompressive surgery for

- malignant cerebral infarction. *Surg. Neurol.* 62, 420–429 (2004).
40. Pérez, C. *et al.* Lesiones Medulares Traumáticas y Traumatismos Craneoencefálicos en España, 2000-2008. *Minist. Sanid.* 190 (2011). at <http://www.msssi.gob.es/profesionales/saludPublica/prevPromocion/Lesiones/JornadaDecenioAccionSeguridadVial/docs/Lesiones_Medulares_WEB.pdf>
41. Teasdale, G. & Jennett, B. ASSESSMENT OF COMA AND IMPAIRED CONSCIOUSNESS. A Practical Scale. *Lancet* 304, 81–84 (1974).
42. Civil, I. D. & Schwab, C. W. The Abbreviated Injury Scale, 1985 revision: a condensed chart for clinical use. *J. Trauma* 28, 87–90 (1988).
43. Baker, S. P. & O'Neill, B. The injury severity score: an update. *J. Trauma* 16, 882–5 (1976).
44. Maas, A. I., Stocchetti, N. & Bullock, R. Moderate and severe traumatic brain injury in adults. *Lancet Neurol.* 7, 728–741 (2008).
45. Sahuquillo, J., Poca, M. a., Pedraza, S. & Munar, X. Actualizaciones en la fisiopatología y monitorización de los traumatismos craneoencefálicos graves. *Neurocirugia* 8, 260–283 (1997).
46. North, S. H., Shriver-Lake, L. C., Taitt, C. R. & Ligler, F. S. Rapid Analytical Methods for On-Site Triage for Traumatic Brain Injury. *Annu. Rev. Anal. Chem.* 5, 35–56 (2012).
47. Mendes Arent, a, de Souza, L. F., Walz, R. & Dafre, a L. Perspectives on Molecular Biomarkers of Oxidative Stress and Antioxidant Strategies in Traumatic Brain Injury. *Biomed Res Int* 2014, (2014).
48. Cheng, G., Kong, R. H., Zhang, L. M. & Zhang, J. N. Mitochondria in traumatic brain injury and mitochondrial-targeted multipotential therapeutic strategies. *Br. J. Pharmacol.* 167, 699–719 (2012).
49. Werner, C. & Engelhard, K. Pathophysiology of traumatic brain injury. *Br. J. Anaesth.* 99, 4–9 (2007).
50. Marshall, L. F. *et al.* A new classification of head injury based on computerized tomography. *J Neurosurg* 15, 14–20 (1991).
51. Gennarelli, T. A. The pathobiology of traumatic brain injury. *Neuroscientist* 3, 73–81 (1997).
52. Marmarou, A. *et al.* IMPACT database of traumatic brain injury: design and description. *J. Neurotrauma* 24, 239–250 (2007).

-
53. Kahle, K. T. *et al.* Molecular mechanisms of ischemic cerebral edema: role of electroneutral ion transport. *Physiology* 24, 257–265 (2009).
54. Hovda, D. A. *et al.* The neurochemical and metabolic cascade following brain injury - moving from animal-models to man. *J. Neurotrauma* 12, 903–906 (1995).
55. Bergsneider, M. *et al.* Cerebral hyperglycolysis following severe traumatic brain injury in humans: a positron emission tomography study. *J. Neurosurg.* 86, 241–251 (1997).
56. Katayama, Y., Becker, D. P., Tamura, T. & Hovda, D. A. Massive increases in extracellular potassium and the indiscriminate release of glutamate following concussive brain injury. *J. Neurosurg.* 73, 889–900 (1990).
57. Kochanek, P. M. *et al.* Biochemical, cellular, and molecular mechanisms in the evolution of secondary damage after severe traumatic brain injury in infants and children: Lessons learned from the bedside. *Pediatr. Crit. Care Med.* 1, 4–19 (2000).
58. Bullock, R. *et al.* Factors affecting excitatory amino acid release following severe human head injury. *J Neurosurg* 89, 507–518 (1998).
59. Rao, V. L. *et al.* Antisense knockdown of the glial glutamate transporter GLT-1, but not the neuronal glutamate transporter EAAC1, exacerbates transient focal cerebral ischemia-induced neuronal damage in rat brain. *J. Neurosci.* 21, 1876–1883 (2001).
60. Nilsson, P., Hillered, L., Olsson, Y., Sheardown, M. J. & Hansen, a J. Regional changes in interstitial K⁺ and Ca²⁺ levels following cortical compression contusion trauma in rats. *J. Cereb. Blood Flow Metab.* 13, 183–192 (1993).
61. Brooks, G. A. & Martin, N. A. Cerebral metabolism following traumatic brain injury: New discoveries with implications for treatment. *Front. Neurosci.* 9, 1–13 (2015).
62. Faden, a I., Demediuk, P., Panter, S. S. & Vink, R. The role of excitatory amino acids and NMDA receptors in traumatic brain injury. *Science (80-)*. 244, 798–800 (1989).
63. Saatman, K. E., Creed, J. & Raghupathi, R. Calpain as a therapeutic target in traumatic brain injury. *Neurotherapeutics* 7, 31–42 (2010).
64. Weber, J. T. Altered calcium signaling following traumatic brain injury. *Front. Pharmacol.* 3 APR, 1–16 (2012).
65. Rosenfeld, J. V. *et al.* Early management of severe traumatic brain injury. *Lancet* 380, 1088–1098 (2012).

-
66. Prins, M., Greco, T., Alexander, D. & Giza, C. C. The pathophysiology of traumatic brain injury at a glance. *Dis. Model. Mech.* 6, 1307–15 (2013).
67. Verweij, B. H., Amelink, G. J. & Muizelaar, J. P. Current concepts of cerebral oxygen transport and energy metabolism after severe traumatic brain injury. *Prog. Brain Res.* 161, 111–124 (2007).
68. Zielke, H. R., Zielke, C. L. & Baab, P. J. Direct measurement of oxidative metabolism in the living brain by microdialysis: a review. *J Neurochem* 109, 24–29 (2010).
69. McGinn, M. J. & Povlishock, J. T. Pathophysiology of Traumatic Brain Injury. *Neurosurg. Clin. N. Am.* 27, 397–407 (2016).
70. Goodman, J. C., Valadka, A. B., Gopinath, S. P., Uzura, M. & Robertson, C. S. Extracellular lactate and glucose alterations in the brain after head injury measured by microdialysis. *Crit. Care Med.* 27, 1965–1973 (1999).
71. Sala, N. *et al.* Cerebral extracellular lactate increase is predominantly nonischemic in patients with severe traumatic brain injury. *J. Cereb. blood flow Metab.* 33, 1815–1822 (2013).
72. Lama, S. *et al.* Lactate storm marks cerebral metabolism following brain trauma. *J. Biol. Chem.* 289, 20200–20208 (2014).
73. Hutchinson, P. J. *et al.* A combined microdialysis and FDG-PET study of glucose metabolism in head injury. *Acta Neurochir. (Wien)*. 151, 51–61; discussion 61 (2009).
74. Merino, M. a, Sahuquillo, J., Borrull, A., Poca, M. a & Expósito, M. R. L. ¿ Es el lactato un buen indicador de hipoxia tisular? Resultados de un estudio piloto en 21 pacientes con un traumatismo craneoencefálico. *Neurosurg. J.* 21, 289–301 (2010).
75. Larach, D. B., Kofke, W. A. & Le Roux, P. Potential non-hypoxic/ischemic causes of increased cerebral interstitial fluid lactate/pyruvate ratio: A review of available literature. *Neurocrit. Care* 15, 609–622 (2011).
76. Nelson, D. W. *et al.* Analyses of cerebral microdialysis in patients with traumatic brain injury: relations to intracranial pressure, cerebral perfusion pressure and catheter placement. *BMC Med.* 9, 21 (2011).
77. Gladden, L. B. Lactic acid: New roles in a new millennium. *Pnas* 98, 395–397 (2001).
78. Reinstrup, P. *et al.* Intracerebral microdialysis in clinical practice: baseline values for chemical markers during wakefulness, anesthesia, and neurosurgery.

Neurosurgery 47, 701-709-710 (2000).

79. Oddo, M. *et al.* Brain Lactate Metabolism in Humans With Subarachnoid Hemorrhage. *Stroke* 43, 1418–1421 (2012).

80. Timofeev, I. *et al.* Cerebral extracellular chemistry and outcome following traumatic brain injury: a microdialysis study of 223 patients. *Brain* 134, 484–494 (2011).

81. Sahuquillo, J. *et al.* Lactate and the lactate-to-pyruvate molar ratio cannot be used as independent biomarkers for monitoring brain energetic metabolism: A microdialysis study in patients with traumatic brain injuries. *PLoS One* 9, (2014).

82. Pellerin, L. & Magistretti, P. J. Glutamate uptake into astrocytes stimulates aerobic glycolysis: a mechanism coupling neuronal activity to glucose utilization. *Proc. Natl. Acad. Sci. U. S. A.* 91, 10625–9 (1994).

83. Connett, R. J., Gayeski, T. E. & Honig, C. R. Lactate production in a pure red muscle in absence of anoxia: mechanisms and significance. *Adv. Exp. Med. Biol.* 159, 327–335 (1983).

84. Richardson, R. S. *et al.* Lactate efflux from exercising human skeletal muscle: role of intracellular PO₂. *J Appl Physiol* 85, 627–634 (1998).

85. Vespa, P. *et al.* Metabolic crisis without brain ischemia is common after traumatic brain injury: a combined microdialysis and positron emission tomography study. *J. Cereb. Blood Flow Metab.* 25, 763–774 (2005).

86. Patet, C. *et al.* Neuroenergetic response to prolonged cerebral glucose depletion after severe brain injury and the role of lactate. *J. Neurotrauma* 32, 1560–1566 (2015).

87. Sanchez, J. J. *et al.* Neuromonitoring with microdialysis in severe traumatic brain injury patients. *Acta Neurochir. Suppl.* 118, 223–227 (2013).

88. Dienel, G. A. Brain lactate metabolism: the discoveries and the controversies. *J. Cereb. Blood Flow Metab.* 32, 1107–1138 (2012).

89. Levasseur, J. E., Alessandri, B., Reinert, M., Bullock, R. & Kontos, H. A. Fluid percussion injury transiently increases then decreases brain oxygen consumption in the rat. *J. Neurotrauma* 17, 101–112 (2000).

90. Obrist, W., Langfitt, T., Jaggi, J. & Cruz, J. Cerebral blood flow and metabolism in comatose patients with acute head injury. *J. Neurosurg.* 61, 241–253 (1984).

91. Fink, M. P. Bench-to-bedside review: Cytopathic hypoxia. *Crit. Care* 6, 491–9 (2002).

-
92. Soustiel, J. F. & Larisch, S. Mitochondrial Damage: A Target for New Therapeutic Horizons. *Neurotherapeutics* 7, 13–21 (2010).
93. Clausen, T., Zauner, A., Levasseur, J. E., Rice, A. C. & Bullock, R. Induced mitochondrial failure in the feline brain: Implications for understanding acute post-traumatic metabolic events. *Brain Res.* 908, 35–48 (2001).
94. Castro, L., Rodriguez, M. & Radi, R. Aconitase is readily inactivated by peroxy nitrite, but not by its precursor, nitric oxide. *J. Biol. Chem.* 269, 29409–29415 (1994).
95. Szabo, C., Zingarelli, B., O'Connor, M. & Salzman, A. L. DNA strand breakage, activation of poly (ADP-ribose) synthetase, and cellular energy depletion are involved in the cytotoxicity of macrophages and smooth muscle cells exposed to peroxy nitrite. *Proc Natl Acad Sci U S A* 93, 1753–1758 (1996).
96. Kristián, T. & Siesjö, B. K. Calcium in ischemic cell death. *Stroke.* 29, 705–718 (1998).
97. Hillered, L., Valtysson, J., Enblad, P. & Persson, L. Interstitial glycerol as a marker for membrane phospholipid degradation in the acutely injured human brain. *J. Neurol. Neurosurg. Psychiatry* 64, 486–491 (1998).
98. Schulz, M. K., Wang, L. P., Tange, M. & Bjerre, P. Cerebral microdialysis monitoring: determination of normal and ischemic cerebral metabolisms in patients with aneurysmal subarachnoid hemorrhage. *J. Neurosurg.* 93, 808–814 (2000).
99. Marklund, N., Salci, K., Lewén, a & Hillered, L. Glycerol as a marker for post-traumatic membrane phospholipid degradation in rat brain. *Neuroreport* 8, 1457–61 (1997).
100. Stahl, N., Ungerstedt, U. & Nordstrom, C. H. Brain energy metabolism during controlled reduction of cerebral perfusion pressure in severe head injuries. *Intensive Care Med.* 27, 1215–1223 (2001).
101. Ståhl, N., Schalén, W., Ungerstedt, U. & Nordström, C.-H. Bedside biochemical monitoring of the penumbra zone surrounding an evacuated acute subdural haematoma. *Acta Neurol. Scand.* 108, 211–5 (2003).
102. Peerdeman, S. M., Girbes, A. R. J., Polderman, K. H. & Vandertop, W. P. Changes in cerebral interstitial glycerol concentration in head-injured patients; correlation with secondary events. *Intensive Care Med.* 29, 1825–1828 (2003).
103. Clausen, T. *et al.* Association between elevated brain tissue glycerol levels and poor outcome following severe traumatic brain injury. *J. Neurosurg.* 103, 233–238 (2005).

-
104. Frykholm, P. *et al.* Increase of interstitial glycerol reflects the degree of ischaemic brain damage: a PET and microdialysis study in a middle cerebral artery occlusion-reperfusion primate model. *J Neurol Neurosurg Psychiatry* 71, 455–461 (2001).
105. Braugher, J. M., Duncan, L. a & Chase, R. L. The Involvement of Iron in Lipid Peroxidation. *J. Biol. Chem.* 261, 10282–10289 (1986).
106. Hall, E. D., Vaishnav, R. A. & Mustafa, A. G. Antioxidant Therapies for Traumatic Brain Injury. *Neurotherapeutics* 7, 51–61 (2010).
107. Shah, D., Mahajan, N., Sah, S., Nath, S. K. & Paudyal, B. Oxidative stress and its biomarkers in systemic lupus erythematosus. *J. Biomed. Sci.* 21, 1–13 (2014).
108. Hanafy, K. A. & Selim, M. H. Antioxidant Strategies in Neurocritical Care. *Neurotherapeutics* 9, 44–55 (2012).
109. Pun, P. B. L., Lu, J. & Mochhala, S. Involvement of ROS in BBB dysfunction. *Free Radic. Res.* 43, 348–64 (2009).
110. Abdul-Muneer, P. M., Chandra, N. & Haorah, J. Interactions of Oxidative Stress and Neurovascular Inflammation in the Pathogenesis of Traumatic Brain Injury. *Mol. Neurobiol.* (2014). doi:10.1007/s12035-014-8752-3
111. Veenith, T., Goon, S. S. & Burnstein, R. M. Molecular mechanisms of traumatic brain injury: the missing link in management. *World J. Emerg. Surg.* 4, 7 (2009).
112. Abdul-Muneer, P. M., Chandra, N. & Haorah, J. Interactions of Oxidative Stress and Neurovascular Inflammation in the Pathogenesis of Traumatic Brain Injury. *Mol. Neurobiol.* 51, 966–979 (2015).
113. Hillered, L., Vespa, P. M. & Hovda, D. a. Translational neurochemical research in acute human brain injury: the current status and potential future for cerebral microdialysis. *J. Neurotrauma* 22, 3–41 (2005).
114. Mendes Arent, A., Souza, L. F. de, Walz, R. & Dafre, A. L. Perspectives on molecular biomarkers of oxidative stress and antioxidant strategies in traumatic brain injury. *Biomed Res. Int.* 2014, 723060 (2014).
115. Kadiiska, M. B. *et al.* Biomarkers of Oxidative Stress Study II. Are oxidation products of lipids, proteins, and DNA markers of CCl₄ poisoning? *Free Radic. Biol. Med.* 38, 698–710 (2005).
116. Morrow, J. D. *et al.* Formation of novel non-cyclooxygenase-derived prostanoids (F₂-isoprostanes) in carbon tetrachloride hepatotoxicity. An animal model of lipid peroxidation. *J. Clin. Invest.* 90, 2502–2507 (1992).

117. Basu, S., Nozari, A., Liu, X. L., Rubertsson, S. & Wiklund, L. Development of a novel biomarker of free radical damage in reperfusion injury after cardiac arrest. *FEBS Lett.* 470, 1–6 (2000).
118. Clausen, F. *et al.* Interstitial F2-Isoprostanes as a Biomarker of Oxidative Stress after Severe Human Traumatic Brain Injury. *J. Neurotrauma* 29, 766–775 (2012).
119. G.-F., Y. *et al.* Increased plasma 8-iso-Prostaglandin F2alpha concentration in severe human traumatic brain injury. *Clin. Chim. Acta* 421, 7–11 (2013).
120. Milne, G. L., Yin, H. & Morrow, J. D. Human Biochemistry of the Isoprostane Pathway. *J. Biol. Chem.* 283, 15533–15537 (2008).
121. Janicka, M. *et al.* LC-MS/MS determination of isoprostanes in plasma samples collected from mice exposed to doxorubicin or tert-butyl hydroperoxide. *Int. J. Mol. Sci.* 14, 6157–6169 (2013).
122. Basu, S. F2-isoprostanes in human health and diseases: from molecular mechanisms to clinical implications. *Antioxid. Redox Signal.* 10, 1405–1434 (2008).
123. Bayir, H. *et al.* Marked gender effect on lipid peroxidation after severe traumatic brain injury in adult patients. *J. Neurotrauma* 21, 1–8 (2004).
124. Starling, E. H. On the Absorption of Fluids from the Connective Tissue Spaces. *J. Physiol.* 19, 312–326 (1896).
125. Lang, G. E., Stewart, P. S., Vella, D., Waters, S. L. & Goriely, A. Is the Donnan effect sufficient to explain swelling in brain tissue slices? *J. R. Soc. Interface* 11, 20140123 (2014).
126. Klatzo, I. Presidential address. Neuropathological aspects of brain edema. *J. Neuropathol. Exp. Neurol.* 26, 1–14 (1967).
127. Simard, J. M., Kent, T. A., Chen, M., Tarasov, K. V & Gerzanich, V. Brain oedema in focal ischaemia: molecular pathophysiology and theoretical implications. *Lancet Neurol.* 6, 258–268 (2007).
128. Aarts, M. M. & Tymianski, M. TRPMs and neuronal cell death. *Pflugers Arch. Eur. J. Physiol.* 451, 243–249 (2005).
129. Simard, J. M. *et al.* Newly expressed SUR1-regulated NC(Ca-ATP) channel mediates cerebral edema after ischemic stroke. *Nat. Med.* 12, 433–40 (2006).
130. Chen, M. & Simard, J. M. Cell swelling and a nonselective cation channel regulated by internal Ca²⁺ and ATP in native reactive astrocytes from adult rat brain. *J. Neurosci.* 21, 6512–21 (2001).

-
131. Simard, J. M., Kahle, K. T. & Gerzanich, V. Molecular mechanisms of microvascular failure in central nervous system injury—synergistic roles of NKCC1 and SUR1/TRPM4. *J. Neurosurg.* 113, 622–629 (2010).
132. Aarabi, B. & Simard, J. M. Traumatic brain injury. *Curr. Opin. Crit. Care* 15, 548–53 (2009).
133. Russell, J. M. Sodium-Potassium-Chloride Cotransport. 80, 211–276 (2000).
134. Nilius, B. & Droogmans, G. Ion channels and their functional role in vascular endothelium. 81, 1415–59. (2001).
135. Brown, R. C. & Davis, T. P. Calcium modulation of adherens and tight junction function: A potential mechanism for blood-brain barrier disruption after stroke. *Stroke* 33, 1706–1711 (2002).
136. Lee, K. R. *et al.* Edema from intracerebral hemorrhage: the role of thrombin. *J. Neurosurg.* 84, 91–96 (1996).
137. Fukuda, S. *et al.* Focal Cerebral Ischemia Induces Active Proteases That Degrade Microvascular Matrix. *Stroke* 35, 998–1004 (2004).
138. Valable, S. *et al.* VEGF-induced BBB permeability is associated with an MMP-9 activity increase in cerebral ischemia: both effects decreased by Ang-1. *J. Cereb. Blood Flow Metab.* 25, 1491–1504 (2005).
139. Wang, X. Y. & Lo, E. H. Triggers and mediators of hemorrhagic transformation in cerebral ischemia. *Mol. Neurobiol.* 28, 229–244 (2003).
140. Thanvi, B. R., Treadwell, S. & Robinson, T. Haemorrhagic transformation in acute ischaemic stroke following thrombolysis therapy: classification, pathogenesis and risk factors. *Postgrad. Med. J.* 84, 361–7 (2008).
141. Abumiya, T., Yokota, C., Kuge, Y. & Minematsu, K. Aggravation of hemorrhagic transformation by early intraarterial infusion of low-dose vascular endothelial growth factor after transient focal cerebral ischemia in rats. *Brain Res.* 1049, 95–103 (2005).
142. Marion, D. W., Darby, J. & Yonas, H. Acute regional cerebral blood flow changes caused by severe head injuries. *J. Neurosurg.* 74, 407–14 (1991).
143. Bouma, G. J. *et al.* Ultra-early evaluation of regional cerebral blood flow in severely head-injured patients using xenon-enhanced computerized tomography. *J. Neurosurg.* 77, 360–368 (1992).
144. Siggaard-Andersen, O., Fogh-Andersen, N., Gøthgen, I. H. & Larsen, V. H. Oxygen status of arterial and mixed venous blood. *Crit. Care Med.* 23, 1284–1293

(1995).

145. Siggaard-Andersen, M. & Siggaard-Andersen, O. Oxygen status algorithm, version 3, with some applications. *Acta Anaesthesiol. Scand. Suppl.* 107, 13–20 (1995).

146. Sahuquillo, J. *et al.* Coexistence of regional cerebral hypoxia with normal or hyperemic brain detected by global monitoring methods. Analysis of apparently contradictory findings based on the Siggaard-Andersen model of tissue hypoxia. *Acta Neurochir. Suppl.* 81, 303–5 (2002).

147. Sahuquillo, J., Poca, M. a & Amorós, S. Current aspects of pathophysiology and cell dysfunction after severe head injury. *Curr. Pharm. Des.* 7, 1475–1503 (2001).

148. Chávez, J. C., Agani, F., Pichiule, P. & LaManna, J. C. Expression of hypoxia-inducible factor-1 α in the brain of rats during chronic hypoxia. *J. Appl. Physiol.* 89, 1937–1942 (2000).

149. Wood, S. M., Gleadle, J. M., Pugh, C. W., Hankinson, O. & Ratcliffe, P. J. The Role of the Aryl Hydrocarbon Receptor Nuclear Translocator (ARNT) in Hypoxic Induction of Gene Expression. *J. Biol. Chem.* 271, 15117–15123 (1996).

150. Wang, G. L., Jiang, B. H., Rue, E. A. & Semenza, G. L. Hypoxia-inducible factor 1 is a basic-helix-loop-helix-PAS heterodimer regulated by cellular O₂ tension. *Proc. Natl. Acad. Sci. U. S. A.* 92, 5510–5514 (1995).

151. Ruscher, K. *et al.* Induction of hypoxia inducible factor 1 by oxygen glucose deprivation is attenuated by hypoxic preconditioning in rat cultured neurons. *Neurosci. Lett.* 254, 117–120 (1998).

152. Sharp, F. R. & Bernaudin, M. HIF1 and oxygen sensing in the brain. *Nat. Rev. Neurosci.* 5, 437–448 (2004).

153. Jiang, B. H., Semenza, G. L., Bauer, C. & Marti, H. H. Hypoxia-inducible factor 1 levels vary exponentially over a physiologically relevant range of O₂ tension. *Am. J. Physiol.* 271, C1172–C1180 (1996).

154. Metzen, E. Intracellular localisation of human HIF-1 α hydroxylases: implications for oxygen sensing. *J. Cell Sci.* 116, 1319–1326 (2003).

155. Pause, A. *et al.* The von Hippel-Lindau tumor-suppressor gene product forms a stable complex with human CUL-2, a member of the Cdc53 family of proteins. *Proc. Natl. Acad. Sci. U. S. A.* 94, 2156–61 (1997).

156. Jeong, J.-W. *et al.* Regulation and Destabilization of HIF-1 α by ARD1-Mediated Acetylation moxic conditions is triggered by the posttranslational hydroxylation of

- prolines (Pro402, Pro564) within a poly. *Cell* 111, 709–720 (2002).
157. Isaacs, J. S. *et al.* Hsp90 regulates a von Hippel Lindau-independent hypoxia-inducible factor-1 alpha-degradative pathway. *J. Biol. Chem.* 277, 29936–29944 (2002).
158. Mahon, P. C., Hirota, K. & Semenza, G. L. FIH-1: A novel protein that interacts with HIF-1?? and VHL to mediate repression of HIF-1 transcriptional activity. *Genes Dev.* 15, 2675–2686 (2001).
159. Hewitson, K. S. *et al.* Hypoxia-inducible factor (HIF) asparagine hydroxylase is identical to factor inhibiting HIF (FIH) and is related to the cupin structural family. *J. Biol. Chem.* 277, 26351–26355 (2002).
160. Maxwell, P. H. *et al.* The tumour suppressor protein VHL targets hypoxia-inducible factors for oxygen-dependent proteolysis. *Nature* 399, 271–275 (1999).
161. Jaakkola, P. *et al.* Targeting of HIF-alpha to the von Hippel-Lindau ubiquitylation complex by O2-regulated prolyl hydroxylation. *Science (80-.).* 292, 468–472 (2001).
162. Semenza, G. L. Hypoxia-inducible factor 1: Oxygen homeostasis and disease pathophysiology. *Trends Mol. Med.* 7, 345–350 (2001).
163. Ratcliffe, P. J., O'Rourke, J. F., Maxwell, P. H. & Pugh, C. W. Oxygen sensing, hypoxia-inducible factor-1 and the regulation of mammalian gene expression. *J. Exp. Biol.* 201, 1153–1162 (1998).
164. Iadecola, C., Zhang, F., Xu, S., Casey, R. & Ross, M. E. Inducible nitric oxide synthase gene expression in brain following cerebral ischemia. *J. Cereb. Blood Flow Metab.* 15, 378–84 (1995).
165. Serrano, J. *et al.* Adrenomedullin expression is up-regulated by ischemia-reperfusion in the cerebral cortex of the adult rat. *Neuroscience* 109, 717–731 (2002).
166. Zhang, F., White, J. G. & Iadecola, C. Nitric oxide donors increase blood flow and reduce brain damage in focal ischemia: evidence that nitric oxide is beneficial in the early stages of cerebral ischemia. *J. Cereb. Blood Flow Metab.* 14, 217–26 (1994).
167. Watanabe, K. *et al.* Adrenomedullin Reduces Ischemic Brain Injury after Transient Middle Cerebral Artery Occlusion in Rats. (2001).
168. Docagne, F. *et al.* Transforming growth factor-beta1 as a regulator of the serpins/t-PA axis in cerebral ischemia. *FASEB J.* 13, 1315–1324 (1999).
169. Marti, H. J. *et al.* Hypoxia-induced vascular endothelial growth factor

expression precedes neovascularization after cerebral ischemia. *Am. J. Pathol.* 156, 965–76 (2000).

170. Ata, K. A. Expression of vascular endothelial growth factor (VEGF) and its ... (1998).

171. Semenza, G. *et al.* Hypoxia Response Elements in the Aldolase A, Enolase 1, and Lactate Dehydrogenase A Gene Promoters Contain Essential Binding Sites for Hypoxia-inducible Factor 1. *J. Biol. Chem.* 271, 32529–32537 (1996).

172. Wenger, R. H. Cellular adaptation to hypoxia: O₂-sensing protein hydroxylases, hypoxia-inducible transcription factors, and O₂-regulated gene expression. *FASEB J.* 16, 1151–1162 (2002).

173. Meixensberger, J. *et al.* Influence of cerebral oxygenation following severe head injury on neuropsychological testing. *Neurol. Res.* 26, 414–417 (2004).

174. Veenith, T. V. *et al.* Pathophysiologic Mechanisms of Cerebral Ischemia and Diffusion Hypoxia in Traumatic Brain Injury. *JAMA Neurol.* 73, 542 (2016).

175. Menon, D. K. *et al.* Diffusion limited oxygen delivery following head injury. *Crit. Care Med.* 32, 1384–1390 (2004).

176. Alves, O. L., Daugherty, W. P. & Rios, M. Arterial hyperoxia in severe head injury: a useful or harmful option? *Curr. Pharm. Des.* 10, 2163–76 (2004).

177. Lin, K.-C. *et al.* Attenuating inflammation but stimulating both angiogenesis and neurogenesis using hyperbaric oxygen in rats with traumatic brain injury. *J. Trauma Acute Care Surg.* 72, 650–9 (2012).

178. Wang, G. H., Zhang, X. G., Jiang, Z. L., Li, X., Peng, L. L., Li, Y. C., & Wang, Y. Neuroprotective effects of hyperbaric oxygen treatment on traumatic brain injury in the rat. *J. Neurotrauma* 27, 1733–1743 (2010).

179. Patet, C., Suys, T., Carteron, L. & Oddo, M. Cerebral Lactate Metabolism After Traumatic Brain Injury. *Curr. Neurol. Neurosci. Rep.* 16, 31 (2016).

180. Stiefel, M. F. *et al.* Reduced mortality rate in patients with severe traumatic brain injury treated with brain tissue oxygen monitoring. *J. Neurosurg.* 103, 805–811 (2005).

181. Brenner, M. *et al.* Association between early hyperoxia and worse outcomes after traumatic brain injury. *Arch. Surg.* 147, 1042–6 (2012).

182. Damiani, E. *et al.* Arterial hyperoxia and mortality in critically ill patients: a systematic review and meta-analysis. *Crit. care* 18, 711 (2014).

-
183. Llitjos, J.-F., Mira, J.-P., Duranteau, J. & Cariou, A. Hyperoxia toxicity after cardiac arrest: What is the evidence? *Ann. Intensive Care* 6, (2016).
184. Jeon, S. B. *et al.* Hyperoxia may be related to delayed cerebral ischemia and poor outcome after subarachnoid haemorrhage. *J Neurol Neurosurg Psychiatry* 85, 1301–1307 (2014).
185. Starke, R. M. & Kassell, N. F. The link between hyperoxia, delayed cerebral ischaemia and poor outcome after aneurysmal SAH: association or therapeutic endeavour. *J. Neurol. Neurosurg. Psychiatry* 85, 308326 (2014).
186. Ko, S. B. Multimodality monitoring in the neurointensive care unit: a special perspective for patients with stroke. *J Stroke* 15, 99–108 (2013).
187. Poca, M. *et al.* Incidence of intracranial hypertension after severe head injury: a prospective study using the Traumatic Coma Data Bank classification. *Acta Neurochir. Suppl.* 71, 27–30 (1998).
188. Carney, N. *et al.* Guidelines for the Management of Severe Traumatic Brain Injury, Fourth Edition. *Neurosurgery* (2016). doi:10.1227/NEU.0000000000001432
189. Mokri, B. The Monro-Kellie hypothesis: applications in CSF volume depletion. *Neurology* 56, 1746–8 (2001).
190. Steiner, L. A. & Andrews, P. J. D. Monitoring the injured brain: ICP and CBF. *Br. J. Anaesth.* 97, 26–38 (2006).
191. Gamal Hamdan Suleiman M.D. Trauma Craneoencefálico Severo: Parte I. *Medicrit* 2, 107–148
192. Poca, M.-A. *et al.* Fiberoptic intraparenchymal brain pressure monitoring with the Camino V420 monitor: reflections on our experience in 163 severely head-injured patients. *J. Neurotrauma* 19, 439–448 (2002).
193. Bullock, M. R. & Povlishock, J. T. Guidelines for the management of severe traumatic brain injury. *J. Neurotrauma* 24, (2007).
194. Poca, M. a *et al.* Percutaneous implantation of cerebral microdialysis catheters by twist-drill craniostomy in neurocritical patients: description of the technique and results of a feasibility study in 97 patients. *J. Neurotrauma* 23, 1510–7 (2006).
195. Hutchinson, P. J. *et al.* Consensus statement from the 2014 International Microdialysis Forum. *Intensive Care Med.* 41, 1517–1528 (2015).
196. Bellander, B.-M. *et al.* Consensus meeting on microdialysis in neurointensive care. *Intensive Care Med.* 30, 2166–2169 (2004).

-
197. Martínez-Valverde, T. *et al.* Characterization of the Ionic Profile of the Extracellular Space of the Injured and Ischemic Brain: A Microdialysis Study. *J. Neurotrauma* 34, 74–85 (2017).
198. Benveniste, H. & Hüttemeier, P. C. Microdialysis--theory and application. *Prog. Neurobiol.* 35, 195–215 (1990).
199. Benveniste, H. Brain microdialysis. *J. Neurochem.* 52, 1667–1679 (1989).
200. Hutchinson, P. J. A. *et al.* Clinical cerebral microdialysis--determining the true extracellular concentration. *Acta Neurochir. Suppl.* 81, 359–362 (2002).
201. Nordström, C. H. Cerebral energy metabolism and microdialysis in neurocritical care. *Child's Nerv. Syst.* 26, 465–472 (2010).
202. Ungerstedt, U. & Rostami, E. in *Handbook of microdialysis* (eds. Westerink, B. & Cremers, T.) 16, 675–686 (2007).
203. Chefer, V. I., Thompson, A. C., Zapata, A. & Shippenberg, T. S. in *Current Protocols in Neuroscience* 1–35 (John Wiley & Sons, Inc., 2009). doi:10.1002/0471142301.ns0701s47
204. Janle, E. M. & Cregor, M. Ultrafiltrate and microdialysis DL probe in vitro recoveries: electrolytes and metabolites. *Curr. Sep.* 15, 31–34 (1996).
205. Abi-Saab, W. M. *et al.* Striking differences in glucose and lactate levels between brain extracellular fluid and plasma in conscious human subjects: effects of hyperglycemia and hypoglycemia. *J. Cereb. blood flow Metab.* 22, 271–279 (2002).
206. Langemann, H. *et al.* Extracellular levels of glucose and lactate measured by quantitative microdialysis in the human brain. *Neurol. Res.* 23, 531–536 (2001).
207. Cavus, I. *et al.* Extracellular metabolites in the cortex and hippocampus of epileptic patients. *Ann. Neurol.* 57, 226–235 (2005).
208. Cesarini, K. G. *et al.* Early cerebral hyperglycolysis after subarachnoid haemorrhage correlates with favourable outcome. *Acta Neurochir. (Wien).* 144, 1121–31 (2002).
209. Sánchez-Guerrero, A. *et al.* Reappraisal of the reference levels for energy metabolites in the extracellular fluid of the human brain. *J. Cereb. Blood Flow Metab.* (2016). doi:10.1177/0271678X16674222
210. Meyerson, B. A., Linderöth, B., Karlsson, H. & Ungerstedt, U. Microdialysis in the human brain: extracellular measurements in the thalamus of parkinsonian patients. *Life Sci.* 46, 301–308 (1990).

-
211. Tisdall, M. M. Cerebral microdialysis: research technique or clinical tool. *Br. J. Anaesth.* 97, 18–25 (2006).
212. Persson, L. *et al.* Neurochemical monitoring using intracerebral microdialysis in patients with subarachnoid hemorrhage. *J. Neurosurg.* 84, 606–16 (1996).
213. Persson, L. & Hillered, L. Chemical monitoring of neurosurgical intensive care patients using intracerebral microdialysis. *J. Neurosurg.* 76, 72–80 (1992).
214. Reinstrup, P. *et al.* Intracerebral microdialysis in clinical practice: Baseline values for chemical markers during wakefulness, anesthesia, and neurosurgery. *Neurosurgery* 47, 701–710 (2000).
215. Nordström, C., Reinstrup, P., Xu, W., Gärdenfors, A. & Ungerstedt, U. Assessment of the lower limit for cerebral perfusion pressure in severe head injuries by bedside monitoring of regional energy metabolism. *Anesthesiology* 98, 809–814 (2003).
216. Marion, D. W. *et al.* Effect of hyperventilation on extracellular concentrations of glutamate, lactate, pyruvate, and local cerebral blood flow in patients with severe traumatic brain injury. *Crit. Care Med.* 30, 2619–25 (2002).
217. Boret, H., Fesselet, J., Meaudre, E., Gaillard, P. E. & Cantais, E. Cerebral microdialysis and PtiO₂ for neuro-monitoring before decompressive craniectomy. *Acta Anaesthesiol. Scand.* 50, 252–254 (2006).
218. Hlatky, R., Valadka, A. B., Goodman, J. C., Contant, C. F. & Robertson, C. S. Patterns of energy substrates during ischemia measured in the brain by microdialysis. *J. Neurotrauma* 21, 894–906 (2004).
219. Diene, G. A., Rothman, D. L. & Nordström, C.-H. Microdialysate concentration changes do not provide sufficient information to evaluate metabolic effects of lactate supplementation in brain-injured patients. *J. Cereb. Blood Flow Metab.* 36, 1844–1864 (2016).
220. Tisdall, M. M. & Smith, M. Multimodal monitoring in traumatic brain injury: current status and future directions. *Br. J. Anaesth.* 99, 61–67 (2007).
221. Martínez-Valverde, T. *et al.* Brain microdialysis as a tool to explore the ionic profile of the brain extracellular space in neurocritical patients: a methodological approach and feasibility study. *J. Neurotrauma* 32, 7–16 (2015).
222. Ehling, S., Tefera, S., Earl, R. & Cole, S. Comparison of analytical methods to determine sodium content of low-sodium foods. *J. AOAC Int.* 93, 628–37 (2007).
223. Chang, J. J. J. *et al.* Physiologic and functional outcome correlates of brain

- tissue hypoxia in traumatic brain injury. *Crit. Care Med.* 37, 283–290 (2009).
224. Narotam, P. K. P., Morrison, J. J. F. & Nathoo, N. Brain tissue oxygen monitoring in traumatic brain injury and major trauma: outcome analysis of a brain tissue oxygen-directed therapy: Clinical article. *J. Neurosurg.* 111, 672–82 (2009).
225. Schell, R. & Cole, D. Cerebral monitoring: jugular venous oximetry. *Anesth. Analg.* 90, 559–66 (2000).
226. Poca, Sahuquillo, J., Mena, M., Vilalta, A. & Riveiro, M. Actualizaciones en los métodos de monitorización cerebral regional en los pacientes neurocríticos: presión tisular de oxígeno, microdiálisis cerebral y técnicas de espectroscopía por infrarrojos. *Neurocirugia* 16, 385–409 (2005).
227. Mena, M. P., Vilalta, A., Poca, M. a, Sahuquillo, J. & Riveiro, M. Actualizaciones en los métodos de monitorización cerebral regional en los pacientes neurocríticos: presión tisular de oxígeno, microdiálisis cerebral y técnicas de espectroscopía por infrarrojos. *Neurocirugia* 16, 385–409 (2005).
228. Sarrafzadeh, a S. *et al.* Cerebral oxygenation in contused vs. nonlesioned brain tissue: monitoring of PtiO₂ with Licox and Paratrend. *Acta Neurochir. Suppl.* 71, 186–189 (1998).
229. Valadka, a B., Gopinath, S. P., Contant, C. F., Uzura, M. & Robertson, C. S. Relationship of brain tissue PO₂ to outcome after severe head injury. *Crit Care Med* 26, 1576–1581 (1998).
230. Dopperberg, E. M. *et al.* Determinants of cerebral extracellular potassium after severe human head injury. *Acta Neurochir. Suppl.* 75, 31–34 (1999).
231. Reinert, M. *et al.* High extracellular potassium and its correlates after severe head injury: relationship to high intracranial pressure. *Neurosurg. Focus* 8, e10 (2000).
232. VALADKA, A. B., GOODMAN, J. C., GOPINATH, S. P., UZURA, M. & ROBERTSON, C. S. Comparison of Brain Tissue Oxygen Tension to Microdialysis-Based Measures of Cerebral Ischemia in Fatally Head-Injured Humans. *J. Neurotrauma* 15, 509–519 (1998).
233. Goodman, J. C. *et al.* Simultaneous measurement of cortical potassium, calcium, and magnesium levels measured in head injured patients using microdialysis with ion chromatography. *Acta Neurochir. Suppl.* 75, 35–7 (1999).
234. Mori, K., Miyazaki, M., Iwase, H. & Maeda, M. Temporal Profile of Changes in Brain Tissue Concentrations after Cerebral Ischemia and the Effects of Mild Cerebral Hypothermia. 19, 1261–1270 (2002).

235. Stahel, P. F., Smith, W. R. & Moore, E. E. Hypoxia and hypotension, the 'lethal duo' in traumatic brain injury: Implications for prehospital care. *Intensive Care Med.* 34, 402–404 (2008).
236. Chesnut, R. M. *et al.* Chesnut1993.Pdf.
237. Meixensberger, J. *et al.* Influence of cerebral oxygenation following severe head injury on neuropsychological testing. *Neurol. Res.* 26, 414–417 (2004).
238. Stiefel, M. F. *et al.* Reduced mortality rate in patients with severe traumatic brain injury treated with brain tissue oxygen monitoring. *J. Neurosurg.* 103, 805–811 (2005).
239. Narotam, P. K., Morrison, J. F. & Nathoo, N. Brain tissue oxygen monitoring in traumatic brain injury and major trauma: outcome analysis of a brain tissue oxygen-directed therapy. *J. Neurosurg.* 111, 672–682 (2009).
240. Frijhoff, J. *et al.* Clinical Relevance of Biomarkers of Oxidative Stress. *Antioxid. Redox Signal.* 23, 1144–1170 (2015).
241. Le Roux, P. *et al.* The International Multidisciplinary Consensus Conference on Multimodality Monitoring in Neurocritical Care: Evidentiary Tables: A Statement for Healthcare Professionals from the Neurocritical Care Society and the European Society of Intensive Care Medicine. *Neurocrit. Care* 21, 297–361 (2014).
242. Evans, W. An Encephalographic Ratio for estimating Ventricular Enlargement and Cerebral Atrophy. *Arch Neurol Psychiatr* 47, 931–937 (1942).
243. Hansen, A. J. Effect of anoxia on ion distribution in the brain. *Physiol. Rev.* 65, 101–48 (1985).
244. Antunes, A. P. *et al.* Higher brain extracellular potassium is associated with brain metabolic distress and poor outcome after aneurysmal subarachnoid hemorrhage. *Crit. Care* 18, R119 (2014).
245. Thomas, R. *Practical Guide to ICP-MS.* *Journal of Chemical Information and Modeling* 53, (2004).
246. Harrington, M. G. *et al.* Cerebrospinal fluid sodium increases in migraine. *Headache* 46, 1128–1135 (2006).
247. Gorji, A. *et al.* Neocortical microenvironment in patients with intractable epilepsy: Potassium and chloride concentrations. *Epilepsia* 47, 297–310 (2006).
248. Strong, A. J. & Dardis, R. Depolarisation phenomena in traumatic and ischaemic brain injury. *Adv. Tech. Stand. Neurosurg.* 30, 3–49 (2005).

249. Hartings, J. A. *et al.* Spreading depolarizations have prolonged direct current shifts and are associated with poor outcome in brain trauma. *Brain* 134, 1529–1540 (2011).
250. LaVerde, G. C., Jungreis, C. A., Nemoto, E. & Boada, F. E. Sodium time course using ²³Na MRI in reversible focal brain ischemia in the monkey. *J. Magn. Reson. Imaging* 30, 219–223 (2009).
251. Hubschmann, O. R. & Kornhauser, D. Effects of intraparenchymal hemorrhage on extracellular cortical potassium in experimental head trauma. *J Neurosurg* 59, 289–293 (1983).
252. Kurland, D., Hong, C., Aarabi, B., Gerzanich, V. & Simard, J. M. Hemorrhagic Progression of a Contusion after Traumatic Brain Injury: A Review. *J. Neurotrauma* 29, 19–31 (2012).
253. Simard, J. M. & Chen, M. Regulation by sulfanylurea receptor type 1 of a non-selective cation channel involved in cytotoxic edema of reactive astrocytes. *J. Neurosurg. Anesthesiol.* 16, 98–99 (2004).
254. Martínez-Valverde, T. *et al.* Sulfonylurea Receptor 1 in Humans with Post-Traumatic Brain Contusions. *J. Neurotrauma* 32, 1478–1487 (2015).
255. O'Donnell, M. E. Blood-brain barrier Na transporters in ischemic stroke. *Adv. Pharmacol.* 71, 113–146 (2014).
256. White, H., Cook, D. & Venkatesh, B. The use of hypertonic saline for treating intracranial hypertension after traumatic brain injury. *Anesth. Analg.* 102, 1836–1846 (2006).
257. Betz, a L., Keep, R. F., Beer, M. E. & Ren, X. D. Blood-brain barrier permeability and brain concentration of sodium, potassium, and chloride during focal ischemia. *J. Cereb. Blood Flow Metab.* 14, 29–37 (1994).
258. Boada, F. E. *et al.* Sodium MRI and the Assessment of Irreversible Tissue Damage During Hyper-Acute Stroke. *Transl. Stroke Res.* 3, 236–245 (2012).
259. Wetterling, F. *et al.* Sodium-23 Magnetic Resonance Imaging Has Potential for Improving Penumbra Detection but Not for Estimating Stroke Onset Time. *J. Cereb. Blood Flow Metab.* 35, 103–110 (2015).
260. Leis, J. A., Bekar, L. K. & Walz, W. Potassium homeostasis in the ischemic brain. *Glia* 50, 407–416 (2005).
261. Sick, T. J., Feng, Z. C. & Rosenthal, M. Spatial stability of extracellular potassium ion and blood flow distribution in rat cerebral cortex after permanent middle

- cerebral artery occlusion. *J. Cereb. Blood Flow Metab.* 18, 1114–1120 (1998).
262. Kawamata, T., Mori, T., Sato, S. & Katayama, Y. Tissue hyperosmolality and brain edema in cerebral contusion. *Neurosurg. Focus* 22, E5 (2007).
263. Maeda, T., Katayama, Y., Kawamata, T., Koyama, S. & Sasaki, J. Ultra-early study of edema formation in cerebral contusion using diffusion MRI and ADC mapping. *Acta Neurochir. Suppl.* 86, 329–331 (2003).
264. Nattie, E. E., Bergin, M. B., Daley, J. & Melton, J. CSF and brain ions, acid-base balance, and ventilation in acute hyponatremia. *J. Appl. Physiol.* 49, 95–101 (1980).
265. Kawamata, T. & Katayama, Y. Cerebral contusion: a role model for lesion progression. *Prog. Brain Res.* 161, 235–241 (2007).
266. Nguyen, M. K. & Kurtz, I. Quantitative interrelationship between Gibbs-Donnan equilibrium, osmolality of body fluid compartments, and plasma water sodium concentration. *J. Appl. Physiol.* 100, 1293–1300 (2006).
267. Merenda, A. *et al.* Validation of Brain Extracellular Glycerol as an Indicator of Cellular Membrane Damage due to Free Radical Activity after Traumatic Brain Injury. *J. Neurotrauma* 25, 527–538 (2008).
268. Prabhakar, H., Singh, G. P., Anand, V. & Kalaivani, M. Mannitol versus hypertonic saline for brain relaxation in patients undergoing craniotomy. *Sao Paulo Med. J.* 133, 166 (2015).
269. Frijhoff, J. *et al.* Clinical Relevance of Biomarkers of Oxidative Stress. *Antioxid. Redox Signal.* 23, 1144–70 (2015).
270. Rosenthal, G. *et al.* The role of lung function in brain tissue oxygenation following traumatic brain injury. *J. Neurosurg.* 108, 59–65 (2008).
271. H., R. *et al.* Quality assurance for cerebrospinal fluid protein analysis: International consensus by an internet-based group discussion. *Clin. Chem. Lab. Med.* 41, 331–337 (2003).
272. Wang, G. H., Zhang, X. G., Jiang, Z. L., Li, X., Peng, L. L., Li, Y. C., & Wang, Y. Neuroprotective effects of hyperbaric oxygen treatment on traumatic brain injury in the rat. *J. Neurotrauma* 27, 1733–1743 (2010).
273. Huang, L. & Obenaus, A. Hyperbaric oxygen therapy for traumatic brain injury. *Med. Gas Res.* 1, 21 (2011).
274. Bennett, M. H., Trytko, B. & Jonker, B. in *Cochrane Database of Systematic Reviews* (ed. Bennett, M. H.) 12, (John Wiley & Sons, Ltd, 2012).

275. Rockswold, S. B., Rockswold, G. L., Zaun, D. a & Liu, J. A prospective, randomized Phase II clinical trial to evaluate the effect of combined hyperbaric and normobaric hyperoxia on cerebral metabolism, intracranial pressure, oxygen toxicity, and clinical outcome in severe traumatic brain injury. *J. Neurosurg.* 118, 1317–1328 (2013).
276. Deng, J. *et al.* Neuroprotective gases - Fantasy or reality for clinical use? *Prog. Neurobiol.* 115, 210–245 (2014).
277. Diring, M. N., Aiyagari, V., Zazulia, A. R., Videen, T. O. & Powers, W. J. Effect of hyperoxia on cerebral metabolic rate for oxygen measured using positron emission tomography in patients with acute severe head injury. *J. Neurosurg.* 106, 526–529 (2007).
278. Nortje, J. *et al.* Effect of hyperoxia on regional oxygenation and metabolism after severe traumatic brain injury: preliminary findings. *Crit. Care Med.* 36, 273–281 (2008).
279. Rockswold, S. B., Rockswold, G. L., Zaun, D. a & Liu, J. A prospective, randomized Phase II clinical trial to evaluate the effect of combined hyperbaric and normobaric hyperoxia on cerebral metabolism, intracranial pressure, oxygen toxicity, and clinical outcome in severe traumatic brain injury. *J. Neurosurg.* 118, 1317–1328 (2013).
280. Tisdall, M. M., Tachtsidis, I., Leung, T. S., Elwell, C. E. & Smith, M. Increase in cerebral aerobic metabolism by normobaric hyperoxia after traumatic brain injury. *J. Neurosurg.* 109, 424–432 (2008).
281. Massabuau, J. C. *From low arterial- to low tissue-oxygenation strategy. An evolutionary theory. Respiration physiology* 128, 249–261 (2001).
282. Arikan, F. *et al.* Intraoperative monitoring of brain tissue oxygenation during arteriovenous malformation resection. *J. Neurosurg. Anesthesiol.* 26, 328–341 (2014).
283. Readnower, R. D. *et al.* Increase in blood-brain barrier permeability, oxidative stress, and activated microglia in a rat model of blast-induced traumatic brain injury. *J. Neurosci. Res.* 88, 3530–9 (2010).
284. Puccio, A. M. *et al.* Effect of short periods of normobaric hyperoxia on local brain tissue oxygenation and cerebrospinal fluid oxidative stress markers in severe traumatic brain injury. *J. Neurotrauma* 26, 1241–9 (2009).
285. Kety, S. S. & Schmidt, C. F. The effects of altered arterial tensions of carbon dioxide and oxygen on cerebral blood flow and cerebral oxygen consumption of normal young men. *J. Clin. Invest.* 27, 484–92 (1948).

286. Johnston, A. J., Steiner, L. A., Gupta, A. K. & Menon, D. K. Cerebral oxygen vasoreactivity and cerebral tissue oxygen reactivity. *Br. J. Anaesth.* 90, 774–786 (2003).
287. JACOBSON, I., HARPER, A. M. & MCDOWALL, D. G. THE EFFECTS OF OXYGEN AT 1 AND 2 ATMOSPHERES ON THE BLOOD FLOW AND OXYGEN UPTAKE OF THE CEREBRAL CORTEX. *Surg. Gynecol. Obstet.* 119, 737–42 (1964).
288. Schmitz, T. *et al.* Cellular changes underlying hyperoxia-induced delay of white matter development. *J. Neurosci.* 31, 4327–4344 (2011).
289. Wu, H.-M., Huang, S.-C., Vespa, P., Hovda, D. a & Bergsneider, M. Redefining the pericontusional penumbra following traumatic brain injury: evidence of deteriorating metabolic derangements based on positron emission tomography. *J. Neurotrauma* 30, 352–60 (2013).
290. Siggaard-Andersen, O., Ulrich, A. & Gøthgen, I. H. Classes of tissue hypoxia. *Acta Anaesthesiol. Scand. Suppl.* 107, 137–42 (1995).
291. Joo, K. M. *et al.* Experimental and clinical factors influencing long-term stable in vitro expansion of multipotent neural cells from human adult temporal lobes. *Exp. Neurol.* 240, 168–177 (2013).
292. Jha, R. M., Liu, X., Chrenek, R., Madsen, J. R. & Cardozo, D. L. The postnatal human filum terminale is a source of autologous multipotent neurospheres capable of generating motor neurons. *Neurosurgery* 72, 118–128 (2013).
293. Varghese, M. *et al.* Isolation of human multipotent neural progenitors from adult filum terminale. *Stem Cells Dev.* 18, 603–13 (2009).
294. Arsenijevic, Y. *et al.* Isolation of multipotent neural precursors residing in the cortex of the adult human brain. *Exp. Neurol.* 170, 48–62 (2001).
295. Murrell, W. *et al.* Expansion of Multipotent Stem Cells from the Adult Human Brain. *PLoS One* 8, (2013).
296. Nam, H., Lee, K.-H., Nam, D.-H. & Joo, K. M. Adult human neural stem cell therapeutics: Current developmental status and prospect. *World J. Stem Cells* 7, 126–36 (2015).
297. Johansson, C. B., Svensson, M., Wallstedt, L., Janson, a M. & Frisen, J. Neural stem cells in the adult human brain. *Exp. Cell Res.* 253, 733–736 (1999).
298. Stevanato, L. *et al.* c-MycERTAM transgene silencing in a genetically modified human neural stem cell line implanted into MCAo rodent brain. *BMC Neurosci.* 10, 86 (2009).

299. Miljan, E. a *et al.* Implantation of c-mycER TAM immortalized human mesencephalic-derived clonal cell lines ameliorates behavior dysfunction in a rat model of Parkinson's disease. *Stem Cells Dev.* 18, 307–19 (2009).
300. Littlewood, T. D., Hancock, D. C., Danielian, P. S., Parker, M. G. & Evan, G. I. A modified oestrogen receptor ligand-binding domain as an improved switch for the regulation of heterologous proteins. *Nucleic Acids Res.* 23, 1686–1690 (1995).
301. Donato, R. *et al.* Differential development of neuronal physiological responsiveness in two human neural stem cell lines. *BMC Neurosci.* 8, 36 (2007).
302. Pollock, K. *et al.* A conditionally immortal clonal stem cell line from human cortical neuroepithelium for the treatment of ischemic stroke. *Exp. Neurol.* 199, 143–155 (2006).
303. Fang, C. M., Shi, C. & Xu, Y. H. Deregulated c-myc expression in quiescent CHO cells induces target gene transcription and subsequent apoptotic phenotype. *Cell Res* 9, 305–314 (1999).
304. Graham, D. I., Adams, J. H. & Doyle, D. Ischaemic brain damage in fatal non-missile head injuries. *J. Neurol. Sci.* 39, 213–34 (1978).
305. Siggaard-Andersen, O., Fogh-Andersen, N., Gøthgen, I. H. & Larsen, V. H. Oxygen status of arterial and mixed venous blood. *Crit. Care Med.* 23, 1284–1293 (1995).
306. Yu, A. C., Gregory, G. A. & Chan, P. H. Hypoxia-induced dysfunctions and injury of astrocytes in primary cell cultures. *J Cereb Blood Flow Metab* 9, 20–28 (1989).
307. Weidemann, A. & Johnson, R. S. Biology of HIF-1 α . *Cell Death Differ.* 15, 621–627 (2008).
308. Kim, J. W., Tchernyshyov, I., Semenza, G. L. & Dang, C. V. HIF-1-mediated expression of pyruvate dehydrogenase kinase: A metabolic switch required for cellular adaptation to hypoxia. *Cell Metab.* 3, 177–185 (2006).
309. Véga, C., R. Sachleben, L., Gozal, D. & Gozal, E. Differential metabolic adaptation to acute and long-term hypoxia in rat primary cortical astrocytes. *J. Neurochem.* 97, 872–883 (2006).
310. Dings, J., Meixensberger, J. & Roosen, K. Brain tissue pO₂-monitoring: catheter stability and complications. *Neurol. Res.* 19, 241–5 (1997).
311. Crowley, L. C. *et al.* Measuring cell death by propidium iodide uptake and flow cytometry. *Cold Spring Harb. Protoc.* 2016, 647–651 (2016).

-
312. Hillered, L., Persson, L., Nilsson, P., Ronne-Engstrom, E. & Enblad, P. Continuous monitoring of cerebral metabolism in traumatic brain injury: a focus on cerebral microdialysis. *Curr. Opin. Crit. Care* 12, 112–118 (2006).
313. Pulsinelli, W. A., Brierley, J. B. & Plum, F. Temporal profile of neuronal damage in a model of transient forebrain ischemia. *Ann. Neurol.* 11, 491–498 (1982).
314. Xu, L., Sapolsky, R. M. & Giffard, R. G. Differential sensitivity of murine astrocytes and neurons from different brain regions to injury. *Exp. Neurol.* 169, 416–24 (2001).
315. Callahan, D. J., Engle, M. J. & Volpe, J. J. Hypoxic injury to developing glial cells: protective effect of high glucose. *Pediatr Res* 27, 186–190 (1990).
316. Kelleher, J. a, Chan, P. H., Chan, T. Y. & Gregory, G. a. Modification of hypoxia-induced injury in cultured rat astrocytes by high levels of glucose. *Stroke.* 24, 855–63 (1993).
317. Zhu, H., Jackson, T. & Bunn, H. F. Detecting and responding to hypoxia. *Nephrol. Dial. Transplant* 17 Suppl 1, 3–7 (2002).
318. Marrif, H. & Juurlink, B. H. J. Astrocytes respond to hypoxia by increasing glycolytic capacity. *J. Neurosci. Res.* 57, 255–260 (1999).
319. Niitsu, Y. *et al.* Exposure of cultured primary rat astrocytes to hypoxia results in intracellular glucose depletion and induction of glycolytic enzymes. *Mol. Brain Res.* 74, 26–34 (1999).
320. Bell, G. I., Burant, C. F., Takeda, J. & Gould, G. W. Structure and function of mammalian facilitative sugar transporters. *J. Biol. Chem.* 268, 19161–19164 (1993).
321. Wood, I. S. & Trayhurn, P. Glucose transporters (GLUT and SGLT): expanded families of sugar transport proteins. *Br. J. Nutr.* 89, 3 (2003).
322. Lutz, P. L. & Nilsson, G. E. Contrasting strategies for anoxic brain survival-glycolysis up or down. *J. Exp. Biol.* 200, 411–419 (1997).
323. Bittar, P. G., Charnay, Y., Pellerin, L., Bouras, C. & Magistretti, P. J. Selective Distribution of Lactate Dehydrogenase Isoenzymes in Neurons and Astrocytes of Human Brain. *J. Cereb. Blood Flow Metab.* 1079–1089 (1996). doi:10.1097/00004647-199611000-00001
324. Tsacopoulos, M. & Magistretti, P. J. Metabolic coupling between glia and neurons. *J. Neurosci.* 16, 877–885 (1996).
325. Larrabee, M. G. Lactate Metabolism and Its Effect on Glucose Metabolism in

an Excised Neural Tissue. *J. Neurochem.* 64, 1734–1741 (1995).

326. Schurr, A., West, C. A. & Rigor, B. M. Lactate-supported synaptic function in the rat hippocampal slice preparation. *Science (80-.)*. 240, 1326–1328 (1988).

327. Ungerstedt, U. & Rostami, E. Microdialysis in neurointensive care. *Curr. Pharm. Des.* 10, 2145–2152 (2004).

SECTION



ANNEXES

7

- 1 HUMAN ORGANOTYPIC CULTURES AS AN IN VITRO MODEL**
- 2 HUMAN ADULT NEURAL STEM CELLS AS AN IN VITRO MODEL**
- 3 LOW EXTRACTIVITY BRAIN HYPOXIA AFTER TRAUMATIC BRAIN INJURY. METABOLIC PROFILE AND IN VITRO MODELING**

ANNEX

This section includes *in vitro* studies related to the development of the objective 4 of this doctoral thesis. For this purpose, the feasibility of using an *in vitro* model from adult human tissue was first studied (**Annex 1** and **Annex 2**). The last section (**Annex 3**) includes the results of a study describing abnormal brain metabolic profiles and the changes in the glycolytic machinery under hypoxic conditions observed in one of the types of hypoxia described by Siggaard-Andersen in 1995 (low extractivity hypoxia).¹ This was accomplished using an *in vitro* model of human cerebral cortex astrocytes.

1. Human organotypic cultures as an *in vitro* model

To reproduce the abnormal metabolic profiles observed under hypoxia, we first studied the feasibility of obtaining a robust *in vitro* slice culture model of human brain specimens from surgical operations in which small resections of cerebral cortex need to be removed. The neuropathological hallmarks and the histological characterization of the cultured slices were determined in the original sample before culture and at different time points during the culture (days *in vitro* -DIV-).

1.1. Material and methods

1.1.1. Cell Culture

Surgically explanted human brain tissue (neocortex with a variable degree of white matter), with no apparent radiological alterations, was obtained from the Vall d'Hebron University Hospital. These samples were processed and destined to culture only if presurgical MRI scan did not show any abnormalities of the normal tissue in T1W, T2W, or FLAIR images. All samples were part of the planned resections and tissue was only collected after sufficient specimen was available for the neuropathological report.

Different strategies were tested for organotypic culture (cutting methods, culture medium, and transport media). In this section, we describe the strategy that gave us better results.

After resection, the harvested tissue was immediately placed into ice cold Hank's balanced salt solution (HBSS; catalog# 14025092; Thermo Fisher Scientific, Waltham, MA) at 4°C (ice cold) and transported immediately to the laboratory where it was processed under sterile conditions. Surgical specimens were cut with a scalpel into rectangular blocks of 5-10 mm by 1-2 mm. These slices were further sectioned into 300 µm-thick slices using a McIlwain tissue chopper (TC752, Lafayette Instruments, Lafayette, IN) and placed into a Petri dish containing phosphate buffered saline (PBS). The brain slices were gently separated under a stereomicroscope (SZ61 Olympus; Olympus Corporation, Tokyo, Japan) with 2 sterile scalpels and individually transferred into membrane culture inserts (catalog# PICM0RG50, Millipore, Billerica, MA) within 6-well plates. Before placing the inserts into these plates, 1.2 mL of Neurobasal medium (catalog# 10888-022, Thermo Fisher Scientific) supplemented with B27 (catalog# 17504044, Thermo Fisher Scientific), L-glutamine (catalog# 25030081, Thermo Fisher Scientific), penicillin/streptomycin (P/S; catalog# 15140122, Thermo Fisher Scientific), and growth factors (20 ng/mL epidermal growth factor -EGF; catalog# 53003018, Thermo Fisher Scientific- and 20 ng/mL basic fibroblast growth factor -bFGF-2; catalog#F0291, Sigma-Aldrich, St. Louis, MO-) were placed into each well. The final pH of the media was maintained between 7,2 and 7,4. The brain slices were incubated at 37°C with constant humidity, 95% air and 5% CO₂, and checked daily with an inverted light microscope for viability. Culture medium was refreshed the first day after preparation and every three days.

1.1.2. Cell culture characterization

In order to evaluate neuropathological hallmarks and the histological characterization of the tissue, all processed specimens were prepared for histological, immunohistochemical staining, transmission electron microscopy (TEM) analysis and cell culture viability. The specimens were analyzed at different time points: at *DIV0*, *DIV7*, *DIV14* and *DIV30*. Additionally, before cultivation, the samples obtained in the operating room were evaluated following the procedures described above.

Histological analysis

The samples were fixed with phosphate-buffered 4% formaldehyde at room temperature (RT) for 48h. After fixation, 10- μ m sections were obtained using a cryostat (Leica CM3050 S, Leica Biosystems, Heidelberg, Germany). At least 4 sections were obtained from each block: one for histological examination using hematoxylin–eosin stain (H&E) and 3 sections for immunohistochemical (IHC) detection of astrocytes, microglia and neurons. Histological studies consisted on H&E staining for evaluating signs of altered structure and specifically for the presence of hypoxia/ischemia and edema.

Immunohistochemical Analysis

For IHC analysis, tissue sections were washed with 0.1M PBS and incubated for 15 minutes in PBS 0.1M containing 0.3 % H₂O₂ and 0.1% methanol to block endogenous peroxidase activity. After this, sections were blocked with 4% donkey serum (catalog# D9663; Sigma, St. Louis, MO, USA), and 0.1% Triton-X (catalog# T8787; Sigma) in PBS 0.1 M for 1 hour. Next, the cryosections were incubated for 1 hour at RT and then overnight with the primary antibody at 4°C in a humidified chamber to prevent dehydration. Primary antibodies used were: rabbit Anti-glia fibrillary acidic protein (GFAP; 1:1000; catalog# Z0334, Dako, Carpinteria, CA, USA), mouse Anti-cluster of differentiation 68 (CD68;1:50; catalog# M081401, Dako) and Anti-mouse 200-kDa phosphorylated and non-phosphorylated neurofilament epitopes (NF200KD; 1:200; catalog# N0142, Sigma). Next day, after washing in PBS, sections were incubated with a species-appropriate biotinylated secondary antibody (1:200; Vector Laboratories, Burlingame, CA) for 1 h at RT. After washing in PBS, sections were incubated in avidin-biotin solution (ABC Kit, PK-6200, Vector Laboratories) and the reaction product was visualized using diaminobenzidine tetrahydrochloride activated with 0.01% H₂O₂. Finally, sections were counterstained with hematoxylin, dehydrated and mounted in DPX. The omission of primary antibodies served as negative controls. The stained sections were visualized using a bright field microscope (D-Sight Fluo, A. Menarini Diagnostics, Florence, Italy), and all sections were digitally registered and documented. The presence and the amount of the different cell type-specific markers

(GFAP and CD68) was evaluated in the whole section. Additionally, a descriptive analysis was conducted for NF200KDa immunolabelling in each sample.

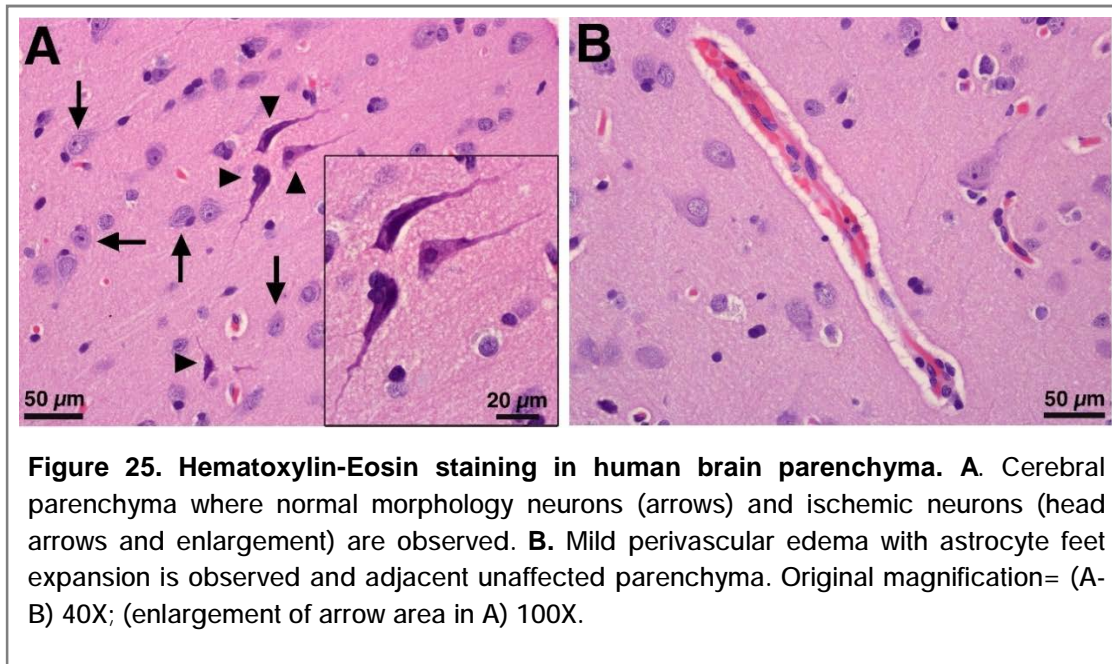
Transmission Electron Microscopy

Ultrastructural studies were performed on tissues fixed in 2% glutaraldehyde and 2% paraformaldehyde in 0.1 M PB, pH 7.4 prepared for TEM analysis. The fixed sections were immersed in 1% osmium tetroxide, rinsed, dehydrated, and embedded in Eponate 12 resin (Ted Pella, Inc., Redding, CA, USA). Semithin sections (1 mm thick) were obtained with a Leica Ultracut UCT microtome (Leica Microsystems GmbH, Wetzlar, Germany) and stained with 1% aqueous toluidine blue solution. To select the areas most suitable for further analysis, semithin sections were examined with a light microscope. Whenever possible, the most suitable sections contained gray matter where different states of tissue were present (healthy, dark, ischemic and hydropic neurons). For ultrastructural analysis, ultrathin sections (70 nm thick) were cut, placed on coated copper grids, and then, contrasted with uranyl acetate and Reynold's lead citrate solution. Sections were examined under a Hitachi H-7000 transmission electron microscope (Hitachi High-Technologies Europe GmbH, Krefeld, Germany) at 100kV and photographed with an ES500W Erlangshen CCD camera (Gatan, Pleasanton, United States). The sections were analyzed for normal or altered cytoarchitecture, cellular composition, tissue integrity, cytoplasmic organelles and synaptic contacts.

1.2. Results and discussion

A total of 8 non-pathological brain specimens were obtained and cultured (5 men and 3 women). The specimens were obtained from patients who underwent selective brain resections to access extra-axial skull base tumors or intraventricular lesions. The patients from which the normal surgical brain tissue was obtained had a median age of 45 years (min: 2; max: 70 years).

Under routine H&E staining, we evaluated the pathologic evidence of edema and hypoxia or ischemia. H&E stained sections of the original samples (pre-culture) showed a variable degree of ischemic changes, extracellular edema, and microvacuolization of the neuropil (**Figure 25**). Perivascular edema was more prominent in the gray matter and at the interface between gray and white matter in all analyzed specimens. All the samples showed a variable presence of dark neurons (basophilic cells with a dark, shrunken nucleus) produced by manipulation or trauma to the brain tissue before sample fixation. Signs of hypoxia/ischemia became more evident over time *in vitro*. At DIV7, the slices showed signs of neural necrosis, and macrophages were observed in some cases. All of these lesions increased at DIV30, with an extensive vacuolization and abundant phenomena of necrosis-apoptosis. The evolution of the cultures differed according to the original characteristics of the tissue.



The high variability observed among the samples was confirmed by IHC analysis. This analysis revealed a variable number of activated microglial cells/macrophages. The amount of GFAP positive cells varied in each sample and ranged from scanty to highly abundant. A descriptive analysis was conducted for NF200KDa in each sample. Axon segmental dilatations occurred in 50% of the samples analyzed. Cell inclusions and axonal spheroids were not detected in the entire collection. Most axonal alterations consisted of larger diameter axons, showing multiple small axonal swellings with

neurofilament displacement or multiple irregular foamy-like axons (**Figure 26**). Under culture, brain organotypic slices showed an increase in astrogliosis and a decrease in the number of viable neurons.

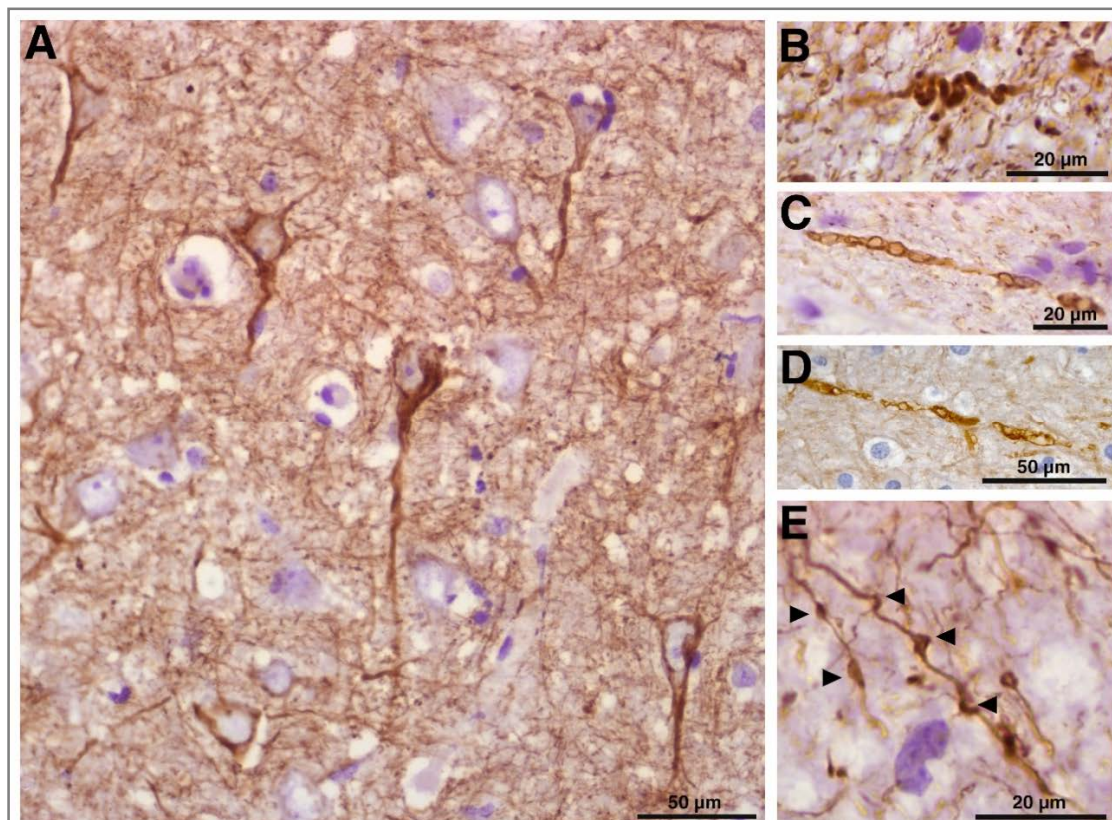


Figure 26. Phosphorylated and non-phosphorylated 200kDa Neurofilament staining (NF-200) in human brain parenchyma. A. neurons labelled for expression of NF-200, indicating absence of axonal spheroids or cellular inclusions. **B-D.** Pathological axon structure. **B.** Tortuous axons. **C.** Larger diameter axons with multiple small axonal swellings with neurofilament displacement towards the periphery giving a chain appearance axon. **D.** Axon varicosities. **E.** Multiple irregular foamy-like axon dilatations. Sections were counterstained with hematoxylin. Original magnification = (A) 40X; (B-E) 100X.

The sections were also analyzed using TEM. Ultrastructural analysis corroborated the histological findings. In all the surgically explanted specimens, there was substantial variability in the evaluated parameters (**Figure 27**).

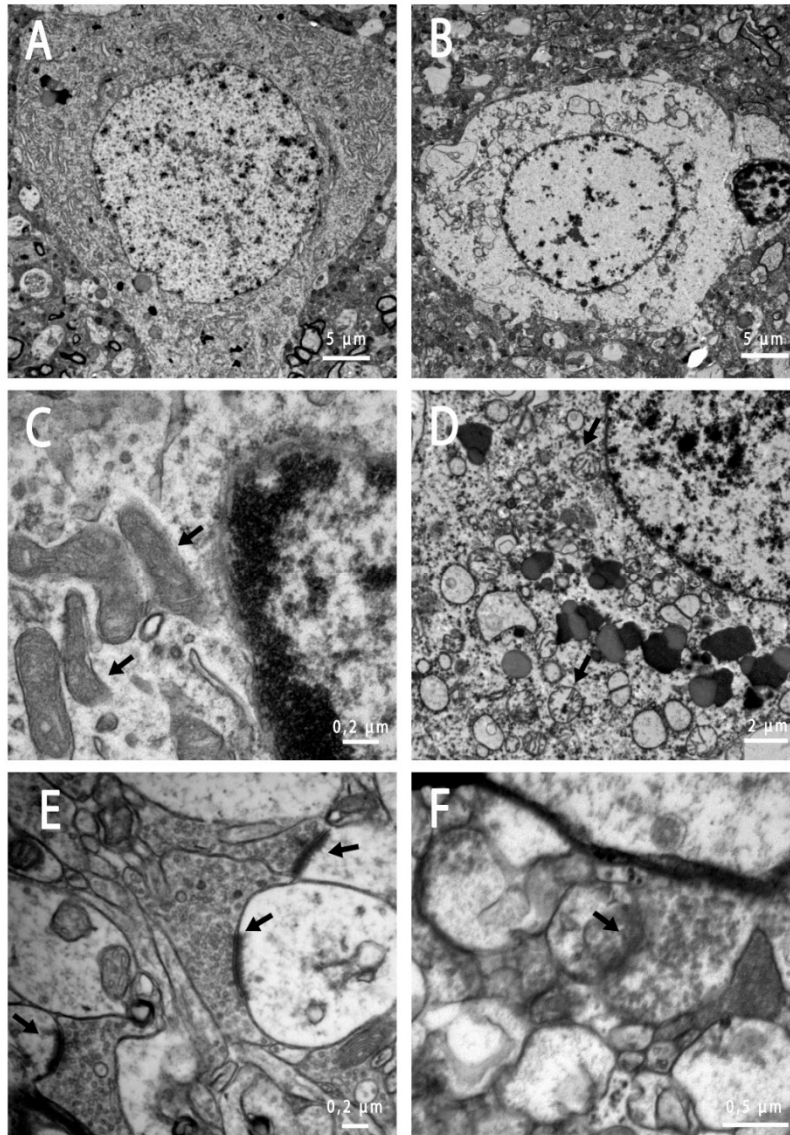


Figure 27. Electron micrographs of two cases of normal human cortex (pre-culture).

A. Neuron with normal-appearing nucleus and cytoplasm without signs of edema or injury.

B. Perikaryon of a neuron severely edematous with few organelles showing most of them a swollen lumen.

C. Typical mitochondrial ultrastructure with no evidence of matrix lucency, intracristal dilatation or other signs of swelling, or condensation (arrow).

D. Swelling mitochondrias (arrow) and rough endoplasmic reticulum with intact surrounding membranes.

E. Asymmetric synapsis containing round to oval clear vesicles (arrow).

F. Synapsis with diffuse and irregular membranes and with amorphous appearance of synaptic vesicles.

In the analysis of samples before culture, the oligodendrocyte structure appeared intact in most of the samples, and microglia were rarely affected. In contrast, all or almost all of the samples presented a severely altered astrocyte structure (mainly hydropic). The presence of astrocytes with altered structure ranged from occasional

to highly frequent. Intact neurons were seldom observed in the explanted specimens, and only one sample showed no structural changes compatible with neuronal damage. The affected neurons were mostly hydropic or ischemic, with numerous dark neurons standing out. Sporadically neuronal necrosis and apoptosis were also observed.

The synaptic contacts and vesicles associated with these structures presented a structural degradation in accordance with the degree of neuronal structural damage. Microvacuolization of the neuropil varied in each case, and the morphology of myelinated and non-myelinated axons was also well preserved in over half of the samples. In conclusion, the TEM analysis of the original samples revealed different degrees of alteration in each case. With the increase of DIV, ischemic lesions became more evident, the numbers of cells and normal neurons were reduced, and a greater disorganization of the neuropil was observed.

The samples came from apparently "healthy/normal" tissue (no radiologic alterations) obtained during brain tumor resections. Nevertheless, the deep histological and ultrastructural study indicated that these samples were not "normal." We can conclude that organotypic cultures cannot be performed from samples of living adult human brain tissue due to the pathological characteristics of the surgically explanted samples (pathological evidence of edema or ischemia) and the great variability between them. Alternative models are proposed in the following sections (**Annex 2** and **Annex 3**).

2. Human adult neural stem cells as an *in vitro* model

We proposed a strategy to obtain an alternative *in vitro* model that is stable over time and could be subjected to different experimental conditions (e.g., hypoxia). The strategy involves the culture of human neural stem cells (hNSCs) from healthy human tissue of the *subventricular zone* (SVZ) and *fillum terminale* (FT), which are explanted during neurosurgical procedures. The hNSCs are isolated, maintained, and expanded, and the differentiated cellular phenotypes (neurons, astrocytes, and oligodendrocytes) are generated after withdrawal of mitogens from the culture medium. This approach allows us to obtain an *in vitro* experimental model for testing new therapeutic strategies, and it could serve as a potential tool for substitution therapy with neural precursors in cases of CNS disease in cell dysfunction due to injury, ischemia, or degeneration.

2.1. Material and methods

2.1.1. Cell culture

Human SVZ and FT specimens were obtained from the Vall d'Hebron University Hospital. After resection, the harvested tissue was immediately placed into ice cold HBSS and transported immediately to the laboratory, where it was processed under sterile conditions. SVZ and FT specimens were dissected in Petri dishes containing phosphate buffer. Under sterile conditions the samples were dissected, mechanically dissociated into small pieces and incubated in papain (catalog# 9001-73-4, Worthington, Lakewood, NJ) for 15 min at 37°C. Small tissue pieces were further dissociated mechanically by gentle trituration through fire-polished Pasteur pipettes. Cell suspension was filtered through a 70-micron cell strainer (catalog# 087712, BD Falcon, Heidelberg, Germany) to remove debris. Cells were then collected by centrifugation and seeded in growth media containing Dulbecco's modified Eagle's medium (DMEM-F12; catalog#11320, Thermo Fisher Scientific) supplemented with 0.6 % glucose, 2 mmol/L L-glutamine (catalog# 25030081, Thermo Fisher Scientific), 1 M HEPES (catalog# 15630080, Thermo Fisher Scientific), 9.6 g/mL putrescine (catalog# P51799, Sigma-Aldrich, St. Louis, MO), 0.025 mg/mL progesterone (catalog# P0130,

Sigma-Aldrich), 5.2 ng/mL sodium selenite (catalog# S5261, Sigma-Aldrich), 0.025 mg/mL insulin (catalog# I6634, Sigma-Aldrich), 0,1 mg/mL transferrin (catalog# T3309, Sigma-Aldrich), 2 g/mL heparin (catalog# H3393, Sigma-Aldrich), and antibiotic/antimicotic (catalog# 15240062, Thermo Fisher Scientific) (control medium). Cells were cultured in serum-free medium on non-coated culture dishes in the presence of 20 ng/mL EGF (catalog# 53003018, Thermo Fisher Scientific) 10 ng/mL bFGF (catalog# F0291, Sigma-Aldrich), BSA and 0.2 % Heparin (Sigma-Aldrich) (-complete medium). Leukemia inhibitory factor (LIF; catalog# L5158, 10 ng/mL; Sigma-Aldrich) was additionally added in human cultures. The number of primary neurospheres was counted after 7 days, for differentiation, proliferation and self-renewal studies. Primary spheres appeared in culture after 7–10 DIV, and were then passaged. Subsequent passages were performed after 4–7 DIV.

Additionally, the effectiveness of an alternative culture method of hNSCs was tested. Human SVZ specimens were cultured using a modification of the methodology proposed by K.M Joo et al. in 2013.² In brief, human SVZ was mechanically minced and placed in the enzyme mixture solution described above for 15 minutes at 37°C. After mild trituration, cells were filtered through a cell strainer. Following Percoll purification (catalog# P1644, Sigma-Aldrich), adherent culture on pre-treated poly-L-ornithin-coated dishes (catalog# P4957, Sigma-Aldrich) was performed in a DMEM/F12 media supplemented with 1% B27 (catalog# 17504001, Thermo Fisher Scientific), 1% P/S cocktail (catalog# 15140122, Thermo Fisher Scientific), EGF (50 ng/mL), bFGF (50 ng/mL), LIF (10 ng/mL) and 0.5% FBS (catalog# 26140087, Thermo Fisher Scientific).

Cell differentiation: The primary neurospheres were mechanically dissociated with accutase (catalog# A6964, Sigma-Aldrich) and cells were then plated in poly-ornithine and poly-D-Lysine (catalog# P6407, Sigma-Aldrich)-coated 24 well plates in the presence of 1.5% FBS, 0.2% Heparin and 10 ng/mL bFGF.

2.1.2. Cell culture characterization

Cells were fixed in 4% formaldehyde for 20 minutes at RT, and washed with PBS. Non-specific binding was then blocked with 10% donkey serum and 0.1% Triton-X in PBS 0.1M for 1 h at room temperature. Cells were then incubated with primary antibodies

to: β -tubulin III (TUJ1; 1:100; catalog# ab9354, Millipore Corporation), Nestin (1:2000; catalog# S1409, Sigma-Aldrich), Glial fibrillary acidic protein (GFAP; 1:1000; catalog# ab4674, Abcam, Cambridge, UK), Doblecortin (DCX; 1:200; catalog# ab18723, Abcam) and Vimentin (1:500; catalog# ab24525, Abcam) at 4°C overnight. Fluorescent-labeled, species-appropriate secondary antibodies (Thermo Fisher Scientific) were used for visualization. Omission of primary antibodies served as negative controls. Cells were then washed with PBS and counterstained with the nuclear dye, 4,6-diamino-2-phenylindole (DAPI, Thermo Fisher Scientific). Fluorescent signals were captured using an epifluorescence microscope (FX100 Olympus or BX61 Olympus; Olympus Corporation), or a confocal microscope (Spectral Confocal Microscope FV1000, Olympus) depending on analysis requirements.

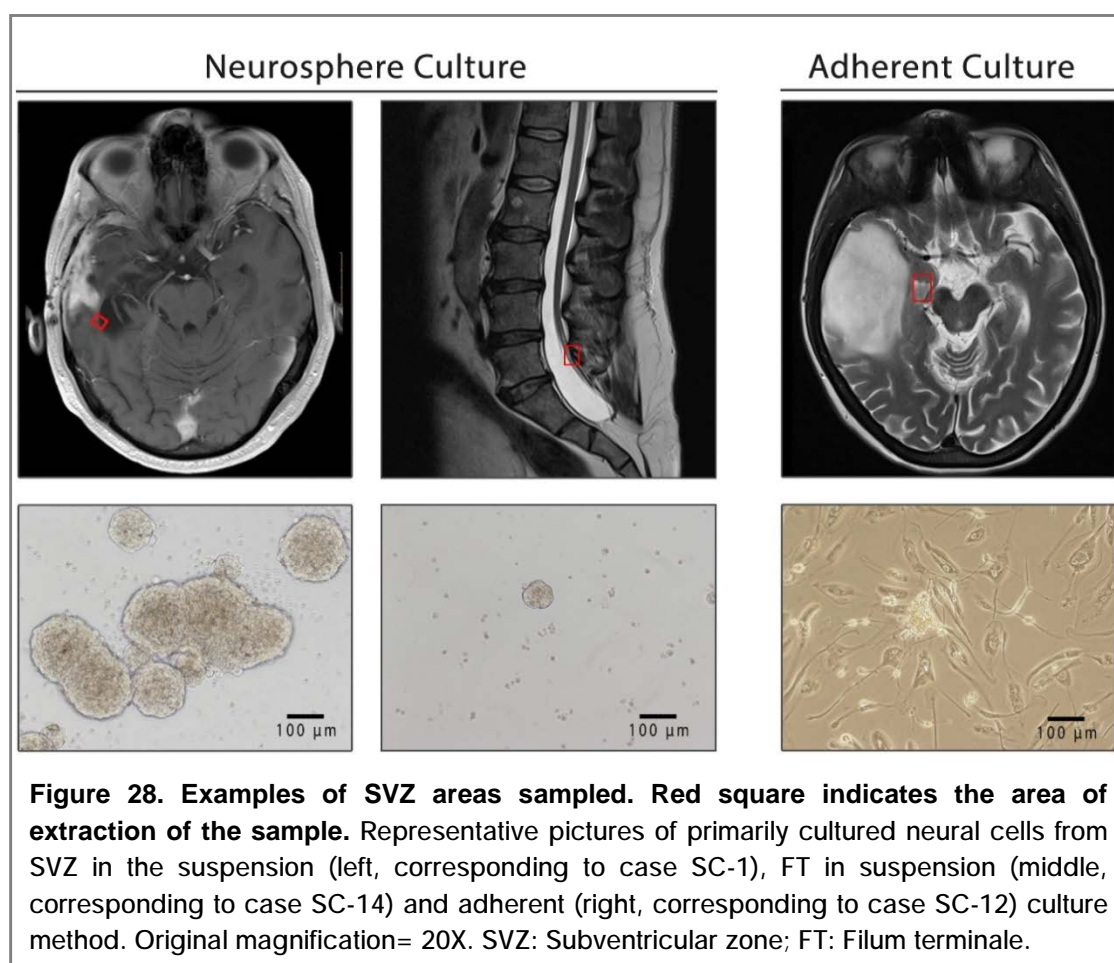
2.2. Results and discussion

A total of 14 specimens were obtained from a cohort of 14 patients (9 males and 5 females) with a median age of 28 years. The specimens obtained from SVZ (n=13) and FT (n=1, case SC-14) were cultured using two different methods: suspension culture (n=13) and adherent culture (n=1, SVZ sample; case SC-13) (**Figure 28**). Due to the lower availability of FT samples, we could only report data from a single case. Demographics and clinical data of the samples are summarized in **Table 12**. The human SVZ and FT specimens contained multipotent neural precursors that could be expanded as neurospheres and differentiated *in vitro*. Neurospheres were observed in over 90% of the specimens obtained from the SVZ (all cases except one). One case was successfully cultured using the attachment culture method.² Under this condition, the dissociated cells proliferated as a monolayer of cells, which were propagated until 70% cell confluence for cultured stem cell characterization. We were also able to produce spheres from the FT, a recently defined source of neural stem cells.^{3,4} The neural progenitors observed from FT samples were small, spherical, non-process bearing cells that were similar to the hNSCs obtained from SVZ. After 7 weeks in culture, the progenitors proliferated and developed spherical aggregates ("neurospheres"). Self-renewal was not tested in this case.

Table 12. Demographics and clinical characteristics of cases used for *in vitro* expansion of stem cells derived from SVZ and FT

Case	Age (years) ¹	Gender	Primary pathology	Tissue analyzed	Neurospheres observed ²
SC-1	49	M	GBM	SVZ	ü
SC-2	31	F	Intraventricular tumor	SVZ	
SC-3	2	M	Rhabdoid tumor	SVZ	ü
SC-4	24	M	Ganglioma	SVZ	ü
SC-5	52	M	Obstructive hydrocephalus	SVZ	ü
SC-6	6	F	Choroids plexus papilloma	SVZ	ü
SC-7	66	M	Pineal Tumor	SVZ	ü
SC-8	1	M	Choroids plexus papilloma	SVZ	ü
SC-9	3	F	Astrocytoma	SVZ	ü
SC-10	0.9	F	Astrocytoma	SVZ	ü
SC-11	66	M	Epidermoid cyst	SVZ	ü
SC-12	42	F	Meningioma	SVZ	ü
SC-13	0.7	M	Oligoastrocytoma	SVZ	ü
SC-14	46	M	Tethered cord	FT	ü

¹ Age at surgery. ² Cases in which neurosphere generation was observed. SVZ: Subventricular zone; FT: Filum terminale; GBM: Glioblastoma multiforme.



The isolation of cells from adult human SVZ resulted in heterogeneous tendencies in the proliferation rates. One of the main reasons is that the research supply of SVZ material from human biopsies is limited, and the characteristics vary between specimens because investigators cannot dictate the amount of tissue where neurosurgical resections will be directed.⁵ We can conclude that clusters of cells appeared after 7 to 20 DIV in the presence of EGF, FGF, and LIF. As the cells continued to proliferate, they formed spheres after 14 to 40 DIV. The shape of these spheres was very similar to that of spheres derived from the adult mouse brain. Neurospheres have limited capacity to generate new spheres. We were able to produce new multipotent spheres until only passage 9. The number of cells also decreased with each passage. We did not quantify proliferation because it varied from specimen to specimen, since samples were obtained from different donors of different ages and during different surgeries.

The identity of the cells composing the spheres was characterized by immunocytochemistry (ICC) techniques. ICC was performed on single neurospheres, which expressed markers of immaturity and undifferentiation (Nestin) that colocalize to a variable degree of phenotypic markers (Vimentin) (**Figure 29**). A similar distribution was observed in the adherent culture. In summary, the expression pattern and the proportion of + cells to each marker was variable among cases. To characterize the neurospheres and their potential to produce neurons and glia, they were tested for the expression of Nestin, GFAP, Tuj1, and Dcx. There was a predominant expression of Tuj1 and Dcx, which are markers present in neuroblasts and migration neurons that colocalize to different degrees with Nestin and GFAP.

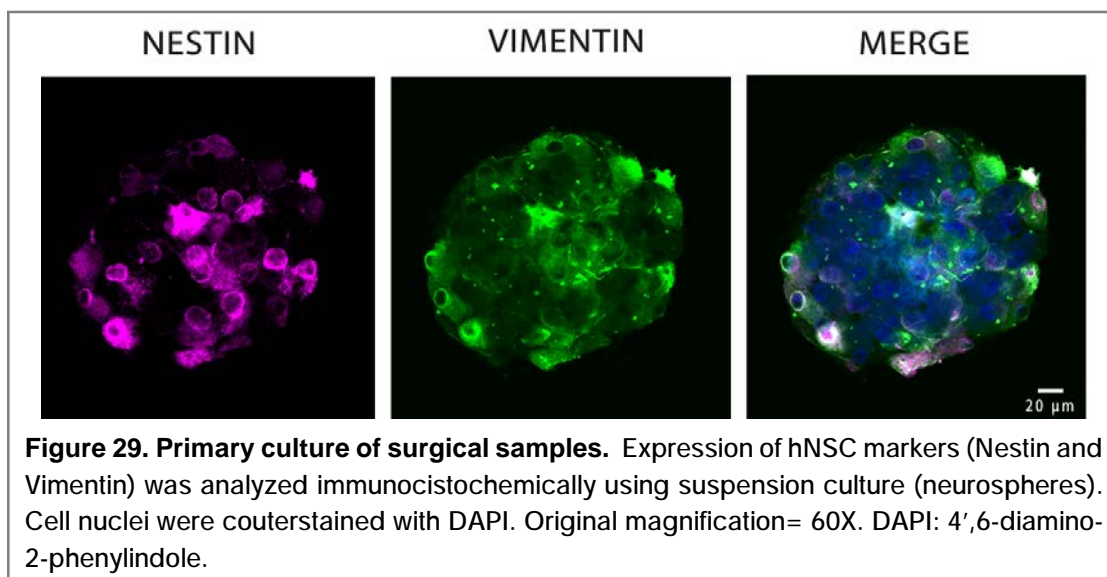


Figure 29. Primary culture of surgical samples. Expression of hNSC markers (Nestin and Vimentin) was analyzed immunocytochemically using suspension culture (neurospheres). Cell nuclei were counterstained with DAPI. Original magnification= 60X. DAPI: 4',6-diamino-2-phenylindole.

Our data suggest that it is technically and clinically challenging to use hNSCs derived from adult human brains for cell therapy due to the limited number of isolated cells and their difficult expansion *in vitro*, which is in accordance with published data.⁶⁻⁹ It is crucial to optimize the expansion potential of these cells in order to use them as therapeutic tools. Thus, we studied the ability of 4-OHT to induce the expression of c-mycER^{TAM}, and its effects on the growth and self-renewal in adult SVZ-derived mouse hNSCs was tested. The c-MycER^{TAM} immortalization technique is an alternative source of implantation material that may overcome existing constraints on the supply and heterogeneity of available brain tissue.¹⁰ The technique is based on the expression of a fusion protein consisting of a growth-promoting gene, human c-Myc, and a modified mouse estradiol receptor (ER). The modification of the ER by site-directed mutagenesis determines that c-Myc protein function is conditional on the presence of the tamoxifen metabolite, 4-hydroxytamoxifen (4-OHT), and therefore, its function is reversible.¹¹ This technique has proven to be successful in generating stable, immortalized embryonic neural stem cell lines,^{12,13} which retain genetic and phenotypic stability. The c-MycER^{TAM} immortalization technique has been successfully applied to embryonic hNSC cells,¹³ the CHO cell line,¹⁴ and fibroblasts, but its use in adult hNSCs had not yet been explored. To our knowledge, this is the first report evaluating the effects of the MycER^{TAM} technique on adult hNSCs and using episomal vectors instead of retroviral vectors for genetic modification.

We will not discuss this part in detail since it is not part of the body of this doctoral thesis. Nevertheless, the main conclusion of this new strategy was that MycER^{TAM} exogenous expression in adult hNSCs can induce mild but insufficient cell proliferation while arresting cell differentiation. Although discouraging, these results have relevant implications in research focusing on adult hNSCs. Far from being beneficial for expanding the scarce hNSCs obtained from adult sources, the effect of c-Myc might be deleterious and is associated with low expansion efficiency and high tumorigenic risk. According to these findings, we believe that alternative modifications should be investigated to achieve transient immortalization of human hNSCs for future therapies that can be applied to humans. For these reasons, human cerebral cortex astrocytes were selected as an *in vitro* model to study the metabolic alterations under hypoxia (**Annex 3**).

3. Low extractivity brain hypoxia after traumatic brain injury. Metabolic profile and *in vitro* modeling.

For both clinicians and researchers, brain hypoxia has been a focus in most secondary lesions occurring in patients with severe TBI. In 1978, Graham et al. raised awareness of the high frequency of ischemic lesions in patients who died from TBI, and in the 1980s, they confirmed that ischemic brain damage is highly prevalent in these patients.^{15,16} Clinical studies showed that CBF was significantly reduced very early after TBI and is an independent predictor of poor neurological outcome. In addition, early extra-cranial insults (hypotension, hypoxemia, anemia, etc.) are frequent after TBI and have devastating effects on the damaged and already vulnerable brain.

In the last two decades, evidence has shown that “brain ischemia” is a reductionist term that has a different meaning for different authors. It includes a wide variety of oxygen/glucose deprivation and thus many classes of tissue hypoxia with different pathophysiological mechanisms. In 1995, Siggaard-Andersen et al. introduced a comprehensive and unambiguous classification system of tissue hypoxia, including ischemia (i.e., ischemic hypoxia).^{1,17} The Siggaard-Andersen classification system stratifies tissue hypoxia into 7 basic types: ischemic hypoxia, low-extractivity hypoxia, shunt hypoxia, dysperfusion hypoxia, histotoxic hypoxia, uncoupling hypoxia, and hypermetabolic hypoxia.^{1,17} The term “oxygen extractivity” was coined by Siggaard-Andersen et al. to define the capacity of the arterial blood that allows the tissues to extract an arbitrary amount of approximately 52 mL/L of oxygen from the arterial blood without a decrease in arterial oxygen tension below the usual venous tension (~38 mmHg).^{1,17} The oxygen extraction tension (P_x) is a variable that indicates the oxygen extractivity and is an indicator of the oxygen reserve of the arterial blood.^{1,17} Following this line of thought, “low-extractivity” hypoxia was introduced by our group and includes three potential causes of hypoxia: hypoxic hypoxia, anemic hypoxia, and high-affinity hypoxia (low P_{50}).

The brain needs a continuous supply of oxygen and glucose for functional integrity.¹⁸ Oxygen deprivation is an important and common indicator of the complex metabolic changes associated with ischemic events. Numerous *in vivo* studies have been performed to elucidate the mechanisms involved in this type of brain injury. However,

the results are difficult to interpret because multiple parameters are liable to change simultaneously in the brain under experimental conditions. This makes it difficult to determine the relevant mechanisms involved.¹⁸

Under normal oxygen tensions, cells catabolize glucose to pyruvate via glycolytic enzymes. Pyruvate is then taken up by the mitochondria for further catabolism through the KC, which transfers electrons to the respiratory chain. Electron transport through the ETC chain results in ATP production and terminates in the donation of electrons to oxygen. In low oxygen tension, hypoxic cells are surmised to undergo anaerobic glycolysis as a default mode to supply the ATP that cannot be generated in the ETC. Increased glycolytic flux requires transcriptional activation of genes encoding glucose transporters (GLUTs) and glycolytic enzymes (e.g., LDH, pyruvate dehydrogenase kinase -PDK-),^{19,20} which are mediated by HIF.²⁰ Moreover, cerebral tissue is composed of many different cell types that have a different susceptibility to hypoxia.^{18,21} Astrocytes are the most abundant cell type in the central nervous system and provide structural and metabolic support to surrounding cells during ischemia. Astrocytes have been implicated in ischemic pathology and are efficiently positioned to preserve neuronal function from injury.²¹ Oxygen supply is critical for brain function, and glucose uptake and metabolism by astrocytes are essential to their metabolic coupling to neurons.²²

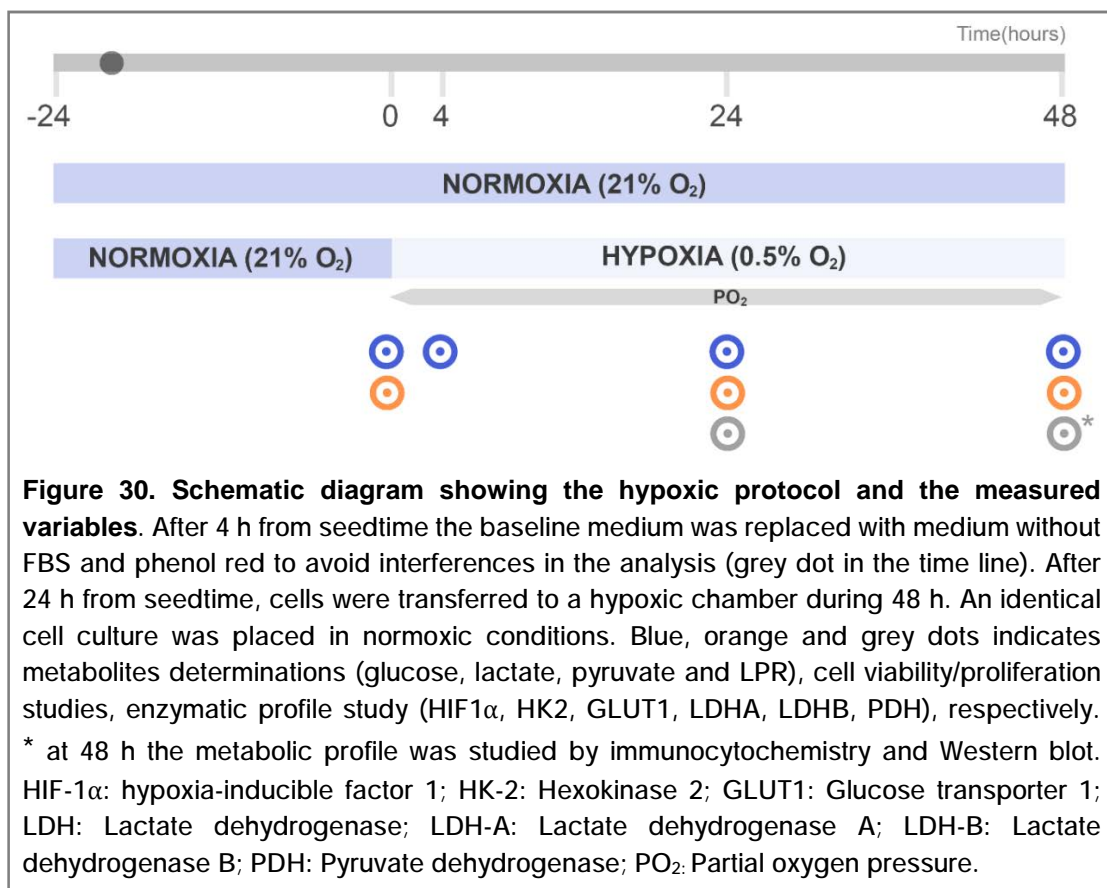
The main goal of this study was to reproduce the energy metabolic profile *in vitro*, as well as the changes in the glycolytic machinery of low-extractivity hypoxia. This condition is characterized by a lack of oxygen supply for the mitochondria, a good delivery of glucose, and a significant reduction in the clearance of metabolites, particularly lactic acid and protons. For this purpose, we used human cerebral cortical astrocytes as a model to explore the metabolic profile and the dysfunction of astrocytes under low, moderate, and severe hypoxia. To study the metabolic profile, the metabolite levels (glucose, lactate, pyruvate, and LPR) and the metabolic enzymatic profile (GLUT1, HK-2, LDH and PDH) were analyzed under hypoxic and normoxic conditions. This is a first step to exploring the consequences of LEH *in vitro* for a better understating of the MD pattern found in neurocritical patients. Our aim in this study is to acquire in-depth knowledge of more complex forms of brain hypoxia found in acute brain injuries, such as mitochondrial dysfunction, in which the available information is still fragmentary and incomplete.

3.1. Material and methods

3.1.1. Cell culture and hypoxic challenge

Human cortical cryopreserved astrocytes (catalog# 1800, ScienCell Research Laboratories, San Diego, CA, USA), isolated from human fetal brain (20 weeks), were incubated in astrocyte medium (AM; catalog# 1801, ScienCell Research Laboratories) in poly-L-lysine (catalog# P4832, Sigma-Aldrich) pretreated plates, according to manufacturer's instructions. AM medium consists of basal media, FBS (catalog# 0010, ScienCell Research Laboratories), P/S (catalog# P0503, ScienCell Research Laboratories) solution and astrocyte growth supplement (AGS; catalog# P1852, ScienCell Research Laboratories).

For the hypoxic challenge, cells were counted, seeded into 6-well plates (at 250,000 cell/mL) containing the complete medium (described above) and acclimated in a regular normoxic incubator for 4h (Galaxy 170R; Eppendorf, Enfield, CT, USA). After this 4h period, the baseline medium was replaced with medium without FBS and phenol red (catalog# 1801-prf, ScienCell Research Laboratories), to avoid interferences in the analysis, and cells were incubated during 24h at 37°C under normoxic conditions (21% O₂, 5% CO₂ at 95% humidity). After 24 h from seedtime, cells were transferred to the INVIVO₂ 200 hypoxic chamber (Ruskin, Bridgend, UK) at a temperature of 37°C filled with 94.5% N₂/ 0.5% O₂/ 5% CO₂ at 95% humidity) and maintained for 48 h. An identical cell culture was placed in normoxic conditions (21% O₂, 5% CO₂ at 95% humidity at 37°C) during 48 h and used as control. A schematic representation of the hypoxic challenge experiment and the studies conducted are summarized in **Figure 30**. The measured PO₂ in the medium was evaluated with a Licox CC1.SB oxygen probe (Integra Neurocare, Plainsboro, NJ, USA) and was 10.0 ± 0.15 mmHg at 4 h, 4.9 ± 0.03 mmHg at 24 h and 2.4 ± 0.05 mmHg at 48 h. At the end of the experiment, a calibration at air pressure (sensitivity-calibration) as well as in oxygen free solution (zero-drift) was carried out, as previously reported by Dings et al. in 1997.²³ The deviation of the sensibility of the sensor was 0.37% and after the calibration at the zero-point the PO₂ fell to 0 mmHg, 20 minutes later.



3.1.2. Cell Viability: Propidium iodide uptake

The propidium iodide (PI) uptake assay and flow cytometry were used to measure cell death.²⁴ Briefly, cells were detached by trypsinization, seeded in 100 mm plates and incubated overnight. After overnight seedtime, cells were then incubated during 24 and 48 h under normoxic and hypoxic conditions, as described above. At each time point, supernatants were collected and cells were harvested by trypsinization. Then cells were stained with PI (catalog#P4864, Sigma-Aldrich) to a final concentration of 5 $\mu\text{g}/\text{mL}$. PI uptake versus exclusion is commonly used to discriminate between dead cells, in which plasma membranes become permeable—regardless the mechanism of death—, and live cells with intact plasma membranes.²¹ PI fluorescence of individual nuclei was detected by a Fortessa LSRII flow cytometer (BD Immunocytometry System, BD Biosciences, San Jose, CA, USA) using FACSDiva software v6.2 (BD Biosciences). In all the samples, 150 μL were analyzed in 75 seconds, giving a relative measure of the number of cells (events). Cells were gated based on forward scatter (FSC) and side scatter (SSC) detectors using a linear scale to gate out cellular debris.

The fluorescence intensity was then determined for PI and plotted using a log scale. Fluorescence emission was detected at the C-Blue channel (600lp, bp610 \pm 20) for PI. The sample flow rate chosen was low (2 μ L/min), and at least 20.000 cells were acquired for analysis. The percentage of viable cells (negative PI fluorescence) was gated and automatically determined by the analysis software. Triplicate counts were made for each procedure.

3.1.3. Metabolic analysis

Briefly, 20 μ L aliquots of the culture medium were collected at baseline (1h before starting the experiments) and at 4, 24 and 48 h in cells exposed to hypoxia and in controls (normoxia). The samples were centrifuged at 800 x g for 3 min to eliminate cell debris and the metabolic profile (glucose, lactate, pyruvate, glycerol and LPR) was analyzed by using an ISCUS Flex analyzer (M Dialysis AB, Solna, Sweden) according to the manufacturer's instructions. Mean values of at least three wells from six independent experiments were calculated.

3.1.4. Western blot (WB)

After 48 h under hypoxia, the cultured cells were washed with cold PBS and harvested with ice-cold RIPA buffer (catalog# R0278, Sigma-Aldrich). Proteases were inhibited by a protease inhibitor cocktail (catalog# 11697498001, Roche Diagnostics, Mannheim, Germany) containing 1 mM orthovanadate Na₃VO₄ (catalog# S6508, Sigma-Aldrich). The protein concentration was quantified by the Bradford's method,²² using bovine serum albumin as the standard (catalog# A2153, Sigma-Aldrich). A total of 10 μ g of protein was loaded on a 10% SDS-polyacrylamide gel together with a standard weight marker (catalog# 161-0374, Precision Plus Protein Standards-Dual Color; Bio-Rad, California, USA), separated electrophoretically and transferred to a polyvinylidene difluoride membrane (catalog# IPVH00010, Millipore Corporation). The transferred membranes were blocked with 5% fat-free milk tris-buffered saline buffer (TBS) containing 0.1% Tween 20 (catalog# P9416, Sigma-Aldrich), at RT. Next, membranes were incubated overnight with the following primary antibodies: mouse anti-Hexokinase II (HK-2; 1:2000; catalog# ab104836, Abcam), rabbit anti-lactate

dehydrogenase (LDH; 1:2000; catalog# ab47010, Abcam), goat anti-lactate dehydrogenase A (LDH-A; 1:200; catalog# sc-33781, Santa Cruz Biotechnology, Dallas, USA), mouse anti-lactate dehydrogenase B (LDH-B; 1:5000; catalog# H00003945-M01, Abnova, Jhongli, Taiwan), mouse anti-pyruvate dehydrogenase (PDH; 1:2000; catalog# ab110330, Abcam), mouse anti-hypoxia inducible factor (HIF1 α ; 1:1000; catalog# NB100-449, Novus Biological, Littleton, USA) and mouse anti-glucose transporter 1 (GLUT1; 1:5000; catalog# ab40084, Abcam). After washing in TBS containing 0.1% Tween 20 (Sigma-Aldrich), the horseradish peroxidase (HRP)-labeled species-appropriate secondary antibody was applied at 1:2000 dilution for 1 h. The blot was washed again in TBS-Tween 20, and then positive signals were developed using enhanced chemiluminescence ECL Prime Western blotting detection reagent (catalog# RPN2232, GE Healthcare, Buckinghamshire, UK) and detected by an exposure to radiographic films (Santa Cruz Biotechnology). The optical density of the resulting bands was determined by Quantity One 1-D Analysis Software v4.6.6 (Bio-Rad). Data were expressed as the ratio of the band intensity of the protein of interest to the loading control protein band (β -Tubulin; 1:100.000; catalog# T4026 Millipore or β -Actin, 1:100.000; catalog# ab8226, Abcam).

3.1.5. Immunocytochemistry

Cells were cultured on coverslips (Macalaster Bicknell, New Haven, CT, USA) during 24 and 48h in 24-well plates under the normoxic and hypoxic conditions as described above. After washing, cells were fixed in 4% formaldehyde for 30 min at RT, then washed twice in PBS and incubated for 1h at RT in a blocking solution containing 5% donkey serum and 0.1% Triton-X in PBS 0.1 M. In the next step, cells were incubated first for 1h at RT and then overnight at 4°C with the following primary antibodies: HK2 (1:20), LDH (1:200), LDH-A (1:50), LDH-B (1:50), PDH (1:100), HIF-1 α (1:100), GLUT1 (1:200). Fluorescent-labeled, species-appropriate secondary antibodies (Thermo Fisher Scientific) were used for visualization. Omission of primary antibodies served as a negative control. Cells were counterstained with DAPI and cover-slipped with polar mounting medium (Thermo Fisher Scientific). Fluorescent signals were visualized using an epifluorescence microscope (BX61 Olympus; Olympus Corporation).

3.1.6. Statistical analysis

Statistical analyses were carried out with R v3.2.0 (R Foundation for Statistical Computing, Vienna, Austria; <http://www.R-project.org>) and the integrated development environment R Studio v0.99.902 (RStudio, Inc., Boston, MA, USA; <http://www.rstudio.com>) and Graphpad Prism 7.00 (GraphPad Software, Inc., La Jolla California USA). Descriptive statistics were obtained for each variable. Data were expressed as the mean \pm SD unless specified. Statistical analysis of cell treatments was carried out using U Mann-Whitney to compare two independent groups. For exploratory data analysis variables were presented graphically using box-plots and line graphs to show treatment time effect. Statistical significance was considered when $p \leq 0.05$.

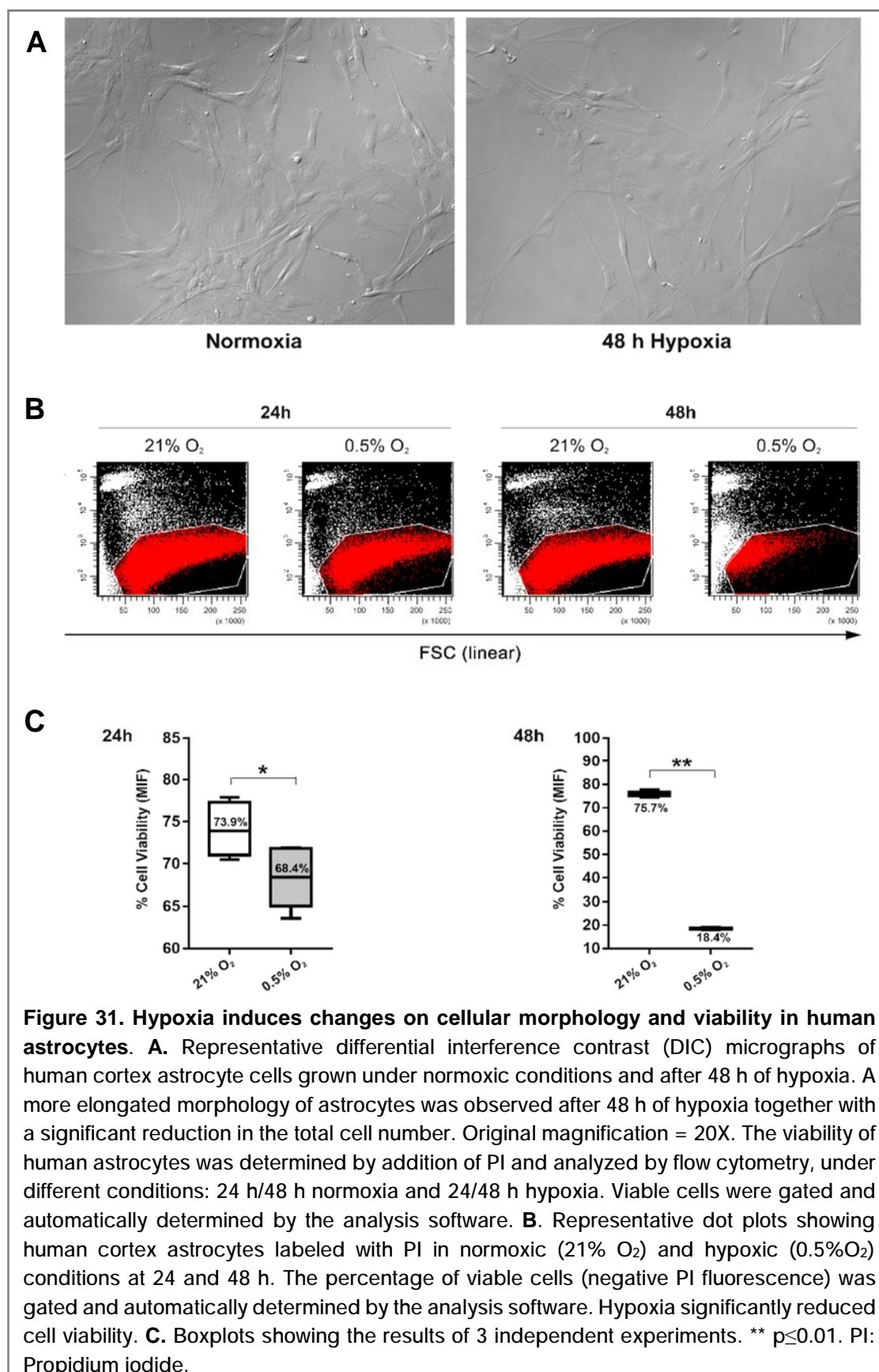
3.2. Results

3.2.1. Effects of hypoxia on cellular proliferation, morphology and viability

Flow cytometry allowed us to quantify the number of cells and the cell viability under different conditions. Under normoxia, a time-dependent increase in the total cell number was observed. The total number of cells increased from 453.804 ± 55.290 cells/mL at baseline to 542.529 ± 43.091 cells/mL at 24 h (+19.6%) and to 624.724 ± 18.229 cells/mL at 48 h (+37.4%). Under hypoxia, the number of cells stabilized from 453.804 ± 55.290 cells/mL at baseline to 395.988 ± 11.985 cells/mL at 24 h (-12.7%) and decreased to 176.796 ± 17.536 cells/mL at 48 h (-61.0%). Protein content also decreased after 48 h of sustained hypoxia. The mean protein content was $1.48 \mu\text{g}/\mu\text{L}$ under normoxia and $1.15 \mu\text{g}/\mu\text{L}$ in hypoxia (-22.3%).

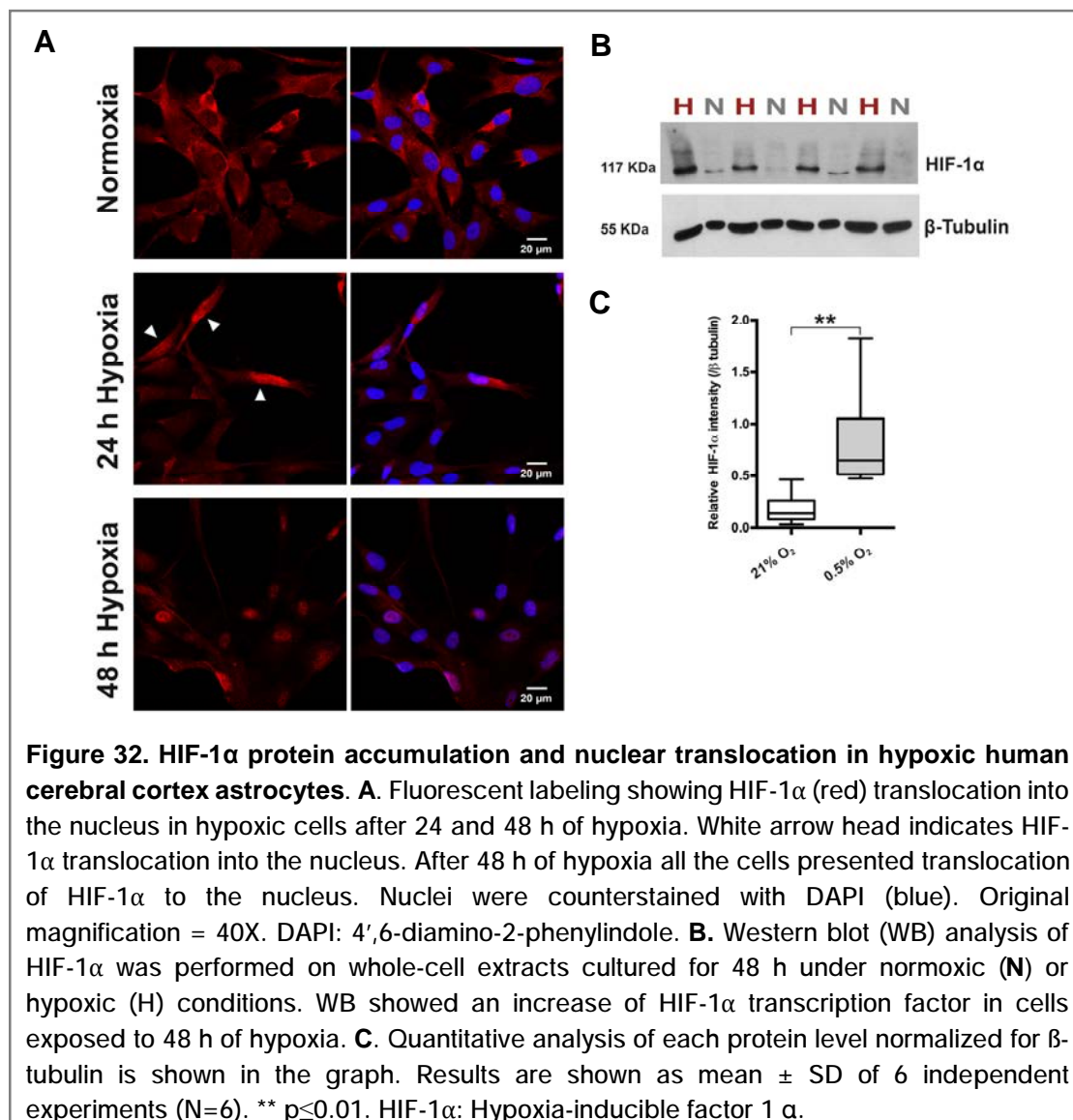
The exposure of astrocytes to hypoxia for 48 h resulted in mild morphologic changes to a more elongated structure and generated less clusters than under normoxia (**Figure 31A**). The effects of hypoxia on cell viability were investigated by the PI uptake using flow cytometry. As shown in **Figures 31B** and **C**, the percentage of viable cells was significantly higher under normoxia than under hypoxia at 24 h (Mann-Whitney test, $p = 0.0260$) and 48 h (Mann-Whitney test, $p = 0.0043$). In normoxia, the percentages of cell viability were $74.08 \pm 3.143\%$ at 24 h and $75.78 \pm 1.14\%$ at 48 h.

Cell viability under hypoxic conditions was $68.27 \pm 3.53\%$ at 24 h and $18.44\% \pm 0.36\%$ at 48 h.



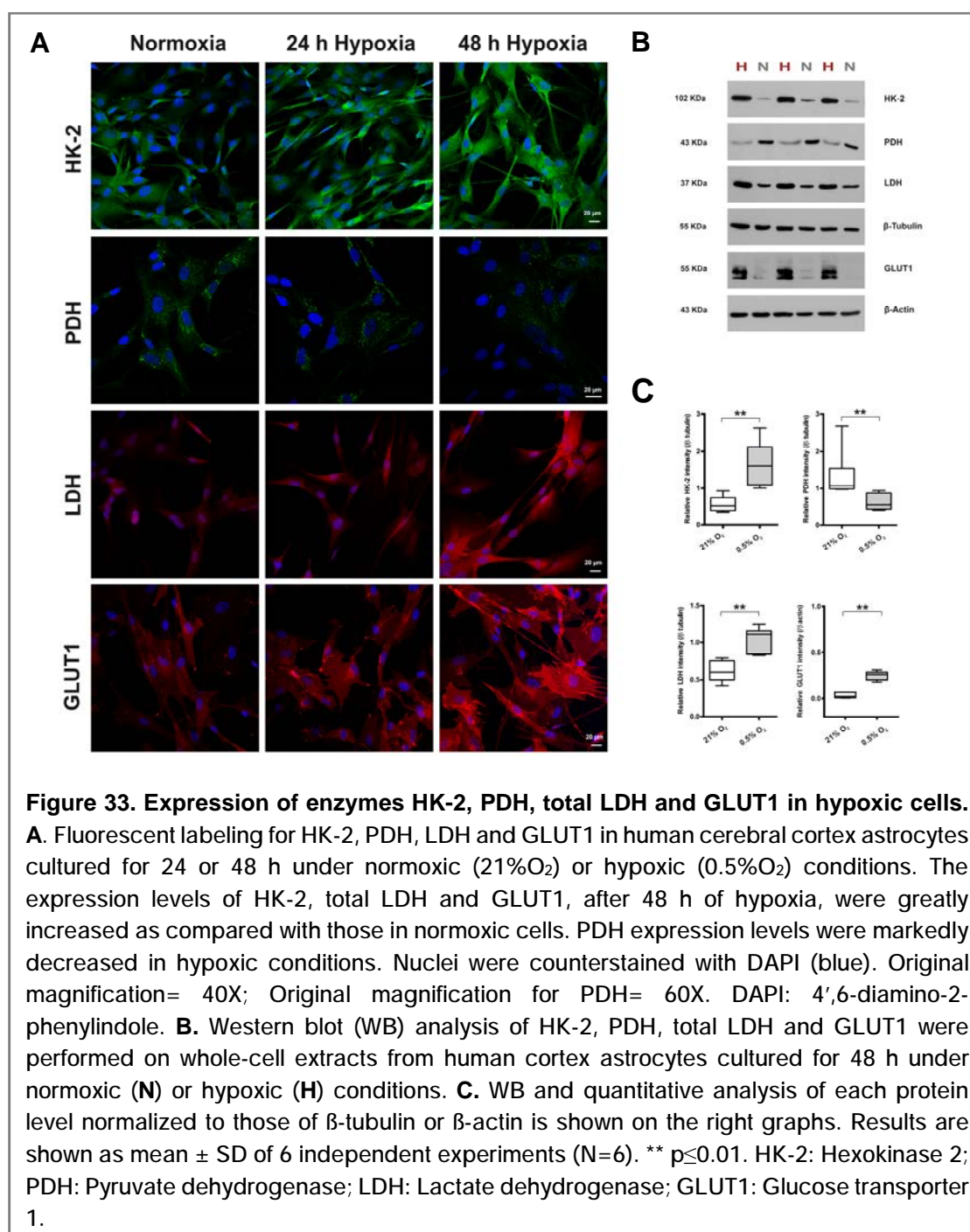
3.2.1. HIF-1 α protein accumulation and nuclear translocation

To compare HIF-1 α protein accumulation and nuclear translocation, astrocytes were studied after 24 and 48 h of hypoxia. Under hypoxic conditions, HIF-1 α protein accumulates and translocates to the nucleus, where it forms an active complex and activates the transcription of target genes. Astrocytes responded to hypoxia by HIF-1 α stabilization according to WB and ICC techniques (**Figure 32**). ICC assessment revealed that HIF-1 α translocated to the nuclei after 24 h of hypoxia and persisted at 48 h. After sustained hypoxia (48 h), most of the cells showed nuclear translocation (**Figure 32A**). HIF-1 α protein accumulation was analyzed in whole-cell lysates incubated at 0.5% O₂ or 21% O₂. HIF-1 α was stabilized in hypoxia with a statistically significant increase in the protein levels in hypoxic conditions compared to normoxic conditions (U Mann-Whitney test, $p=0.002$; **Figure 32B**).

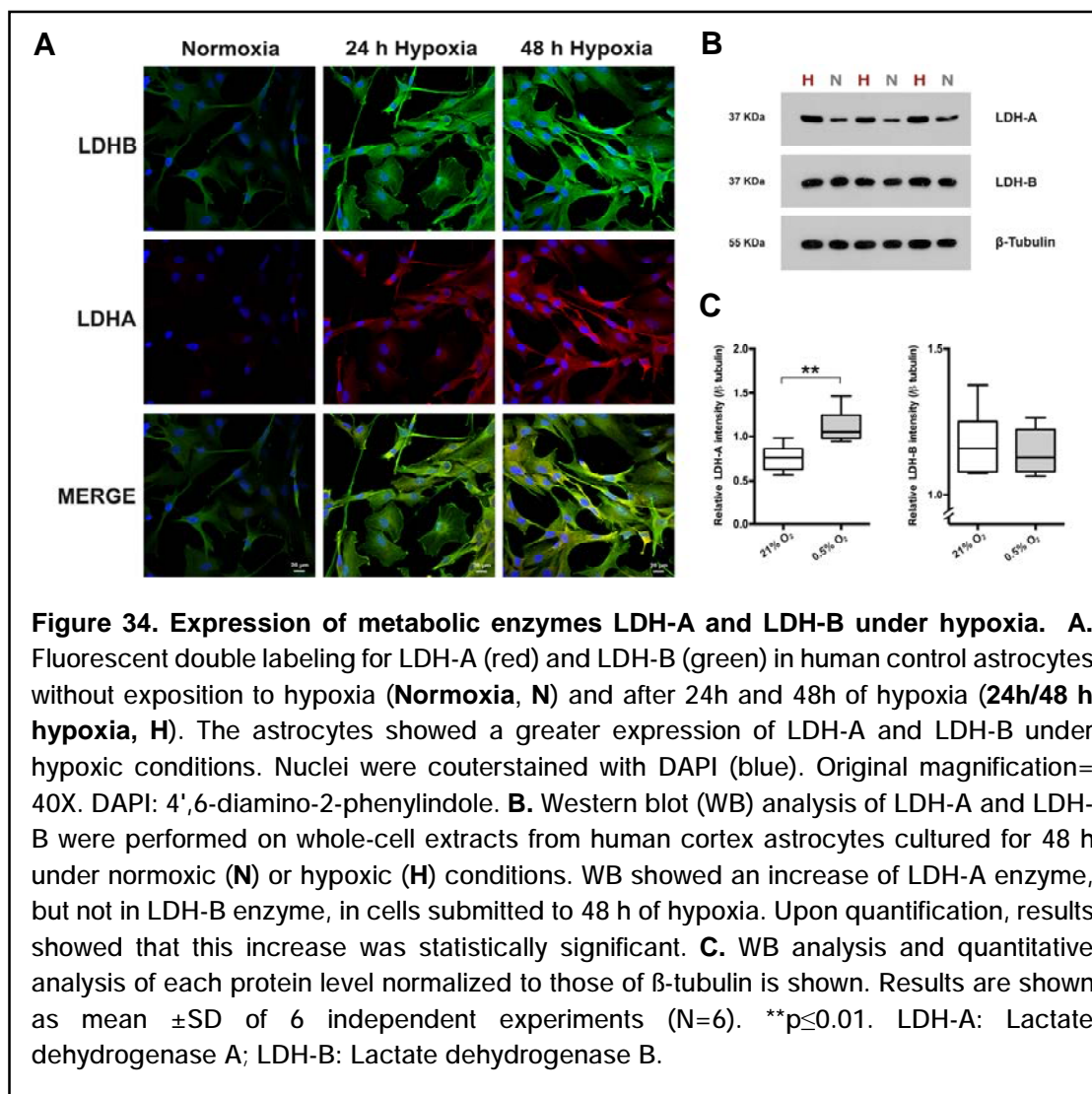


3.2.2. Expression of glycolytic enzymes in hypoxic cells

To determine the metabolic profile of human cortex astrocytes under sustained hypoxia, the protein levels and expression of HK-2, PDH, total LDH (LDH-A and LDH-B subunits), and GLUT1 were determined by WB and ICC. Experiments were conducted in parallel, and the cells exposed to hypoxia were compared with astrocytes maintained in normoxic conditions. Representative immunoblots and quantitative analysis for each protein are shown in **Figures 33** and **34**.



We first examined the expression by ICC. As shown in **Figures 33A** and **34A**, the expression of these metabolic enzymes was detectable in all the conditions (normoxia, 24 h of hypoxia, and 48 h of hypoxia). The protein levels of HK-2, total LDH, GLUT1, LDH-A, and LDH-B after 48 h of hypoxia were significantly increased in comparison with those in normoxic cells, especially for the LDH and GLUT1 enzyme (**Figures 33** and **34**). However, PDH expression levels were markedly decreased after exposure of the astrocytes to hypoxic conditions (**Figure 33**).



The next experiments examined the effect of hypoxia on glycolytic enzymes. WB analyses demonstrated significantly higher expressions of GLUT1, HK-2, and total LDH after hypoxic conditions (U Mann-Whitney test, $p=0.0022$ in all 3 comparisons; **Figure 33C**). In contrast, PDH levels were significantly decreased under hypoxic

conditions compared to normoxia (U Mann-Whitney test, $p=0.002$; **Figure 33C**). To confirm the LDH expression levels, LDH-A and LDH-B isoforms were also analyzed by WB. Different expression of these isoforms was observed. In the hypoxic astrocytes, a statistically significant increase of LDH-A protein levels was observed compared to the normoxic cells (U Mann-Whitney test, $p=0.0022$; **Figure 34C**). However, we did not observe any significant change in LDH-B (U Mann-Whitney test, $p=0.6753$, **Figure 34C**).

3.2.3. Effects of hypoxia on astrocytes energy metabolism

The metabolic profiles (glucose, lactate, pyruvate, and the lactate-to-pyruvate ratio (LPR) levels) of astrocyte cultures corresponding to short (4 h), intermediate (24 h), and prolonged (48 h) periods of hypoxia were analyzed in the cell culture supernatants. The changes in absolute values of all metabolites are summarized in **Table 13**. Under normoxic conditions, the glucose consumption increases in a time-dependent manner (**Figure 35**). Lactate levels increase as a consequence of cell proliferation and because lactate is the main product of astrocytes (**Figure 35**). As a result of the lactate level increase, a decrease in pyruvate levels was observed (**Figure 35**). On the other hand, hypoxia caused an increase in glucose consumption relative to its homologous control, showing statistically significant differences after 48 h of the hypoxic challenge (Mann Whitney test, $p = 0.0260$, **Figure 35**). As expected, lactate levels showed a statistically significant increase after 24 and 48 h of hypoxia (Mann Whitney test, $p = 0.0022$ and $p = 0.0043$, respectively; **Figure 35**).

The levels of pyruvate remained relatively stable over time, probably because the observed hyperglycolysis led to the saturation of the enzyme (LDH) and thus the accumulation of its substrate (pyruvate). Statistically significant differences were also observed for pyruvate at 24 and 48 h (Mann Whitney test, $p = 0.0022$ and $p = 0.0095$, respectively; **Figure 35**). These changes were reflected in the LPR (**Figure 35**). In our opinion, this index must be carefully considered in this scenario under *in vitro* conditions because there is no wash-out of lactate, unlike *in vivo* conditions. This results in lactate accumulation in the culture media.

Table 13. Metabolite concentrations in the culture media at baseline and during short (4h), intermediate (24 h) and prolonged (48 h) periods of hypoxia

	Glucose (mmol/L)	Lactate (mmol/L)	Pyruvate (μ mol/L)	LPR
Baseline				
N	4.26 \pm 0.26	1.67 \pm 0.16	567 \pm 45.2	2.98 \pm 0.46
H	4.29 \pm 0.23	1.64 \pm 0.20	575 \pm 46.2	2.89 \pm 0.52
4h				
N	4.05 \pm 0.20	2.25 \pm 0.23	547 \pm 36.3	4.19 \pm 0.65
H	4.13 \pm 0.20	2.49 \pm 0.27	565 \pm 33.7	4.47 \pm 0.67
24h				
N	3.23 \pm 0.23	4.29 \pm 0.58	367 \pm 32.4	12.0 \pm 2.41
H	2.63 \pm 0.39	7.45 \pm 1.02	559 \pm 40.8	14.2 \pm 2.46
48h				
N	2.32 \pm 0.40	6.20 \pm 0.76	222 \pm 38.3	32.5 \pm 7.40
H	0.77 \pm 0.70	14.8 \pm 2.20	530 \pm 61.9	25.7 \pm 4.86

Results are shown as mean \pm SD of 6 independent experiments (N=6). N: Normoxia; H: Hypoxia; LPR: Lactate-to-pyruvate ratio; SD: Standard Deviation.

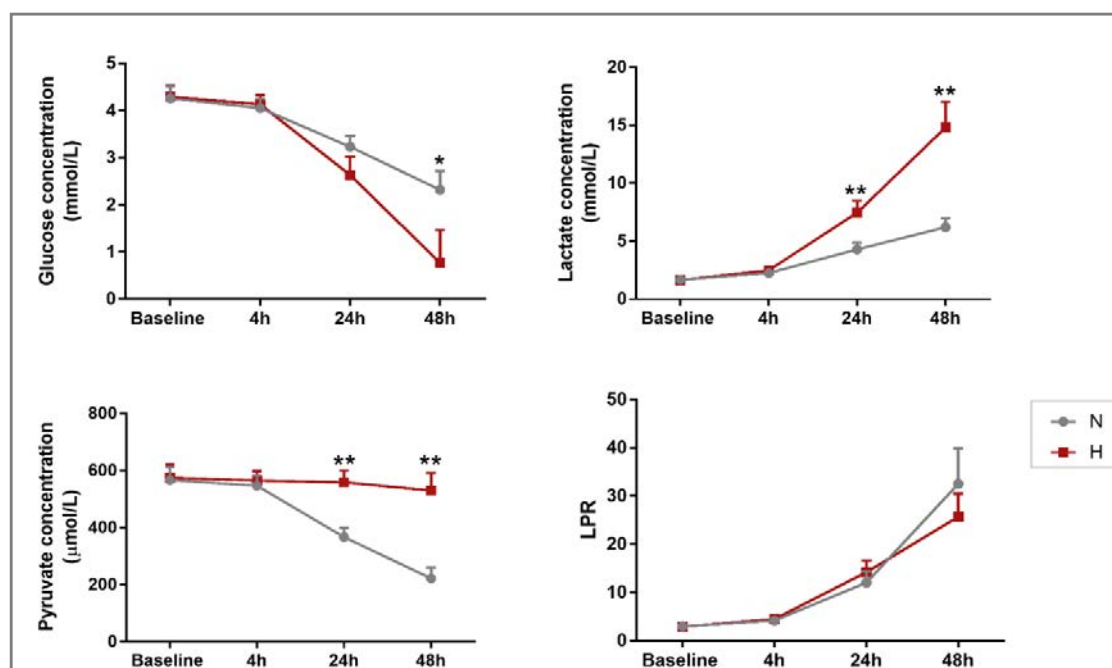


Figure 35. Graphical representation of the metabolic response of human cortex astrocytes to normoxic and hypoxic conditions. Human cortex astrocyte cells were grown at normoxic (N, 21%O₂) or hypoxic (H, 0.5%O₂) conditions and the corresponding conditioned culture media was analyzed at baseline, 4, 24 and 48 h. The hypoxic modulation of glycolysis associated metabolites was analyzed on the analyzer ISCUS Flex (M Dialysis AB, Solna, Sweden) according to the manufacturer's instructions. Statistical analysis confirming the differences in the consumption/production of metabolites: glucose, lactate, pyruvate and LPR in human cortex astrocytes submitted to hypoxia. Results are shown as mean \pm SD of 6 independent experiments (N=6). * $p \leq 0.05$, ** $p \leq 0.01$.

The metabolic levels after 48 h of the hypoxic challenge were normalized to the total protein content. As expected, no changes were observed in the metabolic trends and in the statistical significance. Data are summarized in **Table 14** for glucose, lactate, and pyruvate.

Table 14. Metabolite concentrations at 48 h of hyperoxia normalized for protein content

	Glucose (mmol/L/ μ g/ μ L)	Lactate (mmol/L/ μ g/ μ L)	Pyruvate (μ mol/L/ μ g/ μ L)
N	1.44 \pm 0.38	4.43 \pm 1.63	138 \pm 23.6
H	0.34 \pm 0.51	12.7 \pm 2.86	441 \pm 68.8
p*	0.0159	0.0043	0.0095

Results are expressed as mean \pm SD. * Comparisons between variables were made using the Mann Whitney test. N: Normoxia; H: Hypoxia; SD: Standard deviation.

Culture media evaporation was observed under hypoxic conditions at 48 h. To overcome differences in the metabolite concentration caused by evaporation of the cell culture media, the metabolite concentrations were corrected according to the culture media volume. After this correction, the metabolic trends were maintained. However, statistically significant differences between conditions were observed only for lactate and pyruvate (**Table 15**).

Table 15. Metabolite concentrations at 48 h of hyperoxia normalized for media volume

	Glucose (mmol/L/ μ L)	Lactate (mmol/L/ μ L)	Pyruvate (μ mol/L/ μ L)
N	0.93 \pm 0.22	2.75 \pm 0.87	88.7 \pm 19.8
H	0.33 \pm 0.42	9.9 \pm 2.6	349.4 \pm 39.9
p*	0.0667	0.0043	0.0095

Results are expressed as mean \pm SD. * Comparisons between variables were made using the Mann Whitney test. N: Normoxia; H: Hypoxia; SD: Standard deviation.

3.3. Discussion

Oxygen deprivation is common in both ischemia and LEH. However, ischemia is characterized by the deprivation of glucose due to the reduction in CBF that accompanies ischemic hypoxia. In addition to the lack of oxygen supply for the mitochondria, the LEH is characterized by good delivery of glucose. A disappointing

paradox is that the pivotal classification system¹⁷ has not received enough attention in intensive care literature or in the framework of brain hypoxia. To date, the seminal paper has received only 44 citations, amounting to 2.59 citations per year according to Harzing's Publish and Perish citation software. However, this classification provides a theoretical framework for the characterization of all types of brain hypoxia found in a clinical setting.

This study investigated LEH using a human *in vitro* model. We aimed to demonstrate the importance of the Sigaard-Andersen classification to differentiate between different forms of brain hypoxia. In neurocritical patients, modern multimodal neuromonitoring is widely used in neurocritical care units, including PtiO₂ and MD monitoring, which allow for the quasi-continuous profiling of the brain oxygen supply and brain metabolism.^{25,26} These probes are generally inserted in the subcortical white matter. The susceptibility to hypoxia differs among brain cells, with astrocytes and endothelial cells being more capable of withstanding hypoxic injury than neurons and oligodendrocytes.^{27,28} Human astrocytes were selected as an *in vitro* model under hypoxia. Human cortex astrocytes with normal levels of glucose (5mM) were selected to study the low-extractivity brain hypoxia that follows TBI.

The present study examined the effect of short, intermediate, and prolonged periods of severe hypoxia on human cortex astrocytes on cell viability and the metabolic profile. Astrocytes have a high glycolytic rate and mainly produce lactate. Our findings suggest that the exposure of human astrocytes to short periods of hypoxia (4 h) elicits no metabolic changes in comparison to a homologous control (**Figure 35** and **Table 13**). In contrast, a fundamentally different glycolytic response was observed after 24 and 48 h of the hypoxic challenge (**Figures 33-35** and **Table 13**). Prolonged periods of hypoxia reduced cell viability in a time-dependent manner. Mild but statistically significant changes were observed after 24 h, probably because astrocytes seem to survive hypoxia as long as there is a supply of glucose for anaerobic glycolysis.^{29,30} At this time point, the mean glucose levels in the culture media were 2.63 mmol/L, whereas those at 48 h were 0.77 mmol/L. After 48 h of hypoxia, a dramatic decrease in glucose levels in the culture media was observed, which can lead to a reduction in cell viability^{29,30} (**Figure 31**) unless other adaptive mechanisms are activated.

The adaptation and response of the brain to hypoxia have been scrutinized for the last 3 decades, and answers to some of the relevant questions are still incomplete.

Intracellular oxygen tension is regulated, and low $[O_2]_i$ triggers the upregulation of genes that initiate the response to hypoxic stress in all cell types. Among them, we found that VEGF and glycolytic enzymes activate erythropoietin (and regulate red blood cell production). Glycolytic enzymes also try to maintain ATP production despite low $[O_2]$.³¹ The debate is still focused on which one functions as the “sensor.” Zhu et al. proposed that cytochrome b5/b5 reductase (b5/b5R) fusion protein is one of the best candidates.²⁴ This protein has low affinity for oxygen and is expressed in a wide variety of human cell lines, organs, and tissues.

Whichever it is, it is quite clear that the oxygen sensor activates the erythropoietin gene through the HIF transcription factors. The HIF transcription factors are instrumental for orchestrating adaptive responses to cope with oxygen shortage, and HIF1 α in particular is a key factor in inducing the expression of glycolytic enzymes. In this study, we observed that HIF1 α activates and translocates to the nucleus after hypoxia. Moderate translocation was observed by ICC after 24 h of the challenge, whereas after 48 h, all the cells presented translocation of the transcription factor to the nucleus (**Figure 32**). In addition, we have demonstrated that HIF1 α induced the expression of glycolytic enzymes, which was reflected by an increase in glucose consumption and lactate release. These strategies have been described previously in primary rat cultures of astrocytes subjected to short anoxia (8 h).³² However, these studies were performed using animal cell culture models and did not look at the profile of the most relevant glycolytic enzymes and the concentration of metabolites, such as pyruvate and the LPR.

Moderate and prolonged periods of hypoxia caused an increase in the glucose consumption rate related to its homologous control. After 4 h of hypoxia, similar consumption rates were observed between normoxia and hypoxia, probably because astrocytes mobilize the glycogen stores as an alternative source of energy production without increasing extracellular glucose uptake.^{32,33} Glucose transport across plasma membranes is achieved by several sodium-independent facilitative glucose transporter isoforms designated as GLUT.^{34,35} The GLUT1 isoform is expressed in both glia and neurons. Our study showed increased GLUT1 expression and increased glucose utilization under hypoxia at 24 and 48 h. Vega et al. observed that the rate of energy consumption was decreased after 3 weeks of sustained hypoxia (5% O_2), which is a sign of metabolic adaptation and part of a strategy called metabolic depression.³⁶ However, we did not observe a decrease in the energy consumption

rate (glucose) after 48 hours of hypoxia. The mean hourly consumption of glucose was quite stable for each condition (normoxia: 0.04 mmol/L/h (24 h) and 0.05 mmol/L/h (48 h); hypoxia: 0.07 mmol/L/h (24 h) and 0.07 mmol/L/h (48 h)). Additionally, reductions in protein synthesis and total cell number were observed at 48 h of hypoxia, which could be considered moderate symptoms of hypoxia adaptation.

Decreased protein synthesis may contribute to the cellular strategy used by astrocytes to maintain their energy balance under hypoxic conditions, as evidenced by the mild changes in cell morphology (**Figure 31**). Energy spared by the reduction in protein synthesis may be reallocated to more critical cell functions.²¹ Nevertheless, we cannot rule out that these effects could be partly related to the reduction in cell viability. Kelleher et al. observed that astrocytes were killed after 24 h of hypoxia in the presence of 7.5 mmol/L of glucose.¹⁸ Four years later, the same group demonstrated that injury of astrocytes occurred after 30 h of hypoxia with higher glucose concentrations, which was related to changes of the media pH (<6.0).³⁰ We reported a significant reduction in cell viability at 48 h after the insult and mild changes in cell viability at 24 h, when the mean glucose concentration was 3.23 mmol/L.

The formation of lactate under aerobic conditions is catalyzed by lactate dehydrogenase 5 (LDH5, constituting 4 LDHA subunits), which is the main LDH isoform found in astrocytes. We determined the levels of LDHA, LDHB, and total LDH. LDHA is predominantly present in glycolytic tissues, while LDHB is found predominantly in aerobic tissues.³⁷ Each one of these isoforms has more affinity (K_m) for a specific substrate and therefore a predominant direction of the same reaction.³⁷ The LDH-B isoform oxidizes lactate to pyruvate, while LDH-A converts pyruvate to lactate. Consequently, we observed an increase in LDHA expression, while LDHB levels were maintained between different conditions (**Figure 34**), which correlates with a statistically significant increase of lactate under hypoxic conditions.

Notably, the lactate concentration in the culture media doubled under hypoxia compared to normoxic conditions at 48 h of the challenge. In the brain, the transport and formation of lactate are essential parts of the metabolic coupling between neurons and astrocytes. Astrocyte-generated lactate is partly taken by neurons, converted to pyruvate, and enters in the Krebs cycle, where it is converted to CO₂ and water.³⁸⁻⁴⁰ Furthermore, the generated lactate is washed out by the blood and enters the Cori cycle. Both mechanisms prevent the accumulation of [Lac]_{brain}. In astrocyte cultures,

the increase in lactate is in part due to the culture medium acting as a sink for lactate, and there are no mechanisms to reduce its concentration. Cell proliferation and the absence of wash-out in the culture media caused an increase in lactate levels under hypoxic and normoxic conditions in a time-dependent manner (**Figure 35**).

Pyruvate must be measured together with lactate in order to discriminate hypoxic from non-hypoxic sources of lactate.⁴¹ Under normoxic conditions, a decrease in pyruvate levels was observed as a result of the lactate increase. In contrast, pyruvate levels remained relatively stable over time in hypoxia, probably because the observed hyperglycolysis led to the saturation of the enzyme (LDH) and thus the accumulation of pyruvate. Véga et al. reported no changes in pyruvate levels in any of their experimental conditions.²¹

To verify these results, the expression of PDH was also determined. This mitochondrial enzyme is part of an enzymatic complex (PDH complex) that is responsible for the oxidative decarboxylation of pyruvate to generate acetyl-CoA. This is the first step after glycolysis that drives pyruvate to oxidative phosphorylation within mitochondria. Under anaerobic conditions *in vivo*, pyruvate is transformed to lactate, and the LPR ratio increases. As expected, we observed decreased expression of PDH in hypoxia. In a clinical environment, the LPR is probably the most important factor for the study of energy metabolism. A high LPR (>25) could represent a warning for the beginning of metabolic crises.⁴² However, LPR should not be considered in isolation since the levels of lactate and pyruvate together may provide more accurate information about the metabolic status of cells.^{41,42} Nevertheless, in our opinion, this index must be carefully considered in this scenario under *in vitro* conditions because of the lack of lactate wash-out and the resulting lactate accumulation in the culture media.

In summary, our results suggest that human cortex astrocytes subjected to sustained hypoxia display different metabolic pathways and different enzymatic profiles. Our findings could have important implications in modeling TBI *in vitro*. Better understanding of the cell behavior under hypoxia is essential for the study of brain metabolism and to translate these findings to the bedside. Moreover, it may open a clear line of research on the effects of neuroprotective drugs on tissue hypoxia. In view of the experimental data, new paradigms are clearly necessary for better understanding of the pathobiology of brain hypoxia and for a more accurate reflection of brain perfusion and oxygenation in patients with head injury.

3.4. Study limitations and future research

One of the main limitations of our study is the culture media evaporation observed under hypoxic conditions, a common problem in the hypoxic chambers. The evaporation may cause changes in osmolarity that eventually cause cell death. In addition, changes in cell culture volume may change the relative composition of the media. To overcome this problem, the media volume was calculated at the end of the experiment, and the levels of the metabolites were corrected accordingly. Another limitation was that the protein concentration was measured at only 48 h of hypoxia, so the normalization of the metabolite levels for the protein concentration was performed only at 48 h. Nevertheless, no changes were observed in the metabolic trends and the statistical significance.

Future studies including the evaluation of intracellular ATP concentrations would provide additional information about brain energetics and metabolism. It is also recommended to develop an LDH functional study to identify kinetic or affinity (K_m) differences of the enzyme that could explain the pyruvate accumulation over time under hypoxic conditions. Once the metabolic patterns in astrocytes are well known, it would be interesting to study the effects of hypoxia on co-cultures of neurons and astrocytes.

4. References

1. Siggaard-Andersen, O., Ulrich, A. & Gøthgen, I. H. Classes of tissue hypoxia. *Acta Anaesthesiol. Scand. Suppl.* 107, 137–42 (1995).
2. Joo, K. M. *et al.* Experimental and clinical factors influencing long-term stable in vitro expansion of multipotent neural cells from human adult temporal lobes. *Exp. Neurol.* 240, 168–177 (2013).
3. Jha, R. M., Liu, X., Chrenek, R., Madsen, J. R. & Cardozo, D. L. The postnatal human filum terminale is a source of autologous multipotent neurospheres capable of generating motor neurons. *Neurosurgery* 72, 118–128 (2013).
4. Varghese, M. *et al.* Isolation of human multipotent neural progenitors from adult filum terminale. *Stem Cells Dev.* 18, 603–13 (2009).
5. Arsenijevic, Y. *et al.* Isolation of multipotent neural precursors residing in the cortex of the adult human brain. *Exp. Neurol.* 170, 48–62 (2001).
6. Murrell, W. *et al.* Expansion of Multipotent Stem Cells from the Adult Human Brain. *PLoS One* 8, (2013).
7. Nam, H., Lee, K.-H., Nam, D.-H. & Joo, K. M. Adult human neural stem cell therapeutics: Current developmental status and prospect. *World J. Stem Cells* 7, 126–36 (2015).
8. Johansson, C. B., Svensson, M., Wallstedt, L., Janson, a M. & Frisen, J. Neural stem cells in the adult human brain. *Exp. Cell Res.* 253, 733–736 (1999).
9. Stevanato, L. *et al.* c-MycERTAM transgene silencing in a genetically modified human neural stem cell line implanted into MCAo rodent brain. *BMC Neurosci.* 10, 86 (2009).
10. Miljan, E. a *et al.* Implantation of c-mycER TAM immortalized human mesencephalic-derived clonal cell lines ameliorates behavior dysfunction in a rat model of Parkinson's disease. *Stem Cells Dev.* 18, 307–19 (2009).
11. Littlewood, T. D., Hancock, D. C., Danielian, P. S., Parker, M. G. & Evan, G. I. A modified oestrogen receptor ligand-binding domain as an improved switch for the regulation of heterologous proteins. *Nucleic Acids Res.* 23, 1686–1690 (1995).
12. Donato, R. *et al.* Differential development of neuronal physiological responsiveness in two human neural stem cell lines. *BMC Neurosci.* 8, 36 (2007).
13. Pollock, K. *et al.* A conditionally immortal clonal stem cell line from human cortical neuroepithelium for the treatment of ischemic stroke. *Exp. Neurol.* 199, 143–

155 (2006).

14. Fang, C. M., Shi, C. & Xu, Y. H. Deregulated c-myc expression in quiescent CHO cells induces target gene transcription and subsequent apoptotic phenotype. *Cell Res* 9, 305–314 (1999).
15. Graham, D. I. *et al.* Ischaemic brain damage is still common in fatal non-missile head injury. *J. Neurol. Neurosurg. Psychiatry* 52, 346–50 (1989).
16. Graham, D. I., Adams, J. H. & Doyle, D. Ischaemic brain damage in fatal non-missile head injuries. *J. Neurol. Sci.* 39, 213–34 (1978).
17. Siggaard-Andersen, O., Fogh-Andersen, N., Gøthgen, I. H. & Larsen, V. H. Oxygen status of arterial and mixed venous blood. *Crit. Care Med.* 23, 1284–1293 (1995).
18. Yu, A. C., Gregory, G. A. & Chan, P. H. Hypoxia-induced dysfunctions and injury of astrocytes in primary cell cultures. *J Cereb Blood Flow Metab* 9, 20–28 (1989).
19. Weidemann, A. & Johnson, R. S. Biology of HIF-1 α . *Cell Death Differ.* 15, 621–627 (2008).
20. Kim, J. W., Tchernyshyov, I., Semenza, G. L. & Dang, C. V. HIF-1-mediated expression of pyruvate dehydrogenase kinase: A metabolic switch required for cellular adaptation to hypoxia. *Cell Metab.* 3, 177–185 (2006).
21. Véga, C., R. Sachleben, L., Gozal, D. & Gozal, E. Differential metabolic adaptation to acute and long-term hypoxia in rat primary cortical astrocytes. *J. Neurochem.* 97, 872–883 (2006).
22. Pellerin, L. & Magistretti, P. J. Glutamate uptake into astrocytes stimulates aerobic glycolysis: a mechanism coupling neuronal activity to glucose utilization. *Proc. Natl. Acad. Sci. U. S. A.* 91, 10625–9 (1994).
23. Dings, J., Meixensberger, J. & Roosen, K. Brain tissue pO₂-monitoring: catheter stability and complications. *Neurol. Res.* 19, 241–5 (1997).
24. Crowley, L. C. *et al.* Measuring cell death by propidium iodide uptake and flow cytometry. *Cold Spring Harb. Protoc.* 2016, 647–651 (2016).
25. Bellander, B.-M. *et al.* Consensus meeting on microdialysis in neurointensive care. *Intensive Care Med.* 30, 2166–2169 (2004).
26. Hillered, L., Persson, L., Nilsson, P., Ronne-Engstrom, E. & Enblad, P. Continuous monitoring of cerebral metabolism in traumatic brain injury: a focus on cerebral microdialysis. *Curr. Opin. Crit. Care* 12, 112–118 (2006).

27. Pulsinelli, W. A., Brierley, J. B. & Plum, F. Temporal profile of neuronal damage in a model of transient forebrain ischemia. *Ann. Neurol.* 11, 491–498 (1982).
28. Xu, L., Sapolsky, R. M. & Giffard, R. G. Differential sensitivity of murine astrocytes and neurons from different brain regions to injury. *Exp. Neurol.* 169, 416–24 (2001).
29. Callahan, D. J., Engle, M. J. & Volpe, J. J. Hypoxic injury to developing glial cells: protective effect of high glucose. *Pediatr Res* 27, 186–190 (1990).
30. Kelleher, J. a, Chan, P. H., Chan, T. Y. & Gregory, G. a. Modification of hypoxia-induced injury in cultured rat astrocytes by high levels of glucose. *Stroke.* 24, 855–63 (1993).
31. Zhu, H., Jackson, T. & Bunn, H. F. Detecting and responding to hypoxia. *Nephrol. Dial. Transplant* 17 Suppl 1, 3–7 (2002).
32. Marrif, H. & Juurlink, B. H. J. Astrocytes respond to hypoxia by increasing glycolytic capacity. *J. Neurosci. Res.* 57, 255–260 (1999).
33. Niitsu, Y. *et al.* Exposure of cultured primary rat astrocytes to hypoxia results in intracellular glucose depletion and induction of glycolytic enzymes. *Mol. Brain Res.* 74, 26–34 (1999).
34. Bell, G. I., Burant, C. F., Takeda, J. & Gould, G. W. Structure and function of mammalian facilitative sugar transporters. *J. Biol. Chem.* 268, 19161–19164 (1993).
35. Wood, I. S. & Trayhurn, P. Glucose transporters (GLUT and SGLT): expanded families of sugar transport proteins. *Br. J. Nutr.* 89, 3 (2003).
36. Lutz, P. L. & Nilsson, G. E. Contrasting strategies for anoxic brain survival--glycolysis up or down. *J. Exp. Biol.* 200, 411–419 (1997).
37. Bittar, P. G., Charnay, Y., Pellerin, L., Bouras, C. & Magistretti, P. J. Selective Distribution of Lactate Dehydrogenase Isoenzymes in Neurons and Astrocytes of Human Brain. *J. Cereb. Blood Flow Metab.* 1079–1089 (1996). doi:10.1097/00004647-199611000-00001
38. Tsacopoulos, M. & Magistretti, P. J. Metabolic coupling between glia and neurons. *J. Neurosci.* 16, 877–885 (1996).
39. Larrabee, M. G. Lactate Metabolism and Its Effect on Glucose Metabolism in an Excised Neural Tissue. *J. Neurochem.* 64, 1734–1741 (1995).
40. Schurr, A., West, C. A. & Rigor, B. M. Lactate-supported synaptic function in the rat hippocampal slice preparation. *Science (80-)*. 240, 1326–1328 (1988).

41. Sahuquillo, J. *et al.* Lactate and the lactate-to-pyruvate molar ratio cannot be used as independent biomarkers for monitoring brain energetic metabolism: A microdialysis study in patients with traumatic brain injuries. *PLoS One* 9, (2014).
42. Ungerstedt, U. & Rostami, E. Microdialysis in neurointensive care. *Curr. Pharm. Des.* 10, 2145–2152 (2004).